

An Investigation of Nitrification Predictors
and Factors in Two Full-Scale Drinking Water
Distribution Systems

by

Daniel Scott

A thesis
presented to the University of Waterloo
in fulfilment of the
thesis requirement for the degree of
Master of Applied Science
in
Civil Engineering

Waterloo, Ontario, Canada, 2012

©Daniel Scott 2012

AUTHOR'S DECLARATION

I hereby declare that I am the sole author of this thesis. This is a true copy of the thesis, including any required final revisions, as accepted by my examiners.

I understand that my thesis may be made electronically available to the public.

Daniel Scott

Abstract

The biologically-mediated process of nitrification can occur in chloraminated drinking water distribution systems. In this process, ammonia is oxidized to nitrite by ammonia-oxidizing bacteria (AOB) and archaea (AOA). In complete nitrification, nitrite is further converted to nitrate by nitrite-oxidizers; however, bacterial mediation of this step is less critical as a chemical-oxidation pathway also exists. The initial conversion of ammonia to nitrite is also more critical due to its role in the degradation of the disinfectant residual. Nitrification is affected by factors such as the concentrations of ammonia and total chlorine, the pH of the drinking water, and the temperature. The key consequence of distribution system nitrification is an accelerated decay of the disinfectant residual; it can also lead to increases in nitrite and nitrate, and a potential proliferation of heterotrophic bacteria.

The goal of this thesis is to enhance understanding of distribution system nitrification; one aspect to this goal is the evaluation of models for nitrification. The approach followed in this study was to collect water samples from two full-scale distribution systems in Southern Ontario. In the first phase, a sampling campaign was conducted at sites in these systems, with water samples being analyzed for parameters considered relevant to nitrification, such as the concentrations of nitrogen species affected by nitrification, the disinfectant residual, and the levels of ammonia-oxidizing microorganisms. In the second phase, batch tests were conducted with water from these same distribution systems.

In the course of the field sampling campaign some indications of nitrification were detected, but there were no severe nitrification episodes as indicated by major losses of the disinfectant or prolonged elevations in nitrite levels. On some occasions at some sites there were small rises in nitrite above baseline levels; moderate declines in total chlorine residual were also seen. Nitrifying microorganisms were present in most samples, as detected by both culture-based and molecular methods (PCR). The latter was able to distinguish AOA from AOB; both were detected in the systems included in this study, with AOB gene counts outnumbering those of AOA at most sites. Using Spearman non-parametric correlations, significant correlations were found between some parameters relevant to nitrification. Notably, AOB were found to be positively correlated with heterotrophic plate counts (HPC), reinforcing the latter's role as a useful indicator of microbial regrowth conditions in a distri-

bution system. Also of interest is the negative correlation between total chlorine residual and levels of microorganisms, reminding drinking water professionals of the value of maintaining a stable disinfectant residual.

Batch testing investigations compared total chlorine decay curves between inhibited and uninhibited samples to provide insight into the microbial contribution to disinfectant decay. Four types of decay curves were identified, with qualitative differences in the microbial contribution to the disinfectant residual decay. Liquid chromatography with organic carbon detection (LC-OCD) was applied to investigate changes in the character of the dissolved organic carbon over the course of the batch tests. Based on the results of this study, it is recommended to evaluate the results of nitrification batch tests based on a visual identification of the curve type and calculation of the decay rates and critical threshold residual (CTR), rather than relying on the microbial decay factor alone to express the results.

An application of this work was in making comparisons to some models for nitrification proposed in the literature. The ultimate goal of these models is to provide drinking water system operators with a prediction of when nitrification episodes will occur so that action may be taken to avert them. The models considered in this study differ in their degree of complexity and in whether they are based on mechanistic considerations. The differences in the underlying principles and data required for analysis make these models suitable for different applications. The results of this evaluation support the use of the model of Fleming *et al.* (2005) in full-scale distribution systems and the use of the model by Yang *et al.* (2008) for research applications, while the other models considered can still offer some useful insights.

The results of this research can be applied to monitoring and operational practices in chloraminated distribution systems where nitrification is a potential concern. The correlations between parameters that have significance to distribution system nitrification that were found in this study, along with the modelling and batch testing evaluated in this work, can provide insight into predicting conditions favourable to nitrification and avoiding or averting nitrification episodes.

Keywords: Ammonia-Oxidizing Archaea (AOA), Ammonia-Oxidizing Bacteria (AOB), Chloramine, Disinfectant Residual, Drinking Water Distribution System, Microbial Decay Factor, Model, Nitrification

Acknowledgements

It has been a long journey to get to the end of this thesis and degree program, and I did not get here on my own. There are many people and organizations I need to thank for their help along the way and their contributions to this research.

First of all, I'd like to acknowledge my supervisors, Dr. Peter M. Huck and Dr. Bill Anderson. Dr. Huck's vision and leadership for the NSERC Chair in Water Treatment at the University of Waterloo have created the environment that makes research such as that found in this thesis possible. His personal encouragement is also appreciated. Dr. Anderson's supervision was irreplaceable—from his frequent contributions to my research direction, to his careful editing of manuscripts and presentations, to his help in navigating university and departmental administrative paperwork, I relied on him immensely. I'd also like to acknowledge Dana Herriman for her hard work that keeps the Chair group running smoothly and for making arrangements for our Information Days and conference attendance.

I owe a ton to Dr. Michele Van Dyke, who was my supervisor in all but name. She performed the enumeration of AOA and AOB and provided much-needed guidance for all of the microbiological aspects to this research. She also proofread my manuscripts and presentations and gave input on all of the areas of my research in regular meetings we had.

Shoeleh Shams was also an enormous help in the lab, processing many of my HPC and Ion Chromatography samples. These samples could not have been processed in a timely fashion without her. For helping me find the equipment I needed for sampling, for teaching me to use the ones I was unfamiliar with, and for trouble-shooting and maintaining it when necessary, Mark Sobon deserves credit. Zhipei Qin conducted the LC-OCD analyses, and Dr. Sigrid Peldszus provided guidance on the DOC and LC-OCD methods and interpretation of results.

My experience doing my Master's degree would not have been the same without my fellow Chair group students during my time here: Avid Banihashemi, Fei Chen, Jamie Croft, Ahmed El-Hadidy, Walid El Henawy, Cynthia Hallé, Mohamed Hamouda, Xiaohui Jin, Leila Munla, Feisal Rahman, Shoeleh Shams, and David Shen. It was fun sharing an office, taking classes, and attending conferences with some of you. Thanks to those of you

who welcomed me when I joined the group and taught me some of the lab methods I needed to use. I really appreciate your cooperation in the lab, sharing TOC or dishwasher runs when needed. I learned a lot from you guys; wherever I go after this, I'll be taking a lot of cutting-edge ideas with me.

The Natural Sciences & Engineering Research Council of Canada (NSERC) has contributed funding to this research. They financially supported my studies through a Canada Graduate Scholarship. The NSERC Chair in Water Treatment at the University of Waterloo is funded by a partnership between NSERC and industrial/municipal partners. A current list of Chair group partners may be found online at <http://www.civil.uwaterloo.ca/watertreatment/pandp/partners.asp>.

This project would not have been possible without the partnership of utilities that allowed me to collect samples from their distribution systems: the Region of Waterloo and Toronto Water. Employees at these utilities (Robert Kozlowski and Alex Lee) were a great assistance to me by providing access to sampling locations and conducting some of the on-site water analyses—and they were a pleasure to work with. David Scott was also very helpful by providing data that I needed and answering some questions I had.

On a personal level, I'd like to thank my housemates—JY Zhang, Brian Woo, Nathan Buchanan, Jason Sau, Isaac Kim, Tristan Kim—for their support and encouragement. When I came to Waterloo they were strangers, but now I count them as good friends.

My family has always been there for me with love, support, and encouragement. I couldn't have accomplished this without them.

Finally, I'd like to end these acknowledgements with a short prayer of thanks to God:

Glory be to the Father, and to the Son, and to the Holy Spirit;
As it was in the beginning, is now, and ever shall be, world without end.

Mention of trade names or commercial products does not constitute endorsement or recommendation for their use by the author, the University of Waterloo, or NSERC.

*To my Dad & Mom,
without whom I wouldn't be here.*

Table of Contents

Author's Declaration	iii
Abstract	v
Acknowledgements	vii
Dedication	ix
List of Tables	xv
List of Figures	xvii
List of Acronyms	xxi
1 Introduction	1
1.1 Problem Statement	1
1.2 Objectives	2
1.3 Approach	2
1.4 Thesis Organization	3
2 Background	5
2.1 Introduction	5
2.2 Impacts and Predictors of Nitrification	7
2.3 Nitrifying Microorganisms	11
2.4 Factors Affecting Nitrification	14

2.5	Controlling Distribution System Nitrification	19
2.6	Modelling Nitrification	20
2.7	Conclusion	22
3	Description of Systems	23
4	Full-Scale Study of Nitrification Factors	31
4.1	Introduction	31
4.2	Methodology	35
	Sampling Procedure	35
	Physico-Chemical Analyses	36
	Microbiological Analyses	37
	Statistical Analysis of Results	37
4.3	Results and Discussion	38
	Distribution System Water Quality	38
	Physico-Chemical Indicators of Nitrification	47
	Occurrence of Nitrifying Microorganisms and Heterotrophs	54
	Statistical Interpretation of Sampling Results	62
4.4	Conclusions and Recommendations	67
5	Application and Evaluation of a Nitrification Batch Test	69
5.1	Introduction	69
5.2	Methodology	71
	Method Summary	71
	Sample Collection	72
	Batch Test Procedure	73
	Analysis of Results	74
5.3	Results and Discussion	77
	Batch Testing Results	77
	Interpretation of Batch Test Results	87
	Evaluation of Batch Test Method	92
5.4	Conclusions and Recommendations	99

6	Evaluation of Models for Nitrification	101
6.1	Introduction	101
6.2	Evaluation and Application of Nitrification Models	107
	Pilot-scale Kinetic Model	109
	Plug-flow Kinetic Model	113
	Nitrification Potential Curves	116
	Nitrification Index	120
	Logistic Risk Model	123
	Carbon-to-Nitrogen Ratio	126
	Alternatives to Modelling	133
6.3	Conclusions and Recommendations	135
7	Conclusions and Recommendations	139
7.1	Major Findings	139
7.2	Recommendations	142
	References	145
	Appendices	152
A	Raw Sampling Data	153
	Nitrification Batch Tests	162
B	Nitrifier Enumeration Methods	169
B.1	Quantitative PCR of AOB and AOA	169
B.2	Culture-based Detection of Nitrifiers	170
C	Supplemental Information	171
D	Calibration of Instruments and Methods	175
E	Sample Model Calculations	181

List of Tables

2.1	Inactivation Rates and Half-Saturation Concentrations	16
3.1	Summary of Systems Studied	24
3.2	Sampling Dates	29
4.1	Nitrifier Growth Test	57
4.2	Spearman Correlations	64
5.1	Coefficients Calculated for Batch Testing Results	78
5.2	Summary of Batch Testing Results	81
6.1	Models for Nitrification	106
6.2	Additional Model Information	108
6.3	Strengths and Weaknesses of Nitrification Models	136
A.1	Physico-Chemical Results from Field Sampling (1)	153
A.2	Physico-Chemical Results from Field Sampling (2)	156
A.3	Microbiological Results from Field Sampling	159

List of Figures

2.1	Flow-chart of Nitrification Processes	6
2.2	Simulation of Nitrification Showing Ammonia Peak	10
3.1	Map of Toronto Sites	27
3.2	Map of Region of Waterloo Sites	28
4.1	Total Chlorine Residuals by Site	40
4.2	pH Levels by Site	42
4.3	CSMR Levels by Site	43
4.4	DOC Levels by Site	44
4.5	Ammonia Levels by Site	46
4.6	Nitrite Levels by Site	48
4.7	Ammonia, Nitrite, and Nitrate at Toronto Sites	50
4.8	Ammonia, Nitrite, and Nitrate at Waterloo Sites	51
4.9	Total Chlorine Residuals at Toronto Sites	52
4.10	Total Chlorine Residuals at Waterloo Sites	53
4.11	AOA and AOB at Toronto Sites	55
4.12	AOA and AOB at Waterloo Sites	56
4.13	AOA:AOB Ratios in Toronto	59
4.14	AOA:AOB Ratios in Waterloo	60
4.15	HPC by Site	61
4.16	Correlations Between AOB and HPC	63
5.1	Layout of Vials for Batch Testing	73

5.2	Illustration of Batch Test Variables	76
5.3	Batch Testing Curve on a Semi-Log Plot	80
5.4	Type I Batch Test	82
5.5	Type II Batch Test	83
5.6	Type III Batch Test	84
5.7	Type IV Batch Test	85
5.8	Check on Second-Order Processes in Batch Tests	90
5.9	A Critique of Using a Single F_m Number	91
5.10	LC-OCD Chromatographs	95
5.11	LC-OND Chromatographs	96
6.1	Simulation Results for Model of Yang <i>et al.</i> (2008)	112
6.2	Fleming Model Illustrated from Waterloo Results	118
6.3	Heterotrophs and Nitrifiers at Waterloo Sites	128
6.4	Carbon-to-Nitrogen Model (Toronto)	130
6.5	Carbon-to-Nitrogen Model (Waterloo)	131
A.1	RCL Batch Test (Preliminary Round)	162
A.2	801 Batch Test (Preliminary Round)	163
A.3	904 Batch Test (Preliminary Round)	163
A.4	RCL Batch Test (Main Round)	164
A.5	801 Batch Test (Main Round)	164
A.6	904 Batch Test (Main Round)	165
A.7	K20S14 Batch Test (Main Round)	165
A.8	WOD61 Batch Test (Main Round)	166
A.9	K20S14+C Batch Test (Follow-Up Round)	166
A.10	K20S14+A Batch Test (Follow-Up Round)	167
A.11	WOD06 Batch Test (Follow-Up Round)	167
A.12	WOD06+C Batch Test (Follow-Up Round)	168
A.13	WOD06+A Batch Test (Follow-Up Round)	168

C.1	Raw Water Agarose Gel	171
C.2	Histograms for Distribution System Parameters	172
C.3	Q-Q Plots for Distribution System Parameters	173
D.1	DOC Calibration Curve	176
D.2	Monochloramine Calibration Factor	176
D.3	IC Calibration Curve (1)	177
D.4	IC Calibration Curve (2)	178
D.5	IC Calibration Curve (3)	179

List of Acronyms

AOA	Ammonia-Oxidizing Archaea
AOB	Ammonia-Oxidizing Bacteria
AOC	Assimilable Organic Carbon
CMFTR	Completely-Mixed Flow Through Reactor
COD	Chemical Oxygen Demand
CSMR	Chloride-to-Sulfate Mass Ratio
CTR	Critical Threshold Residual
DBP	Disinfection By-Products
DO	Dissolved Oxygen
DOC	Dissolved Organic Carbon
GAC	Granular Activated Carbon
HPC	Heterotrophic Plate Count
HRT	Hydraulic Retention Time
LC-OCD	Liquid Chromatography with Organic Carbon Detection
LC-OND	Liquid Chromatography with Organic Nitrogen Detection
LMW	Low Molecular Weight
MPN	Most Probable Number
N.I.	Nitrification Index
NOB	Nitrite-Oxidizing Bacteria
NOM	Natural Organic Matter
PCR / qPCR	(quantitative) Polymerase Chain Reaction
SMP	Soluble Microbial Products
THM	Trihalomethanes
TOC	Total Organic Carbon
TSS	Total Suspended Solids
WTP	Water Treatment Plant

Chapter 1

Introduction

1.1 Problem Statement

Nitrification is a biologically-mediated reaction whereby ammonia is converted to nitrite and then nitrate. In chloraminated drinking water distribution systems, nitrification is possible due to the presence of ammonia, added at water treatment plants to create a monochloramine disinfectant residual. Nitrification promotes the decay of the chloramine residual by consuming ammonia, thereby reducing the stability of monochloramine, and by producing nitrite, which reacts with monochloramine in its chemical oxidation to nitrate. In drinking water distribution systems, the first stage of nitrification, the initial conversion of ammonia to nitrite, is the most critical as it results in the degradation of the disinfectant residual. This step is performed by ammonia-oxidizing bacteria (AOB) and archaea (AOA).

The most prominent consequence of distribution system nitrification is the accelerated decay of the chloramine residual, which can make regulatory compliance more difficult and potentially decrease the robustness of the distribution system as the final barrier for safe drinking water before it is delivered to consumers. Other possible consequences of nitrification include promoting pipe corrosion and possibly contributing to the regrowth of heterotrophic bacteria (autotrophic ammonia-oxidizing microorganisms have the capability to fix inorganic carbon).

Several questions about distribution system nitrification remain unanswered. From the perspective of drinking water distribution system operators, further understanding is needed about the precise conditions that can lead to nitrification episodes. Being able to predict the development of these episodes earlier would allow action to be taken to avert them. Other questions relate to nitrifying microorganisms, such as the relative importance of AOB and AOA in distribution system nitrification, and whether nitrifiers and heterotrophs have a competitive or synergistic relationship.

1.2 Objectives

The objectives of this research were to:

1. Monitor indicators of nitrification in two full-scale drinking water distribution systems.
2. Evaluate the specific systems participating in this research with respect to nitrification potential.
3. Enhance understanding of the factors contributing to and affected by nitrification.
4. Use the data collected to evaluate proposed models for nitrification.

1.3 Approach

The work described in this thesis is composed of two experimental phases. The first phase was a nine month period of sampling and analysis from two full-scale distribution systems in Southern Ontario. The data collected from these experiments was compared to models that have been proposed for nitrification; the data was also analyzed statistically, looking for important correlations. The second phase involved carrying out small-scale laboratory batch testing for nitrification using water samples from these same distribution systems.

In the sampling campaign, water samples were collected regularly from sites in the two distribution systems involved in this study. These samples were analyzed for a number of water quality parameters thought to be relevant to nitrification. These parameters included pH, temperature, total chlorine, ammonia, nitrite, nitrate, dissolved organic carbon (DOC), heterotrophic plate counts (HPC), and nitrifying microorganisms.

The batch testing performed for this research was based on the method of Sathasivan *et al.* (2005). Untreated and microbially inhibited samples were tested in parallel. Comparing the total chlorine decay curves between the two cases reveals the microbial contribution to the decay of the total chlorine residual. An effort was made to evaluate the method and offer suggestions for interpreting the results.

Data analysis involved graphical analysis of the results, statistical tests such as non-parametric correlations (Spearman), and comparisons to models for nitrification found in the literature.

1.4 Thesis Organization

This thesis comprises seven chapters followed by an appendix section. The three chapters discussing the results of this research (4–6) are formatted as individual papers. They are intended for potential submission to peer-reviewed journals.

This introduction makes up the first chapter. Chapter 2 provides a review of literature related to nitrification in chloraminated drinking water distribution systems. It addresses the occurrence and consequences of distribution system nitrification, its kinetics, pathways, factors, and indicators, the microorganisms responsible, and some models for nitrification that have been developed.

Chapter 3 describes the two full-scale distribution systems that participated in this study. Information is given on the water quality at the entrance to each distribution system, and the sites that were sampled are described.

Chapter 4 presents the results from the full-scale distribution system sampling campaign. It focuses on physico-chemical factors and indicators of nitrification, the occurrence of nitrifying microorganisms, and statistical analyses of these parameters.

As a second phase to this research, bench-scale batch tests were conducted using water from some of the same sites sampled earlier. The purpose of these batch tests was to assess the respective contributions of microbial and chemical factors to the decay rate of the monochloramine residual, along with evaluating the usefulness of this method as an indication of the nitrification potential in distribution system samples. These results are presented in Chapter 5.

Chapter 6 compares the experimental results to some proposed models for distribution system nitrification. Particular attention is paid to the models of Fleming *et al.* (2005), and Yang *et al.* (2008), along with the critical carbon-to-nitrogen (C/N) ratios proposed by Verhagen and Laanbroek (1991) and Zhang *et al.* (2009b).

Finally, Chapter 7 integrates the different aspects of this research. Conclusions and recommendations are summarized.

Chapter 2

Background

2.1 Introduction

Nitrification occurs in a wide range of environments; chloraminated drinking water distribution systems are one of these environments due to the presence of ammonia, which is added to the water to react with free chlorine and form a monochloramine disinfectant residual. In contrast with other disinfectant residual options used in distribution systems, chloramination adds a substrate for microorganisms, in addition to a disinfectant (Zhang *et al.*, 2009b). Many utilities in North America have adopted chloramines because they form lower amounts of disinfection by-products (DBPs), are better at penetrating and disinfecting biofilms (LeChevallier *et al.*, 1990), and in many situations are more persistent than free chlorine in distribution systems (Zhang and Edwards, 2009). Therefore, it is important for the drinking water industry to understand the process, risk factors, and consequences of nitrification in chloraminated drinking water distribution systems.

In chloraminated drinking water distribution systems, the first step of nitrification, the conversion of ammonia to nitrite by ammonia-oxidizing microorganisms, is usually considered to be more critical than the subsequent conversion of nitrite to nitrate. Ammonia can be oxidized by autotrophic microorganisms from the domains *Bacteria* (Ammonia-Oxidizing Bacteria, AOB) and *Archaea* (Ammonia-Oxidizing Archaea, AOA). The nitrite produced by AOB and AOA provides a substrate for Nitrite-Oxidizing Bacteria (NOB), which can convert nitrite to nitrate; nitrite can also be chemically oxidized by chloramine (Vikesland *et al.*, 2001; Yang *et al.*, 2008). Some free ammonia will typically be available to AOB and AOA in water leaving the treatment plant, based on the relative dosing of chlorine and ammonia, and more will become available as the monochloramine residual undergoes decay. The mechanisms of monochloramine decay include autodecomposition (Vikesland *et al.*, 2001), reaction with nitrite, and reactions with organic matter, including the cells of microorganisms and

their metabolic products (Yang *et al.*, 2008). It is important to realize that nitrification in chloraminated drinking water distribution systems has a self-reinforcing feedback loop since its products (nitrite, and increased organic matter from nitrifier growth) promote chloramine decay, which provides more ammonia, the substrate for nitrification (Oldenburg *et al.*, 2002). Some authors have raised the possibility of nitrate being “recycled” to ammonia via reactions with corrosion products (Zhang *et al.*, 2008, 2009b). In such situations, more ammonia would be made available for nitrification. Figure 2.1 illustrates the key processes in distribution system nitrification. Some free ammonia is present at equilibrium in chloraminated distribution systems and more becomes available as monochloramine decays via autodecomposition or reaction with organic matter, nitrite, or other drinking water constituents. This ammonia is available to be converted to nitrite by AOB or AOA. Nitrite is then further oxidized to nitrate by NOB or by reaction with chloramine (accelerating the disinfectant residual decay rate).

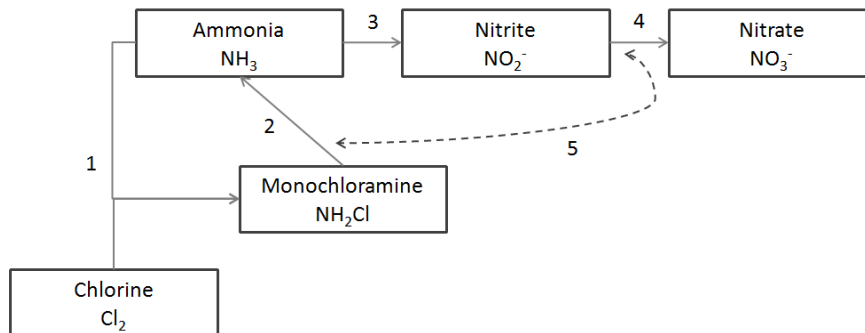


Figure 2.1: A simplified view of the key chemical and biologically-mediated processes in distribution system nitrification: 1, Formation of monochloramine; 2, Decomposition of monochloramine, liberating free ammonia; 3, Ammonia oxidation, carried out by AOB and AOA; 4, Nitrite oxidation, carried out by NOB and via reaction with disinfectant residual; 5, Reaction between monochloramine and nitrite (Snoeyink and Jenkins, 1980; Vikesland *et al.*, 2001; Yang *et al.*, 2008).

Nitrification is a widespread issue in chloraminated drinking water distribution systems. In a landmark survey fifteen years ago, Wilczak *et al.* (1996) found that two thirds of U.S. utilities that applied chloramination had observed some degree of nitrification. Cunniffe (1991) reported similar findings, with 64% of samples from a number of chloraminated drinking water distribution systems in Australia testing positive for nitrifying bacteria. This widespread presence of nitrifiers was consistent with the long inactivation times for nitrifying bacteria at typical monochloramine doses, determined in the same study. Oldenburg *et al.* (2002) also noted that the long inactivation times they found for a species of AOB could explain the persistence of nitrifiers in distribution systems. Even in cooler climates, the po-

tential for nitrification episodes arising from the presence of nitrifying microorganisms can be widespread. Lipponen *et al.* (2002) surveyed AOB and NOB in drinking water distribution systems in Finland and found that nitrifying bacteria were common in chloraminated distribution systems (the mean water temperature was 12°C in their study).

The remainder of this chapter includes detailed discussions about the key impacts of nitrification, the ammonia-oxidizing microorganisms responsible, and some of the factors affecting nitrification. The topic of modelling nitrification will be introduced. These topics will be revisited later in this thesis for the discussion of related results.

2.2 Impacts and Predictors of Nitrification

Fundamentally, nitrification results in the conversion of ammonia to nitrite and nitrate. Inorganic carbon and dissolved oxygen are consumed in the process, and nitrifying microorganisms multiply. In chloraminated drinking water systems, nitrification will result in a decline of the disinfectant residual and will often lead to elevated heterotrophic plate counts (HPCs). In some situations, nitrification may impact corrosion in the distribution system. The consequences of nitrification are not likely to be a direct risk to public health; rather, they may lead to operational or regulatory-compliance challenges. The impacts of nitrification are described in greater detail in this section, and can serve as useful operational indicators that nitrification is occurring.

One of the primary consequences of nitrification is an accelerated rate of monochloramine loss. The responsible mechanisms include the consumption of ammonia which can shift the equilibrium stability of monochloramine, the production of nitrite which reacts with the disinfectant residual, and an increase in microorganisms and organic matter which exerts a chloramine demand (Vikesland *et al.*, 2001; Yang *et al.*, 2008). A decline in the disinfectant residual may be an early indication of nitrification. According to Pintar *et al.* (2005) a partial loss of the total chlorine residual preceded a rise in nitrite levels in a full-scale distribution system. They concluded that a falling total chlorine residual can be an early warning of a developing nitrification episode. Sathasivan *et al.* (2005) developed a batch test methodology to distinguish the chemical and microbial contributions to chloramine decay. An increase in the microbially-mediated chloramine decay rate is associated with nitrification.

From the perspective of regulatory compliance, a loss of the disinfectant residual is expected to be the most critical consequence of distribution system nitrification. Maintaining an adequate disinfectant residual throughout the distribution system is a key element of the Multi-Barrier Approach paradigm applied in Canada to protect drinking water quality from its source to consumers' taps (Health Canada, 2002).

By decreasing the chloramine residual, nitrification can make the distribution system environment more conducive to microbial growth. It can also promote the proliferation of heterotrophic bacteria by contributing to the organic carbon available (Rittmann and Snoeyink, 1984). Rittmann *et al.* (1994) confirmed nitrifiers could produce SMP (soluble microbial products) that could serve as a substrate for heterotrophic microorganisms. For one species of AOB (*Nitrosomonas europaea*), the measured yield was 0.021–0.027 mg COD/mg NH_4^+ -N. In environments which are carbon-limited, this contribution of SMP could promote heterotrophic growth.

Heterotrophic plate count (HPC) bacteria are not a direct health concern, but they are recommended for use as a water quality indicator in Canada. Drinking water system operators are advised to investigate the cause of a rise in HPCs, especially when it is rapid or unexpected (Health Canada, 2011). Similarly, the Committee on Public Water Supply Distribution Systems of the US National Research Council recommended monitoring HPCs as a non-specific indicator of microbiological water quality (National Research Council, 2006). In drinking water distribution systems, HPCs have been observed to rise during nitrification episodes (Skadsen, 1993). Wilczak *et al.* (1996) also reported that high HPCs may accompany nitrification in their survey of U.S. utilities. Odell *et al.* (1996) listed HPCs as one of the indicators of nitrification. Zhang *et al.* (2009b) also recommended HPCs as a nitrification indicator, but cautioned that other factors can lead to high HPCs beside nitrification, so it cannot be used in isolation. On the other hand, Pintar *et al.* (2005) did not see a correlation between HPCs and the onset of nitrification.

A change in the ammonia concentration resulting from a nitrification episode can be difficult to interpret. It appears that free ammonia (NH_3) concentrations initially increase during many nitrification episodes, and then drop off as nitrification takes its course. Many researchers have shown this effect in their results, but few (e.g. Liu *et al.* 2005) have explicitly discussed it. This trend of an initial rise in free ammonia followed by a decline in its concentration as a nitrification episode progresses is supported by chloramine chemistry. The decay of monochloramine releases ammonia, thus the ammonia concentration will increase if the rate at which free ammonia becomes available is greater than its consumption by ammonia-oxidizing microorganisms. Liu *et al.* (2005) observed that ammonia levels initially increased due to chloramine decay, and then decreased as the nitrification rate increased in pilot-scale experiments. This trend also appeared in the results of Yang *et al.* (2008) and Yang *et al.* (2007). A simulation using the model of Yang *et al.* (2008) clearly shows the ammonia trend described here (Figure 2.2). This model applies mass-balance differential equations to chemical and microbiological constituents associated with nitrification. It is described in detail in Chapter 6.

Because the free ammonia concentration either increases or decreases depending on when it is measured during a nitrification event, the impact of nitrification on the ammonia con-

centration is unclear in practice. Wilczak *et al.* (1996) reported that ammonia was not a sensitive nitrification indicator. Since measurements taken at various stages of nitrification can show an increase, decrease, or no change in the ammonia concentration, it is not surprising that using ammonia as an indicator of nitrification would be difficult in practice. The existence of a temporal peak in free ammonia could also explain why some authors (Odell *et al.*, 1996; Yang *et al.*, 2007) did not determine that the ammonia concentration was a significant factor affecting nitrification (in addition to the hypothesis given above that it was present in excess of limiting quantities). Researchers attempting to delineate ammonia concentrations that promote or result from nitrification should take care to measure it at the appropriate point in the curve (before, at, or following the ammonia peak, depending on the purpose of the measurements) described here.

An intrinsic consequence of nitrification is a rise in nitrite and nitrate levels. For this reason, nitrite and nitrate are probably the most frequently recommended indicators of nitrification. Nitrite is an especially good indicator of nitrification because it is normally below detection levels in water entering a distribution system. Nitrate concentrations have more background variability from source water variations. Wilczak *et al.* (1996) strongly recommended that drinking water utilities develop an accurate nitrogen balance for their distribution systems as part of nitrification monitoring. However, Pintar *et al.* (2005) tested a nitrite-nitrogen threshold of 0.05 mg-N/L as an indicator of nitrification and found that it lagged a drop in the total chlorine residual. A rise in nitrite could confirm a nitrification episode in progress, but could not serve as an early warning.

Although nitrification will produce elevated nitrite and nitrate levels, it is not likely to lead to a regulatory violation for these parameters (Zhang *et al.*, 2009b). For example, with 1.5 mg-Cl₂/L of monochloramine (0.30 mg-N/L) and 0.30 mg-N/L of ammonia at the entrance to a distribution system, the maximum amount of nitrite that could be formed is 0.60 mg-N/L, which is less than the regulatory limit of 3.2 mg/L NO₂⁻ (≈ 1 mg-N/L) (Health Canada, 2010). However, higher levels of nitrite may be possible in a situation where nitrate is recycled to ammonia through corrosion-coupled reactions as discussed by Zhang *et al.* (2009b).

Some studies have investigated the impact that nitrification can have on corrosion in distribution systems as well as in household plumbing. Zhang *et al.* (2009a) confirmed that nitrification can reduce pH in low-alkalinity waters, which can lead to a greater release of lead to solution. High alkalinity can provide buffering that limits a pH drop even in the presence of nitrification. The authors concluded that a drop in pH from nitrification could increase lead solubility, but it is not likely to be a serious problem at the initial pH and alkalinity levels of most utilities. In another study, Zhang *et al.* (2010a) found that nitrification led to decreased pH and DO, which reduced release of zinc from galvanized iron (attributed to lower DO) and had little significant impact on corrosion of other materials they tested

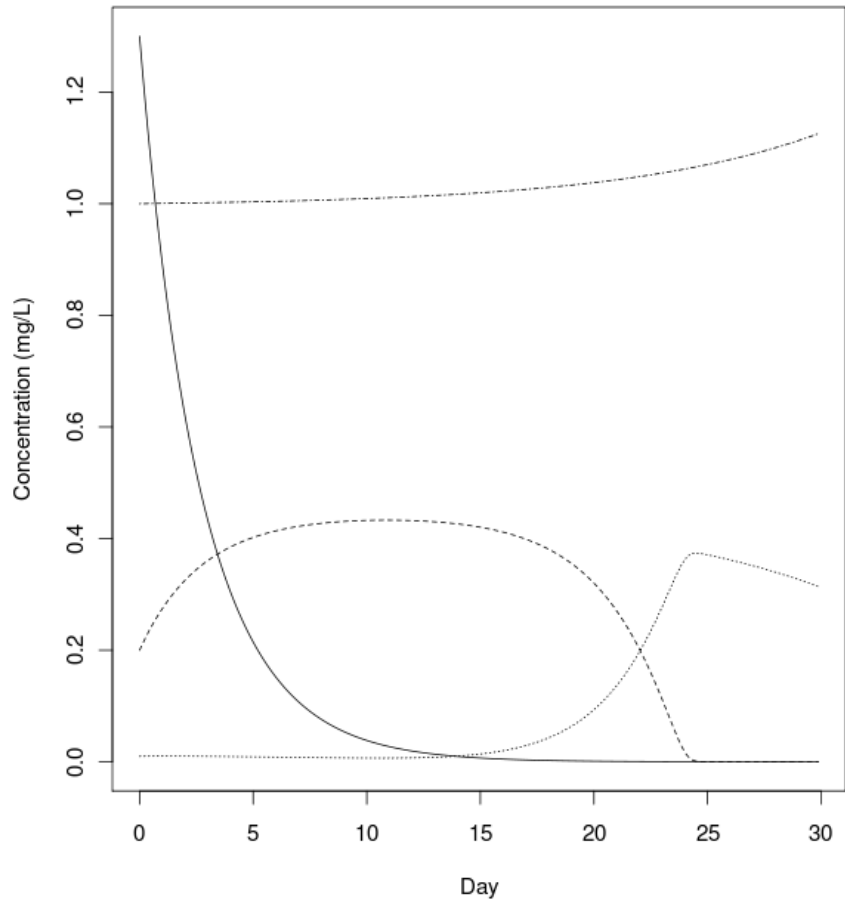


Figure 2.2: A nitrification scenario generated using the model of Yang *et al.* (2008) showing a wide peak in ammonia (dashed line, - - -) following a decline in the total chlorine residual (solid, ___) and preceding a rise in nitrite (dotted, ...). Nitrate is shown alternately dashed and dotted (- . -).

(cast iron, lead, copper, galvanized iron, stainless steel, and concrete). These recent studies suggest that corrosion will typically not be a critical consequence of nitrification.

Odell *et al.* (1996) suggested DO as a good indicator of nitrification; AWWA (2006) listed it as an indicator of limited usefulness. Odell *et al.* (1996) did not recommend pH and alkalinity as good indicators of nitrification. For most drinking water system operators, the most critical consequences of nitrification will be the difficulty in maintaining a chloramine disinfectant residual and the resulting potential increase in heterotrophic bacteria.

2.3 Nitrifying Microorganisms

As mentioned in the introduction, ammonia oxidation is carried out by two types of microorganisms: ammonia-oxidizing bacteria (AOB) and ammonia-oxidizing archaea (AOA). Nitrite-oxidizing bacteria (NOB) have also been found in distribution systems (Regan *et al.*, 2003; Lipponen *et al.*, 2002), but they are not a focus of this research as the first step of nitrification (the conversion of ammonia to nitrite) is considered more critical for distribution system operation, since it causes a decline in the disinfectant residual concentration. In fact, the presence of NOB has the potential to reduce problems associated with distribution system nitrification by consuming nitrite that would otherwise react with chloramine (Regan *et al.*, 2002).

Ammonia-oxidizing bacteria have been widely studied. They are slow-growing, autotrophic (i.e. they fix inorganic carbon to support their growth), aerobic bacteria that inhabit a wide range of terrestrial and aquatic environments. Nitrifiers have slow growth rates due to the high energy cost of fixing inorganic carbon (Rittmann and Snoeyink, 1984). Low levels of dissolved oxygen (DO) could limit nitrification because biological oxidation of ammonia is an aerobic process. The activity of nitrifying bacteria produces H^+ , which can acidify poorly-buffered waters. Ammonia can take both an ionized (NH_4^+ , ammonium) and non-ionized (NH_3) form in water, with the distribution depending on pH; Claros *et al.* (2010) showed that the non-ionized form is the substrate for AOB. Also of relevance in chloraminated drinking water distribution systems, AOB may have some degree of chloramine resistance. This is supported by their persistence in distribution systems, even when the disinfectant residual is high, and by laboratory inactivation experiments that showed long inactivation times (Cunliffe, 1991; Oldenburg *et al.*, 2002). The species of AOB found in one environment may have different properties to those found in drinking water systems. There can even be a difference in which species are dominant between bench-scale and pilot-scale experiments, as Claros *et al.* (2010) observed.

Evidence for the existence of ammonia-oxidizing archaea (AOA) has only appeared within the past ten years. AOA are difficult to culture and only a few strains of AOA have been isolated to date. For example, Könneke *et al.* (2005) successfully cultured an oceanic species of AOA. They were able to show that it converted ammonia to nitrite while fixing inorganic carbon. It was aerobic and its generation time was at least 21 h. Hallam *et al.* (2006) analyzed the genome of another marine AOA. They found genes that were homologous to bacterial genes for oxidizing ammonia (i.e. ammonia monooxygenase). Therefore the existence of AOA has been confirmed by genetic and metabolic evidence.

A topic of particular interest is the way in which AOA differ from AOB. Martens-Habbena *et al.* (2009) found a very low half-saturation coefficient (K_s) for ammonia for a strain of AOA. This high affinity for ammonia suggests it could successfully compete with heterotrophs

for nitrogen and that it could thrive in low-substrate environments. It is not clear whether other species of AOA would share this property. A study performed by Kasuga *et al.* (2010b) raised the possibility that *Archaea* may be more susceptible than *Bacteria* to chlorination.

AOB and, recently, AOA have been previously studied in drinking water distribution systems. van der Wielen *et al.* (2009) conducted one of the only studies to date that has investigated AOB and AOA together in three drinking water distribution systems. This study was conducted in the Netherlands and the distribution systems investigated did not contain a disinfectant residual. In one of these distribution systems only AOA was detected; they increased in numbers toward the distant areas of the distribution system. Ammonia was below the detection limit in the source water for the WTP feeding this distribution system. In the other two distribution systems, AOB outnumbered AOA at most sites, but AOA were still detected. These two systems did not have significant trends in nitrifier numbers with increasing distance from the WTP. AOA had greater diversity than AOB in the samples taken for their study.

Earlier studies on nitrifying microorganisms in drinking water distribution systems were limited to AOB. Factors associated with the presence or abundance of nitrifying bacteria have been identified. Lipponen *et al.* (2004) did a study on the development of biofilms containing nitrifiers on PVC pipes that received water from full-scale drinking water distribution systems. Nitrifiers were found to be more numerous further from the WTP. There was a positive correlation between nitrifiers and heterotrophs. Both heterotrophic and nitrifying microorganisms were positively correlated with turbidity and retention time and negatively correlated with pH and total chlorine. In earlier work, Lipponen *et al.* (2002) surveyed AOB and NOB in water and sediment samples from drinking water distribution systems in Finland. They found a positive correlation between HPC and AOB in both water and sediments. Piping material and the use of GAC filtration were not found to significantly affect the number of nitrifiers, and dissolved oxygen (DO) was not a limiting factor in any of the systems they studied. Cunliffe (1991) investigated the abundance of nitrifying bacteria in chloraminated distribution systems in Australia. Using stepwise multiple logistic regression and Spearman correlations, they found that total chlorine and nitrite plus nitrate were statistically significant indicators for the presence of nitrifying bacteria; temperature and standard plate counts were not statistically significant indicators of nitrifiers.

Other studies have investigated the specific species of nitrifiers that are present in distribution systems. Regan *et al.* (2002) surveyed species of AOB and NOB in a pilot-scale distribution system. This study targeted the 16S rRNA gene. The most abundant AOB species were related to *Nitrosomonas oligotropha* (a species with a low K_s). Regan *et al.* (2003) also studied the dominant genera of AOB and NOB in full-scale distribution systems. *Nitrosomonas oligotropha*-type AOB were the most abundant ammonia-oxidizing species, as in their previous pilot scale study (Regan *et al.*, 2002). They suggest these types of AOB

might be selected for in distribution systems because of their strong affinity for ammonia. Knowing which nitrifying bacteria are most significant in drinking water distribution systems can direct future laboratory studies on AOB growth and inactivation to focus on the relevant species.

The traditional technique for enumerating nitrifying bacteria is the culture-based most-probable number (MPN) method (APHA *et al.*, 2005). However, Hoefel *et al.* (2005) compared culturing methods with a number of culture-independent techniques to study AOB and found that culture-based techniques for detecting AOB are limited because these bacteria are very slow-growing, making growth-dependent analyses too time-consuming. They also provide evidence that MPN underestimates total AOB numbers. In addition, not all species of AOB were detected by MPN due to the selectivity of the media used.

Molecular techniques, especially quantitative polymerase chain reaction (qPCR), are increasingly being adopted to study nitrifiers. PCR primers have been developed that target the ammonia monooxygenase genes that are specific to either AOB or AOA (Rotthauwe *et al.*, 1997; de la Torre *et al.*, 2008). This allows ammonia-oxidizing microorganisms to be specifically and sensitively enumerated. The function of ammonia monooxygenase is to catalyze the conversion of ammonia to hydroxylamine, an intermediary which is then converted to nitrite (Nicolaisen and Ramsing, 2002). Primers have been developed that target a sub-unit of the ammonia monooxygenase gene called *amoA*. The primers used for bacterial *amoA* only work on species from the β -*Proteobacteria*, to which all but two species of known autotrophic AOB belong (Nicolaisen and Ramsing, 2002).

An area of active research is the relative importance of archaeal and bacterial ammonia oxidizers to nitrification. This may be reflected by their relative numbers in environments where nitrification is occurring. Many researchers are also working to gain a better understanding of factors that cause niche separation between AOA and AOB to discover which conditions favour one or the other. Most of these studies have not been performed in drinking water environments, but some of the insights should be transferable.

Leininger *et al.* (2006) were among the first to investigate the relative numbers of AOA and AOB in soil environments. They found that AOA were always more abundant than AOB. AOA:AOB ratios were greatest in non-fertilized soils and at greater depths. They did not test the relative nitrification activity of AOA and AOB. The main factor that has been suggested to cause niche separation between AOA and AOB is the concentration of their substrate, ammonia (Schleper, 2010). As mentioned earlier, Martens-Habbena *et al.* (2009) found a high affinity for ammonia in a strain of AOA, which suggests they may have a competitive advantage in low ammonia niches. Di *et al.* (2010) found that higher ammonia seemed to favour AOB in soils they studied; the nitrification rate also correlated with AOB abundance. Reed *et al.* (2010) observed that both AOA and AOB were stimulated by the addition of nutrients (sequential addition of organic carbon and then nitrogen) to ground-

water. AOA were more abundant before the nutrient addition, and remained so throughout the experiment, but AOB showed a stronger response to the addition of nitrogen. In their research on the formation of nitrifying biofilms in fresh water flow channels, Herrmann *et al.* (2011) observed positive Spearman correlations (0.92 and 0.96, respectively) for both AOA and AOB *amoA* gene copy numbers with the ammonia concentration in water sources. The ratio of AOB/AOA gene copies was also positively correlated with ammonia ($r_s = 0.87$). That is, AOB seem to have been favoured at higher ammonia levels. Interestingly, AOB became dominant in all biofilms, even when AOA were higher in the source water. Sauder *et al.* (2011) conducted a study on ammonia-oxidizing microbial communities in freshwater aquarium biofilters and found that AOA contributed a higher percentage of *amoA* gene copies when ammonium levels were low while AOB had greater relative abundances when ammonium levels were higher. Other water quality parameters were not correlated significantly with the relative abundances of AOA and AOB in their study.

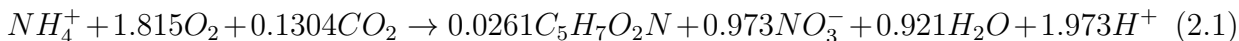
De Vet *et al.* (2009) conducted one of the first studies in a drinking water environment that considered AOA and found that both bacteria and archaea contributed to ammonia oxidation in a full-scale sand filter treating groundwater. The magnitudes of their respective contributions to biofilter nitrification were not determined, however. Kasuga *et al.* (2010a) investigated AOA on pilot-scale biological activated carbon (BAC) filters. AOA gene copies were higher (1–2 orders of magnitude) than those of AOB. The greater numbers of AOA suggested that they may be the dominant ammonia oxidizers. In a further study on full-scale GAC filters, Kasuga *et al.* (2010b) concluded that AOA were responsible for 75–93% of the ammonia removal. van der Wielen *et al.* (2009) looked at AOB and AOA in three drinking water treatment plants using groundwater as a source, and their attached distribution systems. Their study found some distribution system locations where AOA were more numerous, some where AOB were more numerous, and some where the numbers of each type of ammonia oxidizer were similar. Total ammonia oxidizer numbers correlated well with ammonia removal in the treatment trains.

Other factors that have been suggested to explain AOA:AOB ratios or relative activities include pH (Prosser and Nicol, 2008), susceptibility to chlorination or other treatment steps (Kasuga *et al.*, 2010b), and the concentration of organic carbon or metals (van der Wielen *et al.*, 2009).

2.4 Factors Affecting Nitrification

In this section, the current state of knowledge concerning the key factors affecting the occurrence and kinetics of nitrification in the drinking water environment are reviewed. The

following equation (Rittmann and McCarty, 2001) gives the stoichiometry for complete nitrification, including cell synthesis of AOB and NOB.



From the terms in this equation, it can be seen that nitrification requires ammonia, oxygen, and inorganic carbon. The monochloramine disinfectant residual, and the temperature are also known to affect nitrification.

Two of the most prominent factors affecting nitrification are the impacts of the substrate (ammonia) and the disinfectant (monochloramine)—their concentrations in the distribution system, and their associated kinetics (for uptake and inactivation, respectively) with nitrifying microorganisms. Ammonia oxidizers (AOB and AOA) get their energy by converting ammonia to nitrite, however the literature is mixed on whether the risk of nitrification is sensitive to the concentration of ammonia available. Skadsen (1993) identified ammonia overdosing as a possible cause of nitrification episodes in a full-scale chloraminated distribution system. Lipponen *et al.* (2002) found a Spearman correlation of 0.74 between ammonium-nitrogen and AOB in Finnish drinking water distribution system samples. Conversely, Odell *et al.* (1996) found that the ammonia concentration did not seem to have a significant influence on nitrification, but that may simply indicate that ammonia was not limiting in the systems they studied. Similarly, Zhang *et al.* (2010b) found that the chlorine-to-ammonia ratio (which determines the initial ammonia availability) did not have a significant effect on nitrification in an annular reactor experiment.

The effect of a chloramine residual on nitrification is much clearer. Odell *et al.* (1996) reported on a case study in which higher chloramine doses limited AOB regrowth. They found that regrowth occurred in 77% of tests when the residual was 1.7 mg/L, but in only 26% of tests when the residual was 2.5 mg/L. In a two-factor experiment, Pintar and Slawson (2003) determined that maintaining a relatively low disinfectant residual of 0.2–0.6 mg/L of chloramine inhibited AOB more than a low temperature (12°C). Laboratory inactivation tests have been done on the AOB species *Nitrosomonas europaea*, by Oldenburg *et al.* (2002), who fit AOB inactivation to standard Chick-Watson kinetics. Using culture-independent enumeration techniques, Wahman *et al.* (2009) found that a modified Chick-Watson model that includes a lag phase ahead of effective disinfection contact time was a better fit to AOB inactivation trends. To date, no disinfection kinetic studies have been done on any AOA species.

Table 2.1 summarizes inactivation rates and half-saturation coefficients found in previous studies. It is difficult to directly compare studies due to differences in experimental conditions and measurement techniques, but it is notable that the ammonia half-saturation

concentrations vary over more than three orders of magnitude, while the disinfection kinetics of monochloramine are quite consistent (for a single species of AOB). The wide range of half-saturation (K_s) values implies that great care must be taken when using literature values for the growth kinetics of nitrifying microorganisms in a model or calculation. This table also emphasizes that some species of AOA and the AOB species *Nitrosomonas oligotropha*, thought to be selected for in distribution system environments (Regan *et al.*, 2002), have a higher affinity for ammonia than the more thoroughly studied *N. europaea*. There is a research need for studies of the inactivation kinetics of these species, as well as further confirmation and comparisons of their growth kinetics.

Table 2.1: Selected monochloramine disinfection rates and half-saturation concentrations for AOA and AOB, from the literature.

Parameter	Species	Source	Value
Ammonia half-saturation concentration, K_s (mg/L as N)*	mainly <i>Nitrosomonas europaea</i> and <i>N. eutropha</i> (AOB)	Claros <i>et al.</i> (2010)	6.705
	<i>N. europaea</i>	Verhagen and Laanbroek (1991)	5.660
	generic AOB	Rittmann and McCarty (2001)	0.599
	non-specific	Yang <i>et al.</i> (2008)	0.482
	mainly <i>N. oligotropha</i> (AOB)	Claros <i>et al.</i> (2010)	0.023
	non-specific	Fleming <i>et al.</i> (2008)	0.005
	<i>Nitrosopumilus maritimus</i> (AOA)	Martens-Habbena <i>et al.</i> (2009)	0.002
Monochloramine inactivation rate (L/mg-min as Cl_2)+	<i>Nitrosomonas europaea</i> (AOB)	Wahman <i>et al.</i> (2009)	1.60E-03
	<i>N. europaea</i>	Oldenburg <i>et al.</i> (2002)	1.20E-03

*Half-saturation coefficients were converted to a total free ammonia ($\text{NH}_3 + \text{NH}_4^+$) concentration to facilitate comparisons between studies, assuming a pH of 8.0 (where ammonia is 5% of ammonium).

+Chloramine inactivation rates are for pH 8.0.

pH is one of the most complicated factors influencing nitrification, as it can affect nitrification via several mechanisms which may act in opposition. Some of the diverse ways in which pH affects nitrification are: changing the balance of ammonia and ammonium (free ammonia is thought to be the true substrate), inorganic carbon loss from CO₂ stripping at low pH values, affecting the chloramine decay rate, and changing the chloramine disinfection rate on nitrifiers (Zhang *et al.*, 2009b). The optimal pH for the growth of nitrifying bacteria has been measured on multiple occasions. Values of 7.8 (Antoniou *et al.*, 1990) and 8.0 (Villaverde *et al.*, 1997) have been found in some wastewater studies, for example.

pH interacts with monochloramine disinfection both by influencing the monochloramine decay rate, and by affecting the inactivation rate of monochloramine on nitrifiers. Vikesland *et al.* (2001) found that monochloramine auto-decomposition was more rapid at lower pH. An interesting result was that higher carbonate concentrations led to more rapid monochloramine decay at a given pH, which was interpreted as evidence for acid catalysis of monochloramine auto-decomposition. The effect of pH on the monochloramine disinfection rate appears to act in opposition to the impact of pH on the stability of the monochloramine disinfectant residual. Oldenburg *et al.* (2002) found higher Chick-Watson disinfection rates at pH 7 than at pH 8 for a species of AOB, and an even lower rate was found at pH 9. The pH effect was interpreted as consistent with the fact that dichloramine was the active disinfecting agent. Other researchers (Speital *et al.*, 2011) disagree that dichloramine is the active agent, although they confirmed the trend with pH, ascribing it to acid-catalysis of monochloramine disinfection. No inactivation experiments have yet been done on AOA.

The net impact of these various pH mechanisms is unclear, and may be system specific. A full-scale system studied by Skadsen (2002) saw a reduced frequency of nitrification episodes by setting pH >9.3. Oldenburg *et al.* (2002) discussed the possibility of raising pH to control nitrification. Increased pH can lower chloramine decay and may be sub-optimal for AOB growth above 8.5, but it can also decrease the disinfection efficiency of chloramines. By applying logistic regression to results from pilot-scale distribution systems, Yang *et al.* (2007) found that pH was a statistically significant variable. The probability of nitrification was reduced by moving away from an optimum pH (of 8.3) according to their risk-factor probability model. Fleming *et al.* (2008) applied their Nitrification Potential Curves model (models for nitrification are introduced in section 2.6 below and investigated in Chapter 6) to full-scale drinking water distribution systems with different pH values and speculated that raising the pH may be a viable control strategy for nitrification. Further research is recommended on this topic.

Closely related to the impact of pH on nitrification is the effect of alkalinity. Inorganic carbon is required by autotrophic ammonia-oxidizers (Rittmann and McCarty, 2001). However, Zhang *et al.* (2009b) point out that there is usually a ratio greater than 14:1 of CaCO₃ alkalinity to NH₃-N ammonia (i.e. it is present in stoichiometric excess) in distribution

systems, so alkalinity is not likely to be a limiting factor for nitrification in most systems.

As with all biological processes, nitrification can be affected by temperature. Even so, nitrification has been observed in drinking water distribution systems across a wide range of temperatures. Higher temperatures have been found to increase the growth rate of nitrifying bacteria (Antoniou *et al.*, 1990; Rittmann and Snoeyink, 1984), and increase abundance of AOB (Pintar and Slawson, 2003) and the risk of nitrification (Yang *et al.*, 2007). Higher temperatures also accelerate the chemical decay rate of monochloramine (Vikesland *et al.*, 2001), which can lead to conditions conducive to nitrification in distribution systems. In pilot-scale biological activated carbon filters where AOA outnumbered AOB, Kasuga *et al.* (2010a) observed incomplete removal of ammonium-nitrogen at temperatures less than 10°C. Because higher temperatures can promote nitrification, climate change may lead to its increased prevalence in distribution systems. Levin *et al.* (2002) listed enhanced distribution system biofilm growth as one of the challenges that climate change could pose for drinking water utilities.

Although higher temperatures are more favourable to distribution system nitrification, it is not prevented by cooler conditions. In a survey of U.S. water utilities, Wilczak *et al.* (1996) reported that most nitrification occurred when temperatures were above 15°C, but it was also observed below 10°C. In a bench-scale study on AOB, Pintar and Slawson (2003) confirmed that AOB could become established in low temperature reactors (12°C), and even when temperatures were dropped to 6°C established AOB remained viable. In the cool climate of Finland (mean water temperature of 12°C), Lipponen *et al.* (2002) found AOB and NOB to be common in chloraminated distribution systems. Pintar *et al.* (2005) conducted a study in a full-scale distribution system (the Region of Waterloo in Ontario, Canada) and observed nitrification at temperatures as low as 6°C, although the nitrification episodes mainly followed a seasonal pattern (i.e. most occurrences were during warmer months).

Other factors are also known or hypothesized to affect nitrification. As it is an aerobic process, dissolved oxygen is required for nitrification. In a study on the metabolism of a strain of AOA, Martens-Habbena *et al.* (2009) found oxygen was consumed at a ratio of 1.52 moles per mole of ammonium. Rittmann and Snoeyink (1984) raised the possibility of DO limitation on nitrification. According to MacPhee (2005), systems with low DO are less susceptible to nitrification. However, in their survey of U.S. utilities, Odell *et al.* (1996) reported that dissolved oxygen was never a limiting factor for nitrification.

The impact of organic carbon on nitrification remains uncertain. Odell *et al.* (1996) reported that the impact of natural organic matter (NOM) on nitrification is not fully understood. Zhang *et al.* (2010b) hypothesized that the TOC level could indirectly influence AOB growth as reactions with NOM would increase the chloramine decay rate. They concluded that higher TOC stimulated nitrification by decreasing the chloramine concentration. Other causes for the stimulation of nitrification in their study cannot be ruled out, how-

ever, as the water samples being used had additional differences beside TOC levels. Other authors have considered the possibility of high organic carbon concentrations leading to heterotrophic bacteria out-competing nitrifying microorganisms. Verhagen and Laanbroek (1991) evaluated competition between a heterotrophic species (*Arthrobacter globiformis*) and an ammonia-oxidizing species (*Nitrosomonas europaea*) of bacteria in situations with limiting ammonium. According to theoretical considerations they presented, heterotrophs will be nitrogen-limited above a critical carbon-to-nitrogen (C/N) ratio—based on ammonia-nitrogen and organic carbon—and will consume all of the available ammonium, assuming they have a higher affinity than nitrifiers. Below the critical C/N ratio, heterotrophs will be carbon-limited and excess ammonia will be available to nitrifiers. Critical carbon-to-nitrogen molar ratios of 11.6 and 9.6 were determined from two experiments they performed. Zhang *et al.* (2009b) extended this work to predict whether heterotrophs or nitrifiers will be dominant based on the level of the carbon-to-nitrogen ratio (in the absence of a disinfectant residual). However, they also discuss possible synergistic effects between nitrifying microorganisms and heterotrophic bacteria, such as the excretion of useful metabolic products or removal of toxic metabolic products.

However, the findings of other studies cast doubt on whether nitrifiers will face significant competition from heterotrophic bacteria in distribution system environments. Bollmann *et al.* (2002) conducted a study on two species of AOB (*Nitrosomonas europaea* and G5-7, a close relative of *N. oligotropha*) under low ammonium conditions. *N. europaea* was found to recover from starvation more quickly, while G5-7 could grow at lower ammonium concentrations. Differences in growth characteristics between AOB strains could explain niche differentiation for nitrifiers, and also have implications for competition with heterotrophic bacteria. Species such as *N. oligotropha*, which have been detected in distribution system environments (Regan *et al.*, 2002), and have a high affinity for ammonia-nitrogen might be able to successfully compete with heterotrophs at any C/N ratio. Similarly, for a strain of AOA, Martens-Habbena *et al.* (2009) found a very high specific affinity for ammonia. More research is recommended on the topic of competition between heterotrophs and nitrifying microorganisms, and the net effect of organic carbon on nitrification.

2.5 Controlling Distribution System Nitrification

A variety of methods for controlling nitrification have been suggested. Once a nitrification episode is underway, it is difficult to bring the affected portion of the distribution system back under control. Breakpoint chlorination is usually effective. However, Odell *et al.* (1996) presented a case-study in which breakpoint chlorination led to a rise in the number of samples testing positive for total coliforms, which was attributed to increased biofilm

detachment caused by the aggressive reactivity of free chlorine. Breakpoint chlorination is usually kept as a last resort. Simply raising the monochloramine residual, on the other hand, has been reported to be ineffective at halting nitrification once it is established (Skadsen, 1993; Odell *et al.*, 1996; Pintar and Slawson, 2003). Another method that is sometimes used to control nitrification episodes already in progress is flushing the affected part of the distribution system with non-nitrifying water. Skadsen (1993) found this to be temporarily effective. Odell *et al.* (1996) reported cleaning the distribution system to provide good improvement in both short-term and long-term control of nitrification. Also of note is the reservoir management strategy developed by Sathasivan *et al.* (2010) in which they used a batch test method (Sathasivan *et al.*, 2005) to determine when a reservoir was at risk of a nitrification episode. At such times the reservoir was refilled with non-nitrifying water by performing serial dilutions.

For preventing nitrification from becoming established, additional control methods have been investigated. Skadsen (2002) did an experiment in a full-scale distribution system on the effectiveness of high pH in controlling nitrification. A very high pH (>9.4) appeared to reduce nitrification. The experiment was deemed successful and a move to a higher pH was made; over an 8 year monitoring period following the increase, the frequency of nitrification in that system was reduced. The author reviewed other studies on the relationship between pH and nitrification which showed that it had potential as a control option, but the data was mixed. Oldenburg *et al.* (2002) discussed the possibility of raising pH to control nitrification based on theoretical considerations. A higher pH lowers chloramine decay (Vikesland *et al.*, 2001) and may be sub-optimal for AOB growth above 8.5 (Villaverde *et al.*, 1997), but as they found it also reduces the disinfection rate of chloramines; they were unable to determine which effect would be most significant. Fleming *et al.* (2008) applied their Nitrification Potential Curves model to full-scale drinking water distribution systems, and based on differences between systems in their study with different pHs, they speculated that raising the pH may be a viable control strategy for nitrification. McGuire *et al.* (2009) tested the use of chlorite (0.6 mg/L) for preventing nitrification in a full-scale system. Their results showed that it was somewhat effective at preventing nitrification. However, chlorite is a regulated parameter in some jurisdictions, so it is not likely to be a preferred option. For example, the Canadian Drinking Water Quality guidelines have a maximum acceptable concentration of 1.0 mg/L (Health Canada, 2010).

2.6 Modelling Nitrification

The topic of modelling nitrification is discussed in detail in Chapter 6. Having effective models for nitrification available can assist drinking water distribution system operators by

predicting when the potential for nitrification exists. With advance warning, nitrification episodes may be avoided or averted.

Based on factors that are known to impact distribution system nitrification, some researchers have developed models to predict when nitrification episodes will occur or how they will develop. Most of these models are based on considerations of the mechanisms by which selected factors impact nitrification, although a statistically-based logistic regression model (Yang *et al.*, 2007) has also been developed.

Fleming *et al.* (2005) developed a model that generated “Nitrification Potential Curves” between conditions considered non-nitrifying and potentially nitrifying. These curves were based on a balance between growth and inactivation rates of nitrifiers, with the ammonia concentration promoting growth, and the total chlorine concentration acting to inactivate the nitrifiers. The same approach was adopted by Speital *et al.* (2011), who also added the effect of trihalomethane (THM) cometabolism and toxicity to their “Nitrification Index” (N.I.) model. More detailed mechanistic models were developed by Liu *et al.* (2005) and Yang *et al.* (2008); they used mass balance equations for a set of chemical and microbiological parameters relevant to distribution system nitrification. The former was developed for steady-state plug-flow scenarios, and the latter was dynamic with completely-mixed hydraulics. Yang *et al.* (2007) developed a risk-factor probability model for distribution system nitrification, using logistic regression to identify significant parameters. Another model is the C/N model of Zhang *et al.* (2009b), which expands on the work of Verhagen and Laanbroek (1991) to predict whether nitrifiers or heterotrophs will be dominant in a distribution system, based on the carbon-to-nitrogen ratio.

Most of the models that have been proposed for distribution system nitrification incorporate substrate and disinfectant effects. The Nitrification potential curves model of Fleming *et al.* (2005) is based on a balance between Chick-Watson kinetics for inactivation of AOB and Monod kinetics for their growth. The semi-mechanistic model of Yang *et al.* (2008) incorporates substrate and disinfectant effects into a mass balance for AOB in the same way. Liu *et al.* (2005), in contrast, included the disinfectant effect in a Monod-type expression as an inhibition on growth, rather than as an inactivating agent, in their nitrification model. Perhaps the most interesting approach to incorporating substrate and disinfectant effects into a nitrification model was in the work of Yang *et al.* (2007). By fitting a logistic risk model to their experimental results, they found that the ammonia concentration was not a statistically significant predictor of the risk of nitrification. A low total chlorine residual was a significant risk factor. They explained the exclusion of ammonia by suggesting that if the dominant forms of AOB in their experiment were adapted to low ammonia concentrations, then higher ammonia levels may not significantly increase the risk of nitrification.

2.7 Conclusion

This chapter has reviewed the issues surrounding nitrification in chloraminated drinking water distribution systems. Ammonia-Oxidizing Bacteria (AOB) and Ammonia-Oxidizing Archaea (AOA) are the microorganisms responsible for converting ammonia to nitrite, the first step in the nitrification process. Factors affecting nitrification include the ammonia and total chlorine concentrations, pH, and temperature. Some researchers have developed models to predict the occurrence or magnitude of nitrification events. The most critical consequence of nitrification is a decline in the disinfectant residual; a potential proliferation of HPCs and changes in the ammonia, nitrite, and nitrate concentrations are other significant impacts.

There are a number of unanswered questions related to distribution system nitrification. Some of these topics are addressed in subsequent chapters, such as the presence of AOA in chloraminated distribution systems and whether nitrifiers can successfully compete with heterotrophs for ammonia-nitrogen. Some of the models that have been proposed are evaluated.

Chapter 3

Description of Systems

To study water quality in drinking water distribution systems, experiments can be done using samples taken directly from full-scale distribution systems or using model water that is prepared in a laboratory to contain constituents of interest at defined concentrations. Work to date on nitrification in chloraminated drinking water distribution systems has been done both with pilot-scale or bench-scale systems (such as Fleming *et al.* 2005, Yang *et al.* 2008, Verhagen and Laanbroek 1991, Regan *et al.* 2002, Pintar and Slawson 2003) and with sampling from full-scale systems (such as Pintar *et al.* 2005, Fleming *et al.* 2008, Sathasivan *et al.* 2005, Sathasivan *et al.* 2008, van der Wielen *et al.* 2009, Lipponen *et al.* 2002).

For this study, it was decided to use water taken from full-scale distribution systems for both phases of the work: first, a full-scale sampling campaign, followed by batch testing of samples from selected sites. The use of water from full-scale systems has the advantage that it will include factors that are missing from model waters, such as contact with pipe surfaces. There were two full-scale distribution systems included in this study. This provides more confidence in interpreting results than a study conducted at a single distribution system. It also provides some differences in water quality (such as different DOC levels) whose impact on nitrification can be evaluated. Within the distribution systems examined in this study, an effort was made to pick sites that were anticipated to have varying degrees of nitrification.

The water utilities of the City of Toronto (Toronto Water) and the Region of Waterloo participated in this study, both of which are located in Ontario, Canada. Sites were selected from portions of their distribution systems that were served by the same water treatment plant. Table 3.1 summarizes the two systems involved in this study, including the average values (over the course of the study) of selected parameters at the point at which treated water entered each distribution system (i.e. sites RCL and K20S14). With the exception of alkalinity data, which was provided by the utilities partnering in this research, these parameters were measured according to the methods listed in Section 4.2 for physical and chemical

parameters while AOA and AOB enumerations were conducted by Dr. Michele Van Dyke, from the NSERC Chair in Water Treatment in the Department of Civil and Environmental Engineering at the University of Waterloo, according to the methodology described in Appendix B. The samples for raw water AOB & AOA were taken from Lake Ontario in Oct. 2010 and from the Grand River in Nov. 2007.

Table 3.1: Descriptions of the two systems involved in this study, including average values at the entrance to their distribution systems (sites RCL and K20S14, respectively) during the sampling campaign.

Parameter	Toronto	Waterloo
Water source	Great Lakes' water	Highly impacted surface water blended with groundwater
pH	7.49 ± 0.17	7.47 ± 0.18
DOC (mg/L)	2.64 ± 0.86	3.57 ± 1.32
Conductivity ($\mu\text{S}/\text{cm}$)	316 ± 34	706 ± 62
Alkalinity (mg/L as CaCO_3)	80.4	222
Total chlorine residual (mg- Cl_2/L)	1.28 ± 0.11	1.47 ± 0.12
Ammonia (mg-N/L)	0.13 ± 0.10	0.15 ± 0.05
Nitrate (mg-N/L)	0.43 ± 0.12	3.48 ± 0.52
Nitrite (mg-N/L)	0.001 ± 0.002	0.004 ± 0.004
Raw water AOB (cells/100mL)	575	210
Raw water AOA (cells/100mL)	0	4370

Values listed in this table are means \pm standard deviations. Alkalinity data was provided by the utilities partnering in this study. Raw water AOB & AOA were taken from Lake Ontario in Oct. 2010 and from the Grand River in Nov. 2007.

The water source for the City of Toronto is Lake Ontario. The portion of the Toronto Water distribution system included in this study is served by a conventional water treatment plant (R.L. Clark WTP; site label RCL in this study) with a capacity of 615 ML/d (City of Toronto, 2011). The process train includes pre-chlorination (for zebra mussel control), coagulation, flocculation, sedimentation, mixed media (anthracite/sand) filtration, post-chlorination, and chloramination.

The water in the Region of Waterloo distribution system is a blend of surface water (20%) and groundwater (80%). The surface water source is the Grand River at Kitchener, which

receives agricultural and urban run-off. In the Region of Waterloo, water from the Grand River passes through a complex treatment train: coagulation, flocculation, sedimentation, ozonation, filtration, UV disinfection, and chlorination, followed by the addition of ammonia to fix the disinfectant residual to a chloramine form (primarily monochloramine). This water is blended with groundwater prior to entering the distribution system (Region of Waterloo, 2011).

There were some similarities and some differences between these systems. Both systems use monochloramine as a secondary disinfectant and they have pH levels in the same range. The Region of Waterloo distribution system is fed by more heavily-impacted source water than the Toronto Water distribution system, but also has a more extensive treatment process and a higher initial disinfectant residual. The DOC concentration, conductivity, and background nitrate levels were higher in Waterloo. Alkalinity was also greater in Waterloo than in Toronto, but both systems were far above the levels where it would be a limiting factor for nitrification (14 mg/L per mg/L of ammonia-nitrogen, Zhang *et al.*, 2009b). A notable difference between the systems was the presence of nitrifying microorganisms in their respective source waters. In Lake Ontario, AOA were below their detection limit when the raw water was sampled but AOB were present. In the Grand River, the surface water source for the Waterloo distribution system (separate samples were not available for the groundwater source prior to blending), AOA were observed to outnumber AOB. These differences between the systems involved in this study may serve to explain the results presented in Chapter 4.

The following sites from the Toronto Water distribution system were sampled in the course of this study:

- RCL—the R.L. Clark Water Treatment Plant (WTP) that feeds the sites below
- 602—tap in a municipal building
- 801—tap in a municipal building
- 804—tap in a municipal building
- 805—tap in a municipal building
- 904—tap in a municipal building
- 905—tap in a municipal building

Sites from the Region of Waterloo distribution system that were included in this study are described below.

- K20S14—this reservoir is immediately outside the Mannheim WTP and feeds the other sites listed
- W21—outflow from an enclosed reservoir
- WOD08—tap in an industrial cafeteria
- WOD05—tap in a commercial building
- WOD06—a dead-end site
- WOD04—this site is near a free-chlorine booster station; the disinfectant residual here is free chlorine (at all other sites the residual is predominantly monochloramine)
- E60T—outflow from an enclosed reservoir
- WOD61—the most distant site from the WTP

Cumulative hydraulic residence times are not available for these sites; they are listed approximately in the order of their distance from their respective water treatment plants, but it cannot be confirmed that the cumulative residence times necessarily follow the same order. Figures 3.1 and 3.2 show the spatial layout of the sites that were sampled in this study.

These sampling sites were chosen such that they all were fed from a single WTP (within each distribution system), yet were spatially dispersed and had some differences in the historical records of their total chlorine concentrations and HPC levels. The goal in the selection process was to include some sites which may be susceptible to nitrification while others would be expected to have stable water quality. This judgement was based primarily on historical total chlorine residual records for each site: whether they were stable or exhibited some predictable decreases in warmer months. Other parameters such as heterotrophic plate count (HPC) bacteria levels were also considered.

In order to determine how water quality varied over time in these distribution systems, to observe seasonal differences, and to capture any nitrification episodes as they might develop, sample collection frequency was targetted at 2 week intervals. The main sampling period lasted from late November 2009 to August 2010 in Toronto (9 months) and from February to August 2010 in Waterloo (7 months). Samples for batch testing (see Chapter 5) were collected on dates in August, October, and November 2010. Table 3.2 provides a record of the dates on which samples were collected.

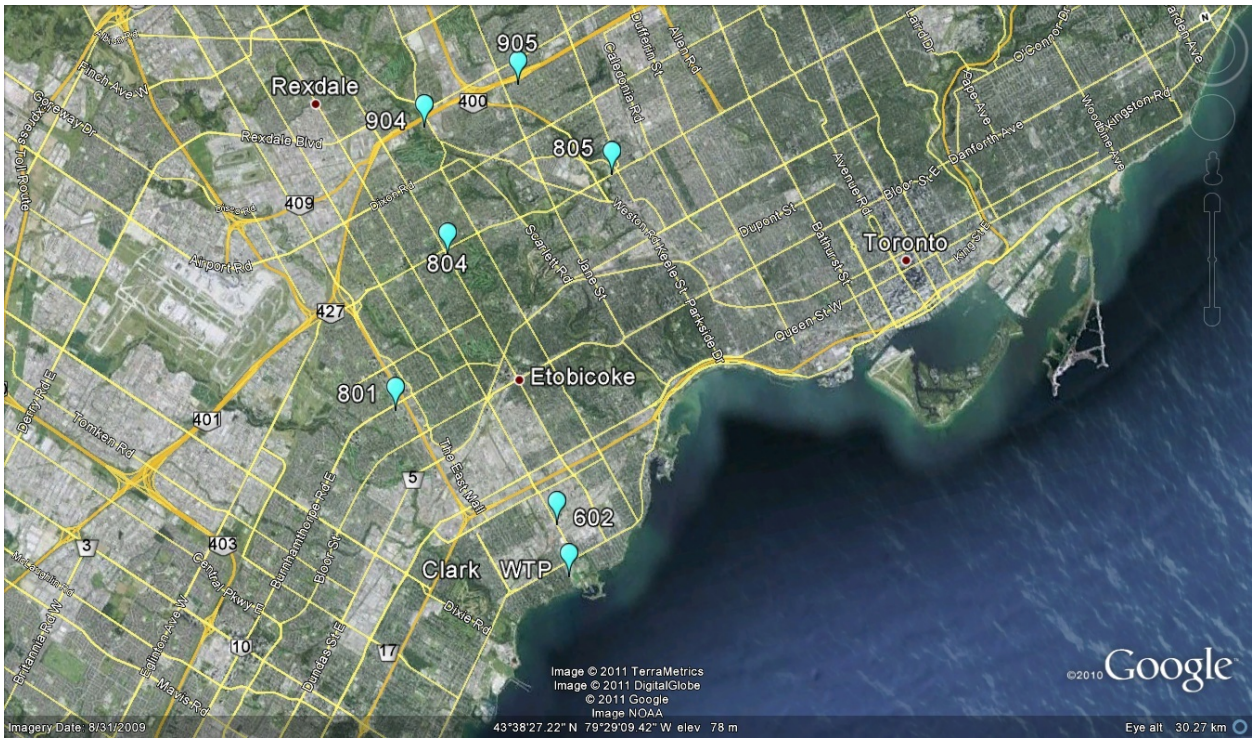


Figure 3.1: Sample sites in the City of Toronto that were monitored for this study (Google Earth). This portion of the distribution system is fed from the R.L. Clark WTP (site RCL in this study).

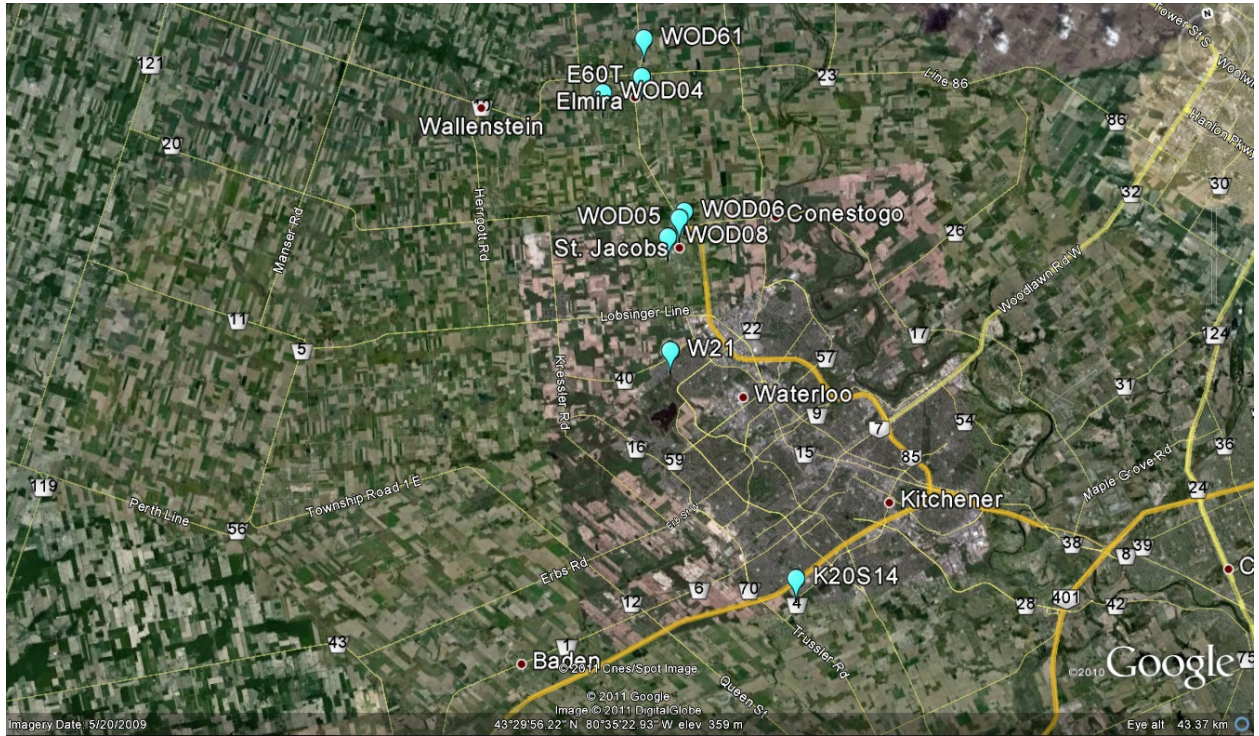


Figure 3.2: Sites in the Region of Waterloo that were monitored for this study (Google Earth). Site K20S14 is a reservoir at the Mannheim WTP that feeds the other sites listed. W21 and E60T are also reservoirs.

Table 3.2: Distribution system sample collection dates in 2009–2010.

Toronto	Waterloo
24-Nov	
8-Dec	
12-Jan	
27-Jan	
9-Feb	16-Feb
23-Feb	3-Mar
	17-Mar
23-Mar	31-Mar
	14-Apr
21-Apr	12-May
18-May	27-May
1-Jun	
7-Jul	15-Jul
17-Aug*+	25-Aug*+
13-Oct+	12-Oct+
	24-Nov+

Samples from dates marked with a “*” were cultured for nitrifying microorganisms; batch testing was conducted on samples collected on dates marked with a “+”.

Chapter 4

Full-Scale Study of Nitrification Factors

4.1 Introduction

Chloramines have been adopted by many drinking water utilities in North America for their lower potential for forming disinfection by-products (DBPs), and their improved persistence and biofilm penetration over free chlorine (LeChevallier *et al.*, 1990; Zhang and Edwards, 2009). It is important for the drinking water utilities using chloramines to understand the process, risk factors, and consequences of distribution system nitrification. This study of nitrification in two full-scale chloraminated drinking water distribution systems was carried out to enhance understanding of factors related to nitrification.

Ammonia-oxidation, the first and rate-limiting step (Francis *et al.*, 2005) of nitrification in distribution systems, is performed by autotrophic microorganisms from the *Bacteria* (ammonia-oxidizing bacteria, AOB) and *Archaea* (ammonia-oxidizing archaea, AOA) groups. This first step of nitrification, known as incomplete nitrification when it occurs alone, is the focus of concern in distribution system environments (Skadsen, 1993; Lipponen *et al.*, 2002) and is the subject of the present research. The amount of free ammonia available to ammonia-oxidizing microorganisms will be supplemented as the monochloramine residual undergoes decay in the distribution system. This creates a positive feedback loop for nitrification since its products (nitrite, and increased organic matter from nitrifier growth) accelerate chloramine decay, providing more free ammonia, and thus further promoting the growth of nitrifying microorganisms (Oldenburg *et al.*, 2002).

The factors that are thought to affect distribution system nitrification include the concentrations of the substrate (ammonia) and the disinfectant (monochloramine), temperature,

dissolved oxygen (DO) and alkalinity concentrations, pH, and organic carbon levels. The literature is mixed on whether the risk of nitrification is sensitive to the concentration of ammonia available. Skadsen (1993) identified ammonia overdosing as a possible cause of nitrification episodes in a chloraminated drinking water distribution system and Lipponen *et al.* (2002) found a positive correlation between ammonium-nitrogen concentrations and AOB in samples from Finnish drinking water distribution systems. Conversely, Odell *et al.* (1996) and Yang *et al.* (2007) reported that the ammonia concentration was not a significant risk factor for nitrification.

The chloramine residual has a clear impact on the risk of nitrification. Odell *et al.* (1996) presented a case study in which higher chloramine doses limited AOB regrowth. Pintar and Slawson (2003) noted that a relatively low disinfectant residual inhibited AOB more than a low temperature did. In their risk-factor model for nitrification, Yang *et al.* (2007) identified the total chlorine residual as a significant factor to predict the probability of a nitrification event. The kinetics of AOB inactivation by chloramine have been studied by Oldenburg *et al.* (2002) and Wahman *et al.* (2009), who both found that long reaction times would be required to inactivate AOB at typical monochloramine doses. No such studies have yet been done on AOA.

As a biological process, nitrification can be affected by temperature, but it has been observed in distribution systems across a wide range of drinking water temperatures. Higher temperatures have been found to increase the growth rate of nitrifying bacteria (Antoniou *et al.*, 1990; Rittmann and Snoeyink, 1984), the abundance of AOB (Pintar and Slawson, 2003), the risk of nitrification (Yang *et al.*, 2007), and the chemical decay rate of monochloramine (Vikesland *et al.*, 2001). However, cooler conditions have not been found to eliminate nitrification or nitrifying microorganisms. Wilczak *et al.* (1996) reported from a survey of U.S. utilities that nitrification was observed below 10°C, although most nitrification episodes did occur when temperatures were above 15°C. Lipponen *et al.* (2002) found AOB and NOB to be common in chloraminated distribution systems in Finland with a mean water temperature of 12°C. In a study conducted in a full-scale chloraminated distribution system operated by the Region of Waterloo (one of the same systems included in work presented in this thesis) Pintar *et al.* (2005) observed nitrification at temperatures as low as 6°C, although the nitrification episodes they observed predominantly occurred during the warmer months of the year.

The impact of organic carbon on nitrification requires further research. Some authors (Verhagen and Laanbroek, 1991; Zhang *et al.*, 2009b) have raised the possibility of high organic carbon substrate concentrations leading to heterotrophic bacteria out-competing nitrifying microorganisms. However, Ammonia-oxidizing species with high substrate affinities would be less susceptible to being out-competed by heterotrophic bacteria. The ability to thrive at low substrate concentrations has been reported for AOB species similar to *Nitro-*

somonas oligotropha, which may be selected for in distribution system environments (Regan *et al.*, 2002), by Bollmann *et al.* (2002). Martens-Habbena *et al.* (2009) had similar findings for a strain of AOA. Dissolved oxygen is required for nitrification by both *Bacteria* (Rittmann and Snoeyink, 1984) and *Archaea* (Martens-Habbena *et al.*, 2009). However, in their survey of U.S. utilities Odell *et al.* (1996) reported that DO was never limiting. Alkalinity is also not likely to be a limiting factor (Zhang *et al.*, 2009a).

The most prominent consequences of distribution system nitrification are an accelerated decay of the chloramine residual, a rise in nitrite and/or nitrate concentrations, and the potential for an increase in heterotrophic bacteria levels. Inorganic carbon and dissolved oxygen are also consumed in the process, and nitrifying microorganisms multiply. These impacts of nitrification have been recommended as indicators that nitrification is occurring in a distribution system (AWWA, 2006; Odell *et al.*, 1996). Nitrification will also impact the ammonia concentration, although the effect is not straight-forward, since some studies have shown an initial rise in the free ammonia concentration during nitrification followed by a peak and subsequent decline (Liu *et al.*, 2005; Yang *et al.*, 2008, 2007; Sathasivan *et al.*, 2008).

The consequences of nitrification are not likely to be a direct risk to public health; rather, they may lead to operational or regulatory-compliance challenges. An accelerated rate of monochloramine loss caused by nitrification can make regulatory compliance more difficult and potentially decrease the robustness of the distribution system as the final barrier for safe drinking water before it is delivered to consumers (Health Canada, 2002). A decline in the disinfectant residual may be an early indication of nitrification (Pintar *et al.*, 2005). Increased levels of nitrite or nitrate arising from nitrification are unlikely to exceed regulatory limits (Zhang *et al.*, 2009b). In addition, nitrification can promote the proliferation of heterotrophic bacteria, by decreasing the chloramine residual, and by contributing to the organic carbon available (Rittmann *et al.*, 1994). In Canada, drinking water system operators are advised to investigate the cause of a rise in HPCs, especially when it is rapid or unexpected (Health Canada, 2011). The National Research Council (2006) in the US also recommended monitoring HPCs as a non-specific indicator of microbiological water quality. HPCs have been reported to rise during nitrification episodes (Skadsen, 1993; Wilczak *et al.*, 1996). They are listed as an indicator of nitrification by Odell *et al.* (1996) and Zhang *et al.* (2009b).

A rise in nitrite and nitrate levels is an intrinsic consequence of nitrification. Therefore, these parameters are probably the most frequently recommended indicators of nitrification. Wilczak *et al.* (1996) strongly recommended that drinking water utilities develop an accurate nitrogen balance for their distribution systems as part of nitrification monitoring. Nitrification is not likely to produce nitrite above regulated limits at typical chloramination dosages applied in North America (Zhang *et al.*, 2009b).

Ammonia oxidizers have been previously studied in drinking water, although only a few studies have specifically examined AOA (Kasuga *et al.*, 2010b; de Vet *et al.*, 2009; van der Wielen *et al.*, 2009). van der Wielen *et al.* (2009) examined three water treatment plants and their distribution systems in the Netherlands that did not maintain a disinfectant residual. In one of these distribution systems, only AOA were detected. In the other two distribution systems, AOB outnumbered AOA at most sites, but AOA were still detected. None of those systems contained a disinfectant residual. Earlier research on nitrifying microorganisms in drinking water distribution systems considered only bacterial nitrifiers (AOB, and also NOB—nitrite oxidizing bacteria). These studies have identified factors associated with the presence or abundance of nitrifying bacteria. Lipponen *et al.* (2004) found positive correlations between nitrifiers and the distance from the WTP, and between nitrifiers and heterotrophs (although confounding variables were not ruled out). Their study also found that all microorganisms were negatively correlated with total chlorine. In earlier work, in which they surveyed AOB and NOB in water and sediment samples from drinking water distribution systems in Finland, Lipponen *et al.* (2002) also found a positive correlation between HPC and AOB in both water and sediments. Cunliffe (1991) identified that total chlorine and nitrite plus nitrate were statistically significant indicators for the presence of nitrifying bacteria in an investigation of chloraminated drinking water distribution systems in Australia; temperature and standard plate counts were not statistically significant.

The ways in which AOA differ from AOB and their relative importance to nitrification are topics of active research. Martens-Habbena *et al.* (2009) reported nearly unprecedented affinity for ammonia in a strain of AOA. If this property is shared by other ammonia-oxidizing archaea, they could thrive in low-substrate environments. This potential difference between the optimal substrate (ammonia) concentrations is the main factor that has been suggested to cause niche separation between AOA and AOB (Schleper, 2010). Other factors that have been suggested to explain AOA:AOB ratios or relative activities include: pH (Prosser and Nicol, 2008), susceptibility to chlorination or other treatment steps (Kasuga *et al.*, 2010b), and the concentration of organic carbon or metals (van der Wielen *et al.*, 2009). Further investigation is required on this topic.

The work presented in this chapter attempts to contribute to the knowledge of nitrification in chloraminated drinking water distribution systems. Some of the unanswered questions related to distribution system nitrification will be addressed in this chapter, such as the presence of AOA in chloraminated distribution systems and whether nitrifiers and heterotrophs have a competitive or synergistic relationship. Another goal of this research was to evaluate the specific systems partnering in this research with respect to nitrification. To achieve these objectives, water samples were collected from two full-scale chloraminated distribution systems in Southern Ontario and parameters relevant to nitrification were monitored. Trends and correlations in these parameters were determined to reveal information

about nitrification.

4.2 Methodology

Sampling Procedure

Samples were collected from a total of 15 sites in two full-scale distribution systems approximately every second week. The distribution systems were located in the City of Toronto and the Region of Waterloo, both in Ontario, Canada. The sampling campaign lasted from November 2009 to August 2010. These systems and sites are described in detail in Chapter 3.

The procedure for collecting the samples was designed to obtain sufficient volume for each parameter of interest. Upon arriving at a site, the aerator was removed from the tap to be sampled, if applicable. Samples for microbiological analyses were collected before the tap was flushed; this was a departure from standard microbiological sampling procedures (Method 9060 A, APHA *et al.* 2005), but was considered more appropriate for this study. Stagnant water has more opportunity to come into balance with biofilm lining the pipes, providing a better measure of the microorganisms present in a distribution system. In addition, stagnant water represents a more critical condition for nitrification, and thus was of greater interest in this research. An exception had to be made for sites RCL and K20S14, which had continuous-flow sampling taps. Microbiological samples to be analyzed for nitrifiers were collected in sterile 1 L plastic bottles containing 1 mL of 3% sodium thiosulfate to quench the disinfectant residual. A separate 250 mL sterile bottle (Systems Plus: Baden, Ont.), also containing sodium thiosulfate, was taken for HPC analysis. Sample bottles were transported back to the lab in a cooler on ice for analysis. Within 48 h (samples were stored in a refrigerator if not filtered immediately), the microbiological samples were analyzed as described below.

Following the collection of the microbiological samples, the taps were flushed until the water reached a steady temperature. A large glass beaker was filled for immediate on-site water quality measurements (pH, DO, temperature, and conductivity).

Samples for further physico-chemical analyses (DOC, ammonia, nitrite, nitrate, chloride, and sulfate) were collected in 300 mL glass bottles and transported to the lab in a cooler on ice. The disinfectant residual was not quenched in these samples. Samples for DOC and anion measurement (Ion Chromatography) were filtered and then kept in a refrigerator until they were analyzed as described below.

Physico-Chemical Analyses

Dissolved oxygen (DO) was measured with a SympHony DO Meter (VWR: Radnor, Penn.). Due to equipment difficulties, DO measurements were only obtained on half of the sampling dates. Temperature and conductivity were measured with a Hach CO150 Conductivity Meter (Hach, Loveland, Colo.). pH was measured with an Orion 290A pH Meter with a standard glass Ag/AgCl electrode probe (Thermo Scientific: Waltham, Mass.). A pH 7 buffer was also measured in the field to calibrate the meter. No temperature corrections were made to pH data. Total chlorine was analyzed by Hach method # 8167 (Hach, 2008), which is based on Standard Method 4500-Cl G (APHA *et al.*, 2005). All of these measurements were taken immediately on-site.

The remainder of the tests on the water samples were done at the University of Waterloo. Samples for dissolved organic carbon (DOC) measurement and ion chromatography were filtered using a 0.45 μm membrane filter (Pall Supor 450; VWR: Port Washington, NY). Membrane filtration was performed with a glass filter unit. 500 mL of ultrapure water was first filtered to rinse the membrane, followed by a second rinse with 100 mL of the test sample (see Karanfil *et al.* 2003). After rinsing the membrane filter, the remainder of the sample was filtered and then divided into three 40 mL vials. One of these vials was set aside for Ion Chromatography analysis while the other two were preserved for DOC quantification by adding 85% phosphoric acid to acidify them to pH 2. All vials were refrigerated at 4°C until they were analyzed.

Monochloramine and free ammonia were measured according to Hach method # 10200 (Hach, 2008). Calibration factors were calculated for monochloramine readings based on measured standards (see Appendix D for details).

Dissolved organic carbon (DOC) was quantified using an automated wet oxidation method (OI Analytical 1010; College Station, Texas). Potassium hydrogen phthalate standards were prepared by adding 53.1 mg of potassium hydrogen phthalate ($\text{C}_8\text{H}_5\text{KO}_4$) to 250 mL of ultrapure water, which was then acidified to pH 2 using phosphoric acid. For each run, calibration curves were created (see example in Appendix D) and used in calculating the results. Due to a break-down of the TOC analyzer, some samples were not analyzed within the one month time frame stipulated by Standard Methods (APHA *et al.*, 2005). Specifically, samples taken between 31 March 2010 and 1 June 2010 were not analyzed until August–November 2010—but were preserved as recommended in the interim.

Ion Chromatography was used to measure the concentrations of four anions in water samples for this research. Chloride, nitrite, nitrate, and sulfate levels were determined for each sample. A Dionex (Sunnyvale, Cali.) ICS-series ion chromatograph was used with an AS4A-SC 4 mm anion exchange column. The eluent was 9 mM sodium carbonate and the regenerant was sulfuric acid. A mixed anion standard solution was prepared by diluting a

stock solution, and standards were included in each run. The stock solution was prepared containing chloride, nitrite, nitrate, and sulfate in a 1:0.5:0.5:1.5 ratio. The chloride concentration was set to 100 mg/L Cl^- . For this solution, 210.3 mg KCl, 75.0 mg NaNO_2 , 68.5 mg NaNO_3 , and 187.0 mg MgSO_4 were added to 1 L of ultrapure water. For each run, individual calibration curves were created in a spreadsheet for each anion; linear or quadratic fits over all or part of the range were chosen based on visual examination of plotted results (see example in Appendix D).

Microbiological Analyses

For heterotrophic plate count (HPC) analysis, 1 mL and 10 mL volumes were separately passed through a sterile 0.45 μm membrane filter (Pall GN-6) by vacuum filtration using aseptic technique. Each sample volume was analyzed once. Following the filtration of each sample volume, the membrane was placed on R2A agar in a petri dish (BD: Mississauga, ON). Samples were incubated at 28°C for 5–7 days. Colonies were then counted at 20x magnification. The optimum colony count per plate was between 20–150. Results were converted to CFU/100 mL. This method is based on Standard Method 9215 (APHA *et al.*, 2005).

Ammonia-oxidizing bacteria (AOB) and ammonia-oxidizing archaea (AOA) were enumerated by quantitative polymerase chain reaction (qPCR). 1 L samples were concentrated by vacuum filtration through sterile 0.22 μm Supor 200 membranes (Pall). Each filter was placed in a 3 mL plastic vial containing 1.5 mL of GITC buffer (Cheyne *et al.*, 2010) and frozen at -80°C. DNA extraction and qPCR were done by Dr. Michele Van Dyke, from the NSERC Chair in Water Treatment in the Department of Civil and Environmental Engineering at the University of Waterloo. The methodology is described in Appendix B.

Statistical Analysis of Results

Statistical analysis for this research was performed using spreadsheets and the statistical software “R” (R Development Core Team, 2009). Notably, non-parametric Spearman correlation coefficients, ρ (the notation r_s is also used), were calculated between parameters. In contrast to traditional correlation coefficients, the Spearman correlation coefficient is based on the ranks of measurements rather than their values, and does not assume a linear relationship. This makes it useful for analyzing distribution system data, where various parameters are not normally distributed or have a large number of non-detects. For example, figures C.2 and C.3 in Appendix C illustrate the differing distributions of a few of the parameters monitored in this study. For this reason, the Spearman correlation coefficient is often used in distribution system research (Rice *et al.*, 1991; Cunliffe, 1991; Lipponen *et al.*, 2002, 2004).

The following equation (Dodge, 2010) defines the Spearman correlation coefficient for the case where there are no tied ranks (a correction should be made if there are many ties). R_X and R_Y are the ranks of the two variables X and Y, respectively.

$$\rho = 1 - \frac{6 \sum_{i=1}^n d_i^2}{n(n^2 - 1)}, \quad (4.1)$$

$$d_i = R_{X_i} - R_{Y_i} \quad (4.2)$$

To explore whether the correlations between certain parameters were due to their mutual correlation with a third factor, partial correlation coefficients were calculated, which control for the third variable (Dodge, 2010). The following equation (Dodge, 2010) was used to calculate partial correlation coefficients between two variables, X and Y, while controlling for a third variable Z. Here, r_{xy} is the correlation coefficient between X and Y, and r_{xz} and r_{yz} are the correlations of Z with X and Y, respectively.

$$r_{xy.z} = \frac{r_{xy} - r_{xz} \cdot r_{yz}}{\sqrt{1 - r_{xz}^2} \cdot \sqrt{1 - r_{yz}^2}} \quad (4.3)$$

According to Kendall (1942), this equation for calculating a partial correlation coefficient is only an approximation when using Spearman's rank correlation, but it was judged to be sufficient for the current study. Therefore, Spearman correlation coefficients (ρ) were used in the equation above.

4.3 Results and Discussion

Distribution System Water Quality

Distribution system water quality parameters were monitored over a period of nine months in two full-scale distribution systems in Southern Ontario. The following parameters were monitored: water temperature, pH, total chlorine residual, dissolved oxygen, DOC, monochloramine, ammonia, nitrite, nitrate, chloride, sulfate, HPC, AOB, and AOA. The water sources are quite different: Lake Ontario water (Toronto) versus a highly-impacted river water blended with groundwater (Waterloo). Concentrations of most water constituents were lower

or at the same level in the Toronto distribution system compared to the Waterloo distribution system. For most parameters, the variability was also lower in the Toronto distribution system than in the Waterloo distribution system, indicating more stable water quality. These general trends are readily apparent in the total chlorine residuals that were measured in this study. These residuals are summarized as boxplots in Figure 4.1. The boxplots presented in this chapter show the median and central 50% (i.e. the interquartile range) of the data values enclosed within a box. Whiskers extend to cover the rest of the range to a distance from the quartiles up to 1.5 times the width of the central box; points outside of these bounds are considered outliers and plotted as individual circles (R Development Core Team, 2009). Sampling sites are listed along the x-axis in the order of their distance from the water treatment plant (WTP). Data on cumulative hydraulic retention times for each site was not available, however, and is not guaranteed to be in the same order. Boxplots for sites from the Toronto Water distribution system are based on 12 samples and boxplots for sites from the Region of Waterloo distribution system are based on 9 samples.

Both distribution systems included in this sampling campaign were able to maintain a disinfectant residual to the most distant points included in this survey. The Toronto distribution system had less variability between sites. In the Waterloo distribution system, the total chlorine residual decreased by about one third from the entrance to the distribution system (site K20S14) to more distant sites. In Waterloo, the disinfectant residual concentrations also had a degree of variability within each site. Site WOD06 is a dead-end location, and site WOD04 is influenced by a reservoir with a free chlorine booster station (and therefore has a lower residual free chlorine target than the rest of the distribution system), so the lower total chlorine residuals at these locations are not unexpected.

The chloramine disinfectant residual concentration can affect the probability of nitrification; sites with a lower disinfectant residual will be more vulnerable to nitrification events. Pintar and Slawson (2003) and Odell *et al.* (1996) both observed a chloramine residual limiting the regrowth of AOB. In their risk-factor model for nitrification, Yang *et al.* (2007) identified the total chlorine residual as a significant factor to predict the probability of a nitrification event. However, some studies have found that AOB have long inactivation times with monochloramine so maintaining a disinfectant residual does not always prevent the growth of nitrifying bacteria in chloraminated distribution systems. Wahman *et al.* (2009), for example, reported a Ct_{99} of 3300 mg-min/L as Cl_2 for *Nitrosomonas europaea*. Oldenburg *et al.* (2002) observed inactivation rates of the same order of magnitude.

pH values, on the other hand, did not display much difference between sites or systems (Fig. 4.2). An early objective of this research was to evaluate the effect of pH on nitrification (see Chapter 2 for a discussion on the complex mechanisms by which pH can affect nitrification), but the minimal variation observed required this objective to be abandoned. Both distribution systems monitored in this study had average pH values near 7.5 and no

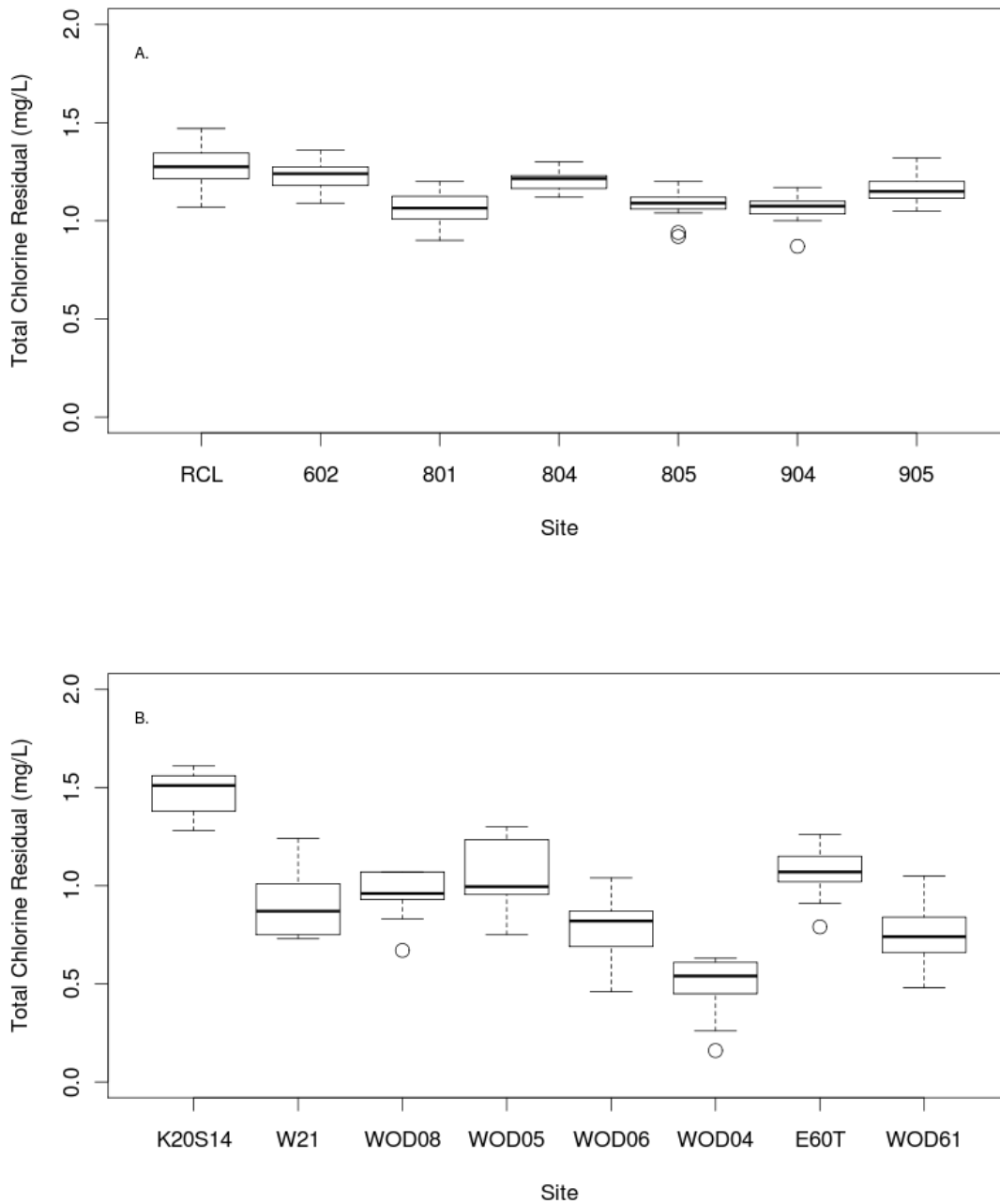


Figure 4.1: Summary boxplots for total chlorine residuals measured in this study for (A) Toronto and (B) Waterloo distribution systems. Sites RCL (Toronto) and K20S14 (Waterloo) are at the entrance points to their respective distribution systems. In Waterloo site WOD04 is free-chlorinated, so its target free chlorine residual is lower, and sites W21 and E60T are reservoirs.

trends between sites.

Chloride and sulfate, while not directly related to nitrification, were of interest due to the bearing they have on corrosion. The chloride-to-sulfate mass ratio (CSMR) is thought to influence distribution system corrosion, specifically with respect to lead. A CSMR greater than about 0.5 may promote galvanic corrosion in distribution systems (Edwards and Triantafyllidou, 2007). Corrosion can consume the disinfectant residual, release metal ions to solution, and promote biofilm attachment; these effects, in turn, could influence nitrification. Additionally, Zhang *et al.* (2009b) describe a mechanism by which corrosion could recycle nitrate to ammonia, increasing the amount of substrate available to nitrifying microorganisms. In Figure 4.3, the CSMR values found in this study are summarized with boxplots for each site. They are slightly higher in the Waterloo distribution system, but are above 0.5 (dotted line) in both systems, with little variability between sites.

Dissolved organic carbon (DOC) concentrations measured in this study are shown in Figure 4.4. DOC readings were slightly higher at the entrance to each distribution system (sites RCL and K20S14) than at more distant sites, suggesting small losses of DOC within the distribution system. Zhang *et al.* (2010b) hypothesized that higher levels of organic carbon would increase the chloramine demand, accelerating the chloramine decay rate and indirectly promoting nitrification. Verhagen and Laanbroek (1991) and Zhang *et al.* (2009b) have proposed that high levels of organic carbon (above a critical carbon-to-nitrogen ratio) could indirectly inhibit nitrification by allowing heterotrophic bacteria to out-compete ammonia-oxidizing bacteria (AOB). The work of other researchers (Bollmann *et al.*, 2002; Martens-Habbena *et al.*, 2009) casts doubt on this concept. The C/N model is evaluated in Chapter 6. Note that due to equipment problems described above, many DOC samples were not analyzed within the one month time frame stipulated by Standard Methods (APHA *et al.*, 2005). Therefore caution must be exercised in drawing any conclusions from this data.

Ammonia concentration is a very important parameter in this research as it is the substrate for nitrifying microorganisms. Ammonia can be released by the decay of a chloramine disinfectant residual and can be consumed by microbial activity, so its concentration in chloraminated drinking water distribution systems can rise or fall under different scenarios and is difficult to interpret in isolation. The ammonia levels measured in this study are summarized for each site in Figure 4.5. In the Toronto distribution system, average ammonia levels were similar between sampling sites. One trend that can be seen in the Waterloo distribution system is that many sites had ammonia levels elevated above those entering the distribution system, likely released from monochloramine decay. As Oldenburg *et al.* (2002) pointed out, the liberation of free ammonia from the decay of the chloramine disinfectant may be seen as a positive feedback loop for nitrification since nitrification promotes the decay of the disinfectant residual while consuming ammonia. A notable exception is site WOD04, which is under the influence of a free-chlorinated reservoir. Another interesting result is the increased

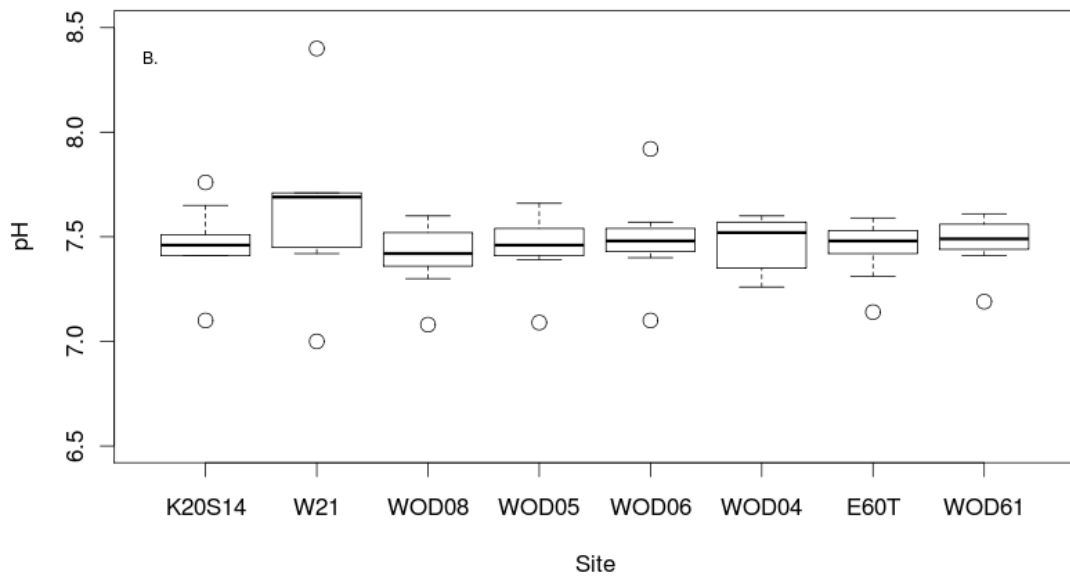
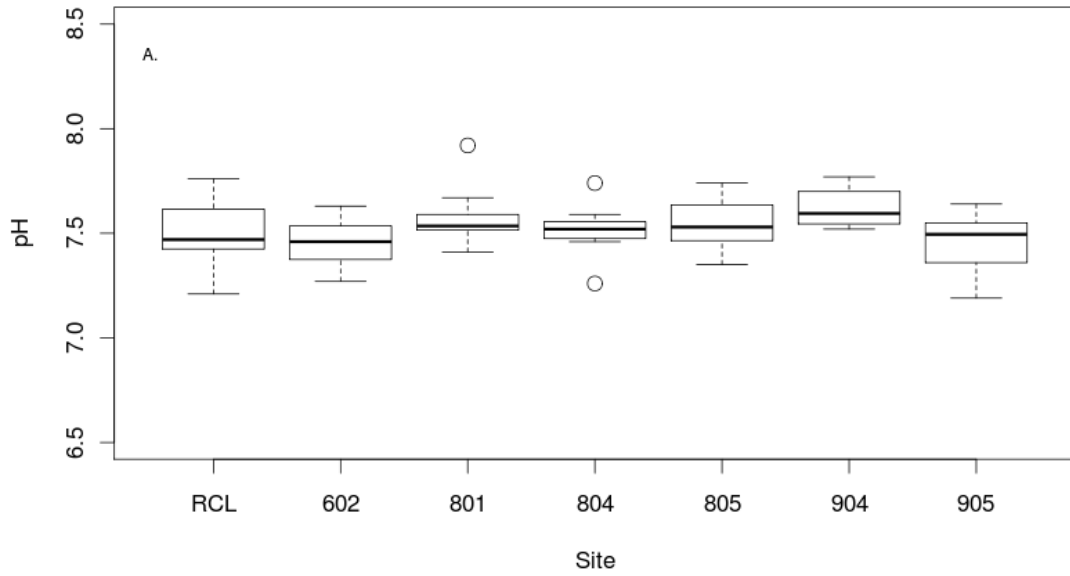


Figure 4.2: Summary boxplots for pH levels measured in this study for (A) Toronto and (B) Waterloo distribution systems.

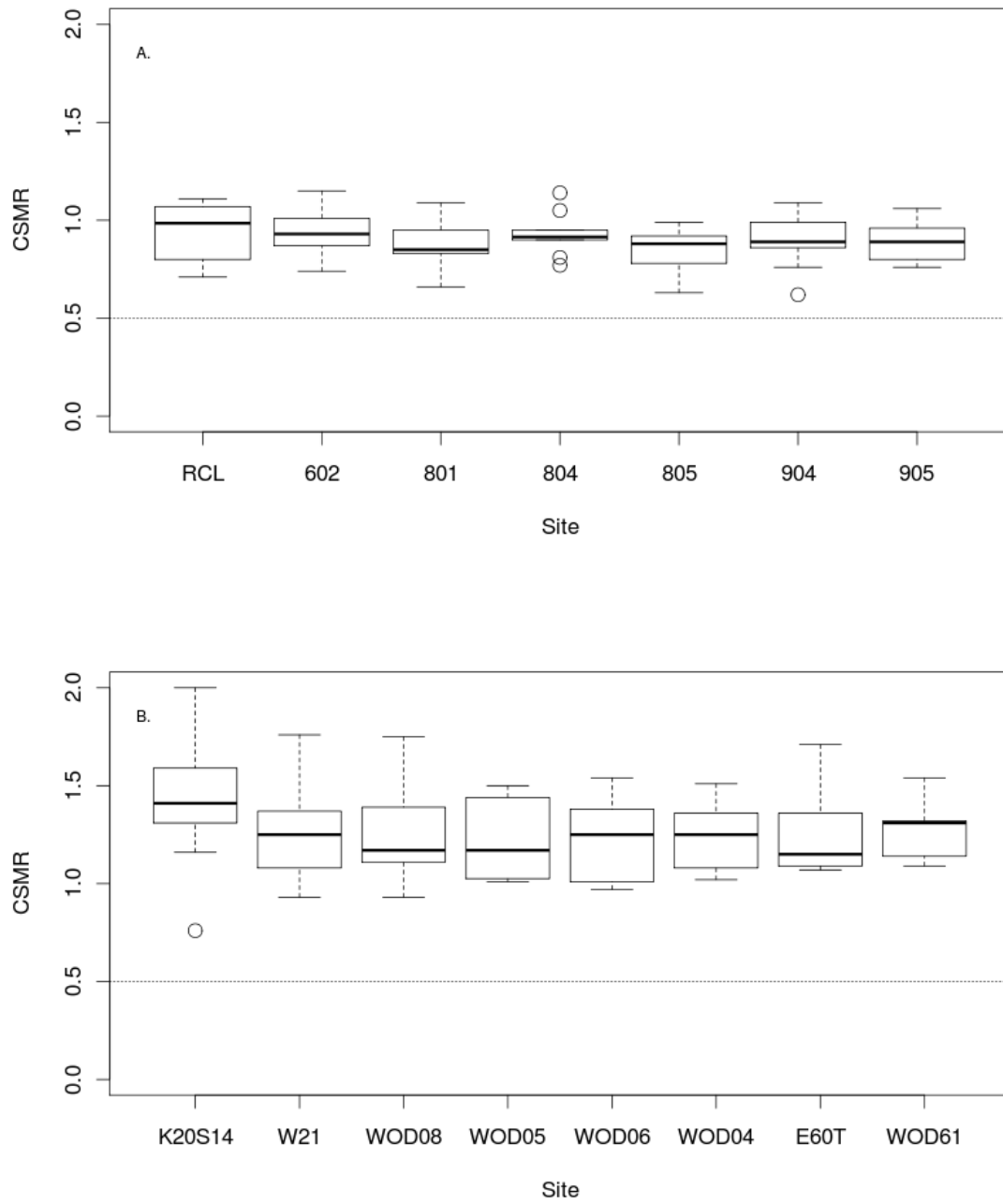


Figure 4.3: Chloride-to-Sulfate Mass Ratios (CSMR) for samples taken from (A) Toronto and (B) Waterloo distribution systems. A dotted line indicates CSMR >0.5, which may promote corrosion.

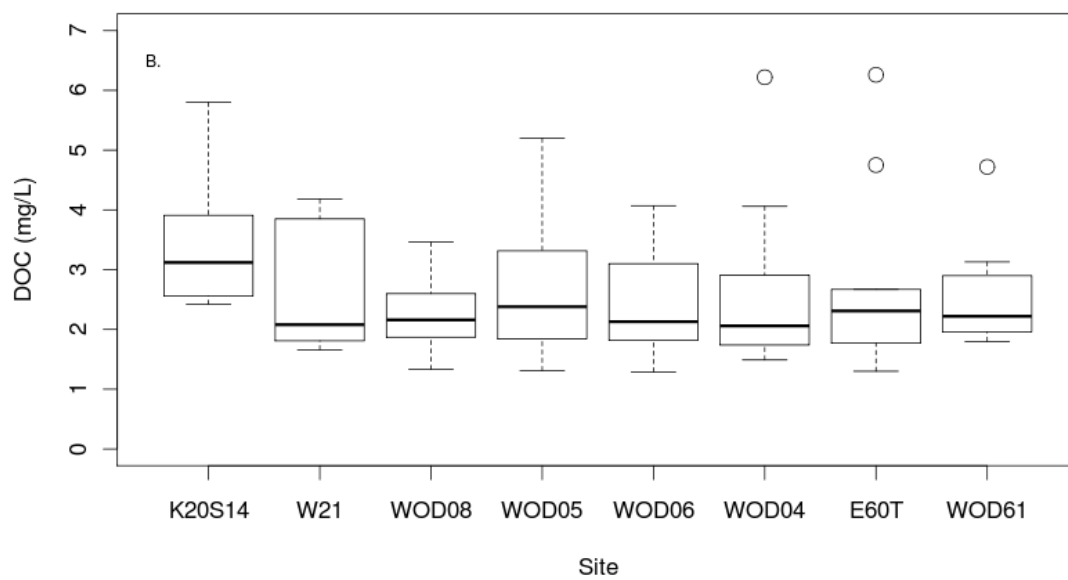
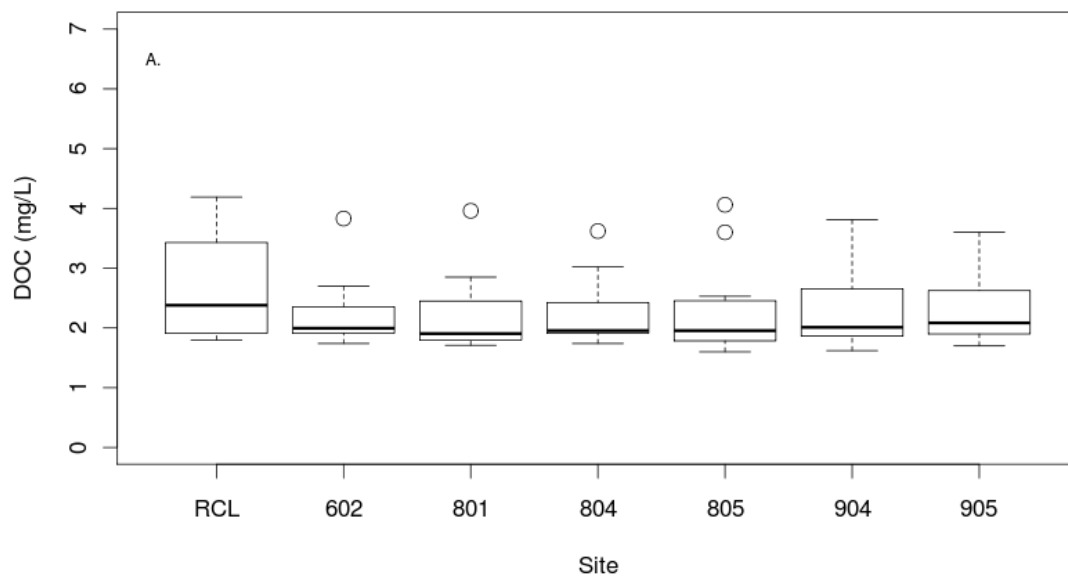


Figure 4.4: Boxplots summarizing DOC measurements for each site (A—Toronto sites; B—Waterloo sites).

variance in free ammonia concentrations at the dead-end site WOD06.

Dissolved oxygen (DO) was also measured in this research. This data is only available for some samples; results are listed in Table A.2 (Appendix A). For the sampling dates when DO measurements were obtained, the average dissolved oxygen concentration at Toronto distribution system sites was 9.5 mg/L, with a range of 6.8–12.9 mg/L. Waterloo distribution system sites had an average of 7.7 mg/L and a range of 3.9–14.9 mg/L. It should be noted that none of the Toronto DO concentrations were obtained in the summer, while the Waterloo DO measurements were evenly divided between summer and winter. Since DO levels are dependent on the water temperature the lower average and greater range observed in the Waterloo distribution system is likely a result of broader seasonal effects. According to Rittmann and McCarty (2001), complete nitrification has an oxygen demand of 4.14 g O₂/g NH₄⁺ so DO will not be a limiting factor for nitrification in either distribution system (both have ammonia-nitrogen <1.0 mg/L). A drop in DO has been suggested as a good indicator of nitrification by Odell *et al.* (1996), while AWWA (2006) listed it as an indicator of limited usefulness. Insufficient data were obtained in this study to evaluate DO as an indicator for nitrification.

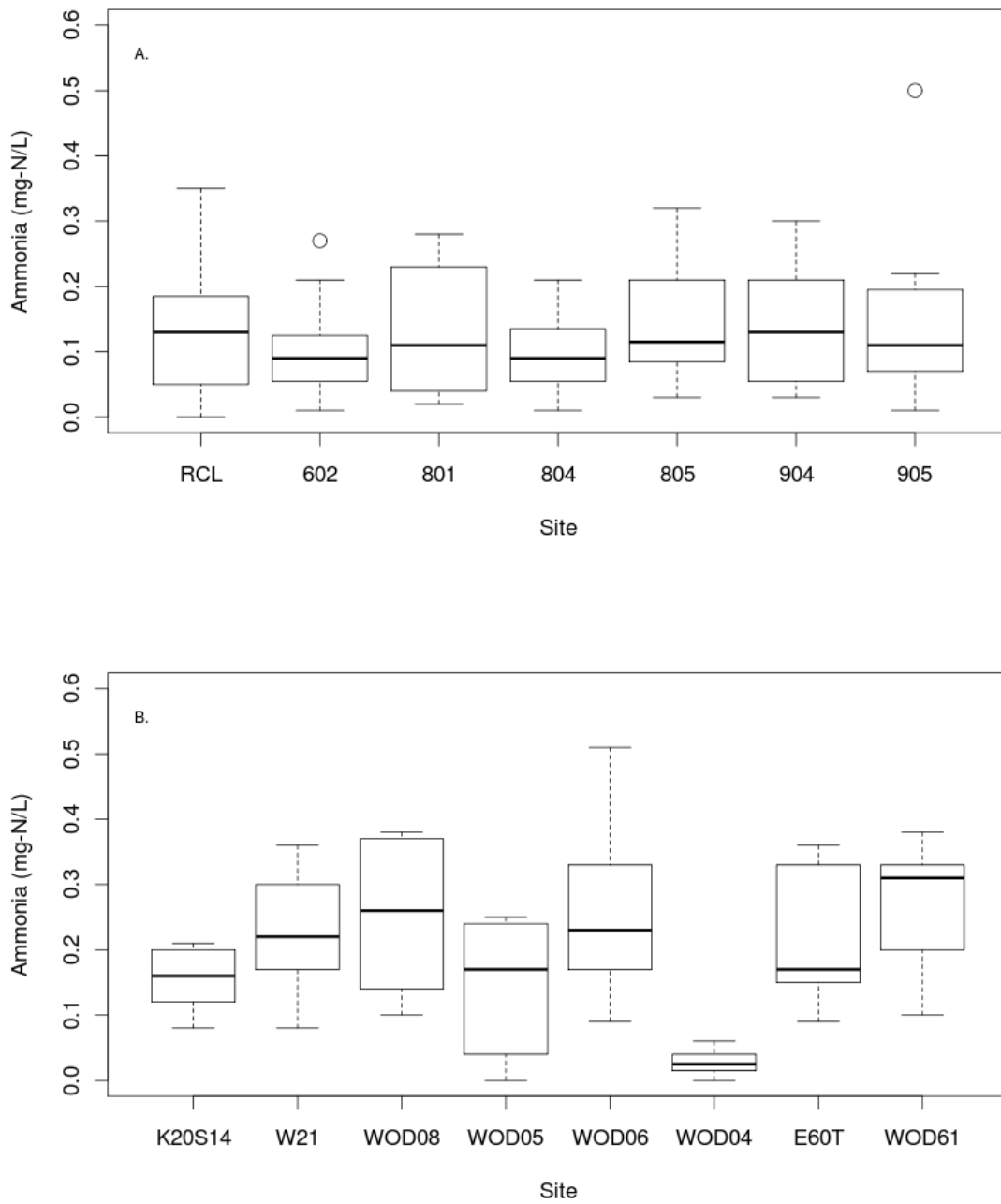


Figure 4.5: Boxplots of the average and range for ammonia-nitrogen (mg/L $\text{NH}_3\text{-N}$) at each site (A—Toronto sites; B—Waterloo sites). Site WOD04 is free-chlorinated, and as expected has negligible ammonia concentrations.

Physico-Chemical Indicators of Nitrification

Because there can be many competing processes impacting water quality in drinking water distribution systems it is not always straight-forward to detect when a complex process such as nitrification is occurring. One indicator that is commonly used is a rise in nitrite levels, since nitrite is normally at very low levels in distribution systems. Figure 4.6 summarizes the nitrite data collected for each site; more detailed results for each sample site are included in Figures 4.7 and 4.8. These results show that the average nitrite levels were well below 0.01 mg-N/L in both distribution systems, although they were slightly higher at most Waterloo sites than in the Toronto distribution system. Typically, the exceedance of some threshold level of nitrite is taken as an indication of nitrification; various threshold values have been proposed. In this study, nitrite levels remained near or below 0.01 mg/L NO₂-N on most occasions, and only once exceeded 0.05 mg/L NO₂-N, a threshold offered by Odell *et al.* (1996). However, Pintar *et al.* (2005) found that this threshold was too high to serve as an effective early warning indicator of nitrification. The reaction between nitrite and monochloramine (Vikesland *et al.*, 2001) can oxidize nitrite while contributing to decay of the disinfectant residual. Other nitrite thresholds for identifying nitrification suggested in the literature are 0.025 mg-N/L (i.e. Fleming *et al.* 2005) and 0.015 mg-N/L (AWWA, 2006). These lower thresholds were sometimes exceeded in the Waterloo distribution system. Other authors (Fleming *et al.*, 2008) have recommended looking for a rise in nitrite above base-line values, rather than any numerical threshold; applying that definition to the data here would add some additional exceedance occurrences. Whatever nitrite threshold is used, the only exceedances were outliers (shown as circles on the plot) rather than entrenched conditions. There were no large or prolonged increases in nitrite in the distribution systems evaluated for this project, indicating that no serious nitrification episodes occurred at any of the sites in this study during the period of the sampling campaign. The outliers of elevated nitrite concentrations are interpreted as probable indicators of minor nitrification instances. In the Waterloo distribution system, five sampling sites (W21, WOD05, WOD06, E60T, and WOD61) had nitrite concentrations >0.025 mg-N/L on a single occasion, all of which occurred on 27 May 2010. However, the total chlorine residual remained above 0.7 mg-Cl₂/L at each of these sites on this date.

Time-series plots of nitrogen species (ammonia, nitrite, and nitrate) are presented in Figures 4.7 (Toronto) and 4.8 (Waterloo). As nitrification converts ammonia to nitrate via nitrite, changes in the balance of nitrogen species can reveal nitrification occurring in a distribution system. In the Toronto distribution system, the most notable trend is a rise in ammonia levels in the warmer summer months. This could be a result of monochloramine decay. This trend is also visible at most of the sites monitored in the Waterloo distribution system, with the exception of WOD04, which is free chlorinated. In Waterloo, small rises in nitrite can be seen at some sites in the warmer months. In many cases (i.e. W21, WOD06,

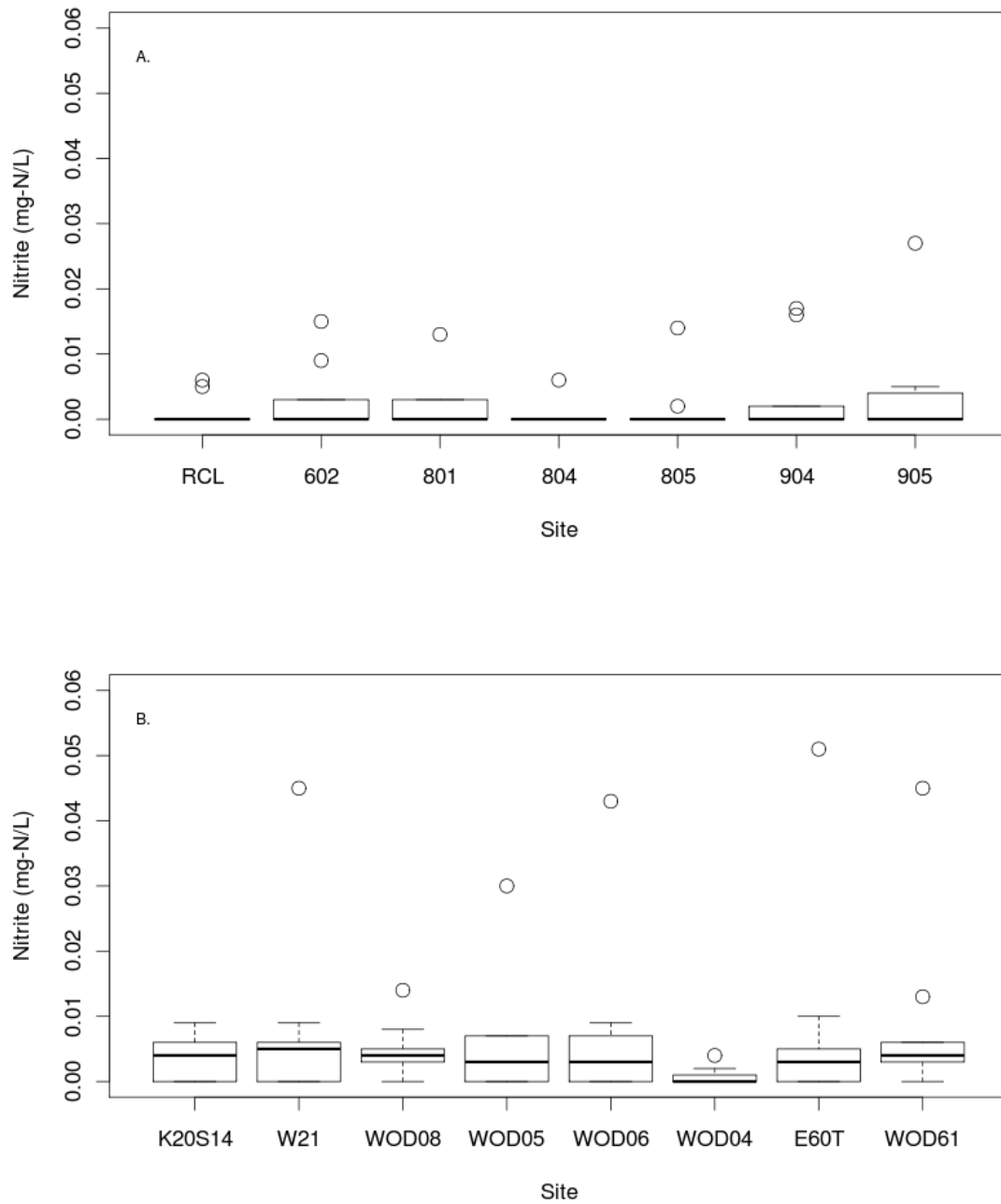


Figure 4.6: Boxplots summarizing nitrite readings (in mg/L NO₂-N) for each site (A—Toronto sites; B—Waterloo sites) over the course of the sampling campaign. Open circles are statistical outliers.

E60T) the rise in nitrite was preceded by an increase in the ammonia concentration on the prior sampling date. For nitrate, there were no clear trends in either distribution system. The nitrate concentrations measured at distribution system sites did not differ greatly from those entering each distribution system (i.e. at sites RCL and K20S14). Complete nitrification would also increase the amount of nitrate present in distribution system samples. However, care needs to be taken to distinguish increases in nitrate due to nitrification from changes in the background concentration entering the distribution system. This study lacks information on distribution system residence times, so it was not able to follow plugs of water through the distribution systems. Therefore, the nitrate data presented here is difficult to use as an indicator of nitrification. Developing an accurate nitrogen balance was one of the top recommendations of Wilczak *et al.* (1996) for drinking water system operators concerned about nitrification.

Time-series plots of total chlorine residuals are presented in Figures 4.9 and 4.10. Temperatures are also shown on these plots. A declining residual can be an indicator of nitrification (Pintar *et al.*, 2005), although there are other potential causes such as long retention times at dead ends (Zhang *et al.*, 2009b). From an operational and regulatory perspective, this decline in the disinfectant residual is usually the most urgent consequence of distribution system nitrification. Canadian drinking water providers are required to maintain a disinfectant residual throughout the entire distribution system to protect water quality until it is delivered to consumers (Health Canada, 2002). Combined chlorine residuals in both systems were always within the 0.25–3.0 mg/L range required for distribution systems in Ontario (Ontario Ministry of the Environment, 2006). In the Waterloo distribution system (Fig. 4.10), a decrease in the total chlorine residual occurred in the summer months at several sites (W21, WOD08, WOD05, WOD06, E60T, and WOD61). The residual at the entrance to the distribution system (site K20S14) remained stable. Disinfectant residuals had less seasonal variability in the Toronto distribution system (Fig. 4.9), although there were slight decreases in July and August at sites 805 and 904. Seasonal variations in the stability of the chloramine residual are expected because the decay rate of monochloramine increases at higher temperatures (Vikesland *et al.*, 2001). Yang *et al.* (2007) found that the water temperature had a statistically significant contribution to the risk of nitrification in a pilot scale distribution system. It should be noted that Pintar *et al.* (2005) conducted an earlier study on nitrification in the Waterloo distribution system, including some sites that were sampled in this study. Compared to their findings, much greater stability (less seasonal variation) of the chloramine residual was observed in the present work.

The results described here may be interpreted to show that there were small amounts of nitrification underway at some sites on some occasions. Specifically, the nitrite threshold of 0.015 mg-N/L given by AWWA (2006) as an indicator of nitrification was exceeded at sites 904 and 905 in the Toronto distribution system and at sites W21, WOD05, WOD06, E60T,

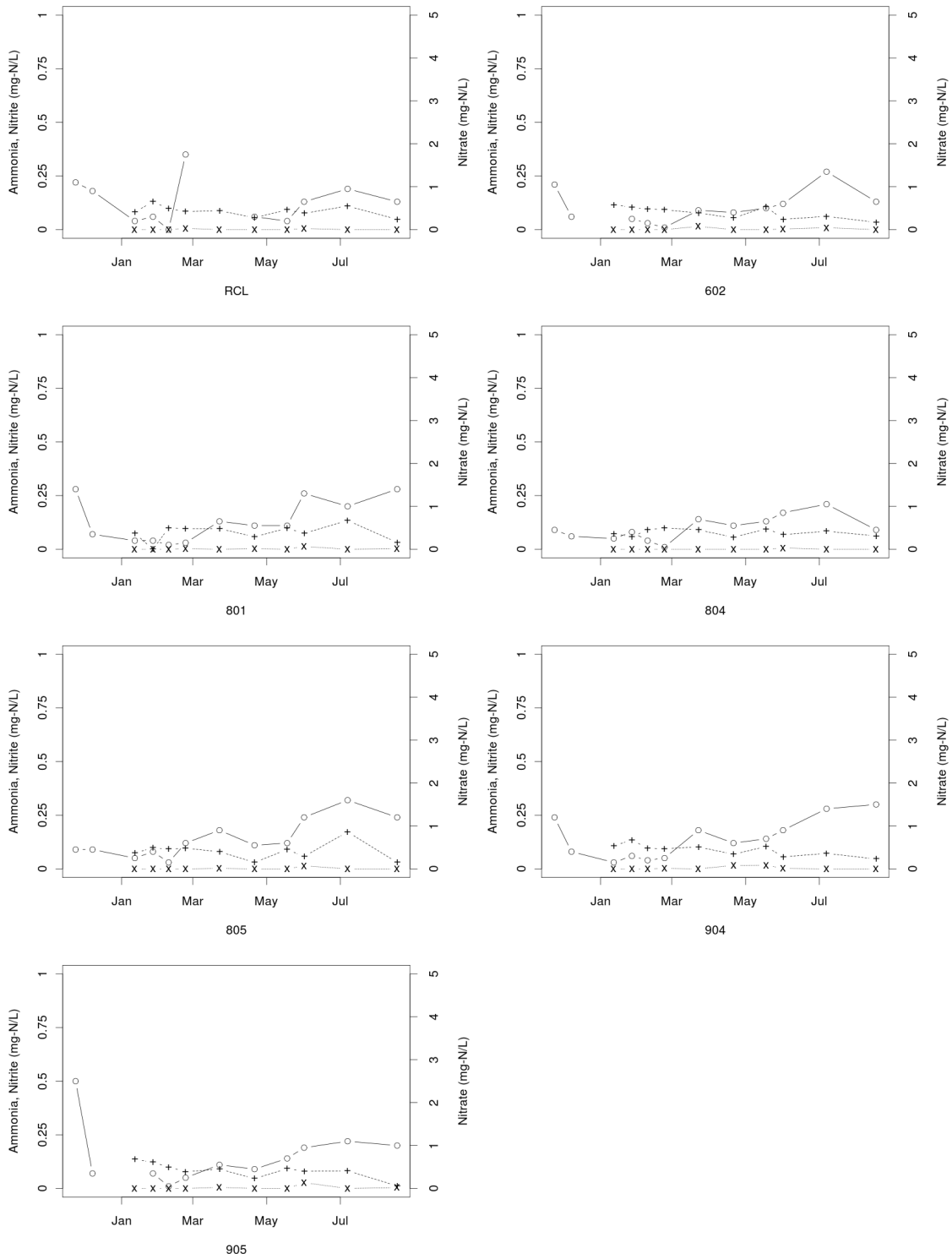


Figure 4.7: Time-series plots of ammonia (o), nitrite (x), and nitrate (+) measured as mg-N/L at each Toronto site. Nitrate is plotted on the right vertical axis.

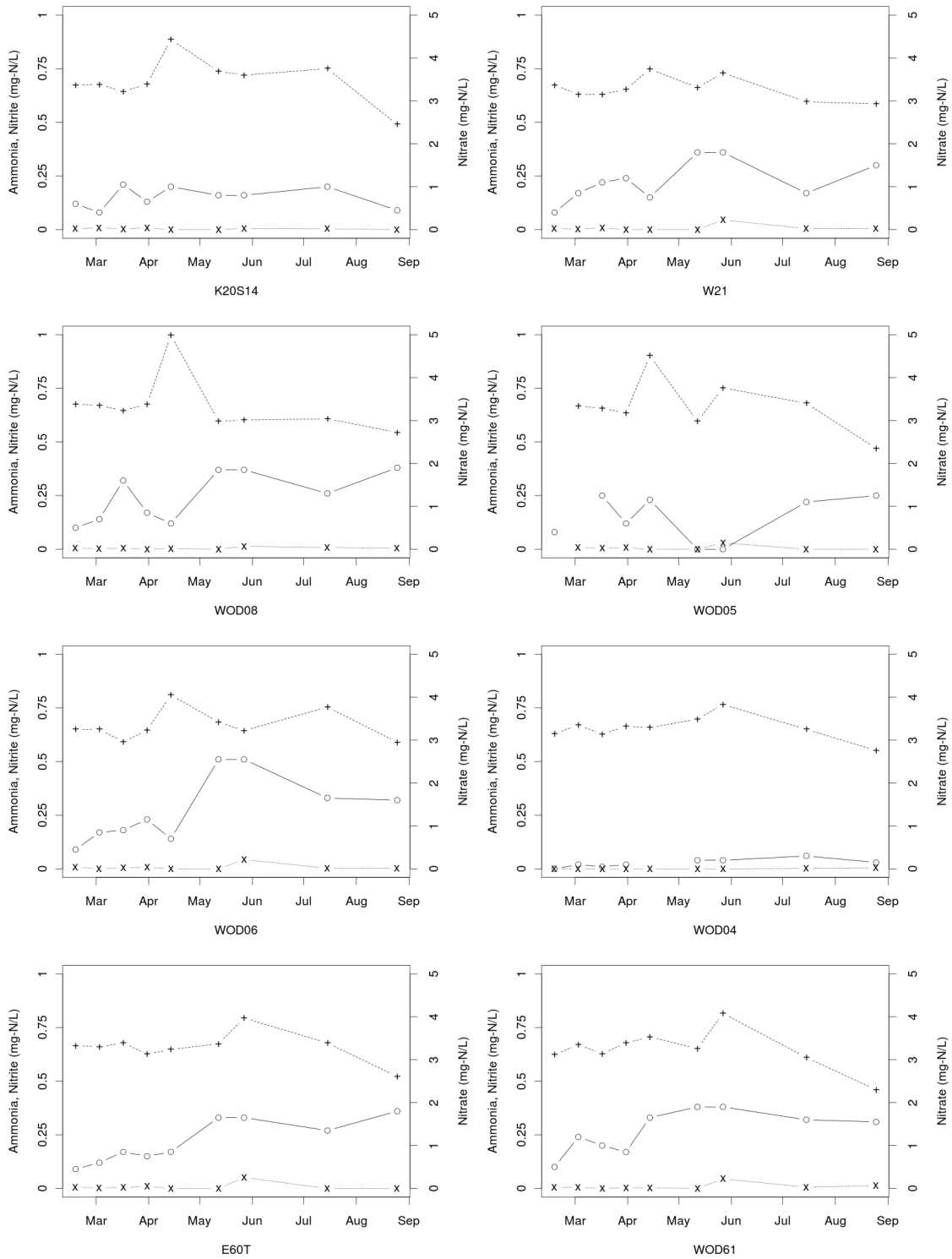


Figure 4.8: Time-series plots of ammonia (o), nitrite (x), and nitrate (+) measured as mg-N/L at each Waterloo site. Nitrate is plotted on the right vertical axis.

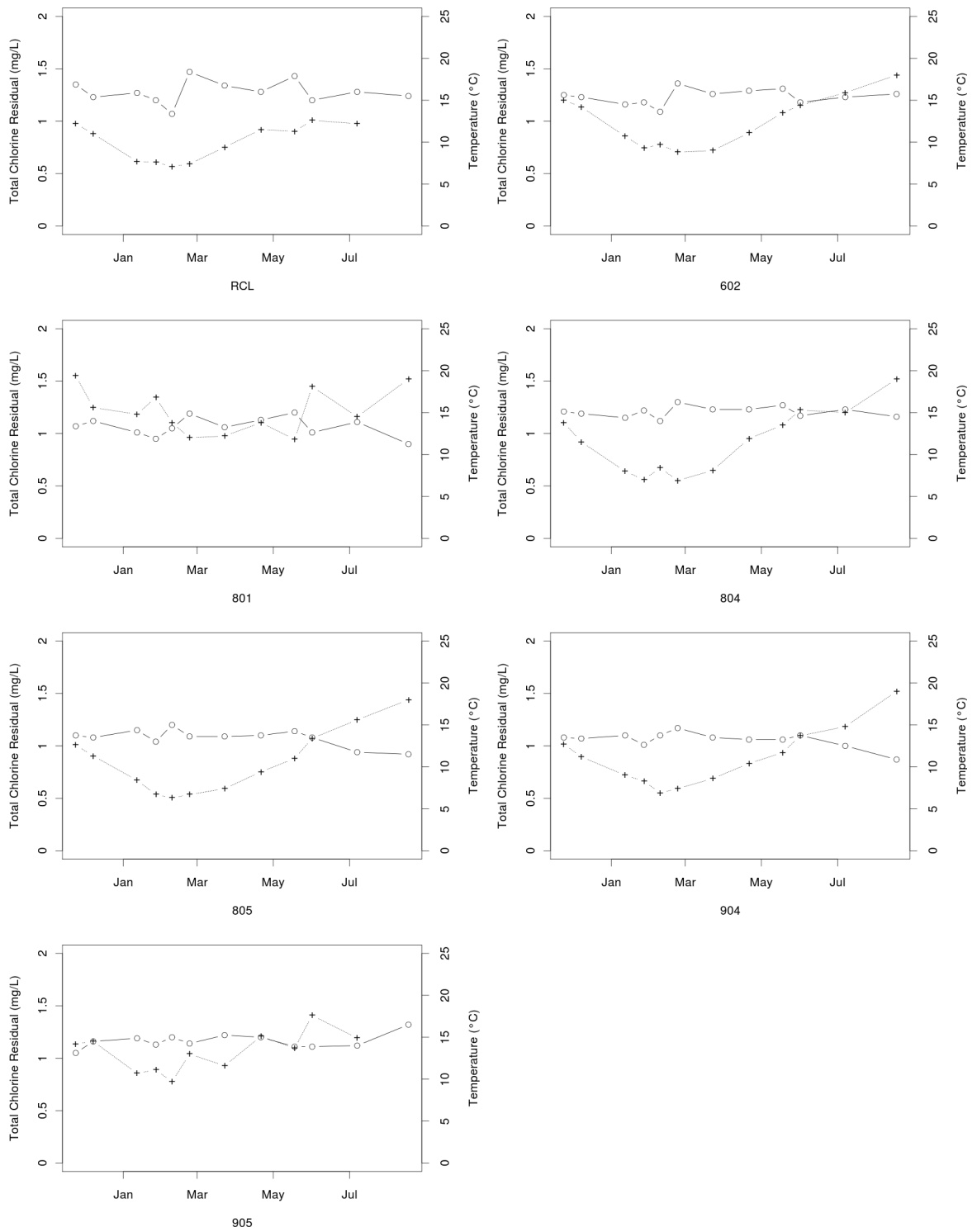


Figure 4.9: Time-series plots of the total chlorine residuals (o), in mg/L Cl_2 , and temperatures (+), in $^{\circ}\text{C}$, at each Toronto site.

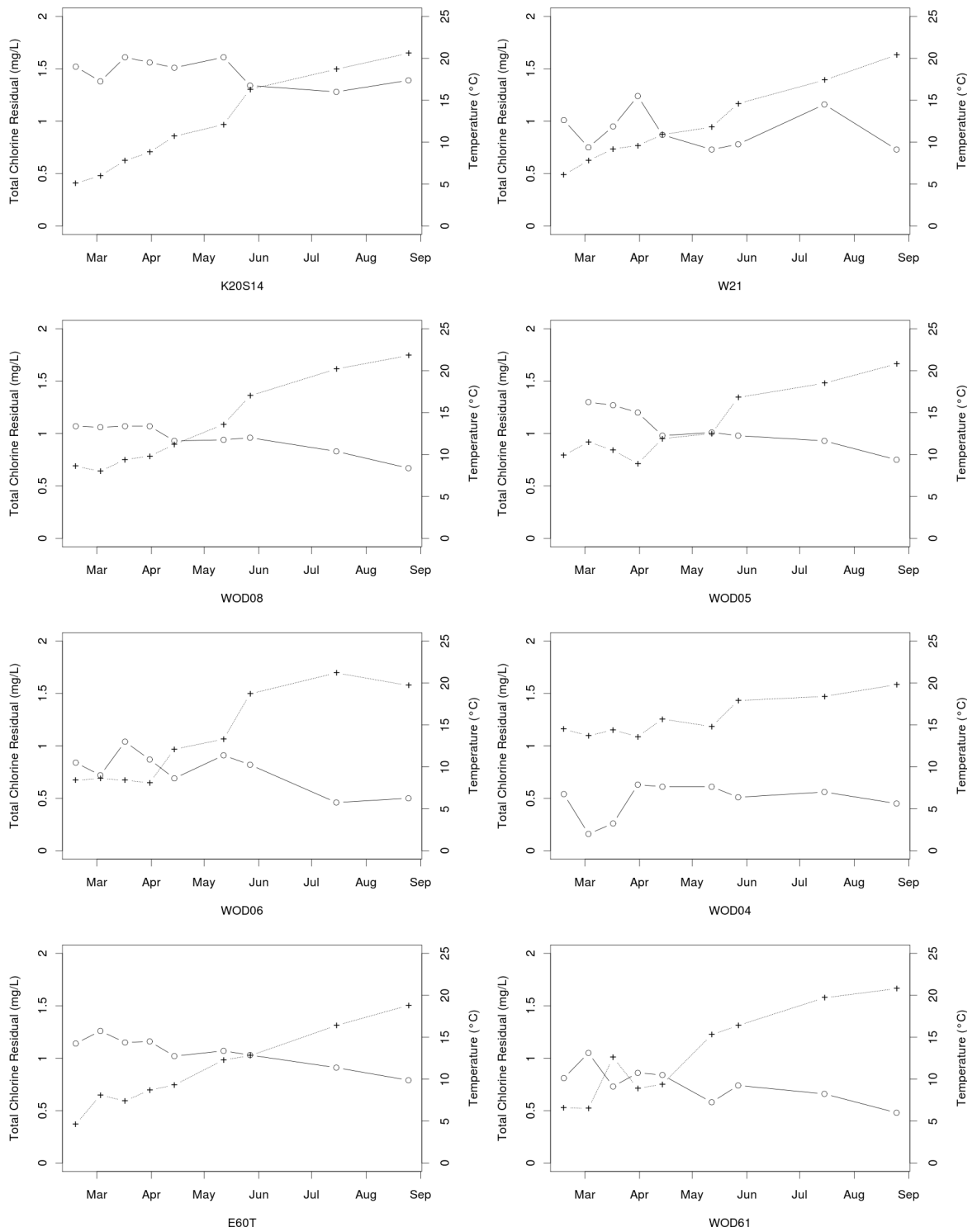


Figure 4.10: Time-series plots of the total chlorine residuals (o), in mg/L Cl₂, and temperatures (+), in °C, at each Waterloo site.

and WOD61 in the Waterloo distribution system. However, in a fully-developed episode of nitrification, a sharp decline in the disinfectant residual would be expected, and there would likely be a greater accumulation of nitrite than was observed here. Based on the parameters monitored in this study, no fully-developed nitrification episodes were observed in the course of this sampling campaign. Compared to the results of Pintar *et al.* (2005), the Waterloo distribution system appears to be better controlled with respect to nitrification. Chloramine residuals only showed moderate declines at some sites and nitrite levels remained below the 0.05 mg-N/L threshold that they evaluated, with only one exception (E60T).

Occurrence of Nitrifying Microorganisms and Heterotrophs

To date only a few studies (van der Wielen *et al.*, 2009; Kasuga *et al.*, 2010b,a) have examined both AOB and AOA in drinking water. Since most existing information on ammonia-oxidizers is for bacteria (AOB), the occurrence of AOA in distribution systems is of interest, as they may have different growth and survival properties in distribution system environments. For example, Martens-Habbena *et al.* (2009) found a half-saturation coefficient for ammonia in a strain of AOA that was lower than any reported for AOB. Kasuga *et al.* (2010b) suggested that AOA and AOB might differ in their resistance to chlorine. Indeed, questions of the relative abundance and respective roles in nitrification of AOA and AOB are topics of active research (Schleper, 2010; Prosser and Nicol, 2008).

Using a PCR approach targeting the *amoA* genes of either AOB or AOA, both groups of ammonia-oxidizing microorganisms were detected. Results are presented in Figures 4.11 and 4.12, for Toronto and Waterloo distribution systems, respectively. These figures show that at Toronto sites AOB are normally more numerous than AOA. Both types of ammonia oxidizing microorganisms were detected intermittently at low levels at the entrance to the distribution system (site RCL). At site 602 (closest to the WTP) AOA were always below the detection level during this sampling campaign, while at site 905 (farthest from the WTP) AOA outnumbered AOB on two sampling dates. In the Waterloo distribution system, the numbers of AOA and AOB were similar at many sites. AOA were more abundant at the entrance to the distribution system (site K20S14), while AOB were more abundant at more distant sites: WOD05, WOD06, and WOD61. Site WOD04, which has a free chlorine disinfectant residual, had very low levels of both types of ammonia-oxidizing microorganisms compared to other sites, in accord with nitrification being an issue primarily in chloraminated drinking water distribution systems. Overall, AOA were more abundant in the Waterloo distribution system, but they were present in both systems investigated in this work. This is a significant result as AOA have not been included in most previous studies of nitrification in drinking water. Future research should not neglect this group of nitrifying microorganisms.

The ratios of AOA to AOB, and how they changed between sites and temporally, are

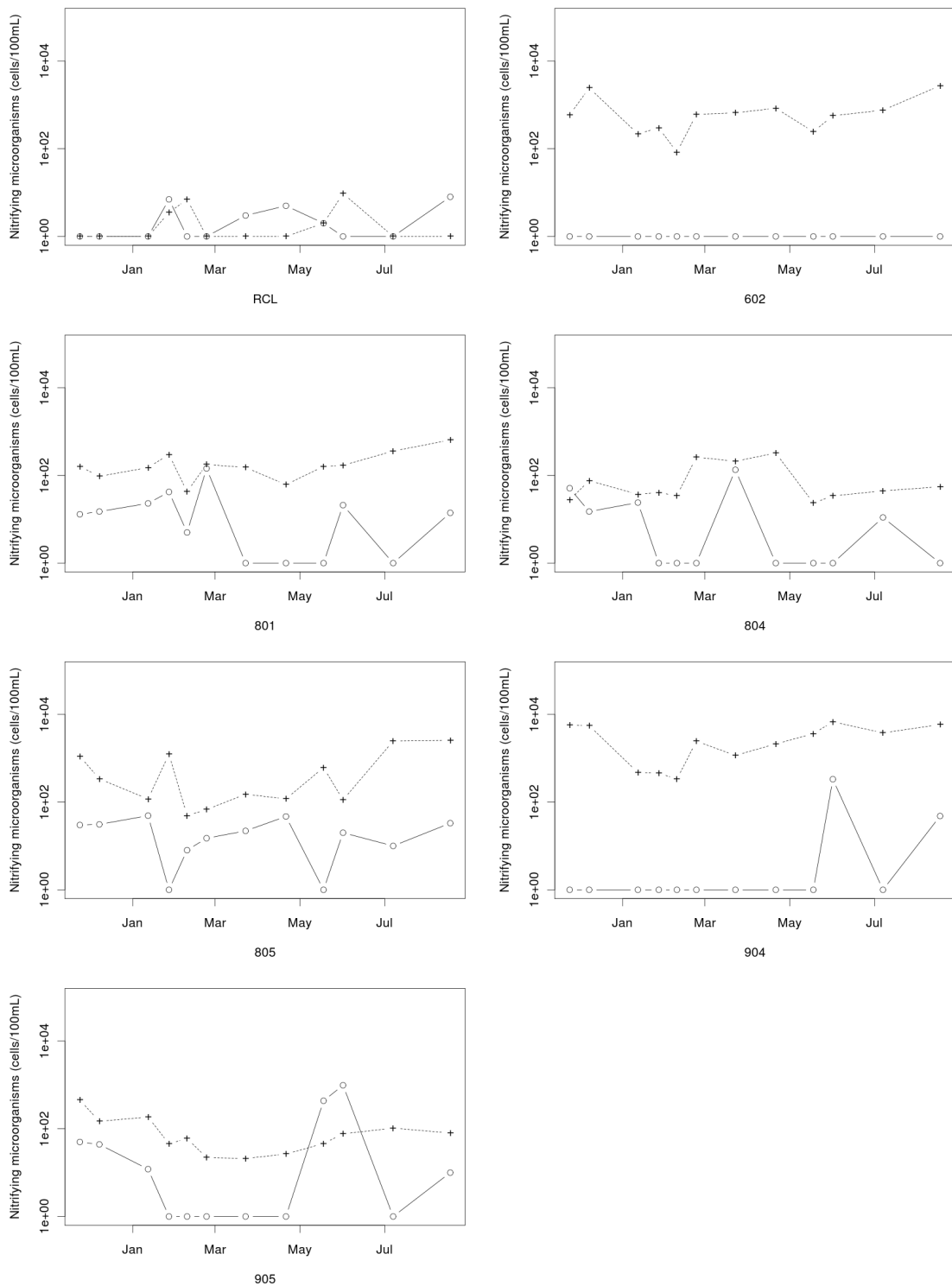


Figure 4.11: Time-series plots of AOB (+) and AOA (o) occurrence at each site in the Toronto distribution system. Ammonia-oxidizing microorganisms are expressed as cells per 100 mL. An arbitrary value of 1 was added to each cell count to facilitate plotting non-detects on a log-scale.

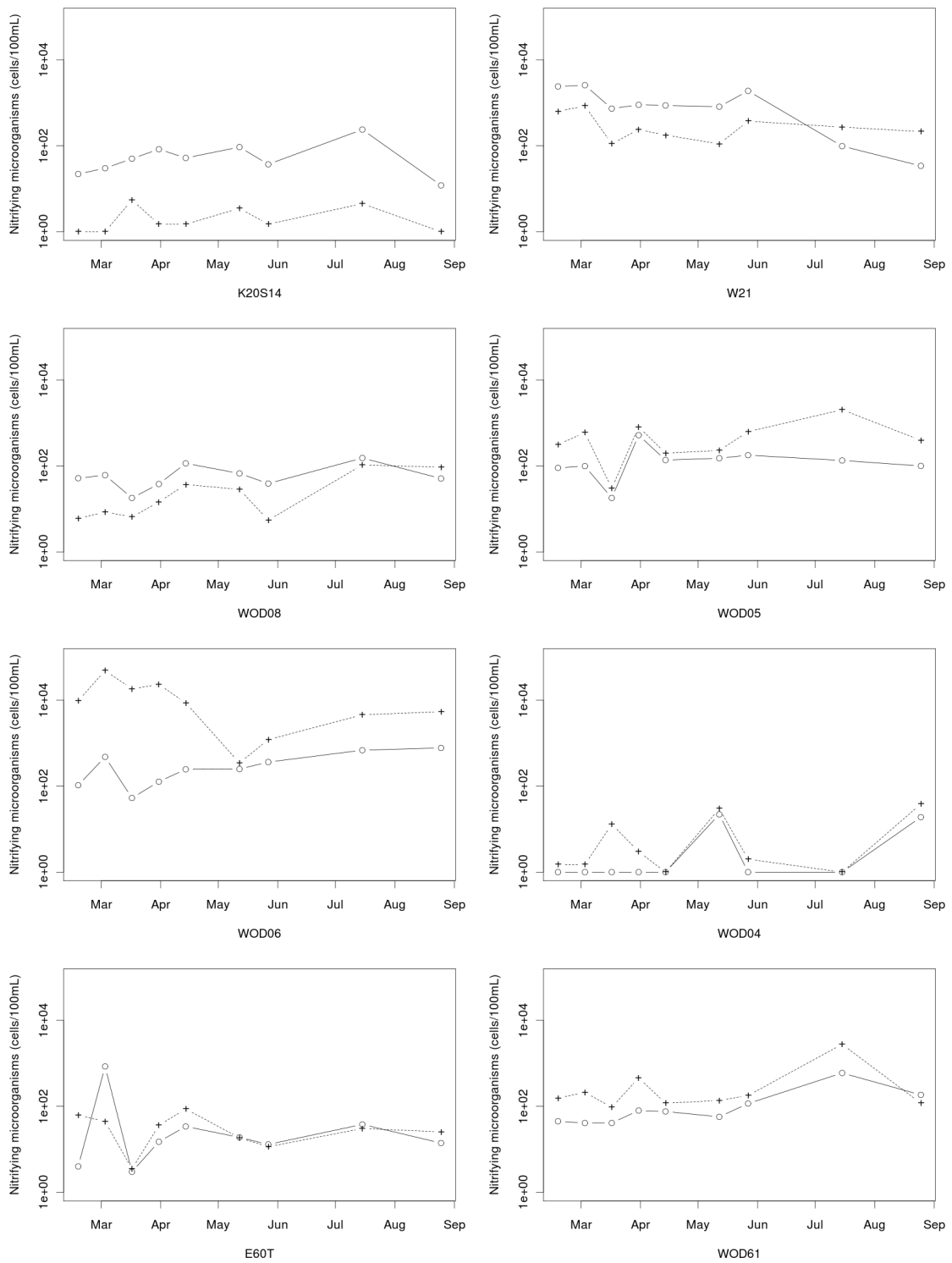


Figure 4.12: Time-series plots of AOB (+) and AOA (o) occurrence at each site in the Waterloo distribution system. Ammonia-oxidizing microorganisms are expressed as cells per 100 mL. An arbitrary value of 1 was added to each cell count to facilitate plotting non-detects on a log-scale.

shown in Figures 4.13 and 4.14. In these figures, ratios are undefined—and thus not plotted—when AOB were below the detection limit. The most interesting observation to be made from these figures is the dominance of AOA in the sites closest to the water treatment plant in the Waterloo distribution system (K20S14, W21, and WOD08). However, this ratio declines in the summer (July and August 2010). One possible reason for the greater numbers of archaeal ammonia oxidizers in the early portion of the Waterloo distribution system is their greater abundance in the source water (see Table 3.1 in Chapter 3). Differences between AOA and AOB in survival through disinfection or other treatment processes have also been suggested (Kasuga *et al.*, 2010b).

To complement the nitrifier occurrence data obtained from molecular methods, a culture-based test for ammonia-oxidizing microorganisms was also employed. This was done because PCR detects intact DNA from both live and dead cells; applying a culture-based test can verify whether any viable cells are present. Table 4.1 shows that the majority of sites were positive for nitrifiers. Both PCR and culture-based testing have thus shown the presence of nitrifying microorganisms, even at sites in these chloraminated distribution systems where little nitrification appears to be occurring. Comparison with PCR results does not reveal a straight-forward threshold of the number of gene copies that must be present to get a positive result with a culture-based test. This is not surprising, as not all bacteria are culturable (Hoefel *et al.*, 2005).

Table 4.1: Summary of the presence/absence (P/A) of culturable nitrifiers from each distribution system site in August 2010 (17th—Toronto, 25th—Waterloo). AOB and AOA cells enumerated by qPCR (reported as cells/100 mL) for the same sample dates are included for comparison. P/A sample volume was 1 L; qPCR sample volume was 100 mL.

Toronto	P/A	AOB	AOA	Waterloo	P/A	AOB	AOA
RCL	Negative	0	7	K20S14	Positive	0	11
602	Positive	2730	0	W21	Positive	213	33
801	Positive	640	13	WOD08	Positive	93	50
804	Negative	54	0	WOD05	Positive	393	99
805	Positive	2545	32	WOD06	Positive	5400	773
904	Positive	5850	47	WOD04	Positive	38	18
905	Positive	79	9	E60T	Positive	25	13
				WOD61	Positive	117	184

In addition to nitrifying microorganisms, heterotrophic bacteria were also enumerated (Figure 4.15). Heterotrophic plate counts (HPC) are presented as colony forming units (CFU) per 100 mL. HPC are commonly recommended as a general indicator of microbiological water quality (Health Canada, 2011; National Research Council, 2006). A rise in

HPC may indicate nitrification (Skadsen, 1993; Wilczak *et al.*, 1996; Odell *et al.*, 1996; Zhang *et al.*, 2009b). Two mechanisms by which nitrification can promote the growth of heterotrophic bacteria are accelerating the decay of the disinfectant residual and contributing to the organic carbon substrate available in the distribution system by the formation of soluble microbial products (SMP) by nitrifiers (Rittmann *et al.*, 1994).

In contrast to normal bacterial sampling procedures, the samples used here, for both nitrifiers and HPC, were taken from the first flush of the tap, rather than after flushing. This was done because conditions in stagnant water are more likely to favour nitrification. First-flush samples also collect bulk water that has had a greater opportunity to approach equilibrium with the biofilm. However, as the taps had other users, constant stagnation times could not be guaranteed between sites or between sampling dates, adding variability to the results. Site WOD08 in the Waterloo distribution system was in a cafeteria kitchen, for example, so the somewhat lower HPC observed there may reflect the shorter stagnation times it was subject to. The lower HPC levels for the sites at the entrance to each distribution system (less than 1 CFU per mL on most sampling dates), as compared to more distant sites, suggests that conditions are supportive for bacterial regrowth in both distribution systems studied here. This supports the comment of Huck and Gagnon (2004), who conceptualized distribution systems as bioreactors, that regrowth in a distribution system is the primary source of HPC bacteria. Also of note is that the site with the free chlorine disinfectant residual, WOD04, has comparable HPC to nearby sites, while its levels of AOB and AOA were much lower. This suggests that nitrifiers are being controlled at this site by the limitation of their ammonia substrate, more than by the superior disinfection strength of free chlorine, which should have a similar effect on HPC.

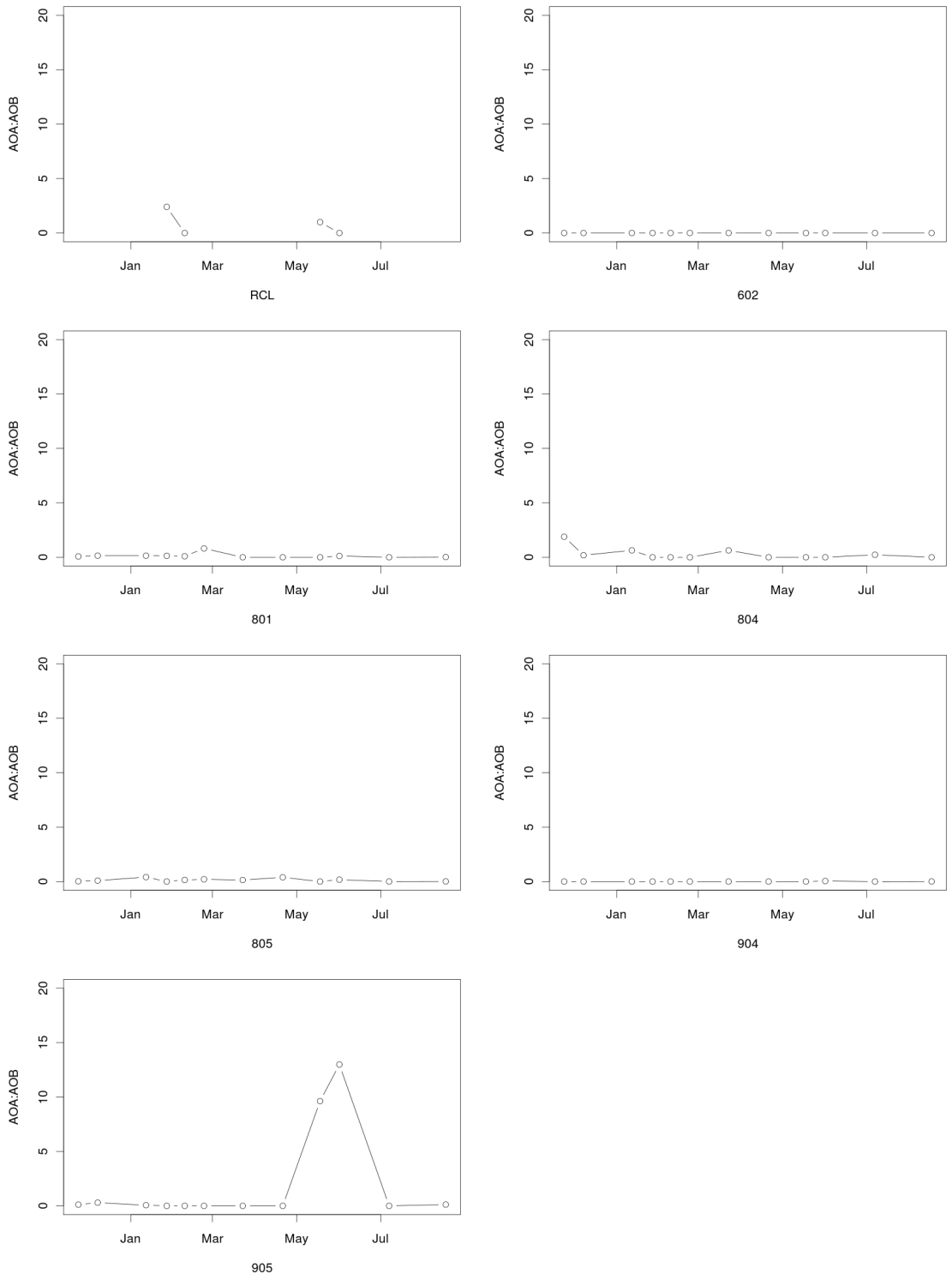


Figure 4.13: Changes in the AOA:AOB ratio over time and between sites in the Toronto distribution system over the course of this study. The ratio is undefined—and not plotted—when AOB were not detected.

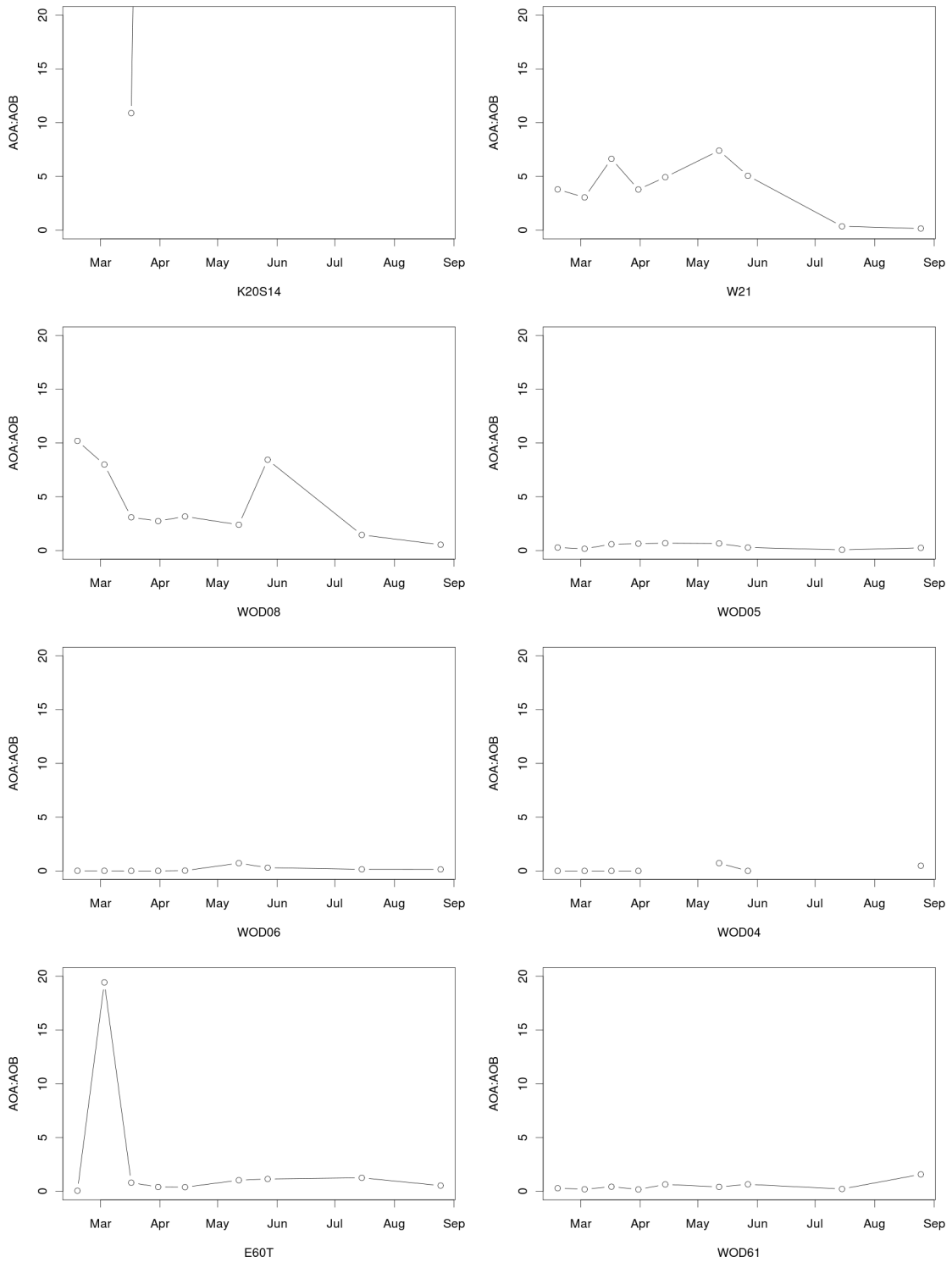


Figure 4.14: Changes in the AOA:AOB ratio over time and between sites in the Waterloo distribution system over the course of this study. Note that the ratio was >20 for some samples from K20S14, but the scale was limited to show more detail. The ratio is undefined—and not plotted—when AOB were not detected.

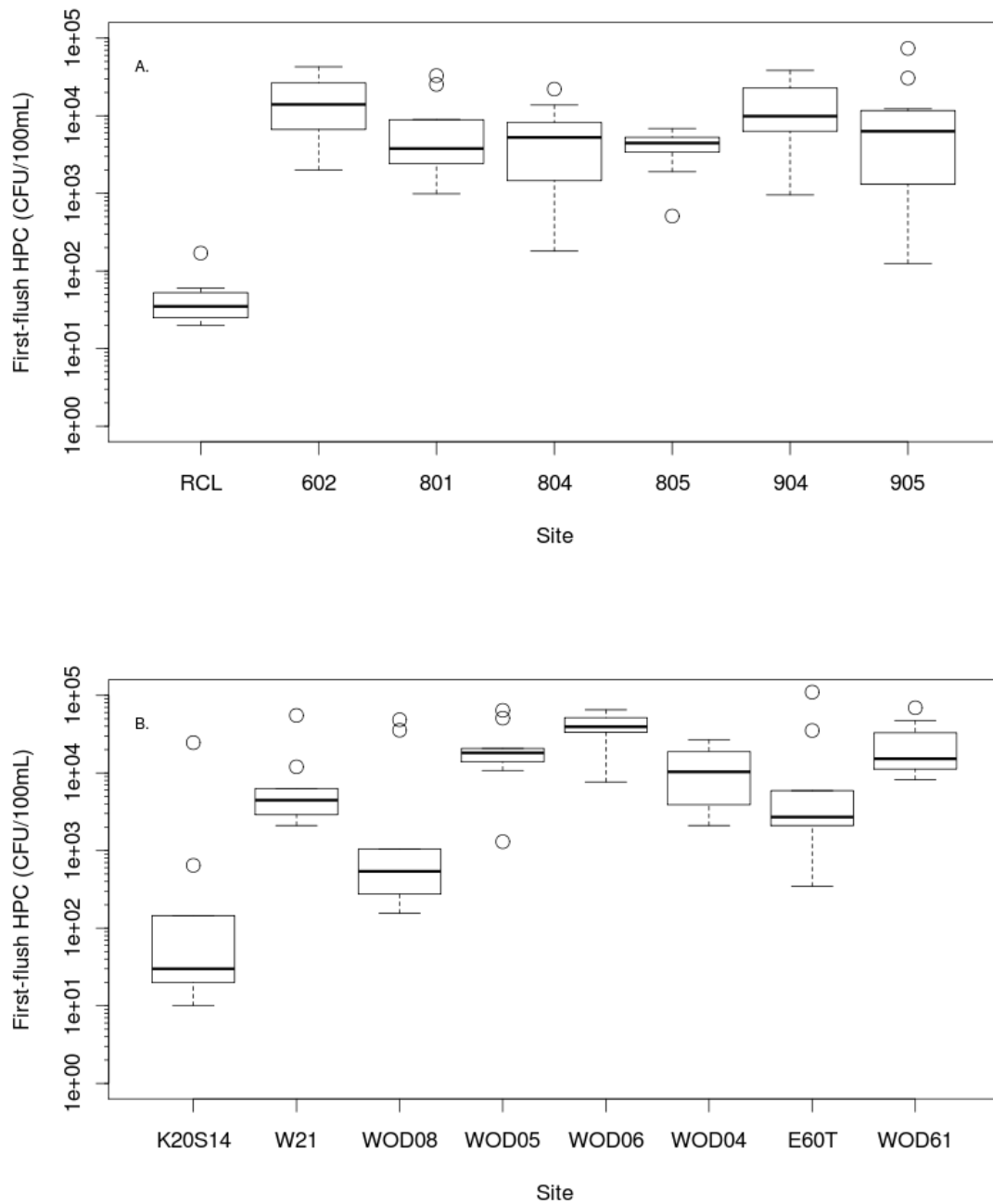


Figure 4.15: Heterotrophic bacteria (HPC) summarized for each site (A—Toronto sites; B—Waterloo sites) as boxplots. Note that the vertical axis is a logarithmic scale, with results expressed in CFU/100 mL and that these results are from first-flush samples.

Statistical Interpretation of Sampling Results

In Table 4.2, Spearman correlation coefficients (ρ) are presented to compare selected water quality parameters in each distribution system, along with the statistical significance of each correlation. Non-parametric Spearman correlations do not necessarily indicate a linear relationship between variables as they are calculated based on the relative ranks, rather than the value, of each data point. Correlations between parameters do not necessarily indicate a causal relationship as a third factor could be influencing both parameters. However, strong correlations have the potential to be useful in distribution system monitoring.

In this table, the total chlorine concentration is shown to have statistically significant negative correlations with AOB, AOA, and HPC bacteria in data from the Toronto distribution system, and with AOB and HPC in the Waterloo distribution system. In both distribution systems, there was a negative correlation between temperature and the total chlorine residual and a positive correlation between temperature and the ammonia concentration. This suggests greater chloramine decay occurs in warmer water. The ammonia concentration had a weak positive correlation with AOB in both distribution systems and with AOA in the Waterloo distribution system. Nitrite is a common chemical indicator for nitrification (AWWA, 2006), but was not found to be correlated with the abundances of ammonia-oxidizing microorganisms in this research. Perhaps of greatest interest are the correlations between the different groups of microorganisms, with AOB positively correlated with HPC levels in both distribution systems and AOA correlated with AOB in the Waterloo distribution system. In figure 4.16, AOB is plotted against HPC for each distribution system to illustrate the correlation that was found.

The negative correlations between total chlorine residuals and microorganism abundances were expected, and serve to remind drinking water system operators of the value of maintaining a suitable disinfectant residual at all sites. Because AOB and HPCs are significantly correlated with each other and with total chlorine in both distribution systems, partial correlation coefficients were determined to check to what degree the correlation between AOB and HPCs can be explained by their respective correlations with total chlorine. The partial correlation coefficients of AOB and HPC with total chlorine as the third factor are 0.48 and 0.54, for the Toronto and Region of Waterloo distribution systems respectively. These partial correlation coefficients are not greatly discounted from the plain Spearman correlations, suggesting that the correlation between AOB and HPC found in both distribution systems studied is not entirely explained by the strength of the total chlorine disinfectant residual. Previous studies have had similar findings on the relationship between the disinfectant residual and microbial occurrences in distribution systems. Lipponen *et al.* (2004) reported a negative correlation between the total chlorine residual and biofilm bacterial densities. Cunliffe (1991) also found a statistically significant relationship between total chlorine and

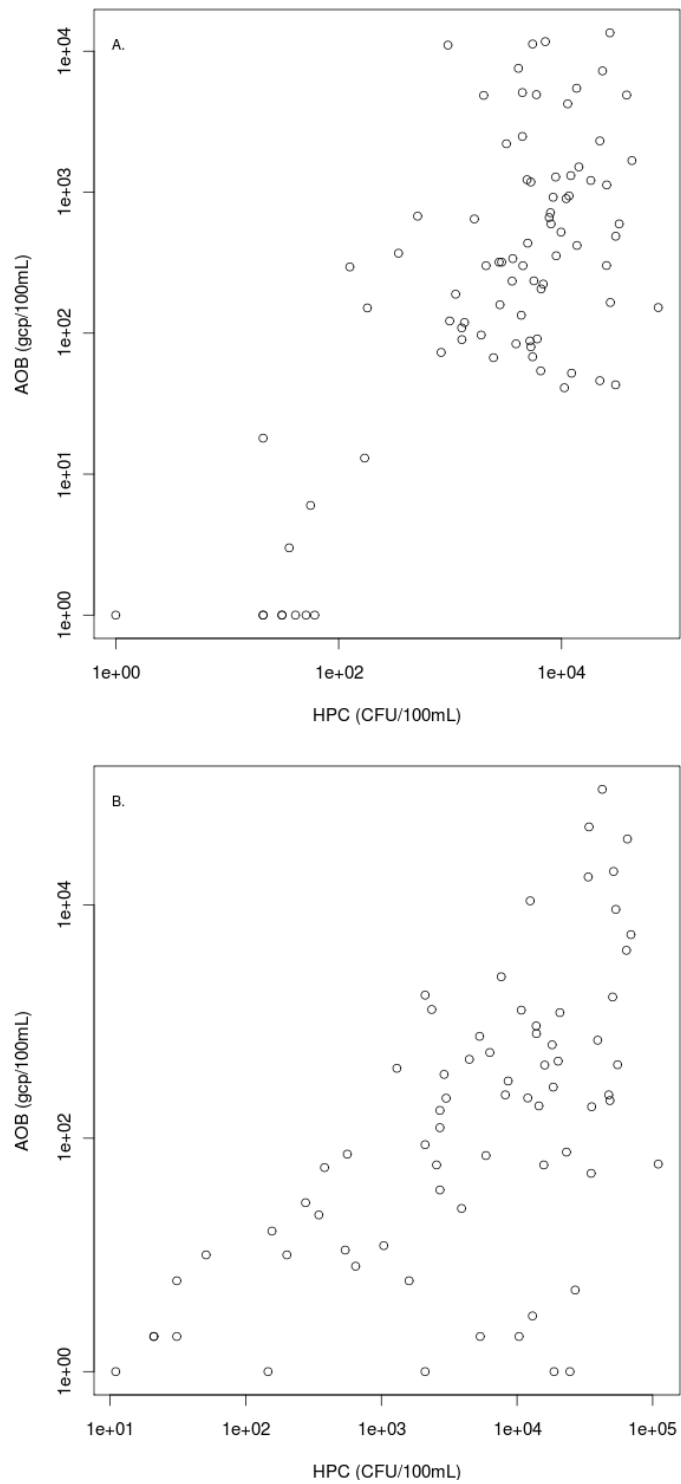


Figure 4.16: These plots illustrate the non-parametric (Spearman) correlations between AOB and HPC in the distribution systems of (A) Toronto and (B) Waterloo. Spearman correlations do not indicate a linear relationship, merely a mutually increasing one.

Table 4.2: Non-parametric Spearman correlations between parameters measured from two full-scale distribution systems.

Correlation		Toronto		Waterloo	
		ρ	p-value	ρ	p-value
Total Chlorine,	AOB	-0.45**	2.0E-05	-0.25*	3.2E-02
	AOA	-0.28**	9.1E-03	0.01	9.3E-01
	HPC	-0.21*	5.4E-02	-0.50**	1.1E-05
Temperature,	AOA	0.22*	4.8E-02	-0.03	8.1E-01
	AOB	0.18	1.1E-01	0.00	1.0E+00
	HPC	0.13	2.5E-01	0.38**	9.2E-04
	Total Cl ₂	-0.23*	4.1E-02	-0.51**	6.5E-06
	Ammonia	0.51**	1.4E-06	0.30*	1.2E-02
	Nitrite	0.20	1.0E-01	-0.11	3.7E-01
Ammonia,	AOB	0.21*	6.6E-02	0.27*	2.3E-02
	AOA	0.13	2.4E-01	0.29*	1.4E-02
	HPC	0.06	5.8E-01	0.16	1.9E-01
Nitrite,	AOA	0.06	6.3E-01	0.15	2.1E-01
	AOB	0.12	3.2E-01	0.17	1.5E-01
	HPC	0.17	1.5E-01	-0.03	8.2E-01
Nitrate,	AOA	-0.28*	1.9E-02	0.09	4.6E-01
	AOB	-0.04	7.7E-01	-0.13	2.8E-01
	HPC	-0.03	7.7E-01	-0.37**	1.6E-03
DOC,	AOA	0.14	2.2E-01	0.02	8.7E-01
	AOB	0.04	7.2E-01	-0.07	5.5E-01
	HPC	-0.15	1.9E-01	0.02	8.7E-01
AOA,	AOB	-0.01	9.1E-01	0.71**	2.7E-12
AOB,	HPC	0.51**	5.7E-07	0.58**	1.1E-07
AOA,	HPC	-0.06	5.9E-01	0.15	2.1E-01

* = significant at $p < 0.1$; ** = significant at $p < 0.01$.

nitrifying bacteria in chloraminated distribution systems.

Nitrification has been reported across a wide range of water temperatures (Wilczak *et al.*, 1996; Lipponen *et al.*, 2002; Pintar *et al.*, 2005), although higher temperatures can increase the growth rate of nitrifying bacteria (Antoniou *et al.*, 1990; Rittmann and Snoeyink, 1984). The ability of AOB to survive at low temperatures (e.g. 6°C; Pintar and Slawson, 2003) could help explain why no correlation between AOB and temperature was observed in this study. The negative correlations observed for temperature and total chlorine are supported by the

chemistry of monochloramine, which decays more quickly at higher temperatures (Vikesland *et al.*, 2001). With present concerns about climate change it is also worthwhile to note that warmer drinking water temperatures could lead to additional microbial regrowth in distribution systems. In this study temperature was positively correlated with AOA in Toronto and with HPC in Waterloo. On this point, Levin *et al.* (2002) cautioned that, “Theoretically, warmer temperatures and especially warmer winters may result in higher microbial and nutrient loadings in drinking water systems, promoting biofilm growth within the distribution system and, in turn, supporting survival of some pathogens and their indicators.” (p.46)

Even though ammonia is the substrate for the first phase of nitrification, it is unclear from previous studies how sensitive the risk of nitrification in a distribution system is to the concentration of ammonia. Some authors have identified high ammonia concentrations as a possible cause of nitrification episodes (Skadsen, 1993), or observed positive correlations between ammonia and AOB levels (Lipponen *et al.*, 2002). Other authors have reported that the ammonia concentration was not a significant risk factor for nitrification (Odell *et al.*, 1996; Yang *et al.*, 2007). One possible explanation for these mixed results is that the ammonia concentration appears to initially rise and then decline later as nitrification progresses (Liu *et al.*, 2005). This implies that ammonia measurements taken during different stages of a nitrification event may show opposite trends (increasing or decreasing). Also, if chloraminated distribution systems are inhabited by species of AOA and AOB with very low half-saturation coefficients for ammonia (Bollmann *et al.*, 2002; Martens-Habbena *et al.*, 2009) then it may be rare for the ammonia concentration to be the main limit on the growth of nitrifying microorganisms. The results of this study, where ammonia was found to have statistically significant ($p=0.1$) positive correlations with AOB in Toronto, and AOB and AOA in Waterloo, indicate that the ammonia concentration is related to the abundance of nitrifying microorganisms, but the relatively low Spearman correlation coefficients (0.21–0.29) suggest a weak relationship.

A lack of correlations observed between DOC and microorganisms is not surprising as DOC levels were fairly consistent. This may also suggest that organic carbon is not a limiting substrate in either system, or that DOC levels are not correlated with the fractions of organic carbon that are readily available to microorganisms. Zhang *et al.* (2002) reported that assimilable organic carbon (AOC) was less than 4% of DOC in their samples so changes in AOC may not be reflected in the DOC concentration.

The fact that HPC and AOB are correlated reinforces that HPC is a good regrowth indicator. It could potentially be used as a surrogate for AOB trends, if the correlations found here can be confirmed for other systems. A correlation between nitrifying bacteria and heterotrophic bacteria has previously been observed by Lipponen *et al.* (2002) in bulk water samples and by Lipponen *et al.* (2004) in biofilms. Health Canada (2011) favours heterotrophic plate counts (HPC) as a useful operational parameter; this study provides

some support for that position. HPCs have also been recommended as a possible nitrification indicator by Zhang *et al.* (2009b), but they caution that other factors can lead to high HPCs aside from nitrification, so it cannot be used in isolation.

4.4 Conclusions and Recommendations

Two full-scale drinking water distribution systems in Southern Ontario were monitored for a nine month period in 2009–2010. The results of monitoring data and analyses thought to be relevant to nitrification have led to the following conclusions and recommendations:

- In general, water quality was well-controlled with respect to nitrification at each site in both distribution systems involved in this study. While some indicators of nitrification were detected, such as small rises in nitrite or dips in total chlorine residual, no fully-developed or severe nitrification episodes were seen.
- Nitrifying microorganisms were detected at all sites, warning of the potential for nitrification in both distribution systems studied if conditions became more favourable for nitrification.
- Statistically significant correlations were detected between several water quality parameters of relevance to nitrification. Total chlorine was negatively correlated with each type of microorganism (nitrifiers and HPC); ammonia levels were positively correlated with nitrifiers. Of special note was the strong correlation between HPC and AOB. This reinforces the usefulness of HPC as an operational parameter measuring general microbiological conditions in distribution systems.
- As nitrification is more likely to occur in warmer waters, it is possible that longer times at summer temperatures would allow nitrification to develop further at some sites. This is something that distribution system operators should consider if climate change affects water temperatures in temperate zones such as Ontario.
- Both AOB and AOA were frequently detected by qPCR in this study. The application of a culture-based presence/absence test confirmed the presence of viable nitrifier cells at most of the sites monitored. AOB were found to typically be present in similar or greater numbers than AOA in both distribution systems, but AOA were more abundant in some samples.
- Further research is recommended to investigate differences between the optimal niches for AOB and AOA, and whether there is any difference in their roles in distribution system nitrification.

Chapter 5

Application and Evaluation of a Nitrification Batch Test

5.1 Introduction

In distribution systems using monochloramine as a secondary disinfectant, the phenomenon of nitrification can promote the loss of the disinfectant residual, among other consequences. Nitrification is the process in which microorganisms, from ammonia-oxidizing bacteria (AOB) and ammonia-oxidizing archaea (AOA), convert ammonia to nitrite, which can be further oxidized to nitrate. Avoiding nitrification is an important operational goal for maintaining a disinfectant residual in chloraminated drinking water distribution systems. However, monitoring for nitrification can be a challenge as chemical indicators, such as a rise in nitrite concentrations, may not provide advance warning of nitrification episodes before they are fully established (Pintar *et al.*, 2005), and enumerating nitrifiers is costly and time-consuming (Hoefel *et al.*, 2005). One approach that shows some promise for understanding the conditions for nitrification in distribution systems is a batch test method developed by Sathasivan *et al.* (2005, 2008). As a batch test, it provides information about bulk water conditions, but not surface-associated effects such as biofilm and corrosion reactions. In this chapter, the batch test method is applied and evaluated on water samples collected from two full-scale chloraminated drinking water distribution systems.

The batch test method considered in this work was initially developed by Sathasivan *et al.* (2005). By inhibiting microbiological activity in a portion of each sample, they were able to separate the chemical and microbial contributions to monochloramine decay. The decay rate in samples in which microorganisms were removed or inhibited was assumed to be due to chemical processes only. The microbial contribution to monochloramine decay was then taken as the difference between the decay rates of the monochloramine residual

in uninhibited and inhibited samples. First-order kinetic coefficients were used to describe the decay rates. Sathasivan *et al.* (2005) defined a quantity they called the microbial decay factor, F_m , as the ratio between the microbial decay coefficient and the chemical decay coefficient. Their test is conducted at a constant temperature (20°C) which facilitates comparisons between samples taken in different seasons. For example, they applied it to samples taken in the winter to provide an indication of a reservoir's susceptibility to nitrification in advance of warmer weather. One of the advantages of this batch test methodology is that it provides a way to quantify the role of nitrifying bacteria (through the microbial decay factor) without enumerating them directly. In their study, Sathasivan *et al.* (2005) verified the effectiveness (and absence of side-effects) of the silver nitrate used to inhibit microbial activity by comparing the inhibited decay coefficient with that from filtered (0.2 μm) samples and in samples that were both filtered and inhibited.

In Sathasivan *et al.* (2008), the authors extended the batch test method they developed earlier (Sathasivan *et al.*, 2005). Their observations showed a point at which the total chlorine decay rate (in uninhibited samples) increases in some situations. They labelled this point the critical threshold residual (CTR). In their study, the average CTR was found to be 0.4 mg/L (the range was 0.20–0.65 mg/L). The pattern of two phases of total chlorine decay (i.e. the decay rate accelerates at the CTR) was seen both in samples collected in summer and in winter, even though initial nitrite levels were different. The phenomenon of two phases of total chlorine decay in these nitrification batch tests was also observed by Sathasivan *et al.* (2010).

This batch test method was further researched by Krishna and Sathasivan (2010), who investigated the phenomenon of elevated chemical decay coefficients (i.e. from inhibited or filtered batch tests) in samples undergoing severe nitrification. Sathasivan *et al.* (2010), for example, had noted a case in which the microbial decay factor, F_m , was lower than would be expected from the amount of microbially-mediated chloramine decay because the chemical decay coefficient (k_C) was elevated. Krishna and Sathasivan (2010) did experiments on mildly and severely nitrifying samples in an attempt to identify the cause of such an increase in k_C . Even after adjusting the mildly nitrifying sample to the same pH and nitrite levels as the severely nitrifying sample, the chemical decay coefficient was not as high. Hypothesized causes for this discrepancy were the presence of SMP or other compounds exerting a chloramine demand in the severely nitrifying sample. They also noted that the decay process deviated from first-order with high nitrite levels present.

The batch test method of Sathasivan *et al.* (2005, 2008) has been applied to studies on full-scale drinking water distribution systems. Fisher *et al.* (2009) applied the microbial decay factor, F_m , to studying reservoir stratification. The method was able to show that microbial stratification persisted in winter, even though the reservoirs were no longer thermally stratified and chemical indicators did not show stratification. They found that the

chemical decay coefficient, k_C , was fairly constant between depths within a season but it appeared to be greater in the autumn than in the winter at all depths. The microbial decay coefficient, k_m , and the microbial decay factor, F_m , had greater variability between depths. The authors recommended using their batch test in the winter or early spring to provide an early warning of the potential for nitrification in the summer.

Sathasivan *et al.* (2010) implemented a successful reservoir management strategy using the microbial decay factor, F_m , as a performance metric. According to the authors, diluting water in reservoirs with a potential for nitrification in the winter, when microorganisms are slow-growing, can yield long term improvements. By conducting batch tests on samples at various dilutions, the authors determined target dilutions that would yield an acceptable F_m (and overall decay rate). In this study, F_m after dilution was found to be proportional to the fraction of the original sample present.

Other researchers have used different batch test methodologies in studies on nitrification. Kasuga *et al.* (2010a) and Herrmann *et al.* (2011) used batch tests that involved incubating biofilm samples on activated carbon and clay tiles, respectively. These tests were not used on distribution system samples, however, and did not contain a chloramine disinfectant residual. Rather, ammonium was added and its oxidation rate determined. These batch tests also did not use an inhibiting agent to separate the contributions of chemical and microbiological processes. Of greater similarity to the batch test method of Sathasivan *et al.* (2005) was that of Zhang *et al.* (2002) who studied the effect of monochloramine on heterotrophic regrowth in treated drinking water. They modelled monochloramine decay with first- and second-order equations and found that both equations provided a good fit to their results. Westbrook and Digiano (2009) also conducted batch tests on monochloramine decay rates, and found an empirical first-order rate model to be appropriate for estimating monochloramine decay in bulk water samples.

In the research presented here, batch tests based on the methodology of Sathasivan *et al.* (2005, 2008) were applied to samples from two full-scale chloraminated drinking water distribution systems. The objectives were to analyze the potential for nitrification at sites in these distribution systems using this batch test method and to evaluate its usefulness.

5.2 Methodology

Method Summary

The batch testing method for nitrification was based on the method of Sathasivan, Fisher, and Kastl (2005). It uses microbially-inhibited and uninhibited batches in parallel to determine the microbial contribution to chloramine decay. The inhibiting agent was 100 $\mu\text{g-Ag/L}$

added as AgNO_3 . To check its efficacy in inhibiting microbiological activity, some comparison batch tests were done using samples that had been filtered through sterile $0.20\ \mu\text{m}$ membrane filters to remove microorganisms. The total chlorine residuals were measured from both the inhibited and uninhibited sets every 1–2 days for approximately three weeks. Monochloramine concentrations were also measured during the main round of batch experiments. Ammonia, nitrite, and nitrate levels were only analyzed before and after most of the batch tests performed in this study. Sampling times became less frequent as each batch test progressed, based on how rapidly the water quality changed. Following each batch test, decay curves were constructed and evaluated as described below.

Sample Collection

Chapter 3 describes the distribution systems and sampling sites that were included in this research. Samples were collected for batch testing from selected sites that were monitored during the full-scale sampling campaign (see Ch. 4); this allowed sites to be selected for batch testing that had shown differing characteristics in water quality testing. Samples for batch testing were collected in 1 L sterile glass bottles. Prior to sampling, the taps were flushed to draw fresh water from the distribution system. Three rounds of experiments using this batch testing method were performed. The preliminary round was conducted to assess the feasibility of the batch test method. Samples for this round were collected on 17 August 2010 from sites RCL, 801, and 904 from the Toronto Water distribution system.

Sample locations for the main round of batch testing were chosen from each distribution system according to the following criteria:

- The entrance to each distribution system (RCL, K20S14)
- The site in each distribution system that experienced the lowest disinfectant residual (801, WOD61)
- The site with the most numerous ammonia-oxidizing bacteria (AOB) in each distribution system (904, WOD06)
- A site from each system that had a stable disinfectant residual over the course of the full-scale sampling campaign (804, E60T)

These samples were collected from sites in the Region of Waterloo distribution system on 12 October 2010 and from sites in the Toronto Water distribution system on 17 October 2010.

A final round of batch testing was conducted with samples collected on 24 November 2010 from sites K20S14 and WOD06 in the Waterloo distribution system. The purpose

of this round was to investigate some questions about the method. Comparisons between filtered and inhibited samples were used to verify the reliability of the inhibiting agent (silver nitrate); the effect of adding ammonia and organic carbon to samples was also evaluated.

Batch Test Procedure

Samples were divided into 15 sterile plastic 50 mL vials, of which half were inhibited and half were uninhibited, in order to provide sufficient data points during the batch tests (Figure 5.1). Vials comprising the inhibited set had 0.25 mL of 20 mg-Ag/L AgNO_3 added, resulting in a final concentration of 100 $\mu\text{g-Ag/L}$.

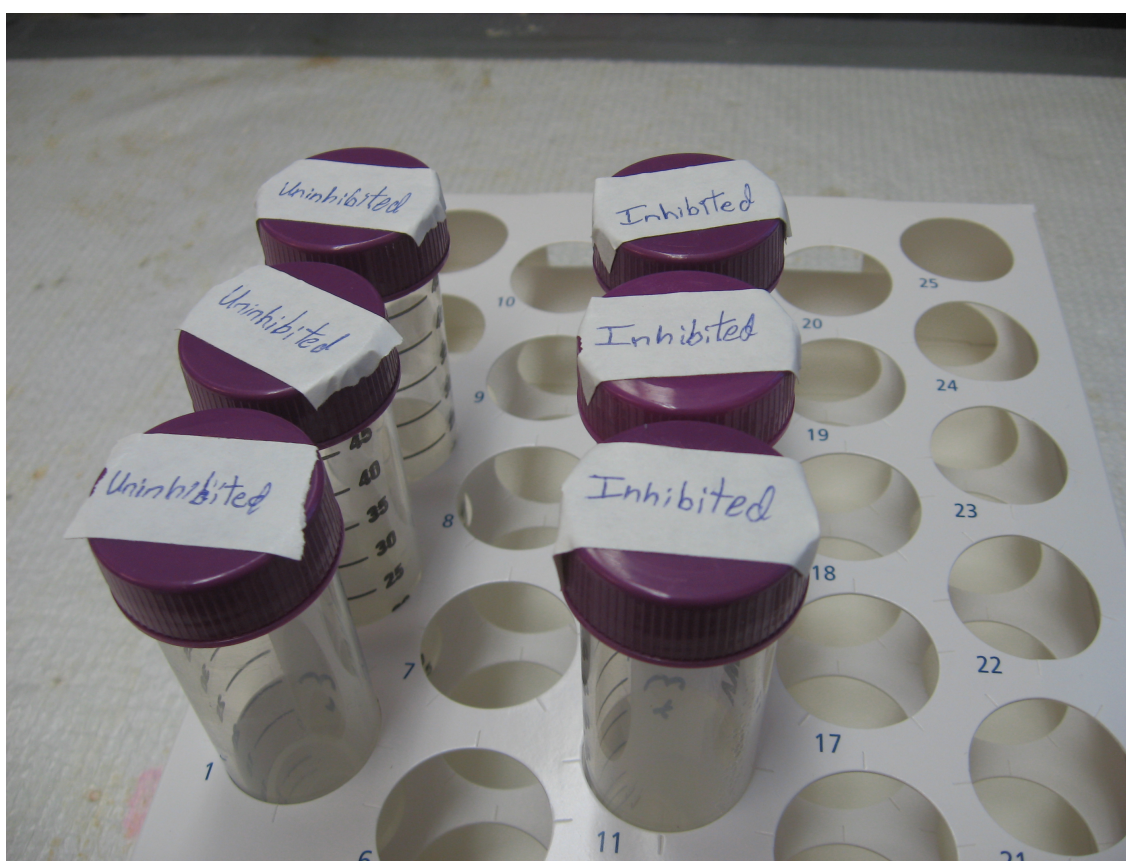


Figure 5.1: The batch test used in this study consists of inhibited and uninhibited batches being run in parallel.

Measurements of total chlorine (and monochloramine during the main round of batch experiments) were performed initially and approximately every two days during the batch test experiments, with the monitoring frequency adjusted as necessary depending on its decay

rate. Free ammonia, nitrite, and nitrate levels were measured at the beginning and end of the main round of the experiment. See section 4.2 for details on the analytical methods used to measure water quality parameters. After the completion of the batch test, chlorine decay curves were constructed and results evaluated as described below.

Another analysis that was done in this work was the characterization of the organic carbon before and after selected batch tests. Organic carbon characterization was performed at the NSERC Chair in Water Treatment at the University of Waterloo, using an automated liquid chromatography with organic carbon detection (LC-OCD) instrument developed by Huber, Balz, Abert, and Pronk (2011).

In the final round of batch testing experiments, the samples were augmented with additional carbon or ammonia. Acetate (1.0 mL of 75 mg-C/L NaCH_3COO for a final concentration of 1.5 mg-C/L) or ammonia (1.0 mL of 10 mg-N/L of NH_4Cl for a final concentration of 0.2 mg-N/L) were added to both the inhibited and uninhibited samples; control samples that did not have nutrient augmentation were included. The final round of batch testing also involved a comparison between inhibited samples and filtered samples to verify that 100 $\mu\text{g-Ag/L}$ of AgNO_3 was an effective microbial inhibitor. Samples were vacuum filtered through sterile 0.20 μm Supor 200 (Pall) membrane filters to remove microorganisms as an alternative method of eliminating microbial activity (to isolate the chemically-mediated fraction of the monochloramine decay rate), and results were compared with inhibited samples.

Analysis of Results

The results of these batch tests were evaluated by calculation of the chemical and microbial decay coefficients (k_C , k_m) for the total chlorine residual, the microbial decay factor (F_m), and the critical threshold residual (defined in Sathasivan *et al.*, 2005 and Sathasivan *et al.*, 2008). To conduct these evaluations, the total chlorine residuals measured over the course of each batch test were plotted against the elapsed time, then decay curves were constructed. Figure 5.2 illustrates the determination of the results of these batch tests and the definition of the variables described above. The differences between inhibited and uninhibited lines are attributed to microbial processes. An acceleration in the residual decay rate defines the start of the second phase of the batch tests. On a semi-log plot, first-order decay rates appear as straight lines; the slopes are the decay coefficients k_C for the inhibited samples, and k_{T1} and k_{T2} for the two phases of decay in the uninhibited samples. The intersection point between lines through the two phases of decay in uninhibited samples is the CTR. The first order microbial decay coefficient and the microbial decay factor were determined from the following equations:

$$k_m = k_{T1} - k_C \quad (5.1)$$

$$F_m = \frac{k_m}{k_C} \quad (5.2)$$

In these equations, k_{T1} is the first-order decay coefficient for the first phase of the disinfectant residual decay (before the decay rate increases) in an uninhibited batch. Although it is not used in the above equations, k_{T2} was also calculated; it is the first-order decay coefficient for the second phase of the residual decay in an uninhibited batch. These decay rates for uninhibited samples are assumed to be the total of chemical and microbial contributions to the disinfectant residual decay. k_C is the first-order decay coefficient in the inhibited batch, which is attributed to chemical processes only. The difference between these variables (for the first phase of the residual decay) is k_m , the first-order decay coefficient that is assumed to be due to microbial processes. The microbial decay factor, F_m , is the ratio between the microbially-mediated and chemical contributions to the overall residual decay rate.

Another parameter is the critical threshold residual (CTR), which cannot be expressed as a simple equation. It is the total chlorine residual at which the decay rate accelerates in the uninhibited sets of samples, and marks the boundary between the two phases of disinfectant residual decay that were observed in most samples. The CTR, and the elapsed time from the start of the test to when it was reached, was determined by finding the intersection point of straight lines through the two phases of total chlorine decay on a semi-log plot (with slopes of k_{T1} and k_{T2}). This was altered from the method of Sathasivan *et al.* (2008) to simplify the calculation process and make it more robust against deviations from first-order decay. Example calculations are shown in Appendix E.

The effect of augmenting the ammonia or organic carbon (as acetate) concentrations in batch test samples was evaluated by comparing the decay rates and by paired t-tests (Dodge, 2010) between corresponding measurements with and without nutrients added. The relative efficacies of filtration and silver nitrate inhibition at eliminating the microbial contribution to chloramine decay were compared in the same way.

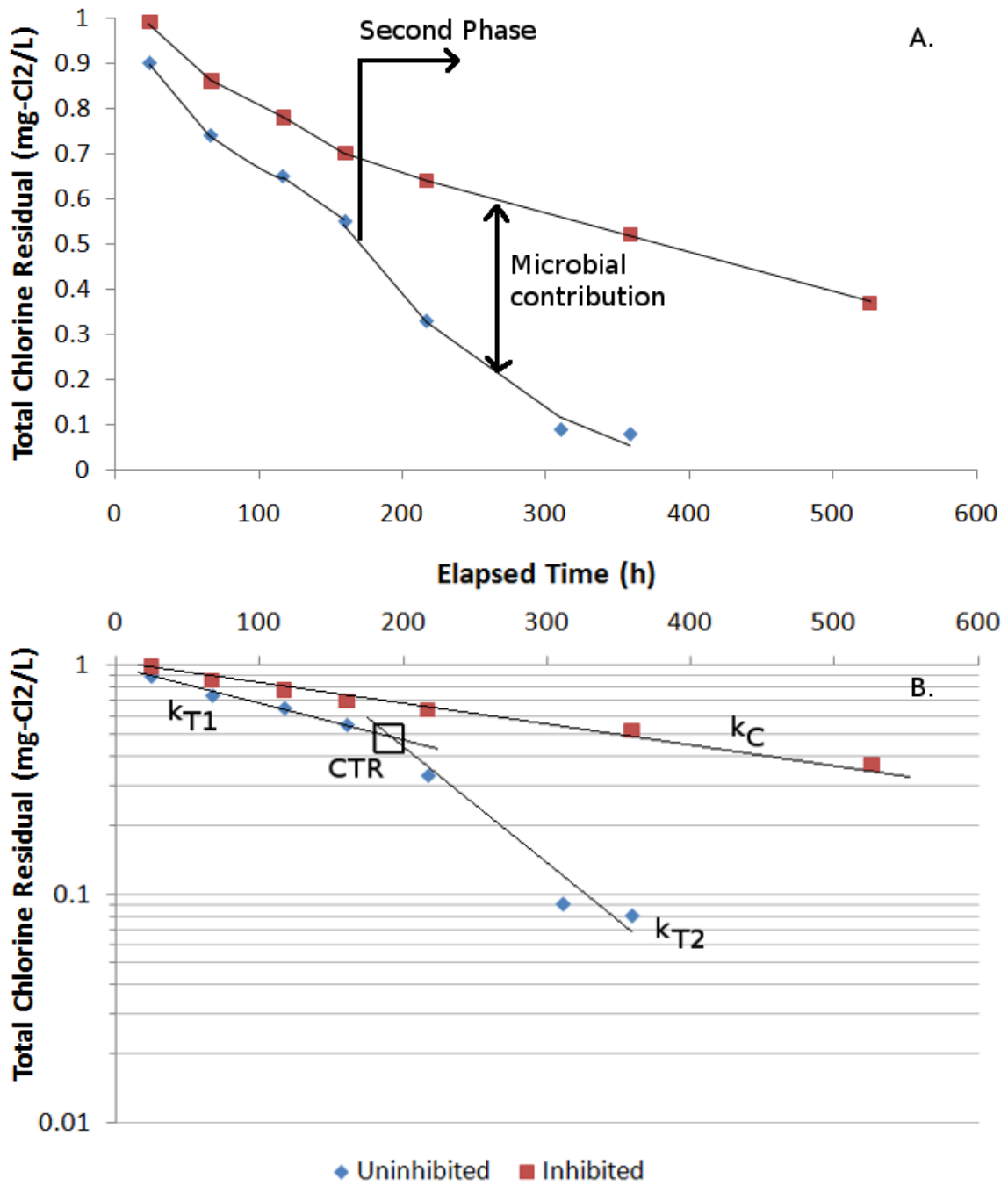


Figure 5.2: An illustration of the variables involved in calculations on the results of these nitrification batch tests. Inhibited (squares) and uninhibited (diamonds) samples are plotted on linear (A) and semi-log (B) graphs.

5.3 Results and Discussion

Batch Testing Results

Batch tests for nitrification were successfully carried out on water samples from a number of sites from full-scale distribution systems in Waterloo and Toronto. There were noticeable differences between results from the various samples, suggesting that this test can provide useful information on the potential for nitrification at distribution system sites. By measuring the total chlorine residuals over time during the batch tests, decay curves were constructed. Silver nitrate was verified to be an effective microbial inhibitor through comparisons between inhibited and filtered samples (detailed in the subsection “Evaluation of Batch Test Method” later in this chapter) and was used in all of the batch test experiments presented in this chapter. The decay of the disinfectant residual in the inhibited sets was attributed to chemical processes only, while that in the uninhibited sets was assumed to be a combination of chemical and microbially-mediated processes. The difference between the total and chemical decay rates was taken as the microbial contribution to total chlorine decay. First-order decay coefficients were determined for each of these elements. The results from the batch tests conducted in this research are presented in Table 5.1. The coefficients k_{T1} and k_{T2} are from uninhibited samples, before and after an increase in the total chlorine rate, respectively. The first order total chlorine decay rate in inhibited batches is given by k_C . The difference in decay rates between uninhibited and inhibited samples is attributed to microbiological processes and is labelled k_m ; the microbial decay factor, F_m , is the ratio between k_m and k_C .

Table 5.1 contains the calculated coefficients for samples from all three rounds of batch test experiments. The preliminary round was conducted on three samples from the Toronto distribution system, collected on 17 August 2010. The main round of batch testing used four samples each from the Waterloo and Toronto distribution systems. Samples were collected on 12 October 2010 from Waterloo sites and on 17 October 2010 from Toronto sites. Some typical results from this round are shown in figures 5.4 (site 804), 5.6 (site E60T), and 5.7 (site WOD06) below. The final round of batch testing included samples with added carbon (denoted with “+C” appended to the sample label) and ammonia (denoted with “+A” appended to the sample label); these samples were collected from the Waterloo distribution system on 24 November 2010. A plot of the results for the control sample from site K20S14 is shown in figure 5.5 below. Plots for the remainder of the samples are shown in Appendix A.

Care must be taken in interpreting the data from Table 5.1. These parameters should be considered together rather than using one of them alone to compare samples or evaluate the results of a batch test. For example, in the main round of batch testing, the sample from

Table 5.1: Coefficients (in h^{-1}) calculated for the batch tests conducted in this research. Sampling dates (in 2010) are indicated.

Sample	k_{T1}	k_{T2}	k_C	k_m	F_m
17 August					
RCL	0.0010	0.0010	0.0011	0.0000	0.0
801	0.0069	0.0069	0.0014	0.0055	3.8
904	0.0039	0.0080	0.0014	0.0025	1.8
17 October					
RCL	0.0018	0.0121	0.0015	0.0003	0.2
801	0.0065	0.0125	0.0013	0.0052	4.0
804	0.0033	0.0015	0.0014	0.0019	1.4
904	0.0033	0.0302	0.0016	0.0017	1.1
12 October					
K20S14	0.0057	0.0090	0.0020	0.0037	1.8
WOD06	0.0075	0.0072	0.0038	0.0037	1.0
E60T	0.0050	0.0105	0.0016	0.0034	2.1
WOD61	0.0062	0.0134	0.0038	0.0024	0.6
24 November					
K20S14	0.0032	0.0069	0.0020	0.0012	0.6
K20S14+C	0.0029	0.0105	0.0020	0.0009	0.5
K20S14+A	0.0029	0.0080	0.0018	0.0011	0.6
WOD06	0.0028	0.0106	0.0020	0.0008	0.4
WOD06+C	0.0026	0.0181	0.0019	0.0007	0.4
WOD06+A	0.0035	0.0105	0.0019	0.0016	0.9

“+C” indicates a sample with organic carbon (acetate) added; “+A” indicates a sample with ammonia added

site 801 had an F_m of 4.0, while for WOD06 the F_m was 1.0, yet the overall total chlorine decay coefficient (in the first phase of decay, k_{T1}) was greater for WOD06 than for 801. This suggests that microbial activity accounted for a larger proportion of the chloramine decay rate in the sample from site 801, while the sample from site WOD06 had a more rapid overall loss of its disinfectant residual. Other notable results include the very low microbial contribution to disinfectant residual decay (quantified by k_m) in the sample from site RCL, and the elevated (above the range of the other samples) decay coefficients associated with chemical processes (k_C) in samples from sites WOD06 and WOD61 in the main round of batch testing of this study. Similar observations of elevated chemical decay coefficients were investigated by Krishna and Sathasivan (2010), but they were not able to conclusively

identify the mechanism causing this increase.

Besides the decay coefficients, and the ratio F_m , the critical threshold residual (CTR) was also calculated for this study. Figure 5.3 shows how the CTR is determined by finding the intersection point of the decay curves from the first and second phase of decay in the uninhibited batch. A clear difference in the decay rate is visible here, reinforcing the validity of the CTR concept. That is, the results of this research (exemplified in Fig. 5.3) support the observations of Sathasivan *et al.* (2008) that monochloramine decay often occurs in two phases, with a greater decay rate in the second phase. The mechanisms responsible for the increase in the total chlorine decay rate below the CTR are unclear. One possible reason for the transition to a higher decay rate could be that a point is reached where the ammonia levels begin to decline. A monochloramine residual is more chemically stable in the presence of ammonia (Vikesland *et al.*, 2001), so the consumption of ammonia by nitrifiers could trigger a more rapid decay of the disinfectant residual. Another factor could be the production of nitrite by ammonia oxidizing bacteria (AOB) and archaea (AOA), since nitrite will react with monochloramine (Vikesland *et al.*, 2001). The results of Sathasivan *et al.* (2008) showed that the beginning of the second phase of the total chlorine residual decay coincided with a decrease in the ammonia concentration and an increase in the nitrite concentration. In this study, ammonia and nitrite concentrations were not monitored while the batch tests were in progress. Two phases of chloramine decay were also observed in the results of a batch test conducted by Zhang *et al.* (2002).

In this study the method of finding the CTR differs from that of Sathasivan *et al.* (2008). Modifications to the analyses described in Sathasivan *et al.* (2008) had to be made to accommodate the fact that the assumption that chloramine decay is a first-order process was not a perfect fit in every test. This made it difficult to apply the calculation procedure for determining CTR given by Sathasivan *et al.* (2008), which depends on calculating pairwise first-order decay coefficients for adjacent points. Instead, the critical threshold residual (CTR) was determined as the intersection point on a semi-log plot between first-order decay curves (which appear as straight lines when plotted in this manner) fitted to measurements before and after a break-point. Example calculations for the procedure are shown in Appendix E. All calculations were performed on total chlorine measurements rather than using monochloramine data to calculate decay rates or CTR. This decision was made due to the lower variability of the total chlorine measurements.

Unlike Sathasivan *et al.* (2005), monochloramine levels were not increased to at least 1.0 mg-Cl₂/L before beginning the batch tests. This simplified the test and preserved the initial sample conditions. Sathasivan *et al.* (2005) raised the initial monochloramine concentration in samples where it was low to ensure a sufficient number of measurements before the residual was depleted and to improve the accuracy of the rate calculations. However, by retaining the initial sample conditions from the distribution system, the time taken to reach the

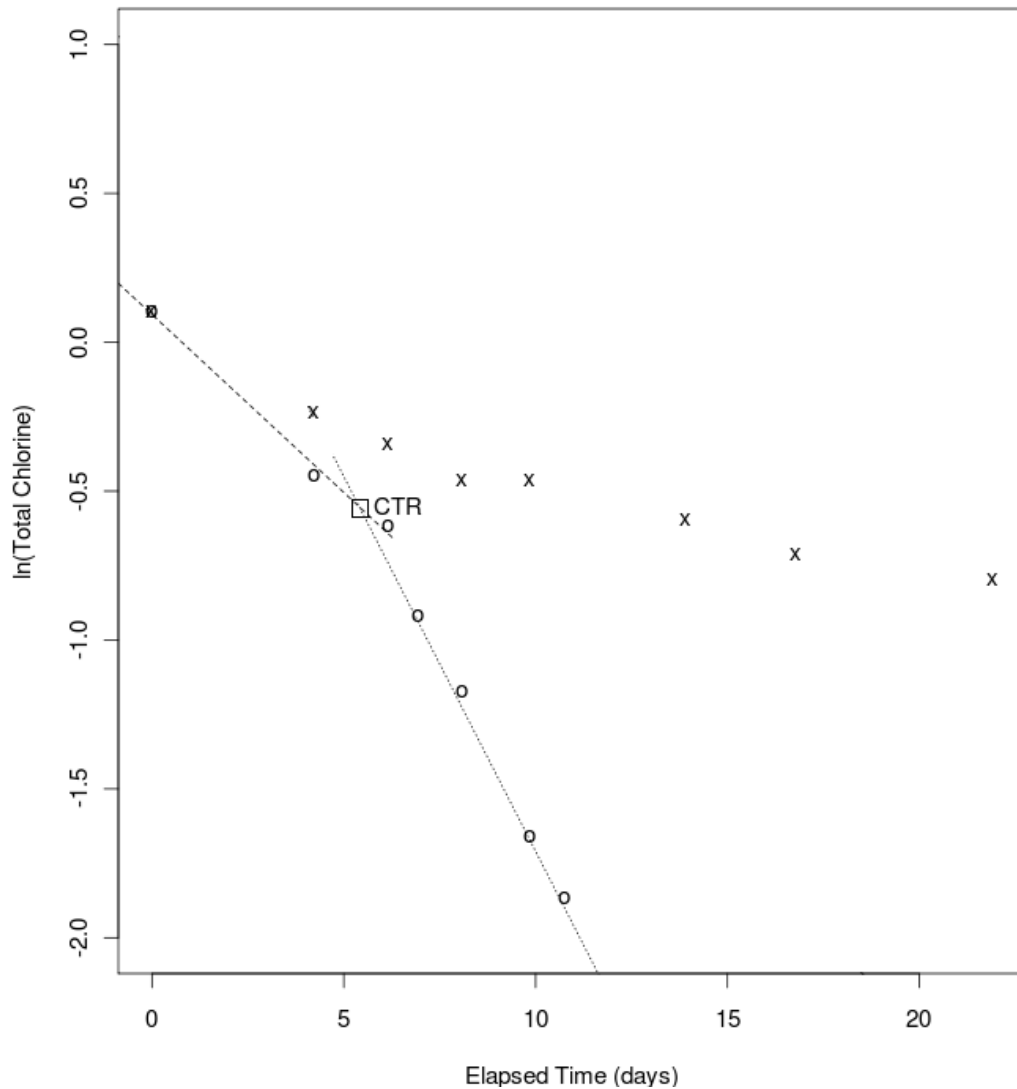


Figure 5.3: A semi-log plot of the total chlorine decay curves from a batch test for nitrification. This figure shows the determination of the CTR as the intersection point between the decay curves for the first phase (dashed line, - - -, slope is k_{T1}) and second phase (dotted line, ..., slope is k_{T2}) of decay in uninhibited (o) sets; inhibited samples (x) are also shown. Sample shown is from site E60T from the main round of batch testing.

CTR becomes a useful basis of comparison between samples. The time taken to reach the critical threshold residual (CTR) may be interpreted as a prediction of the hydraulic retention time allowable at that point in the distribution system before the decay rate of the chloramine residual accelerates. As such, it is recommended as an operationally useful

Table 5.2: Chlorine decay curve types for each sample based on batch tests. The CTR and the incubation time it took to reach the CTR are also given. Sampling dates (in 2010) are indicated.

Sample	Type	CTR (mg/L)	Time to CTR (d)
17 August			
RCL	I	NA*	NA
801	IV	NA	NA
904	II	0.50	5.2
17 October			
RCL	II	0.54	12.0
801	III	0.44	1.4
804	I	0.46	7.1
904	III	0.38	5.6
12 October			
K20S14	II	0.85	4.6
WOD06	IV	NA	NA
E60T	III	0.57	5.4
WOD61	II	0.26	7.1
24 November			
K20S14	II	0.62	11.9
WOD06	II	0.62	7.0

*CTR is not available (NA) for decay curves of types I and IV.

parameter, especially for samples from reservoirs, where the bulk water processes at work in batch tests will be the main effects. The critical threshold residuals, and the incubation time taken to reach them, are listed in Table 5.2 for each sample.

In addition to calculating the microbial decay factor (F_m) and critical threshold residual (CTR) values, this study also evaluated the batch test results by assigning each sample to one of the following types based on a visual examination of its decay curves. This approach was taken to provide a more robust and holistic way of presenting the batch test results than relying on any single parameter from Table 5.1. Here are the types of total chlorine decay curves that were observed in the current study:

- I. Inhibited and uninhibited samples track closely together (fig. 5.4)
- II. Inhibited and uninhibited samples track together initially, and then diverge at the CTR (fig. 5.5)
- III. Inhibited and uninhibited samples have some initial divergence, with an increase in divergence at the CTR (fig. 5.6)

IV. Inhibited and uninhibited samples diverge initially, and no second phase of accelerated decay in the uninhibited batch is observed (fig. 5.7)

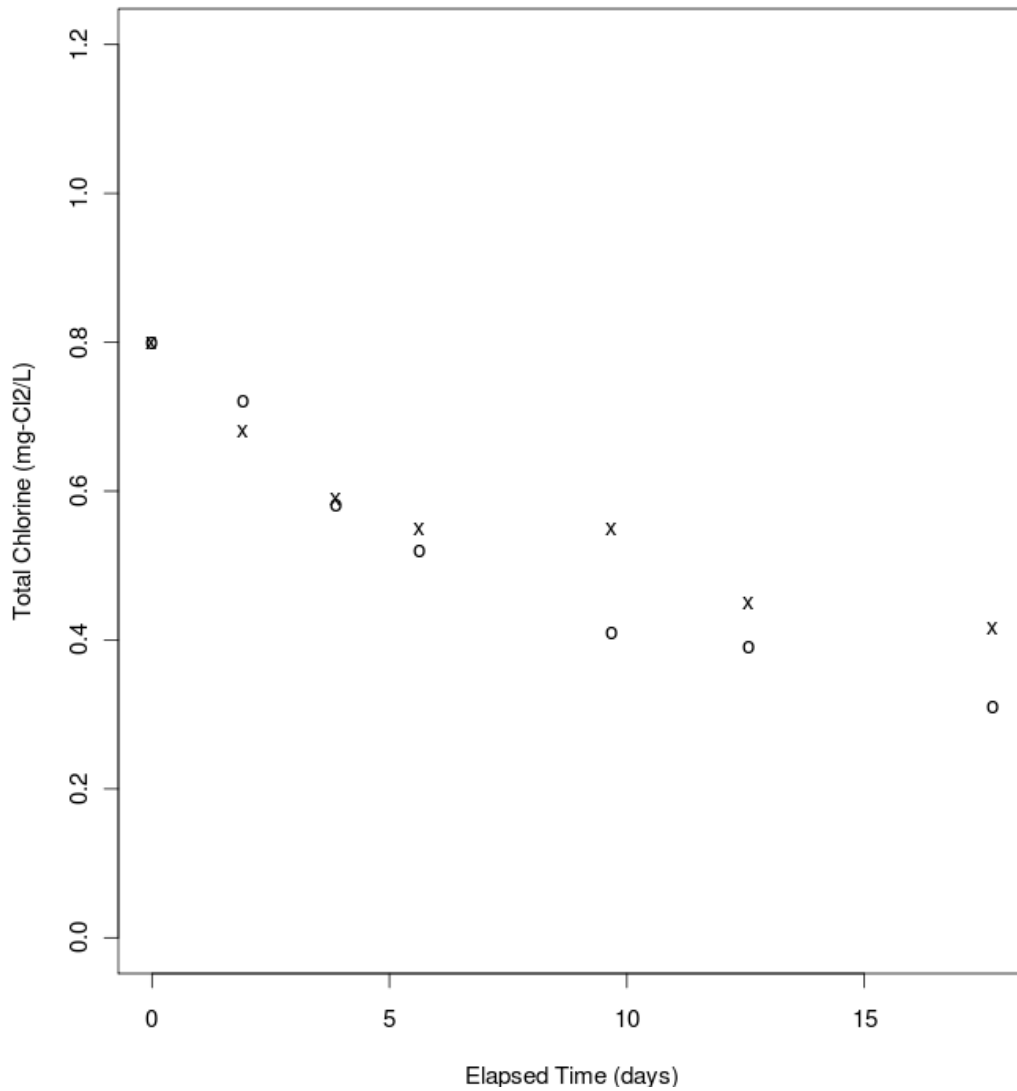


Figure 5.4: Representative Type I chlorine decay curve from site 804 from main round of batch testing. In this type of trend, the inhibited (x) and uninhibited (o) samples track closely together for the entire incubation period.

The advantage of categorizing results from these batch tests into the types described above is that it provides a holistic description of the trends observed. It facilitates comparisons between sites by grouping those that showed similar trends in their residual decay

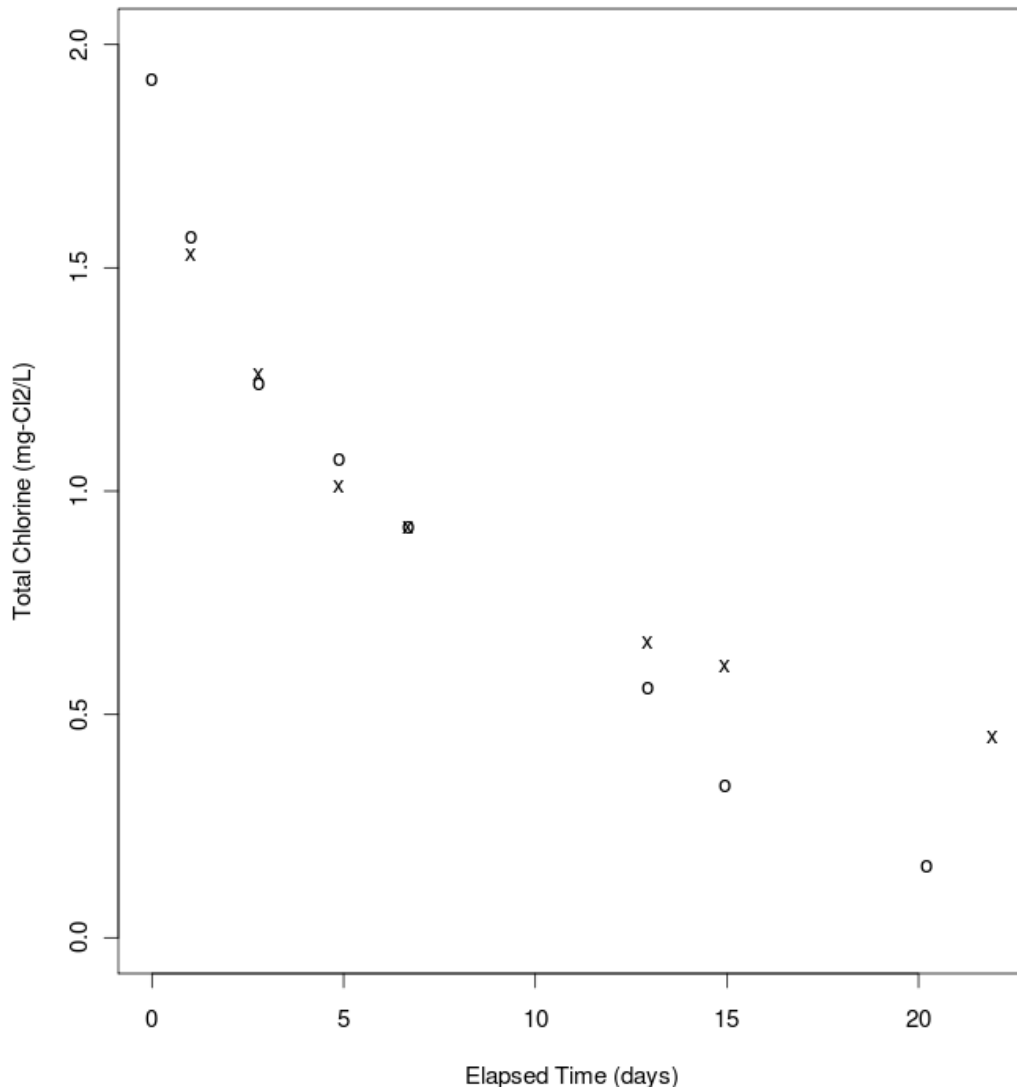


Figure 5.5: Representative Type II chlorine decay curve from site K20S14 from final round of batch testing. In this type of trend, the inhibited (x) and uninhibited (o) samples track closely together initially, and then diverge at a point known as the Critical Threshold Residual (CTR).

into specific types. The chlorine decay curve types defined here can be compared to the categorization system used by Sathasivan *et al.* (2008). They presented their results as three representative samples, A, B, and C. Representative samples A and B in their work would both be classified as type III according to the criteria used here—the total chlorine decay rates were greater in the uninhibited batches than in the inhibited batches from the beginning, and had clear points where they accelerated. The main difference between samples

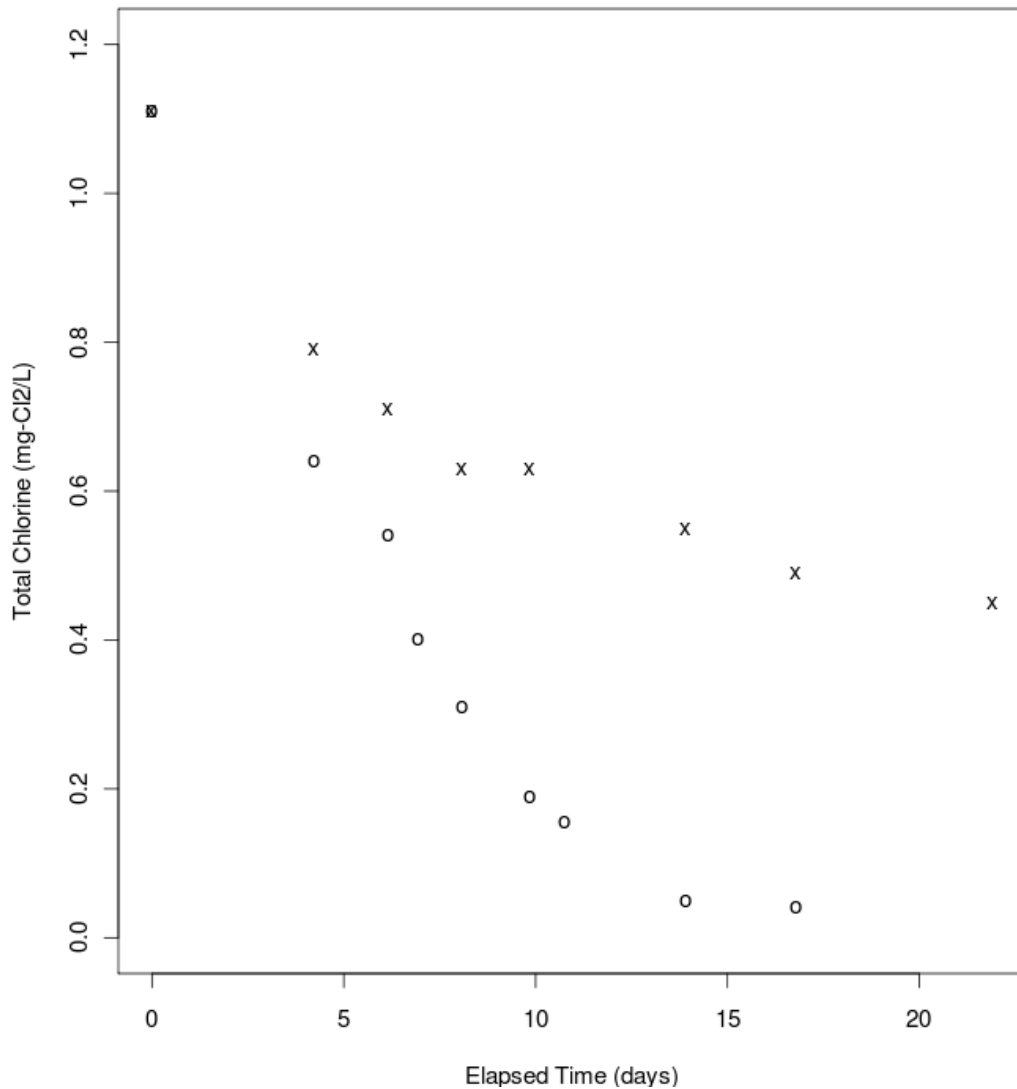


Figure 5.6: Representative Type III chlorine decay curve from site E60T from main round of batch testing. In this type of trend, the inhibited (x) and uninhibited (o) samples have some initial divergence, and then the decay rate in the uninhibited batch accelerates at the CTR.

A and B in the study of Sathasivan *et al.* (2008) was that A was collected in the summer while B was collected in the winter. In contrast, their representative sample C did not show two phases of total chlorine decay and had no significant difference between inhibited and unprocessed samples (i.e. $F_m = 0$); these characteristics make it equivalent to type I in the classification system outlined above. The trends observed in type II and type IV chlorine decay curves, however, are believed to be novel to the current research. Type II fits be-

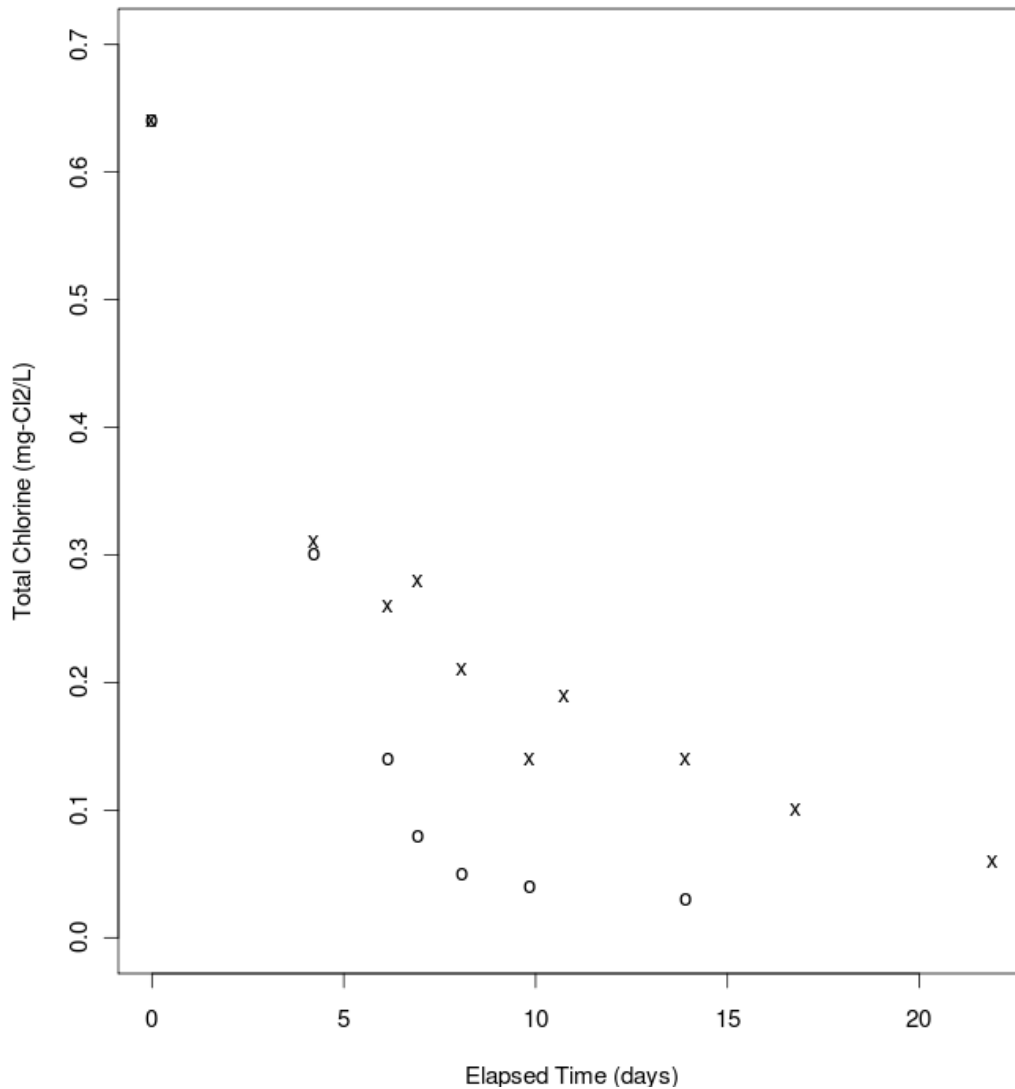


Figure 5.7: Representative Type IV chlorine decay curve from site WOD06 from main round of batch testing. With this type of trend, a Critical Threshold Residual (CTR) cannot be determined due to the lack of a clear breakpoint in the decay rate of the uninhibited portion of the sample. Measurements from the inhibited batch are shown with “x” and measurements from the uninhibited batch are shown with “o.”

tween types I and III, with the chloramine decay rate approximately equal in uninhibited and inhibited batches, until the critical threshold residual (CTR), when the decay rate in uninhibited samples accelerates. Type IV trends likely occur in samples where the initial total chlorine residual is at or less than the CTR, since having the sample start in the accelerated

chlorine decay phase would preclude observing a breakpoint where the acceleration occurs. This idea is supported by the initial decay coefficients (k_{T1}) in uninhibited portions of type IV samples (see Table 5.1), which are greater than in other samples.

Table 5.2 summarizes the results of the batch testing experiments by providing the type and CTR for each sample. Since batch tests undergo bulk water processes rather than wall/biofilm processes, they can be considered a useful tool to investigate reservoirs, as wall/biofilm processes are usually dominated by bulk water processes there. This information may be useful in the operation of reservoirs, by providing values for minimum disinfectant residual and maximum retention time. The site E60T, for example, is a reservoir and results from the batch testing performed in this study suggest that it should be operated to maintain the residual above 0.57 mg/L and with a retention time less than 5.4 days—at least with the water quality conditions at the time the sample was taken (mid October).

Three complementary ways of evaluating the results from these nitrification batch tests have been presented above. The microbial decay factor, F_m (and the decay coefficients used in its calculation, which should be considered in tandem), and the critical threshold residual (CTR) are quantitative, and the assignment of a decay curve type is qualitative.

Interpretation of Batch Test Results

Further discussion is warranted regarding the interpretation of the results from this batch test method for nitrification in chloraminated drinking water distribution systems. The validity of assuming the chloramine decay process can be modeled with first-order rate equations and the robustness of relying on a single metric to compare samples have been questioned above. In this section, these topics are investigated in greater detail. Understanding the limitations and assumptions of the microbial decay factor (F_m) and critical threshold residual (CTR) will guide their proper interpretation and application.

The calculation of the decay coefficients (k_{T1} , k_{T2} , k_C , k_m) depends on the assumption that the chlorine decay in the batch tests is first-order. By plotting the total chlorine decay curves on a semi-log plot (refer to fig. 5.3, for example), it can be seen that the decay process is approximately first-order (linear on a semi-log plot) with some initial deviation from a first-order rate. Sathasivan *et al.* (2005) validated the first-order assumption in their work by obtaining R^2 values for exponential regression >0.98 . However, second-order decay curves can also be fitted successfully, as shown in figure 5.8. This agrees with what other researchers have found about the kinetics of monochloramine decay. Zhang *et al.* (2002) and Westbrook and Digiano (2009) fitted chloramine decay successfully to both first- and second-order equations. Westbrook and Digiano (2009) pointed out that assuming the decay process was first-order was preferable for its greater mathematical simplicity. These observations also accord well with theoretical approaches to modelling chloramine decay. Yang *et al.* (2008) used second-order kinetics for chloramine auto-decomposition and pseudo first-order kinetics for the oxidation of natural organic matter (NOM) in their model. Therefore it is reasonable to see a blend of first- and second-order effects in batch tests for nitrification. To resolve this, the approach taken here was to exclude early data points from decay coefficient calculations if they significantly violated the first-order assumption; a first-order decay rate was then calculated from the remaining data points.

Due to the deviations sometimes seen from first-order decay at early times in these batch tests, it was difficult to determine the critical threshold residual following the calculation procedure of Sathasivan *et al.* (2008). Their method involves piece-wise computations of the median total chlorine residual and the first-order slope between two measurements taken during batch testing. Then the critical threshold residual (CTR) is taken as the point when the first-order slope reaches double its baseline value. However, where the initial measurements did not follow a first-order curve, it was difficult to establish a baseline. The modified method shown earlier in this chapter of calculating CTR as the intersection between the first-order decay curves from the first and second phases of total chlorine decay was adopted as an alternative. It also has the advantage of being more straightforward in its calculation procedure.

Since it is a ratio, the F_m number (microbial decay factor) can have the same value under differing sample conditions. Consequently, comparing samples on the basis of their F_m values alone could result in misleading interpretations of batch test results. Figure 5.9 illustrates this weakness of the microbial decay factor by plotting pairs of k_m and k_C values. In the figure, the plus signs are from batch experiments performed for this study and the open circles are from literature (Sathasivan *et al.*, 2005, 2008; Fisher *et al.*, 2009; Sathasivan *et al.*, 2010). A variety of samples and experimental conditions are included, providing a range of k_C (chemical decay coefficient—from inhibited samples) and k_m (microbial decay coefficient—difference between inhibited and uninhibited samples) values. Each line is a single F_m number (recall that $F_m = k_m/k_C$). It can be seen that reporting the results of nitrification batch tests as an F_m value alone can miss some important details, since any point along one of these lines will have the same F_m , but the residual decreases more rapidly for points further from the origin. Krishna and Sathasivan (2010) reported k_C values that were greatly elevated, and varying k_C values were also measured in these experiments. Due to this effect, reporting both the chemical and microbial decay coefficients should be seen as more useful and informative than just reporting the ratio F_m .

Figure 5.9 also shows that the results for this type of batch test typically cluster together. Chemical decay coefficients normally fall in the range 0.001–0.002 h⁻¹. This is very similar to the range reported by Sathasivan *et al.* (2005) (0.0011–0.0019 h⁻¹). Microbial decay rate coefficients also typically cluster, albeit in a wider range of 0.000–0.005 h⁻¹. Results falling outside of this region have more rapid than normal rates of chlorine decay. This may be a result of nitrification, or due to other processes or water quality effects. In future research, an attempt should be made to identify the mechanisms leading to increases in k_m and k_C .

Another important factor to consider when interpreting results from these batch tests is that only bulk water processes will be applicable (Sathasivan *et al.*, 2005). Therefore this batch test method could significantly underestimate the total chlorine decay rate for samples from distribution system locations where pipe-wall processes, such as corrosion and biofilm-associated reactions, are important factors. However, for samples from reservoirs this test should be very useful since their relatively low surface-to-volume ratios imply that bulk water reactions will usually be the dominant effects on water quality changes.

In addition to having low surface-to-volume ratios, reservoirs also have residence times that are much easier to determine compared to other parts of distribution systems. For these reasons, this batch test method is especially recommended for reservoir operation. For example, the CTR and the incubation time taken to reach it in a reservoir sample can be regarded as the minimum allowable disinfectant residual and maximum allowable retention time for that reservoir, after safety factors are added to the batch test results. Another example application is the project of Sathasivan *et al.* (2010), who used the microbial decay factor, F_m , to develop an operational strategy for a reservoir to prevent nitrification

episodes. The authors used the batch test method of Sathasivan *et al.* (2005) to determine a target dilution that would yield an acceptable F_m (and overall decay rate) since diluting the reservoir water with freshly treated water was their strategy for improving water quality. The authors used serial fill-draw cycles to reach the target F_m ; with each cycle, the proportion of original bulk water remaining was the low level (as a percent of volume) divided by the high level of the cycle:

$$\frac{F_{m,new}}{F_{m,old}} \approx \prod_N \left(\frac{\text{low level}}{\text{high level}} \right)_{cycle} \quad (5.3)$$

These serial dilutions need to be performed quickly enough that nitrifier growth is not a significant factor.

In view of these points, the strengths and weaknesses of the three ways to present the results of these nitrification batch tests can be compared. The microbial decay factor is prone to misinterpretation if it is used in isolation, but this can be mitigated by reporting the decay coefficients that were used in its calculation. These decay coefficients are based on the assumption that the residual decay during the batch test is a first-order process. The validity of this assumption should be checked when using these decay coefficients. The critical threshold residual was difficult to determine via the original procedure of Sathasivan *et al.* (2008) when there were deviations from first-order trends, but the new calculation procedure proposed here should be more robust. Classifying a nitrification batch test into one of the four types described above has the limitation of being qualitative rather than quantitative, but does provide a useful broad categorization of the trends observed. Using all of these parameters in combination provides a robust, holistic view of the results of these batch tests.

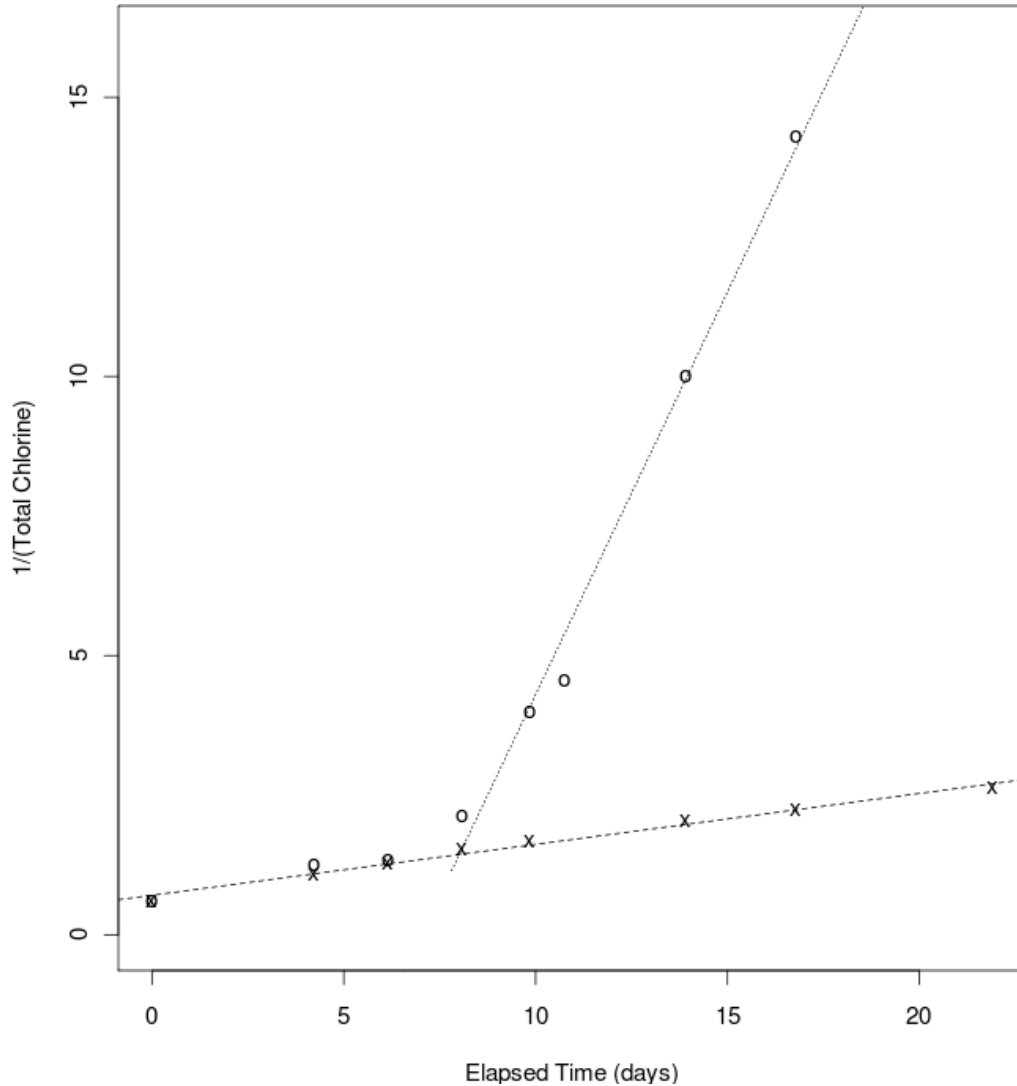


Figure 5.8: The reciprocal of the total chlorine residual plotted against the elapsed time for a batch test following the method of Sathasivan *et al.* (2005). The dashed line (- - -) is fitted for inhibited samples (x) and the dotted line (...) is fitted for the second phase of decay in uninhibited samples (o). On this kind of plot, a second-order process will follow a straight line (Sample shown is from site K20S14 from the main round of batch testing).

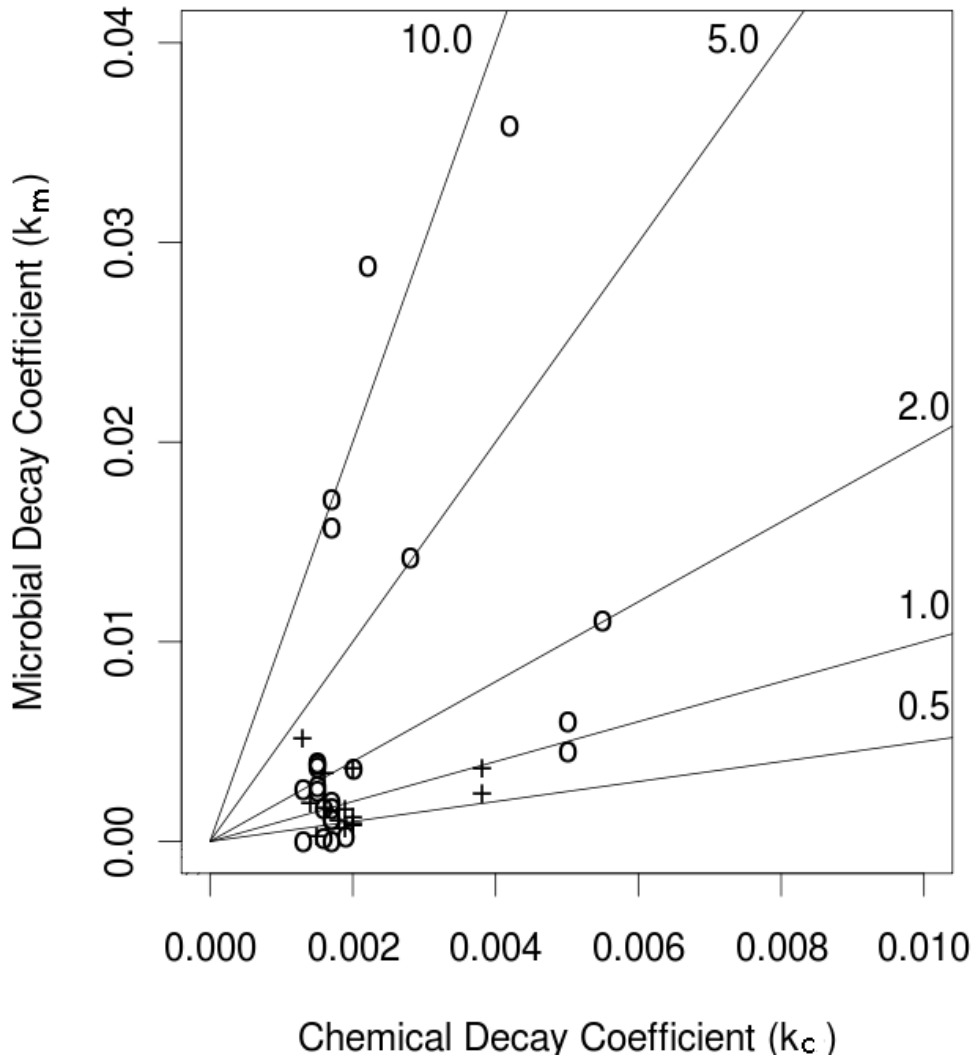


Figure 5.9: An illustration of the range of observed F_m values from batch tests done as part of this research (+), and from literature (o) (Sathasivan *et al.*, 2005, 2008; Fisher *et al.*, 2009; Sathasivan *et al.*, 2010). Constant F_m numbers are shown as straight lines and labelled with their value.

Evaluation of Batch Test Method

For the present research, some aspects of this batch test method for nitrification were investigated further in an attempt to better understand the processes at work, and to validate its effectiveness. First of all, the effectiveness of the silver nitrate inhibitor used was evaluated by comparing the total chlorine decay in inhibited and filtered samples. Organic carbon and ammonia-nitrogen substrates were added to some samples in an effort to assess the effect of nutrient concentrations on chloramine decay. Further data was obtained by liquid chromatography with organic carbon detection (LC-OCD) testing. Finally, the results of the batch testing described in this chapter are compared to disinfection times from literature (*Ct* concept) and to the full-scale sampling results presented in the previous chapter (Chapter 4).

To evaluate the reliability of the batch test method for nitrification used in this research the efficacy of the inhibition agent, silver nitrate, was assessed by comparing inhibited samples (100 $\mu\text{g-Ag/L}$ of AgNO_3) to filtered samples (sterile 0.20 μm membrane filter). Both of these techniques were intended to eliminate microbial activity. Tests of filtered and inhibited sets of samples gave comparable results. A paired t-test (Dodge, 2010) on measurements from inhibited and filtered sets of samples did not find a significant difference ($p=0.22$). If anything, adding silver nitrate appeared to be more reliable than filtration at curtailing microbial activity. Figures A.11 and A.12 (Appendix A) show the total chlorine residual in filtered samples differed from the inhibited sample curves after 200 hours of incubation time, suggesting that some microorganisms may have passed through the filters for site WOD06. In samples from site K20S14, the measured chemical decay rate of filtered samples decreased by 14% from that of inhibited samples. A possible explanation is that filtering the sample removed some particulate or colloidal material that was exerting a chlorine demand. These results reinforce the use of silver nitrate for inhibiting samples to separate the chemical contribution to chloramine decay from the microbial contribution in batch tests, supporting the work of Sathasivan *et al.* (2005).

Also in the final round of batch testing, some samples were augmented with additional ammonia or organic carbon (acetate) to determine if they would accelerate the decay of the total chlorine residual. These results are included in table 5.1 above, marked with “+C” for organic carbon addition (1.5 mg-C/L of acetate) and with “+A” for ammonia-nitrogen addition (0.2 mg-N/L). The impact of augmenting samples with ammonia or organic carbon does not appear to have been investigated in previous applications of this batch testing method for nitrification. The effect of adding these nutrients was assessed by comparing the total chlorine decay coefficients between samples with and without nutrients added. The disinfectant residual concentrations at constant incubation times were compared using paired t-tests (Dodge, 2010) to indicate whether differences were statistically significant. The

samples tested were collected from sites K20S14 and WOD06 in the Waterloo distribution system on 24 November 2010. There were small decreases in k_C , k_{T1} , k_m from adding ammonia. Adding acetate led to large increases in k_{T2} (52% for K20S14, 71% for WOD06), while k_{T1} and k_m had small decreases. Paired t-tests on total chlorine concentrations at equal incubation times yielded the following results:

- Adding ammonia to uninhibited vials did not have a significant effect ($p=0.49$)
- Adding acetate to uninhibited vials led to lower total chlorine concentrations ($p=0.0003$, $\Delta=0.04$ mg/L)
- Adding ammonia to inhibited vials maintained higher total chlorine concentrations for longer periods of time ($p=0.0001$, $\Delta=0.10$ mg/L)
- Adding acetate to inhibited vials did not have a significant effect ($p=0.11$)

Some causes can be suggested for the impacts observed from adding organic carbon and ammonia to samples for batch testing. The addition of acetate to uninhibited samples likely stimulated the growth of heterotrophic microorganisms, which use organic carbon as their substrate. Since it did not have a significant effect in inhibited portions of samples, acetate does not appear to exert a noticeable chlorine demand at the concentration used here. The increases in k_{T2} but not k_{T1} (i.e. the total chlorine decay rate was only greater during the second phase of decay) suggests a lag that fits with the idea that increased heterotrophic growth resulted in more rapid chlorine decay. This has implications in how these batch test results should be interpreted. This method was developed (Sathasivan *et al.*, 2005) and applied here in the context of nitrification. However, it is important to remember that the microbial contribution to chloramine decay (quantified by k_m) also includes heterotrophic activity. Further research is recommended to clarify the relative contributions of nitrifiers and heterotrophs to the total chlorine decay rate in chloraminated drinking waters. The addition of ammonia affected the sample trends in an opposite manner from acetate. It had a significant effect on inhibited samples but not on uninhibited samples. This suggests that a chemical mechanism was most important here. Vikesland *et al.* (2001) noted that monochloramine is more stable in the presence of ammonia, so a decrease in k_C in sample portions with added ammonia matches theoretical considerations. Being able to separate the chemical and microbially-mediated elements of chloramine decay makes this batch test methodology a valuable tool for investigating questions of this nature, and its future use in research is recommended.

The magnitude of the impacts of adding organic carbon and ammonia are not comparable in this study since different concentrations were applied (1.5 mg-C/L versus 0.2 mg-N/L). This was targeted to increase the concentrations of DOC and ammonia by 50–100% each.

When considering the true substrate of heterotrophic microorganisms (assimilable organic carbon, AOC), however, the acetate added represents a much larger augmentation.

A liquid chromatography-organic carbon detector (LC-OCD) (Huber *et al.*, 2011) was used to determine changes in the organic carbon fractions present at the beginning and end of some of the batch tests—both in inhibited and uninhibited samples. This technique was also able to provide some information on nitrogen fractions that were present. The characterization of organic carbon fractions and how they change during the batch testing employed here is a novel aspect to this work on distribution system nitrification. Even though the motivation for these batch tests was the evaluation of nitrification potential in distribution system samples, heterotrophic microorganisms are also expected to be present and active. Furthermore, nitrifiers are able to fix inorganic carbon (Rittmann *et al.*, 1994). These microbial processes will influence the organic carbon that is present in the water sample, so the LC-OCD analysis can provide insight into them.

Figure 5.10 shows how the character of dissolved organic carbon changed during a typical batch test. The largest decreases in the batch test carbon concentrations come from low molecular weight (LMW) acids and humic substances (HS) fraction, with contributions from the “building blocks” and humic substance (HS) fractions that were almost as great in some cases. LMW neutrals appear to increase during the course of the batch testing. Since these batch tests were carried out in plastic vials, it is possible that some of the changes in the character of the organic carbon present—especially the increase in LMW neutrals and the overall TOC content (first peak)—are due to interactions with the container walls, such as adsorption or leaching. These possibilities should be controlled for in future experiments using this method. Krishna and Sathasivan (2010) speculated that the chlorine demand exerted by soluble microbial products or other metabolic byproducts could be the cause of an increase in the chemical decay coefficient (k_C) in samples undergoing severe nitrification; they were not able to fully explain this increase in reference to other water quality changes. LC-OCD testing may be a promising avenue for further investigation of this topic.

The LC-OCD instrument also provided information on the fractions of nitrogen that were present. Figure 5.11 shows organic nitrogen chromatographs from before and after the uninhibited set of a batch test on a sample from site 904. Ammonium is the last peak to the right while nitrate is the large peak near the center of the graph (Huber *et al.*, 2011). This figure shows that some nitrogen was oxidized from ammonium to nitrate over the course of this batch test. The trend seen here conforms to expectations if nitrifiers are indeed active in these samples.

Another way in which the results of the batch tests presented in this chapter were evaluated was the calculation of Ct values (Chick-Watson disinfection times) for comparison with published disinfection kinetics for nitrifying microorganisms (refer to Table 2.1 in chapter 2). This was done by finding the area under the total chlorine decay curves in uninhibited

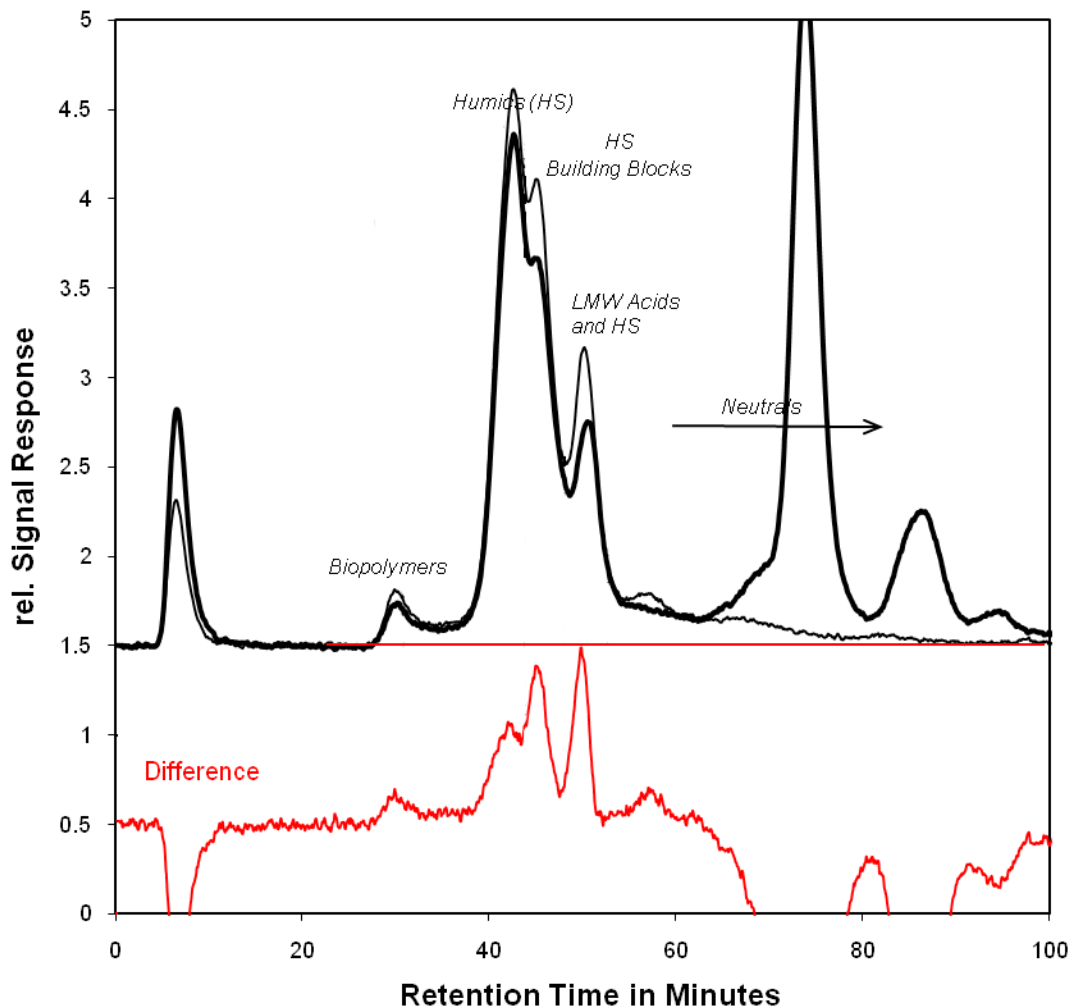


Figure 5.10: Changes in LC-OCD chromatographs over the course of batch testing on an uninhibited sample from site WOD61. The thin line represents a sample which was filtered, acidified, and refrigerated at the start of the testing period while the bold line comes from an uninhibited vial at the end of the testing period. The red curve at the bottom of the figure shows the differences, magnified by a factor of 2.

samples; this area is the product of the disinfectant concentration and contact time, so it has the correct dimensions for a Ct value. For the samples shown above exemplifying each type of trend seen in these batch tests, it ranged from 4010 mg-min/L as Cl_2 for Fig. 5.7 (Type IV sample from site WOD06) to 22070 mg-min/L as Cl_2 for Fig. 5.5 (Type II sample

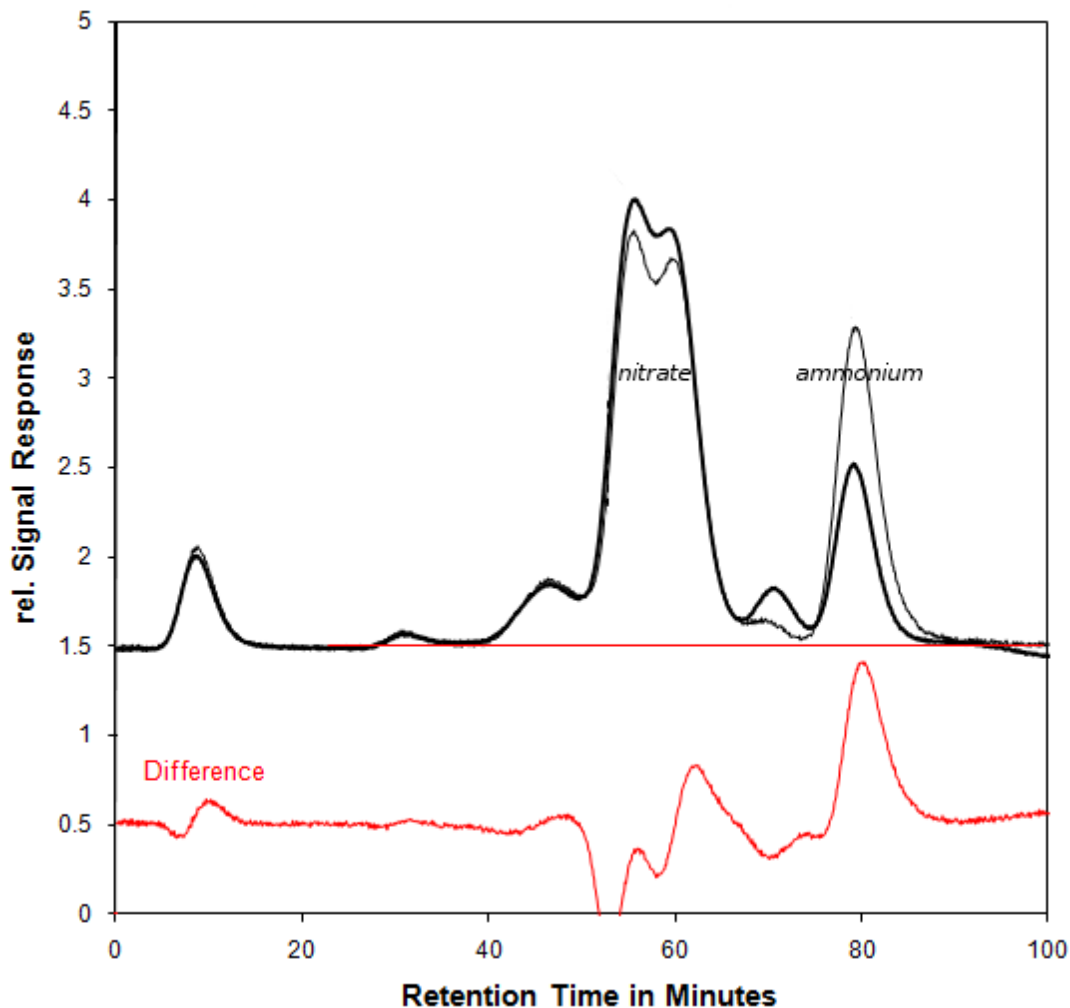


Figure 5.11: Changes in LC-OND Chromatographs over the course of batch testing on a sample from site 904. The thin line was filtered, acidified, and refrigerated at the start of the testing period while the bold line comes from an uninhibited vial at the end of the testing period. The red curve at the bottom of the figure shows the differences. The first peak after the vertical dashed line is nitrate, while the last peak is ammonium.

from site K20S14). In both of these batches microbial activity was detected, as evidenced by $k_m > 0$, even though they were both above the Ct_{99} of 3300 mg-min/L as Cl_2 calculated by Wahman *et al.* (2009) from monochloramine inactivation kinetics on *Nitrosomonas europaea* in a controlled disinfection test. This apparent microbial survival at long inactivation times

may indicate that species of AOB and AOA (and heterotrophic bacteria, which can also contribute to chloramine decay) found in distribution systems have high chloramine resistances (see Cunliffe 1991). Microorganisms in these samples could also be protected by attachment to particles.

The results in this chapter were also compared to the results for the same sites from the sampling campaign presented in Chapter 4. Overall, there were not straight-forward relationships between these batch tests and the full-scale results. This may be significant in itself, suggesting that this batch test methodology may provide information that is complementary rather than redundant to parameters that are usually monitored in distribution systems. For example, the microbial decay rate coefficients (k_m) for samples in the main round of batch testing conducted for this study were not in the same order as the AOA or AOB or HPC abundances on the final sampling date (closest to when the batch tests were conducted) from the full-scale distribution systems. Sathasivan *et al.* (2005) and Fisher *et al.* (2009) have used this batch test method to obtain information about the potential for nitrification at distribution system locations that is not available from traditional physico-chemical indicators.

The closest matches with the full-scale results were between the total chlorine decay curve types defined above and the culture-based AOB test (Table 4.1) and the average HPC (Figure 4.15). Samples collected from sites RCL (Toronto) and K20S14 (Waterloo) in August and October 2010 were identified as types I and II and these sites had low HPCs over the course of the full-scale sampling campaign. Sites RCL and 804 from the Toronto distribution system both tested negative for ammonia oxidizers in a culture-based presence/absence test (Table 4.1) and were identified as types I and II in batch testing on samples collected in August and October 2010. Both of the samples (from sites K20S14 and WOD06) collected on 24 November 2010 were type II. The full-scale sampling campaign had concluded by this time, but the cold water conditions make it reasonable to expect low microbial activity in these samples. This similarity makes sense, since these batch experiments have microorganisms growing in a closed environment, as do the HPC test and nitrifier growth test. Furthermore, both the total chlorine decay curve types and the ammonia-oxidizer presence/absence test are qualitative assessments. This similarity also suggests that the initial concentration of microorganisms is an important factor to this batch test for nitrification. In addition, it supports the common recommendation of heterotrophic plate counts as a gauge of general microbiological water quality in distribution systems (Health Canada, 2011; National Research Council, 2006).

As part of the present research, the batch test method for nitrification being used was evaluated on a number of points. A comparison between filtered and inhibited samples supported the use of silver nitrate as a microbial inhibitor. An initial evaluation was also made regarding the impact of augmenting the organic carbon and ammonia concentrations, al-

though further testing will be necessary to strengthen confidence in the results. The addition of organic carbon appeared to promote chloramine decay associated with microorganisms, while the addition of ammonia seemed to reduce the chemical decay rate coefficient. A novel aspect of the evaluation conducted in this research was the use of LC-OCD to determine changes in the characterization of organic carbon and nitrogen species over the course of batch tests. Calculating the Chick-Watson disinfection time (Ct value) equivalent over the course of the batch tests suggested that some of the microorganisms present in the samples may have some capacity to survive chloramine disinfection under the test conditions. Finally, comparing the results from the batch testing conducted for this portion of the study with the full-scale sampling campaign described earlier indicated that the information obtained is complementary—rather than fully overlapping—with parameters that are normally monitored in distribution systems.

5.4 Conclusions and Recommendations

It is expected that the batch test methodology for investigating the nitrification potential of a distribution system sample used in this study will prove useful in future research and for drinking water system operations, provided its limitations are kept in mind.

The following are the key findings from this chapter.

- The two phases of decay of the total chlorine residual first noted by Sathasivan *et al.* (2008) were confirmed.
- This batch test method is able to isolate the microbially-mediated and chemical components of the total chlorine decay rate.
- Four types of decay trends that can be used to classify samples were identified.
- The assumption of first-order decay is only an approximation, but is usually valid; the calculation procedure for determining the critical threshold residual (CTR) was modified to depend less on this assumption.
- The microbial decay factor (F_m) should be used with caution (not in isolation, but in conjunction with other parameters) since this ratio can have the same value under contrasting conditions.
- A normal range of 0.001–0.002 h⁻¹ was identified for k_C ; samples that fall outside of this range should be examined more closely.
- Liquid Chromatography with Organic Nitrogen Detection (LC-OND) results confirmed nitrification taking place.
- The efficacy of silver nitrate as an inhibiting agent was supported by comparisons between filtered and inhibited samples.
- This batch test method may be seen as complementary to the models discussed in Chapter 6—another tool for predicting distribution system nitrification.

These findings lead to the following recommendations:

- The CTR and the incubation time required to reach it are recommended for use in reservoir operation.
- Further investigation into what causes the acceleration of the decay rate is recommended.

- Further research is recommended on the impact of nutrients and which type of microorganisms have a larger role in chloramine decay.

Chapter 6

Evaluation of Models for Nitrification

6.1 Introduction

Nitrification in chloraminated drinking water distribution systems can lead to operational challenges such as difficulty in maintaining a total chlorine residual and the potential for bacterial regrowth resulting in an increase in heterotrophic plate counts (HPC). Once a nitrification episode is fully established, it can be costly and difficult to bring under control. Raising the monochloramine residual is often ineffective at halting nitrification once it is established (Skadsen, 1993; Odell *et al.*, 1996; Pintar and Slawson, 2003). This is because the products of nitrification (nitrite, and increased organic matter from nitrifier growth) promote chloramine decay, which provides more ammonia, allowing further nitrification (Oldenburg *et al.*, 2002). Breakpoint chlorination or flushing may be necessary once a nitrification episode is fully established.

In addition to challenges in controlling nitrification, detecting episodes before they become fully established can also be a challenge. Commonly used indicators of distribution system nitrification, such as the presence of nitrite, may not provide early warnings of nitrification episodes. Pintar *et al.* (2005) found that using a nitrite threshold concentration of 0.05 mg-N/L could confirm a nitrification episode but appeared too late to be useful as an early warning. Wilczak *et al.* (1996) reported that ammonia was not a sensitive nitrification indicator, which may be explained by the observation of Liu *et al.* (2005) that ammonia levels initially increased due to chloramine decay, and then decreased as the nitrification rate increased. The long times (28 d) required for culture-based analysis of ammonia-oxidizing bacteria (AOB) has historically meant that detecting or enumerating the microorganisms responsible for nitrification could not be used for time-sensitive operational decisions in distribution systems (Hoefel *et al.*, 2005). One approach to dealing with the weaknesses of traditional indicators for nitrification is to use models that can predict distribution system

conditions that could promote nitrification. Some researchers have developed models to predict when nitrification episodes will occur or how they will develop. In this chapter, some of these models are examined and evaluated.

Most of the following models are based on theoretical considerations of the mechanisms by which selected factors impact nitrification, although a statistically-based logistic regression model (Yang *et al.*, 2007) has also been developed. There is a wide range in the complexities of models that have been proposed for nitrification in chloraminated drinking water distribution systems. For example, the model of Fleming *et al.* (2005) has only two variables, while the model of Liu *et al.* (2005) has eight variables.

The most detailed and complex of the models discussed in this chapter are the mechanistic models developed by Liu *et al.* (2005) and Yang *et al.* (2008). They both used mass balance equations for a set of chemical and microbiological parameters relevant to distribution system nitrification. The model of Liu *et al.* (2005) was developed for steady-state plug-flow scenarios, while that of Yang *et al.* (2008) was dynamic with completely-mixed hydraulics.

Yang *et al.* (2008) developed a model for nitrification that is based on suspended growth mass balances. This model was developed for completely mixed flow-through reactors (CMFTR) to predict the dynamics of several chemical and microbiological constituents related to nitrification on a semi-mechanistic basis. The authors attempted to delve deeper into the underlying mechanics and dynamics of nitrification episodes than previous models. As a mechanistic model, it requires the concentrations of a large number of constituents: total chlorine, free ammonia, nitrite, nitrate, HPC, AOB, and NOB.

The model of Yang *et al.* (2008) was a good fit for the pilot-scale systems used in their study, including ones that were not used in the regression analysis but were saved for verification. One of the key simplifications used in this model was to neglect biofilm processes. This makes it most suitable for portions of a full-scale distribution system with low surface-to-volume ratios (i.e. reservoirs). One interesting implication of this model was that the heterotrophic contribution to chloramine decay via soluble microbial product oxidation was found to be statistically significant.

Liu *et al.* (2005) developed a steady-state plug flow kinetic model for nitrification in drinking water distribution systems. It was based on experiments done on pilot-scale distribution systems that used cast-iron pipes with flow velocities typical of dead zones in distribution systems. Their model predicts concentrations of nitrogen species and AOB and NOB biomass. They used Monod kinetics for net cell growth and rate of substrate utilization; these growth equations allowed for the possibility of DO limitation. In contrast to the other models described here, Liu *et al.* (2005) treated the monochloramine concentration as an inhibiting factor for nitrifying microorganisms and not an inactivating agent. The main

portion of this model are plug flow mass-balances that were derived for monochloramine, ammonia, nitrite, and nitrate, assuming a constant total concentration of inorganic nitrogen. A major simplification of this model was that the chemical oxidation of nitrite was not accounted for. This model requires that the hydraulic retention time (HRT) be known for each pipe segment modelled in order to define a concentration gradient (inflow – outflow / HRT), since the transformation processes are expressed as rates. Therefore, this model would be difficult to apply to most full-scale distribution systems where retention times are variable or not known with sufficient precision.

Fleming *et al.* (2005) developed the “Nitrification Potential Curves” model that delineates between conditions considered non-nitrifying and potentially nitrifying based on a balance between growth and inactivation rates of nitrifiers. Growth rates were treated as a function of the ammonia concentration promoting growth, and the total chlorine concentration was taken as the factor affecting the inactivation rate. The nitrification potential curves of Fleming *et al.* (2005) are defined by equation 6.2.

An important advantage of the nitrification potential curve model of Fleming *et al.* (2005) is that it only requires measurements of chemical parameters (total chlorine, ammonia, and nitrite), which are relatively simple to obtain. Nitrification potential curves do not use direct measurements of kinetic parameters, as the precise nitrifier strains present are usually unknown, but are instead fitted to system monitoring data.

A generalized biological stability curve was presented by Srinivasan and Harrington (2007) that has the same basis as the nitrification potential curve of Fleming *et al.* (2005)—a balance between substrate and disinfectant concentrations—but can be applied to heterotrophs or nitrifiers. They explored the mathematics of this type of curve and provided a procedure for fitting its parameters to a specific system. Like Fleming *et al.* (2005), Srinivasan and Harrington (2007) conceptualized biological stability in a distribution system as the outcome of the interaction between bacteria, their substrates, and the disinfectant residual. They pointed out that each species of bacteria in a distribution system would have its own biostability curve, based on its growth and inactivation kinetics, but showed that in practice a conservative biostability curve can be fitted to a system empirically.

This approach to modelling biological stability in drinking water distribution systems has a basis in earlier literature. LeChevallier *et al.* (1996) identified disinfectant and nutrient levels as variables affecting the biological quality of drinking water. They hypothesized that adequate water quality could be attained by limiting the nutrient level or by maintaining a strong enough disinfectant level. Huck and Gagnon (2004) hypothesized a critical disinfectant residual, C_{crit} , above which the substrate concentration has a minimal effect on microbial accumulation; this is analogous to the asymptote (R_{gi}) of the biostability curves of Srinivasan and Harrington (2007) and Fleming *et al.* (2005).

Fleming *et al.* (2008) applied the nitrification potential curves model to three full-scale drinking water distribution systems. They were able to successfully fit their model to all of the distribution systems they studied. A notable outcome of their study is that the K_s values fitted for the nitrification curves were much lower than half-saturation coefficients found in literature for *N. oligotropha*, a species of AOB with a high affinity for ammonia. Therefore, they suggested that K_s values for full-scale systems will be much lower than those found from culture-based studies. This may be because nitrification potential curves can encompass the behaviour of many species, as shown by Srinivasan and Harrington (2007). Nitrification potential curves can be used to identify changes in total chlorine and ammonia concentrations that could reduce the risk of nitrification.

The same approach as Fleming *et al.* (2005) was adopted by Speital *et al.* (2011), who also added the effect of trihalomethane (THM) cometabolism and toxicity to their “Nitrification Index” (N.I.) model. Wahman *et al.* (2006) found that nitrifiers could degrade THMs, although toxic by-products were generated in the process. The rate constants that Wahman *et al.* (2006) found for THM removal were highly variable. As this was a cometabolism process, it was promoted by higher ammonia (i.e. the primary metabolic substrate) concentrations. The removal of THMs by AOB cometabolism was also observed by Wahman *et al.* (2011) in biofilters they studied. The “Nitrification Index” model of Speital *et al.* (2011) builds on the work of Wahman *et al.* (2006) and Fleming *et al.* (2005). It is defined by equation 6.3. N.I. >1 implies nitrification will occur. THM cometabolism was found to have a small effect (20% versus 70–90% for monochloramine disinfection) at N.I. <1.5.

A different approach from the models discussed above—statistical rather than based on mechanistic considerations—was applied by Yang *et al.* (2007), who developed a risk-factor probability model for distribution system nitrification, using logistic regression to identify significant parameters. They used factorial experiments in pilot-scale distribution systems to ascertain the impact of selected factors on the probability of nitrification. The significant factors determined in their experiments were: pH, total chlorine residual, hydraulic detention time, and temperature. Interestingly, they did not find the ammonia concentration to significantly affect the probability of nitrification. By applying logistic regression they fit equation 6.5 to their system.

The authors identified the simplicity of statistical models, as compared with mechanistic models, as one of their advantages. However, they caution that the accuracy of their model is not guaranteed beyond the conditions for which it was developed, so it may be necessary to fit a similar equation to a specific system being studied.

The final model to be examined in this research is the “carbon-to-nitrogen ratio” (C/N) model of Zhang *et al.* (2009b), which is based on the work of Verhagen and Laanbroek (1991). It uses the carbon-to-nitrogen ratio in the water to predict whether nitrifiers or heterotrophs will be dominant in a distribution system. Unlike the previous models discussed, which

concern nitrification in general, this model has a more specific focus, namely competition for ammonia-nitrogen between ammonia-oxidizing and heterotrophic bacteria. Verhagen and Laanbroek (1991) evaluated competition between a heterotrophic species (*Arthrobacter globiformis*) and an ammonia-oxidizing species (*Nitrosomonas europaea*) of bacteria in situations with limiting ammonium. In theory, heterotrophs will be nitrogen limited above the critical C/N ratio and will consume all of the available ammonium (assuming they have a higher ammonium affinity than nitrifiers); below the critical C/N ratio, heterotrophs will be carbon-limited and excess ammonia will be available to nitrifiers. In two bench-scale competition experiments, Verhagen and Laanbroek (1991) found critical carbon-to-nitrogen ratios of 11.6 and 9.6. These critical C/N ratios were determined as the glucose concentration at which ammonium oxidation ceased in mixed cultures of a heterotrophic and AOB species.

Zhang *et al.* (2009b) developed the C/N model from the work of Verhagen and Laanbroek (1991). It does not account for the effect of a disinfectant residual, so if one type of microorganism had a greater resistance to monochloramine, competition may not have a large impact. The model uses equations 6.9 and 6.10 to delineate conditions under which nitrifiers will be out-competed by heterotrophic bacteria and conditions where they will be the most abundant.

However, there is debate in the literature on the two main assumptions of the C/N model: whether heterotrophs and nitrifiers have a competitive relationship, and whether heterotrophs have a stronger affinity for ammonia-nitrogen than nitrifying microorganisms. Zhang *et al.* (2009b) discussed possible synergistic effects between nitrifying microorganisms and heterotrophic bacteria, such as the excretion of useful metabolic products or removal of toxic metabolic products. For example, *Nitrosomonas europaea* produce 0.073 mg COD (chemical oxygen demand) of soluble microbial products per mg of NH₃-N oxidized, which could provide a substrate for heterotrophs in low organic carbon environments (Rittmann *et al.*, 1994). Some studies have found a higher ammonia affinity in certain species of AOB and AOA compared with the AOB *Nitrosomonas europaea* used by Verhagen and Laanbroek (1991). Bollmann *et al.* (2002) compared the growth at low ammonium concentrations of *N. europaea* with G5-7 (a close relative of *N. oligotropha*, which has been reported in distribution systems (Regan *et al.*, 2002, 2003)). *N. europaea* was found to recover from starvation more quickly, while G5-7 could grow at lower ammonium concentrations. For a strain of AOA, Martens-Habbena *et al.* (2009) found a very low half-saturation coefficient, corresponding to a very high ammonia affinity. The C/N model would not apply to species of ammonia-oxidizers with a higher ammonia affinity than heterotrophic microorganisms, as they would not be out-competed for ammonia even when heterotrophs are nitrogen-limited for their growth.

The models listed in Table 6.1 were examined and evaluated in this chapter. These models were applied to data collected from two full-scale chloraminated drinking water distribution

systems (see Chapter 4). For models where this data was insufficient for their application, more general assessments were made.

Table 6.1: Nitrification models evaluated in this study.

Model	Reference	Basis
Pilot-scale Kinetic Model	Yang <i>et al.</i> (2008)	A mechanistic approach
Plug-flow Kinetic Model	Liu <i>et al.</i> (2005)	A steady-state mechanistic approach
Nitrification Potential Curves	Fleming <i>et al.</i> (2005)	Separation of nitrifying and non-nitrifying sites based on free ammonia and total chlorine levels
Nitrification Index	Speital <i>et al.</i> (2011)	Incorporates THM co-metabolism as an inactivating factor
Logistic Risk Model	Yang <i>et al.</i> (2007)	Logistic regression on nitrification factors
Carbon-to-Nitrogen Ratio	Zhang <i>et al.</i> (2009b)	Predicts dominance of heterotrophic or nitrifying bacteria based on substrates DOC & NH ₃

6.2 Evaluation and Application of Nitrification Models

Modelling is a diverse endeavour, in which different approaches are appropriate depending on the circumstances and purpose to which a model will be applied. Models can be distinguished from each other by a broad range of criteria, including their scale, degree of abstraction and approximation, whether they are intended to be mechanistic or merely descriptive, and whether they include dynamic and probabilistic considerations. Peierls (1980) classified models in physics according to their degree of simplification. The author argued that all types of models can be useful so long as their limitations are recognized and their use is restricted to appropriate circumstances, whether calculations, teaching, or thought experiments. The models presented in this chapter mostly fit in the middle of the categorization scheme of Peierls (1980) as “Simplifications” or “Approximations” where some features of the phenomenon being studied (nitrification in this case) are omitted to provide clarity or considered negligible enough to ignore. Murthy *et al.* (1990) provided additional means for classifying models. They divided types of models based on whether they include changes with time and whether they are deterministic or include randomness. Most of the models evaluated below are static and deterministic, although the model of Yang *et al.* (2008) involves changes with time. Murthy *et al.* (1990) suggest that models may be further categorized based on the number of independent variables that they use and whether those variables are mathematically discrete or continuous. Dym (2004) emphasized the importance of using a proper level of detail and physical scale when selecting or designing a model.

Table 6.2 lists the scales at which each of the models considered in this chapter have been tested and the number of variables and coefficients used, which may be taken as quantifying the complexity of the model. These items are used as criteria in evaluating the models in this chapter.

In the following subsections, each of the models is evaluated and discussed in detail. Where possible, they are applied to the results of the full-scale distribution system sampling campaign that was covered in Chapter 4 of this thesis. However, some of these models require parameters that were not measured or were not available at the level of detail required for the analysis. For example, applying the plug-flow model for nitrification developed by Liu *et al.* (2005) would require detailed information about hydraulic retention times that was not available for the distribution systems being studied. Models that could not be applied to the full-scale results of the current research project are discussed at a theoretical level.

The first models to be discussed are the mechanistic models of Yang *et al.* (2008) and Liu *et al.* (2005). These models are the most complex since they attempt to account for the important processes involved in nitrification and track the concentrations of relevant parameters. Even so, they still rely on many simplifying assumptions. The complexity of these models makes them best suited for research applications. They are presented first to

Table 6.2: The scale at which each model has been tested and the number of input variables and fitting coefficients for the models evaluated in this chapter.

Model	Scale Tested	Variables	Coefficients
Pilot-scale Kinetic Model	Pilot	8	18
Plug-flow Kinetic Model	Pilot	8	8
Nitrification Potential Curves	Full (Fleming <i>et al.</i> , 2008)	2	2
Nitrification Index	Bench	6	14
Logistic Risk Model	Pilot	3	5
Carbon-to-Nitrogen Ratio	Bench (Verhagen and Laanbroek, 1991), Theory (Zhang <i>et al.</i> , 2009b)	2	NA

provide a contrast with other models discussed in this chapter that may be more feasible for application to full-scale drinking water distribution systems. The next two models discussed (Fleming *et al.*, 2005; Speital *et al.*, 2011) are conceptually much less complex. These models still have some basis in the mechanisms of nitrification, but focus on only a few key processes. Additionally, they merely predict whether the conditions for nitrification exist at a distribution system site, rather than predicting the concentrations of relevant parameters. The model of Yang *et al.* (2007) used a statistical approach that did not depend on mechanistic considerations. This model predicts the probability of a nitrification event. The final model discussed is the Carbon-to-Nitrogen model (Verhagen and Laanbroek, 1991; Zhang *et al.*, 2009b) which relates to a niche topic (i.e. the ecological balance between nitrifiers and heterotrophs) rather than making predictions about nitrification in general.

Pilot-scale Kinetic Model

The first model considered here is the kinetic nitrification model that Yang *et al.* (2008) developed from pilot scale experiments. The inputs to this model are the influent concentrations of the chloramine residual, HPC bacteria, ammonia, AOB, nitrite, NOB, and nitrate, and the hydraulic retention time. It returns predictions for the concentrations of the chloramine residual, ammonia, AOB, nitrite, NOB, and nitrate. This model is based on mass balances in the bulk water phase for chemical and biological quantities relevant to nitrification. This is the most complex model evaluated in the present study, having a large number of variables and fitting coefficients. Like the other models considered in this chapter, it is deterministic; it has no stochastic elements. In contrast to the other models, the kinetic nitrification model of Yang *et al.* (2008) is the only one that is truly dynamic.

This model is defined by a set of differential equations for the model parameters. For example, the following equation is their mass balance for the total chlorine disinfectant residual (Yang *et al.*, 2008):

$$\frac{dC_d}{dt} = \frac{C_{d0} - C_d}{\tau} - k_A C_d^2 - k_{NOM} C_d - r_{mn} - k_{SMP} C_{HPC} C_d \quad (6.1)$$

In this equation, C_d represents the concentration of the total chlorine disinfectant residual, τ is the hydraulic residence time, k is used for the rate coefficients for various reactions, and r_{mn} is the reaction rate between nitrite and monochloramine. Mass balances similar to equation 6.1 for ammonia, AOB, nitrite, NOB, and nitrate comprise the remainder of the model. See Yang *et al.* (2008) for further details and the remaining mass balances.

Chloramine autodecomposition was given a second-order decay coefficient in this model. Reaction with NOM (natural organic matter) was taken as the other chemical contribution to chloramine decay and was modelled as a pseudo-first order process, with NOM assumed to be non-limiting. In addition to chemical factors driving chloramine decay, the complete model considered other mechanisms contributing to chloramine decay, including chemical oxidation of nitrite, and reaction with soluble microbial products (SMP). Temperature was accounted for in their model by adjusting the maximum specific growth rates for AOB and NOB. Some of the required coefficients were obtained from literature, and others from calibrating the model to the pilot-scale distribution system used in its development.

For the evaluation of the kinetic model developed by Yang *et al.* (2008) some simulations were conducted using the statistical language “R” (R Development Core Team, 2009). The code used for these simulations is given in Appendix E. For purposes of this evaluation, a small adaptation was made to the equations of Yang *et al.* (2008) to convert them from completely mixed flow-through reactor (CMFTR) hydraulics to batch hydraulics. That is, terms for influent and effluent concentrations were removed. This was done to simplify the

calculations involved, and to facilitate comparisons with the batch testing results presented in Chapter 5. This model was too complex to directly apply to the results in Chapter 4—in either hydraulic configuration—due mainly to its dynamic nature. The samples analyzed in Chapter 4 of this thesis were not collected frequently enough to evaluate a dynamic model. The aim of conducting simulations with this kinetic model was to obtain some indication of the reasonableness and consistency of its results, since it was not possible to apply it to the data collected in this research. Performing the simulations involved setting the initial values for each parameter and recording changes in their concentrations for a simulated period of 30 days, long enough to observe all the trends of interest.

Even though this model was not applied to data collected in this research, an effort was made to use realistic initial values in the following simulations. Initial total chlorine and ammonia concentrations of 1.3 mg/L and 0.15 mg-N/L, respectively, were assumed. These concentrations are within the ranges observed in both distribution systems involved in this study. HPC bacteria were assumed to be present at a level of 10 000 cells per 100 mL; HPC levels of this order of magnitude were observed in first-flush samples at a number of sites in both distribution systems involved in this research. In order to emphasize nitrification effects in simulations using the model of Yang *et al.* (2008), a high initial concentration was assumed for AOB: 100 000 cells per 100 mL, which approximates the maximum AOB level observed in first-flush distribution system samples in this study (at site WOD06 in the Waterloo distribution system). NOB were not monitored in this study, so they were set at one fifth of the initial AOB level (this ratio is based on the relative numbers of NOB and AOB observed by Lipponen *et al.* (2002) in chloraminated drinking water distribution systems). Assumed cell abundances were converted to biomass concentrations using a factor of 10^{-9} mg/cell (Rittmann and McCarty, 2001). All of these assumed biomass concentrations (HPC, AOB, and NOB) were chosen as high values to ensure a dramatic response from the model of Yang *et al.* (2008), since nitrification would not be expected to have a large effect at typical concentrations in well-controlled chloraminated drinking water distribution systems. Nitrite and nitrate were given arbitrary starting concentrations of 0.01 mg-N/L and 1.0 mg-N/L, respectively.

To investigate the properties and behaviour of the kinetic model of Yang *et al.* (2008), some tests were conducted to observe the impact on the model output when the initial values were varied. Starting from the set of initial values described above, one variable at a time was doubled and changes in the time that the model took to exceed a nitrite threshold of 0.05 mg-N/L were noted. The following observations were made from sensitivity testing on this model:

- Doubling the initial disinfectant residual led to a 57% increase in the time taken to exceed the nitrite threshold.

- From their default values, doubling HPC or the ammonia concentration had only a small effect, decreasing the time taken for a rise in nitrite by less than 5%.
- Doubling the assumed initial AOB abundance led to a 14% reduction in the time taken for nitrite to rise above 0.05 mg-N/L.
- Doubling the assumed initial NOB abundance led to an 8% increase.

These impacts generally fit expectations; the model did not yield noteworthy surprises in these simulations. A greater disinfectant residual is expected to prevent or delay the onset of nitrification. Similarly, starting with a larger AOB population would be likely to hasten the onset of a nitrification episode, as occurred in these simulations. The delay in the rise of nitrite when a larger starting NOB population was simulated is interesting. This illustrates how NOB activity could complicate monitoring for nitrification in real distribution systems. If a drinking water operator relies primarily on nitrite data for monitoring nitrification and there is a significant NOB population consuming nitrite, then there will be a longer delay before a nitrification episode is noticed. Additionally, as Regan *et al.* (2002) proposed, an NOB population could possibly slow the rate of the disinfectant residual decay by consuming nitrite that would otherwise react with monochloramine.

Figure 6.1 shows simulations that were conducted with the model of Yang *et al.* (2008) at two different initial ammonia concentrations (0.15 mg-N/L and 0.30 mg-N/L; other values are as listed above). It can be seen that there was not a great deal of difference in the model behaviour between these conditions; the model did not exhibit much sensitivity to the initial ammonia concentration. A simulation using this model was also applied to generate Figure 2.2 in Chapter 2.

The small impact seen from doubling the ammonia concentration in these simulations has some support in literature on nitrification. Many authors have reported high affinities for ammonia nitrogen in AOB species found in distribution system environments (Regan *et al.*, 2002; Bollmann *et al.*, 2002), as well as in AOA (Martens-Habbena *et al.*, 2009). For species with high ammonia affinities, the ammonia concentrations used in the above simulations may be in excess of growth requirements; in that case, the small impact on nitrification from a further increase in ammonia levels is a realistic output from the model. The half-saturation coefficient for AOB used by Yang *et al.* (2008) in their model fits well within the range reported in the literature (see Table 2.1).

One effect of the ammonia concentration that was not included in this model is increasing the stability of the monochloramine residual (Vikesland *et al.*, 2001). The authors included the effect of ammonia on biological processes related to nitrification, specifically the growth and metabolic activity of ammonia oxidizers, but assumed the effects of ammonia on chemical processes relevant to distribution system nitrification could be neglected.

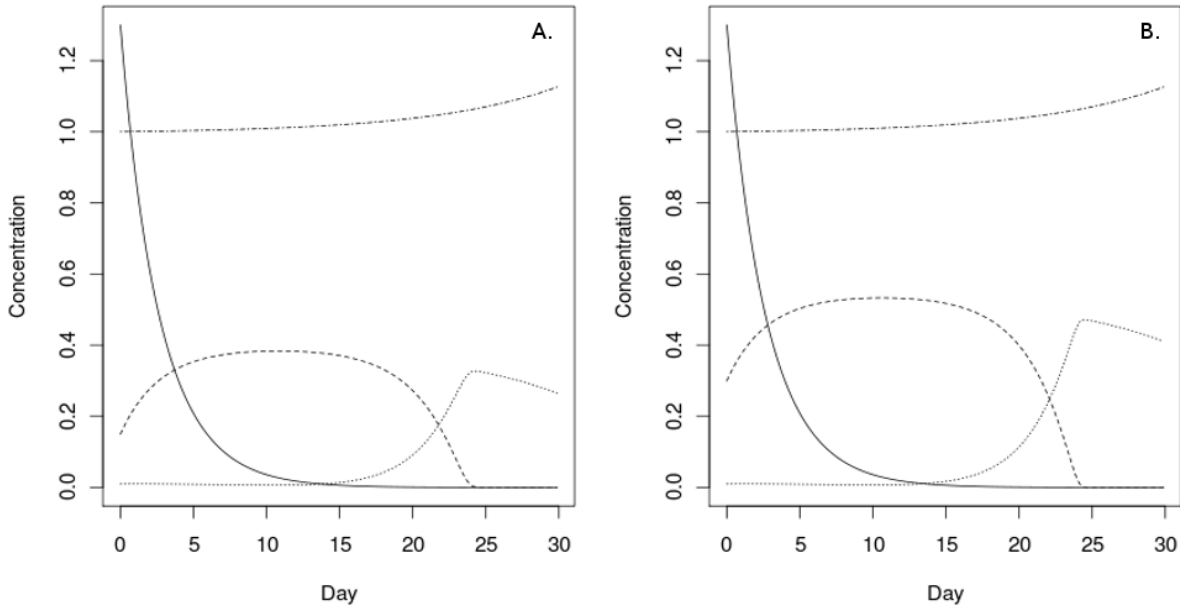


Figure 6.1: A pair of simulations conducted using the model of Yang, Harrington, and Noguera (2008). Initial conditions were the same except for the ammonia concentration (A—0.15 mg-N/L; B—0.30 mg-N/L). Ammonia is shown as a dashed line (---), the total chlorine residual is shown as a solid line (—), nitrite is shown as a dotted line (...), and nitrate is shown alternately dashed and dotted (-.-.).

However, in batch tests conducted for this study—described in Chapter 5—adding ammonia to distribution system samples in which microbial activity was inhibited yielded a decrease in the total chlorine decay rate. This suggests that accounting for the increased stability of monochloramine in the presence of ammonia might be a useful improvement to this model.

Since the simulations based on the model of Yang *et al.* (2008) have been modified to a batch hydraulic regime for simplicity, they can easily be compared to the results of the batch tests presented in Chapter 5. A prominent contrast exists between the above simulations and the batch testing results from this research, which is the absence of a second phase of total chlorine decay where the decay rate accelerates. Sathasivan *et al.* (2008) labelled the point at which the decay rate of the total chlorine residual accelerates in nitrification batch tests as the critical threshold residual (CTR). The existence of the CTR was confirmed in the work presented in Chapter 5 of this thesis (see Figures 5.5 and 5.6), but does not appear in the simulations conducted with the kinetic nitrification model of Yang *et al.* (2008). Since this model is mechanistically-based and the mechanisms causing the increase in the total chlorine decay rate below the CTR are unknown, it is not surprising that that effect was not included in the model. However, this does represent a possible opportunity to improve the

model performance.

A strength of this model is that it includes reactions that are sometimes overlooked in discussions of nitrification, namely the oxidation of nitrite by monochloramine and the contribution of heterotrophic bacteria to chloramine decay. Both chemical and biological pathways for the conversion of nitrite to nitrate should be considered for an accurate model. Also, nitrification is not the only biological process at work in chloraminated drinking water distribution systems that can promote the loss of the disinfectant residual, so attempting to account for the effect of heterotrophic bacteria should also assist the accuracy of a nitrification model. By way of comparison, both of these processes were left out of the other kinetic model considered in this chapter (Liu *et al.*, 2005).

One of the simplifications in the model of Yang *et al.* (2008) is that biofilm activity was assumed to be negligible; all of the reactions included take place in the bulk water phase. This simplification makes their model best suited for applications to portions of distribution systems with low surface-to-volume ratios, such as reservoirs, where biofilm activity is less significant.

Compared to the other models to be considered in this chapter, the kinetic nitrification model of Yang *et al.* (2008) has high complexity. Because of this, it would be difficult to apply it directly to a full-scale drinking water distribution system. However, it has the potential to be useful in research applications and to provide insights into nitrification processes.

Plug-flow Kinetic Model

The model of Liu *et al.* (2005) takes a similar approach to that of Yang *et al.* (2008). Both of these models use a set of mass balance equations to estimate the concentrations of chemical and microbiological parameters associated with nitrification. They are both deterministic and mechanistic; these models incorporate reactions that are relevant to distribution system nitrification although there are necessarily simplifications involved. The model of Liu *et al.* (2005) predicts the concentrations of ammonia, nitrite, nitrate, and monochloramine in the effluent from each pipe segment modelled. Ammonia, nitrite, and nitrate are each calculated in a separate mass balance equation while monochloramine is calculated by assuming that the total inorganic nitrogen concentration remains constant. In addition to these parameters, the model also requires the hydraulic retention time (HRT) for each pipe segment, the dissolved oxygen concentration, and estimates for AOB and NOB biomass in the system. A prominent contrast between the models of Yang *et al.* (2008) and Liu *et al.* (2005) is that the latter is based on plug-flow hydraulics as opposed to the completely mixed reactor assumed by the former. The plug-flow kinetic model of Liu *et al.* (2005) is only applicable to steady-state conditions, but it is not completely static since distance along a pipe under a plug-flow hydraulic regime is an analogue for time.

As with the kinetic model of Yang *et al.* (2008), this plug-flow kinetic model (Liu *et al.*, 2005) was too complex to apply to the full-scale distribution system sampling data collected for this research and presented in Chapter 4. In a full scale distribution system the hydraulic retention times between sampling locations—required by the model of Liu *et al.* (2005)—are very difficult to determine precisely, and the assumption of steady-state conditions will rarely be met. The inherent complexity of kinetic models for nitrification dictates the conditions under which they can be used. The plug-flow steady-state hydraulic constraints specified in the model of Liu *et al.* (2005) require data that has high resolution in both time and space. This sort of data is simply not available in most full-scale distribution systems at the present time. As it is, the applications for this model are probably limited to pilot-scale distribution systems like the one the authors used, where a high degree of control can be maintained, and possibly in long distance pipelines where it would be feasible to sample the same plug of water repeatedly as it travels along the pipe. It may also be possible to incorporate a nitrification model like this into a hydraulic model. However, lessons and insights gained from using the plug-flow kinetic model of Liu *et al.* (2005) in research situations may be applied to the issue of nitrification in chloraminated drinking water distribution systems more generally. Since a full evaluation was not possible, this model is discussed at a more general level in the current chapter. Many of the discussion points from the previous model apply to this one as well, so the focus here is placed on their differences.

Although the basic structure of the model of Liu *et al.* (2005) is similar to that of Yang *et al.* (2008), discussed above, there are some notable differences. Some of these differences are in reference to simplifying assumptions regarding assorted distribution system nitrification mechanisms while others follow from their respective focus on pipeline (Liu *et al.*, 2005) or suspended growth (Yang *et al.*, 2008) environments. One difference is that the equations Liu *et al.* (2005) use for the growth of AOB and NOB include the possibility of dissolved oxygen being a limiting factor, whereas Yang *et al.* (2008) ignore this possibility. Dissolved oxygen limitation is a possibility, according to Rittmann and Snoeyink (1984), while Odell *et al.* (1996) did not report dissolved oxygen concentrations below levels expected to be limiting in their survey of U.S. utilities. Thus, there may be specific distribution systems where accounting for dissolved oxygen as a growth factor for nitrifying microorganisms will yield improved model accuracy, while in other distribution systems it may be ignored.

The biomass of nitrifiers was dealt with differently in these kinetic models. Liu *et al.* (2005) assumed that bulk water and biofilm microorganism activity could be combined into a function of a single biomass concentration for each type of nitrifying microorganism. In contrast, Yang *et al.* (2008) assumed that biofilm microorganisms would have negligible activity in their system. This difference accords with the different hydraulic regimes—plug-flow (Liu *et al.*, 2005) compared to a completely mixed reactor (Yang *et al.*, 2008)—in the pilot-scale distribution systems used for each study; the importance of biofilms to nitrification

would be expected to differ between the pilot scale distribution systems used to develop these two models.

Perhaps the most important practical difference between the two kinetic models considered in this chapter is in their handling of the chloramine disinfectant residual. Liu *et al.* (2005) modelled the effect of monochloramine as merely inhibiting the growth of nitrifying microorganisms, in contrast to other models discussed in this chapter (Yang *et al.*, 2008; Fleming *et al.*, 2005; Speital *et al.*, 2011) that assumed the chloramine residual would inactivate nitrifiers. Laboratory disinfection experiments by Oldenburg *et al.* (2002) and Wahman *et al.* (2009) have demonstrated inactivation of the AOB species *Nitrosomonas europaea* by monochloramine, although the disinfection rates observed were slow. Therefore, it is probably a better modelling approach to treat the chloramine residual as an inactivating agent on nitrifying microorganisms. Another difference in the treatment of monochloramine was that Yang *et al.* (2008) provided an explicit mass-balance equation for the chloramine residual while Liu *et al.* (2005) left it to be determined by balancing the equations for other parameters. Given the operational importance of the disinfectant residual (Health Canada, 2002), calculating it explicitly seems preferable. Liu *et al.* (2005) note that their model overestimates nitrite concentrations because the chemical reaction between monochloramine and nitrite was not included, that is, only biological conversion of nitrite was assumed to be significant.

A final point of comparison between the two kinetic models for nitrification considered in this chapter relates to their use of literature values for the model coefficients. Both Liu *et al.* (2005) and Yang *et al.* (2008) relied on a mixture of literature sources and fitting to the systems they were studying to set the kinetic coefficients of their models. However, Liu *et al.* (2005) drew a larger proportion of their coefficients from literature. Table 2.1 in Chapter 2 of this thesis illustrates the large range of values that have been reported in previous studies for the half-saturation coefficients of ammonia-oxidizing microorganisms. Kinetic coefficients sourced from literature may not always match well with a specific distribution system a model is being applied to. On the other hand, obtaining these coefficients through mathematical fitting procedures has its own challenges, so judgment is required.

Since some of the differences between the two mechanistic kinetic models for nitrification examined here (Liu *et al.* 2005 and Yang *et al.* 2008) are due to the differences in their hydraulic regime, the circumstances to which the model will be applied can guide in choosing between them. In circumstances where nitrification within pipes is more of a concern, the plug-flow kinetic model of Liu *et al.* (2005) may be a better starting point. Conversely, if a model is needed for nitrification in a reservoir, the suspended growth kinetic model of Yang *et al.* (2008) may be more appropriate.

The plug-flow kinetic nitrification model of Liu *et al.* (2005) discussed here was not able to be applied to data collected for this thesis due to its complexity. This illustrates a significant

aspect to modelling nitrification in chloraminated drinking water distribution systems: even though a mechanistic model like this has many simplifying assumptions included, it still requires a lot of data that is not presently feasible to obtain for most full-scale distribution systems. However, it can find use in research with pilot-scale distribution systems, and could possibly be incorporated with a hydraulic model at some point. In any case, models such as this can provide insight into the mechanisms and processes of distribution system nitrification and can give valuable lessons for the development of future models. For example, a lesson from the work of Liu *et al.* (2005) is that the chemical oxidation of nitrite should be accounted for in order to accurately model its concentration. A number of such issues that are relevant to nitrification models have been discussed above, mainly with reference to the other mechanistic model considered in this chapter (Yang *et al.*, 2008).

Nitrification Potential Curves

The Nitrification Potential Curve model of Fleming *et al.* (2005) is at the other end of the complexity spectrum from those of Yang *et al.* (2008) and Liu *et al.* (2005). This model has a much higher degree of simplification and far fewer variables (2 instead of 7 or 8), but still attempts to have a mechanistic basis for its structure. The purpose of the model of Fleming *et al.* (2005) is restricted when compared to the kinetic models already discussed in this chapter; rather than predicting the concentrations of a number of chemical and microbiological constituents, it simply seeks to identify distribution system conditions that have the potential for nitrification. There are no dynamic elements. The Nitrification Potential Curve model uses curves of the form of equation 6.2 to separate distribution system conditions that are deemed potentially nitrifying from conditions where the potential for nitrification does not exist:

$$[\text{Total Chlorine}] = \frac{R_{gi} * [\text{Free Ammonia}]}{[\text{Free Ammonia}] + K_s} \quad (6.2)$$

Here, R_{gi} is the ratio of the growth and inactivation rates of nitrifying microorganisms and K_s is the half-saturation coefficient for these microorganisms growing on an ammonia substrate. In theory, these parameters could be calculated from Chick-Watson disinfection kinetics and Monod growth kinetics, but in practice they are treated as fitting parameters to distribution system measurements, as experiments based on laboratory strains may not accurately reflect the distribution system ecosystems. To derive this model, the authors assumed that endogenous decay of ammonia oxidizers was negligible, and that neither dissolved oxygen (DO) nor alkalinity would be limiting. R_{gi} theoretically incorporates the maximum specific growth rate (μ_{max}), dichloramine:monochloramine ratio (α), and disinfection rate of

AOB (k_i): $R_{gi} = (\mu_{max}/\alpha k_i)$; in practice, it represents a chlorine concentration above which nitrification will always be prevented (Fleming *et al.*, 2008).

By design, the Nitrification Potential Curve model of Fleming *et al.* (2005) only requires simple chemical measurements (total chlorine residual, ammonia concentration, and nitrite concentration), making it feasible for application in most full-scale distribution systems. In a subsequent study, Fleming *et al.* (2008) successfully applied the Nitrification Potential Model to three full-scale chloraminated drinking water distribution systems in the United States. It is the only model discussed in this chapter that has previously been applied to full-scale systems (see Table 6.2).

To evaluate the model of Fleming *et al.* (2005), it was applied to the results of sampling from two full-scale chloraminated drinking water distribution systems in Southern Ontario (see Chapter 4). Because the distribution systems involved in this study generally remained well controlled with respect to nitrification, a more stringent criteria for nitrification episodes was used here than in Fleming *et al.* (2008), in order to have enough data for analysis. Fleming *et al.* (2008) identified sites as nitrifying where two consecutive samples had nitrite above 0.025 mg-N/L. For the purpose of illustrating the application of the Nitrification Potential Curves model in this research, a single sample above 0.025 mg-N/L of nitrite was categorized as a point of interest. None of the sites used in this illustrative example would be classified as nitrifying using the criteria of Fleming *et al.* (2008), however. The data for this model comprised the concentrations of total chlorine and ammonia in the sample prior to nitrite exceeding the threshold for points of interest and overall average concentrations of total chlorine and ammonia for other sites. Since sampling frequency was only biweekly, going back further than one sample for calculating the concentrations to be used in the model at points of interest was not reasonable. Once the total chlorine and ammonia concentrations to be used for the points of interest and other sites were determined, Nitrification Potential Curves were fit to the data. Two curve-fitting procedures were applied. The first method was modified from Srinivasan and Harrington (2007) while the second was adapted from Fleming *et al.* (2005, 2008). These procedures are listed in detail in Appendix E.

Figure 6.2 demonstrates the application of the Nitrification Potential Curve model (Fleming *et al.*, 2005) to data from the Region of Waterloo distribution system collected in the present research. The two curves are from the two fitting methods used; the region beneath these curves is predicted to have the potential for nitrification. Using the data collected in this study from the Waterloo distribution system, it was possible to construct Nitrification Potential Curves that captured all but one of the sites classified as points of interest within the area predicted to have the potential for nitrification. One point of interest (WOD05) had zero ammonia and thus could not be included beneath a Nitrification Potential Curve. It is unclear whether this was an anomalous or erroneous measurement, or if it was taken at a time when there was indeed no free ammonia. All of the other points of interest, however,

had ammonia concentrations that were greater than those of all the non-nitrifying sites. Only two points of interest were identified in the Toronto Water distribution system, which were insufficient to apply this model effectively.

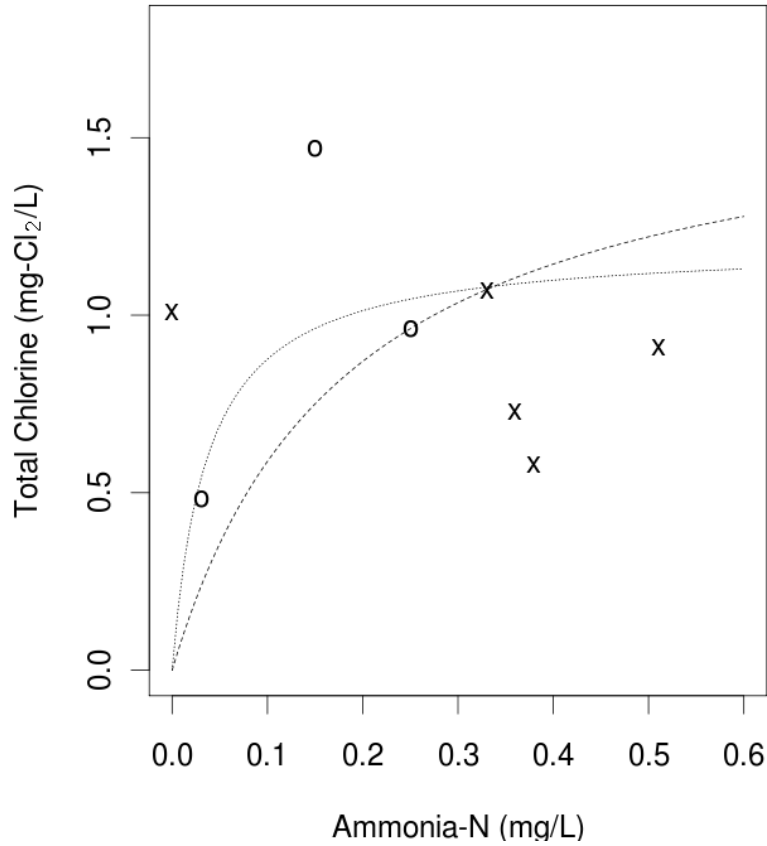


Figure 6.2: Illustration of the output from the model of Fleming, Harrington, and Noguera (2005) using data from the Waterloo distribution system. Distribution system sites were classified as points of interest (x) or other sites (o). Curve coefficients are $R_{gi}=1.67$ and $K_s=0.184$ for the dashed line (- - -), and $R_{gi}=1.20$ and $K_s=0.037$ for the dotted line (...).

There are important points to note when using this model. First of all, the equation for the Nitrification Potential Curves is flexible; changing the coefficients (R_{gi} and K_s) can result in a variety of possible curves. As there were only four points of interest (excluding WOD05 which had an unusual ammonia concentration) in the data set from this study, many possible Nitrification Potential Curves could fit these points within the region of potential nitrification on the graph shown. Having a larger number of points of interest (fully established nitrification events would be even more useful) in the data set available would provide greater confidence in the selected curve. Secondly, the sensitivity of the threshold used for

classifying a site as nitrifying will determine how conservative this model is in application. As mentioned above, if the standard used by Fleming *et al.* (2008) for categorizing a site as nitrifying (i.e. two consecutive samples with nitrite >0.025 mg-N/L) was used in this study, none of the sites would have been labelled as nitrifying. The frequency and timing of collecting samples could also affect this model. In this study, concentrations of total chlorine and ammonia for points of interest were taken from samples two weeks prior to a rise in nitrite since sampling was conducted biweekly. But these concentrations are not static in distribution systems, so a different sampling schedule might find different concentrations of disinfectant and substrate leading up to a rise in nitrite.

Since this model simplifies the complex process of nitrification down to only two variables, it is vital that the variables selected are significant. There is a consensus that the disinfectant residual is a significant factor on whether nitrification will occur or not. All of the models considered in this chapter, except for the Carbon-to-Nitrogen ratio (Verhagen and Laanbroek, 1991; Zhang *et al.*, 2009b)—which deals with a niche topic—include the concentration of the disinfectant residual. Other studies have also found the total chlorine concentration to have a strong impact on the potential for nitrification. In bench scale experiments, Pintar and Slawson (2003) determined that maintaining a chloramine disinfectant residual inhibited AOB more than a low temperature. Earlier in this study, a negative Spearman correlation was found between total chlorine concentrations and AOB levels in both distribution systems studied; this correlation was also seen for AOA in one of the distribution systems that was analyzed (see Table 4.2). The ammonia concentration is not as clear a choice for a two-variable model for nitrification. The model of Yang *et al.* (2007) did not find it to be significant in a logistic regression analysis. In their survey of full-scale chloraminated distribution systems in the U.S., Odell *et al.* (1996) reported that the ammonia concentration did not seem to be a significant factor toward nitrification risk. In support of the significance of the ammonia concentration to the risk of nitrification, Lipponen *et al.* (2002) reported positive Spearman correlations between ammonium-nitrogen levels and AOB in the distribution systems they studied. Positive Spearman correlations between ammonia and AOB were found in both distribution systems involved in this study; this correlation was also seen for AOA in one of the distribution systems (Region of Waterloo) that was analyzed (see Table 4.2). In the evaluation of the Nitrification Potential Curve model presented here, ammonia was equal or greater in nitrifying sites (in the sample prior to a nitrification event) than in non-nitrifying sites (overall averages) for both distribution systems, with the exception of site WOD05, which had zero ammonia measured. Therefore the inclusion of the ammonia concentration as one of the two variables in the highly simplified nitrification model of Fleming *et al.* (2005) appears to be justified by the results of this study. Further research is recommended, however, as to why not all studies find the ammonia concentration to have a significant impact on the potential for nitrification. It is also unclear from these

results whether the higher ammonia levels prior to a rise in nitrite are a leading indicator of nitrification or a causative factor.

The area under the curve in the model of Fleming *et al.* (2005) is predicted to have the potential for nitrification. The model does not predict that nitrification will necessarily occur under those conditions. In the current study, for example, some samples taken from sites not classified as points of interest would lie beneath one or both of the curves shown in Figure 6.2. This model takes a conservative and cautionary approach rather than trying to predict precisely when nitrification will occur. In contrast, the logistic regression risk factor model (Yang *et al.*, 2007) assessed later in this chapter estimates the probability that nitrification will be prevented at given states of water quality. However, a model such as that will require much more data to fit it to a distribution system properly.

The greatest strength of the Nitrification Potential Curves model of Fleming *et al.* (2005) is its applicability. Its low complexity makes it feasible for operational use. This model achieved a reasonable fit to data collected from the Waterloo distribution system in this research, although the study was not carried on long enough to test the predictions against any nitrification events in future years. This model assumes that the ammonia concentration in drinking water can be a useful predictor of nitrification episodes, but the literature is divided on this question. Further research is recommended on this topic. When applying this model, it is important to recall that it predicts conditions with the potential for nitrification, rather than predicting individual nitrification events. That is, its output is cautionary as opposed to being a precise forecast.

Nitrification Index

The Nitrification Index model of Speital *et al.* (2011) follows the same structure as the Nitrification Potential Curve model of Fleming *et al.* (2005), in that it is based on a balance of factors promoting the growth of ammonia oxidizers and factors promoting their inactivation. As in the model of Fleming *et al.* (2005), the ammonia-nitrogen substrate concentration is taken as a factor promoting growth and the chloramine disinfectant concentration is taken as a factor promoting inactivation. Speital *et al.* (2011) add two other inactivating factors: endogenous decay of ammonia oxidizers, and toxicity derived from cometabolism of trihalomethanes (THM). The trihalomethane cometabolism behaviour of AOB has been studied by Wahman *et al.* (2006) and Wahman *et al.* (2011). The Nitrification Index (N.I.) is the quotient of the factors promoting growth and the factors promoting inactivation of ammonia oxidizing microorganisms; N.I. >1 indicates that a nitrification event is likely to occur. It is calculated by equation 6.3 and requires the concentrations of the monochloramine residual, ammonia, and the four THMs as input variables.

$$N.I. = \frac{Y k_{NH_3} \left(\frac{\alpha S_{NH_3}}{K_s + \alpha S_{NH_3}} \right)}{b + k_i S_{NH_2Cl} + \left(\sum_{THM} \frac{k_{1,THM} S_{THM}}{T_c, THM} \right) \left(\frac{\alpha S_{NH_3}}{K_s + \alpha S_{NH_3}} \right)} \quad (6.3)$$

In the above equation, the numerator represents growth processes (on the consumption of ammonia) and the denominator represents inactivation processes, including THM cometabolite toxicity and endogenous decay as well as chloramine disinfection. Concentrations of the constituents included in this model (ammonia, monochloramine, and 4 trihalomethanes) are denoted with “S.” The half-saturation coefficient for ammonia, K_s , the maximum AOB specific substrate utilization rate, k_{NH_3} , and the chloramine inactivation rate, k_i , are included in this model, similar to the nitrification potential curve equation used by Fleming *et al.* (2005). THM by-product toxicity is quantified by the transformation capacity, T_c , which is the maximum amount of cometabolite that can be transformed before the nitrifiers are completely inactivated by the toxic by-products. The cometabolism rate for each trihalomethane is denoted by $k_{1,THM}$. Their model also accounts for the pH sensitivity of AOB growth and their inactivation rate. The endogenous decay rate of nitrifiers is represented by b , and α is the fraction of ammonia that is available in the non-ionized form (NH_3).

Since the model of Fleming *et al.* (2005) has been evaluated previously in this chapter, the discussion here will focus on the addition of the THM cometabolism toxicity effect to the model of Speital *et al.* (2011).

The evaluation performed on the Nitrification Index model in this study was quite simple. The N.I. was not applied to all of the data collected in Chapter 4 since trihalomethanes (THM) were not monitored in the present research. Additionally, the model of Fleming *et al.* (2005), which the Nitrification Index is built on, was already evaluated. Therefore, the evaluation of the model of Speital *et al.* (2011) consisted of calculations to determine the magnitude of the THM cometabolism effect, in order to determine whether it was necessary to include when modelling nitrification in the distribution systems participating in this research.

Average annual total THM concentrations for the Toronto and Waterloo distribution systems were obtained from City of Toronto (2011) and Region of Waterloo (2011), respectively. The annual average concentrations of total trihalomethanes were 17.3 $\mu\text{g/L}$ for the Toronto distribution system and 28.9 $\mu\text{g/L}$ for the Waterloo distribution system. Since the average was higher—but still far below Canadian guidelines of 100 $\mu\text{g/L}$ (Health Canada, 2010)—in the Waterloo distribution system, data from Waterloo was used to evaluate the Nitrification Index. The average total chlorine concentration in samples from the Waterloo distribution system over the course of this study was 0.93 $\text{mg-Cl}_2/\text{L}$ and the average ammonia concentration was 0.20 mg-N/L . These concentrations were used to calculate a Nitrification Index value and check the magnitude of the THM cometabolism effect as predicted by the model of Speital *et al.* (2011). Most of the coefficients for the model are given by Speital *et al.*

(2011). Since only the total THM concentration was available, rather than concentrations for each species, the average coefficients were used for the THM effects: $k_{1,THM} = 0.125$ mg TSS/L-d for the cometabolism rate, and $T_{c,THM} = 40.6$ $\mu\text{g/L}$ THM/mg TSS for the transformation capacity before a critical toxicity is reached. A pH of 7.5 was assumed, giving $\alpha = 0.0156$. Finally, for the following calculations the monochloramine disinfection rate, $k_i = 2.3$ L/mg-Cl₂ d, was taken from Wahman *et al.* (2009) because the model of Speital *et al.* (2011) assumes an acid-catalysis process for chloramine disinfection, making the disinfection rate coefficient a function of alkalinity (and other proton donors), which was not monitored in the present study. The following calculations show that effects from THMs in the Nitrification Index of Speital *et al.* (2011) are small enough to be neglected for the distribution systems involved in this research. Only the denominator (refer to equation 6.3), which contains inactivation effects, of the N.I. is shown since that is the portion of the model that deals with THM cometabolism and toxicity.

$$b + k_i S_{NH_2Cl} \gg \left(\sum_{THM} \frac{k_{1,THM} S_{THM}}{T_{c,THM}} \right) \left(\frac{\alpha S_{NH_3}}{K_s + \alpha S_{NH_3}} \right) \quad (6.4)$$

$$(0.015) + (2.3)(0.93) \gg \left(\frac{(0.125)(28.9)}{(40.6)} \right) \left(\frac{(0.0156)(0.20)}{(2.39) + (0.0156)(0.20)} \right)$$

$$2.15 \gg 0.00385$$

In these calculations, the effect from endogenous decay and chloramine inactivation of ammonia oxidizers was much greater than the effect of toxicity from THM cometabolites. Including this latter effect increases the denominator (calculated total inactivation rate on ammonia oxidizers) by only 0.2%; under these conditions THMs have a smaller impact on nitrification than the endogenous decay rate.

Overall, the Nitrification Index was calculated as $N.I. = 0.015$ using the average values from the Waterloo distribution system. Since this value is <1 , the model of Speital *et al.* (2011) indicates that the Waterloo distribution system is not susceptible to nitrification at its average concentrations of total chlorine and ammonia. As there were only a small number of occasions when there were slight increases in nitrite in this distribution system, these results seem reasonable.

The Nitrification Index model of Speital *et al.* (2011) represents a large increase in complexity over the Nitrification Potential Curve model of Fleming *et al.* (2005) which it is based on (i.e. it has 6 variables compared to 2). In distribution systems like the ones in this study where THM effects have very small impacts, this added complexity is probably not

worthwhile. In their study, Speital *et al.* (2011) found THM cometabolism and toxicity to account for up to 20% of inactivation when N.I. <1.5. It is a matter of judgment whether a potential 20% increase in model accuracy is enough of a benefit for the large increase in complexity over the model of Fleming *et al.* (2005). Furthermore, since trihalomethanes are undesirable in distribution systems, system operators should aim to prevent nitrification without any reliance on THM cometabolism and toxicity effects. In any case, operational targets should be set on conditions that would yield an N.I. <1 (i.e. where nitrification is predicted to not occur) where ignoring the impact of THM cometabolism will not cause a significant reduction in accuracy.

Outside of research on THM cometabolism and any full-scale distribution systems where it is expected to be a significant issue, the model of Speital *et al.* (2011) does not appear to offer compelling benefits over the model of Fleming *et al.* (2005) that it is based on. Given its large increase in complexity, the use of the Nitrification Index (Speital *et al.*, 2011) appears not to be justified under normal circumstances.

Logistic Risk Model

The logistic regression risk model for nitrification developed by Yang *et al.* (2007) differs from the other models evaluated in this chapter, in that it is not based on any mechanistic considerations, but a statistical fit to data from the system being studied. Yang *et al.* (2007) conducted factorial experiments in pilot-scale distribution systems to obtain sufficient data to fit their model. The model of Yang *et al.* (2007) takes input variables of the disinfectant residual concentration, temperature, and pH, and predicts the probability that a nitrification episode will be prevented (i.e. the complementary probability of nitrification). Equation 6.5 defines this model, as fitted to the pilot-scale distribution systems the authors studied:

$$\log\left(\frac{p}{1-p}\right) = 13 + 5.9(pH - 8.3)^2 - 0.49T + 2.5C_d \quad (6.5)$$

Hydraulic detention time is not included in the above equation since it was redundant with the total chlorine concentration, C_d . In the notation above T is the temperature (in °C) and p is the probability of preventing the occurrence of nitrification. For the development of this model, a nitrification occurrence was recorded when two consecutive nitrite samples and their 14-day average were >0.1 mg-N/L, which is a much higher nitrite threshold than most studies have used (i.e. Fleming *et al.* 2005; Pintar *et al.* 2005). The optimal pH for nitrification was determined to be 8.3. Yang *et al.* (2007) also considered interaction effects between some of the variables, such as pH and the disinfectant concentration, but these did not improve the model fit.

Their risk factor model has the potential to be very useful in distribution systems where it provides accurate predictions since it provides the predicted probability of preventing nitrification. This allows system operators to determine the distribution system water quality values that will yield an acceptable level of risk. The model coefficients also provide a rapid indication of the relative impacts of different water quality changes on the risk of nitrification. For example, in the equation of Yang *et al.* (2007) a 1 mg/L increase in the disinfectant residual concentration (coefficient of 2.5) is expected to have five times the impact at reducing the risk of nitrification as compared with a 1°C decrease in the water temperature (coefficient of -0.49). Different distribution systems should have their own unique coefficients fitted by logistic regression if this model is to be used.

The model of Yang *et al.* (2007) was applied to the data collected from the two full-scale chloraminated drinking water distribution systems presented in Chapter 4. Initially, their equation (6.5) was applied with its existing coefficients to pH, temperature, and total chlorine residual data from the distribution system sites sampled in the current study. Next, a more general approach was taken and logistic regression was applied to this data (using the statistics language “R” (R Development Core Team, 2009)) in an attempt to fit an equation of the same form as that of Yang *et al.* (2007) with more suitable coefficients. Logistic regression is a statistical method for fitting a model to data that has a binary response. It takes the form of the following equation, in which Y is the response variable that can take the values 1 or 0, X_i are the independent variables, and β_i are the corresponding coefficients. A logistic regression model provides probabilities for the dependent variable, Y, taking the value of 1 or 0, rather than an estimate of its value as in linear regression (Dodge, 2010).

$$\log \left(\frac{P(Y = 1)}{P(Y = 0)} \right) = \beta_0 + \sum_{i=1}^n \beta_i X_i \quad (6.6)$$

When the equation of Yang *et al.* (2007) was applied to data from two full-scale distribution systems investigated in this research, it predicted that nitrification would be prevented (with greater than 99.9% probability) for all sites on all sampling dates. One possible reason for this is that this type of logistic risk model should be fitted to the systems it will be applied to, as Yang *et al.* (2007) note. Another reason is that the model was developed based on a very high nitrite threshold (>0.1 mg-N/L) for verifying nitrification that was not, in fact, exceeded in the data set used here. Following this initial application of the logistic risk model, an attempt was made to fit a similar model to the data from this research using logistic regression. To obtain positive data to work with, a lower nitrite threshold (nitrite-N >0.015 mg/L) than Yang *et al.* (2007) was used; this threshold was used for the purposes of these calculations and does not imply an established nitrification event. An example R

session is shown in Appendix E. The first and last sites from each distribution system were excluded from the fitting procedure to reserve part of the data set for checking the fit. The same variables tested by Yang *et al.* (2007) were included in the regression analysis: pH (specifically, the squared difference from a pH of 8.3, which Yang *et al.* (2007) identified as optimal), ammonia concentration (C_s), total chlorine residual (C_d), and the water temperature (T). The hydraulic retention time was not available in this study and therefore was not included as a variable for logistic regression. For the Toronto distribution system, the following equation (6.7) was fitted. However, none of the variables were identified as significant by the regression analysis. Recall that p is the probability of preventing the occurrence of nitrification, according to the definitions used by Yang *et al.* (2007).

$$\log\left(\frac{p}{1-p}\right) = -10.33 + 3.67(pH - 8.3)^2 + 0.176T - 0.475C_s + 8.82C_d \quad (6.7)$$

This equation, with coefficients determined for the Toronto distribution system, still did not predict any nitrification episodes there.

For the Waterloo distribution system, the application of regression analysis identified the pH and water temperature as significant variables ($p=0.1$), so logistic regression was repeated with only these variables to obtain the following equation:

$$\log\left(\frac{p}{1-p}\right) = 3.91 + 4.82(pH - 8.3)^2 - 0.305T \quad (6.8)$$

The signs on these coefficients imply that the probability of preventing a nitrification episode will be increased away from the optimal pH, and will be decreased as the temperature rises. These effects are in accordance with theoretical considerations and with the findings of Yang *et al.* (2007). When this equation was applied to the Waterloo distribution system data presented in Chapter 4 it did not predict any nitrification events.

There was not enough data available from the two distribution systems investigated in this research to achieve a good fit with a logistic risk model. During the course of this study, there were only a small number of occurrences of mild nitrification which may be insufficient to effectively fit a statistically-based model. For comparison, the Nitrification Potential Curve model (Fleming *et al.*, 2005) evaluated above requires less data to fit to a given distribution system compared to this model, since it includes fewer variables. However, the model of Fleming *et al.* (2005) only indicates whether there is a potential for nitrification or not, rather than assigning a risk probability as the logistic regression model evaluated here does. Since there was only enough data to apply the model of Fleming *et al.* (2005) to one of the distribution systems in this study (i.e. the Waterloo distribution system), it is not

surprising that the model of Yang *et al.* (2007), which requires much more data, could not be evaluated effectively.

An important point to note about the logistic risk factor model of Yang *et al.* (2007) is that it does not make any attempt to deal with nitrification from a mechanistic perspective, so the variables identified as significant in their work, or when fitting a model of the same form to another distribution system, should be seen strictly as predictors of nitrification rather than causative factors.

While the accuracy of this model could not be evaluated effectively in the present study, it is judged to have good ease of application. Therefore, in distribution systems where a large enough data set on nitrification is available to obtain a good fit from logistic regression, it may provide useful information on predicting nitrification and identifying relevant risk factors.

Carbon-to-Nitrogen Ratio

Verhagen and Laanbroek (1991) and Zhang *et al.* (2009b) developed a model to predict the ecological balance between heterotrophic and ammonia-oxidizing bacteria based on the carbon-to-nitrogen ratio (i.e. organic carbon and ammonia-nitrogen). Starting from theoretical considerations that two species with the same limiting nutrient (ammonia-nitrogen in this case) cannot coexist in equilibrium within the same ecological niche, Verhagen and Laanbroek (1991) experimentally determined a critical C/N ratio of approximately 10 (11.6 and 9.6 in two experiments they performed) above which ammonia oxidizing bacteria would be out-competed for ammonia by heterotrophic bacteria. Zhang *et al.* (2009b) extended this model to also predict conditions of AOB dominance, based on calculations comparing growth rates. Above the critical C/N ratio (equation 6.9), nitrifiers are predicted to have a negligible presence, while for C/N ratios that fall below the curve given by Equation 6.10 nitrifiers are predicted to outnumber heterotrophic bacteria.

$$\frac{C}{N} \geq \approx 10 \quad (6.9)$$

$$C \leq \frac{0.17N}{0.806 + 0.586N} \quad (6.10)$$

In the above equations, C and N are the concentrations of organic carbon, and ammonia-nitrogen, respectively. The first equation (6.9) defines where heterotrophic bacteria will be nitrogen limited and out-compete ammonia-oxidizing microorganisms for ammonia; the

value of 10 for the critical C/N ratio is an approximation to the critical ratios found in the experiments of Verhagen and Laanbroek (1991). The second equation (6.10) predicts when nitrifiers will be more abundant than heterotrophic microorganisms in a distribution system; it was derived by setting their growth rates to be equal and using Monod coefficients found in the literature. Both of these critical lines (i.e. equations 6.9 and 6.9) could be adjusted if more accurate information was available on the growth kinetics of microorganisms in a specific distribution system.

This model differs from the previous models considered in this chapter, in that it does not apply to distribution system nitrification generally, but to the specific question of ecological competition between nitrifiers and heterotrophs.

Figure 6.3 illustrates the topic covered by the C/N model, which is the relative abundance of heterotrophic bacteria and nitrifying microorganisms. This figure shows the ammonia-oxidizing microorganisms (sum of AOA and AOB) and HPC bacteria over the course of the sampling campaign (see Chapter 4) in the Waterloo distribution system (this data is also available in Table A.3). HPC were almost always greater than the total of ammonia oxidizers, but the ratio varied over several orders of magnitude between sites and over the course of the sampling period. Site WOD04 was free chlorinated while the other sites had a chloramine disinfectant residual, explaining its much greater difference between heterotrophs and nitrifiers. Comparing the relative levels of heterotrophs and nitrifiers from the sampling data obtained in this research to the carbon to nitrogen ratio provides an opportunity to evaluate the C/N model.

The sample results from both distribution systems involved in this research project were divided into groups based on the order of magnitude of the relative abundances of ammonia oxidizers and heterotrophs. The following groups were defined:

- Group A: Nitrifiers/HPC ≥ 1.0
- Group B: $1 > \text{Nitrifiers/HPC} \geq 0.1$
- Group C: $0.1 > \text{Nitrifiers/HPC} \geq 0.01$
- Group D: $0.01 > \text{Nitrifiers/HPC}$

In these groups, nitrifiers included both AOA and AOB, although it is debateable whether the C/N model should apply to both. AOA may have high enough affinity for ammonia that they are not susceptible to being out-competed by heterotrophic microorganisms for this nutrient (Martens-Habbena *et al.*, 2009). Some authors have also suggested that AOA may be able to use substrates besides ammonia (Di *et al.*, 2010; Leininger *et al.*, 2006). Additionally, the concept of a critical C/N ratio was only tested for AOB by Verhagen

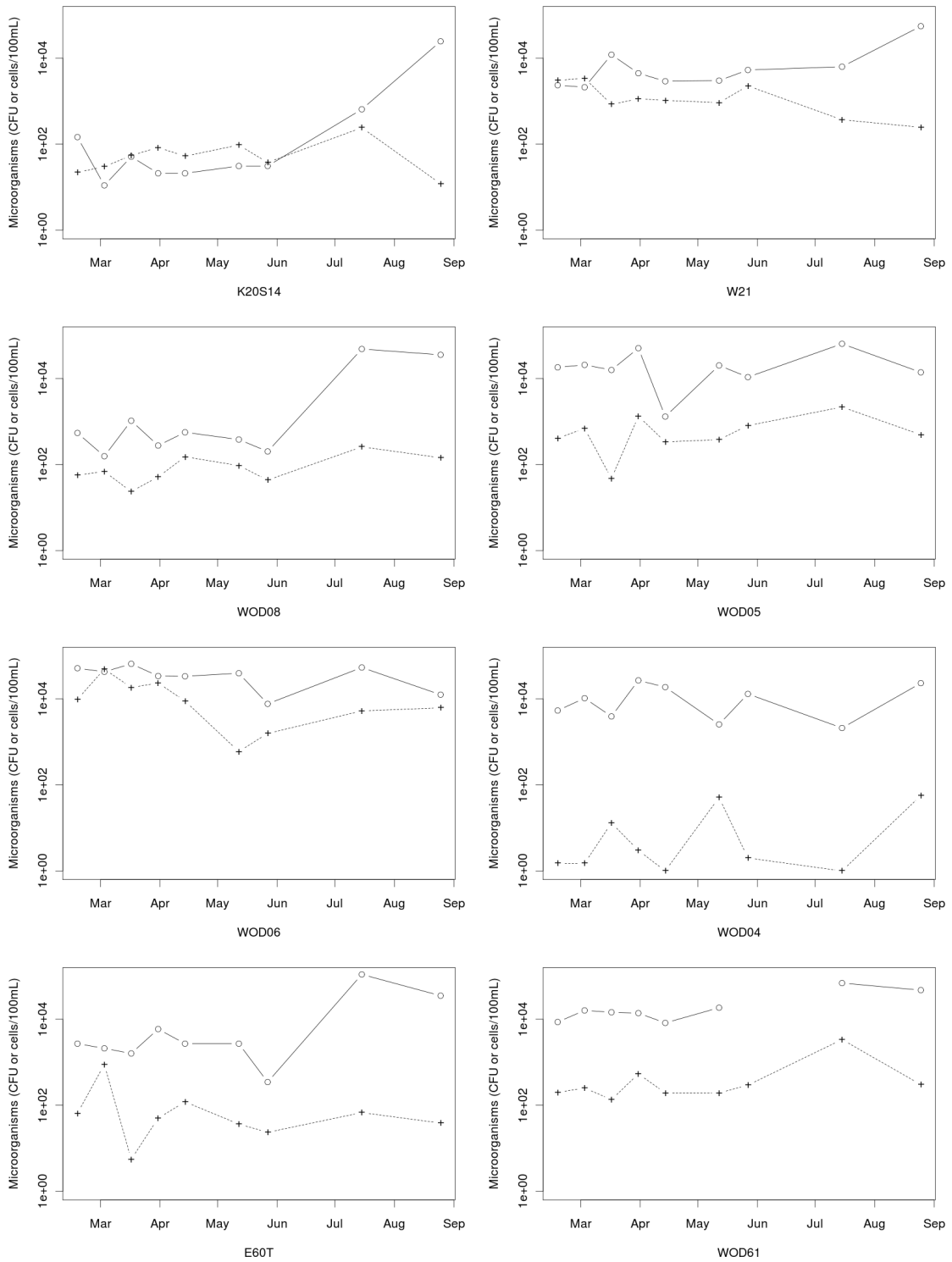


Figure 6.3: Time-series plots of ammonia oxidizing microorganisms (AOA + AOB) in cells/100 mL (+) and HPC bacteria in CFU/100 mL (o) occurrence at each site in the Waterloo distribution system. An arbitrary value of 1 was added to each cell count to facilitate plotting non-detects on a log-scale.

and Laanbroek (1991)—and only for one species (*Nitrosomonas europaea*). However, it was decided to include the whole ammonia-oxidizing community measured in this project in the analysis of the C/N model since both are capable of nitrification.

The C/N model was evaluated by comparing the carbon-to-nitrogen ratios between these groups, both graphically and using the ANOVA statistical technique. ANOVA tests whether there are any significant differences between groups by comparing the variance within groups and the variance between groups (Dodge, 2010). If the C/N model is valid and applicable to the distribution system sites investigated in this study, significant differences between the groups would be expected. These differences should show up as clustering of the groups of nitrifier to heterotroph ratios on graphs of carbon versus nitrogen concentrations and as statistically significant outcomes from the ANOVA test. For example, Group A samples would be expected to have C/N ratios less than the critical value since heterotrophs are not dominant, while Group D samples would have C/N ratios greater than the critical value.

The C/N model was applied to the sampling results from this research, using a graphical approach after the manner of Zhang *et al.* (2009b). These graphs are presented as Figures 6.4 and 6.5, for the Toronto and Waterloo distribution systems, respectively. The Nitrifier/HPC ratio group for each sample was plotted at its concentrations of ammonia (mg-N/L) and dissolved organic carbon (DOC, in mg-C/L). As noted in section 4.2 of this thesis, not all of the samples had their DOC measurements conducted within the stipulated timeframe of 1 month (APHA *et al.*, 2005). Samples with DOC measurements taken after >60 days were excluded from these graphs, and from the following statistical analysis. However, plots including all DOC data (not shown) were similar to Figures 6.4 and 6.5. A critical C/N ratio of 10 (Zhang *et al.* 2009b, Verhagen and Laanbroek 1991) is shown as a solid line (equation 6.9) on these plots; ammonia oxidizing bacteria were predicted to be outcompeted by heterotrophic bacteria above this line. A dashed line (equation 6.10), based on setting their growth rates equal, predicts the environmental conditions (i.e. below this line) where ammonia-oxidizers would become more abundant than heterotrophs (Zhang *et al.*, 2009b). In the region between these lines, it was predicted that heterotrophs would be more numerous than ammonia oxidizing bacteria, but they would coexist in environmental equilibrium.

By examination of Figures 6.4 and 6.5 the C/N model does not appear to fit the systems investigated for this study. As explained above, DOC and ammonia concentrations would be expected to cluster together for each grouping (A–D) of relative abundances of ammonia oxidizers and HPC bacteria if the model fit these real distribution systems. However, this does not appear to be happening. Additionally, the lines on the graphs did not have strong predictive power. Only a few data points fell below the C/N = 10 line, even though most of the samples had ammonia oxidizing microorganisms present above negligible levels. None of the points fell in the region below the dotted line where ammonia oxidizers were predicted to be numerically dominant, even though they did out-number HPC in some samples.

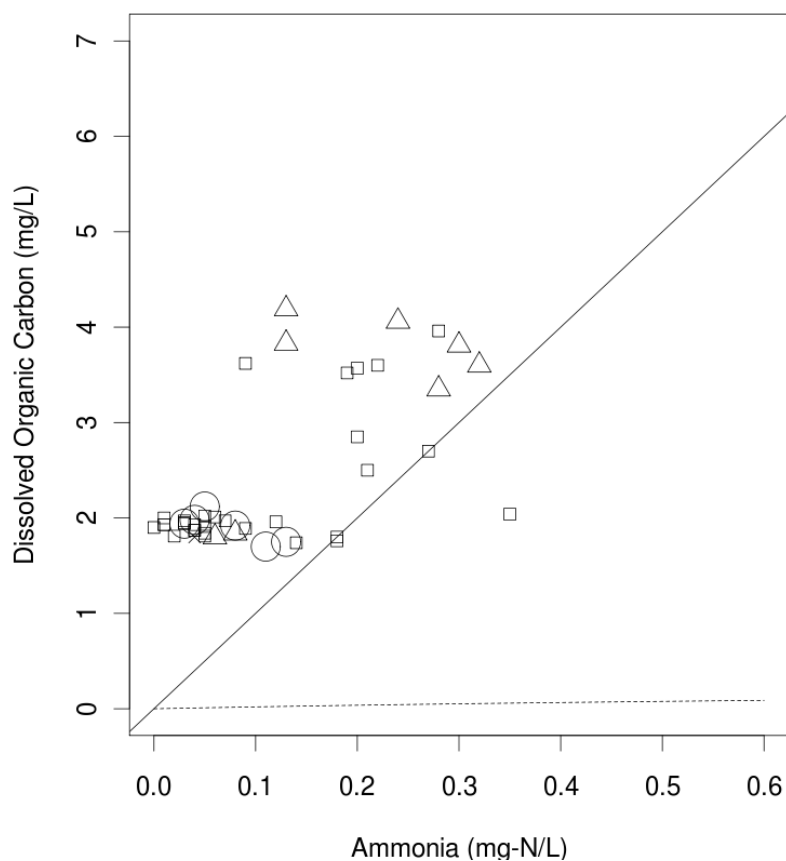


Figure 6.4: Graph of the C/N model applied to samples from the Toronto distribution system. Above the solid line (---) nitrifiers were predicted to be negligible and below the dashed line (- - -) nitrifiers are expected to be dominant. DOC and ammonia concentrations are grouped based on the Nitrifier/Heterotroph quotient: group A, ≥ 1.0 (\times); group B, ≥ 0.1 (Δ); group C, ≥ 0.01 (\square); group D, <0.01 (\circ).

The lack of visual clustering on the graphs in which the C/N model was applied was verified with the statistical ANOVA test. The groupings (A–D) of ammonia oxidizer to HPC quotients were tested for significant differences in their carbon-to-nitrogen ratios, using the same data as in Figures 6.4 and 6.5. p-values of 0.50 and 0.21 were obtained for the Toronto and Waterloo distribution system data, respectively, showing that there were no significant differences between the carbon-to-nitrogen ratios associated with different groups (relative abundances of nitrifiers and heterotrophs).

These results are in accord with findings presented earlier in this thesis. In chapter 4, a positive correlation was found between HPC and AOB (see Table 4.2). Since the C/N model

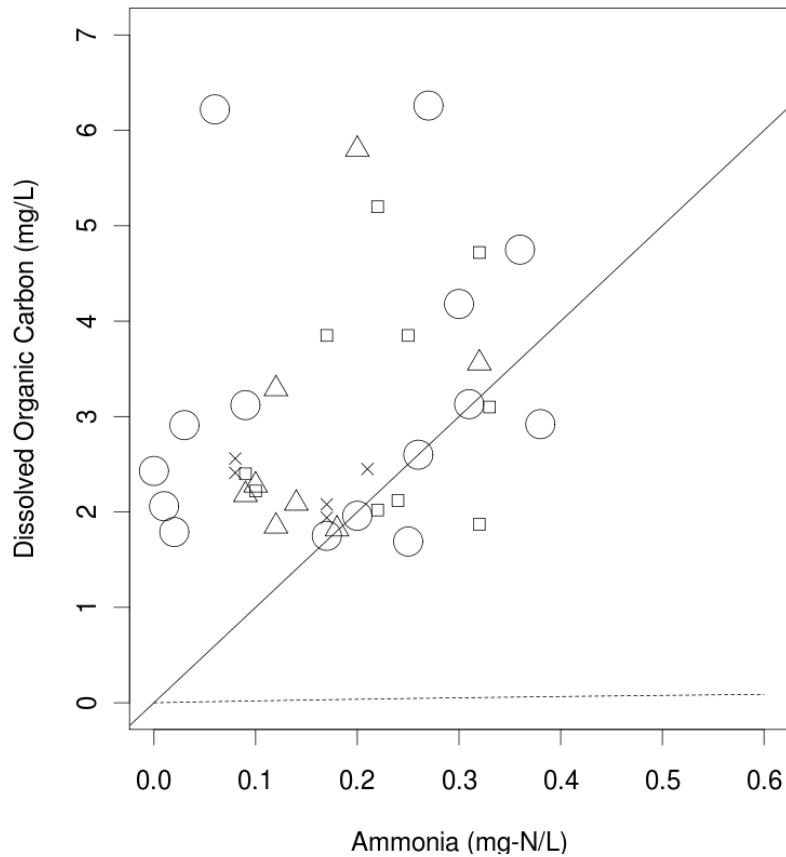


Figure 6.5: Graph of the C/N model applied to samples from the Waterloo distribution system. Above the solid line (—) nitrifiers were predicted to be negligible and below the dashed line (---) nitrifiers are expected to be dominant. DOC and ammonia concentrations are grouped based on the Nitrifier/Heterotroph quotient: group A, ≥ 1.0 (x); group B, ≥ 0.1 (Δ); group C, ≥ 0.01 (\square); group D, <0.01 (\circ).

being discussed here is based on the assumption that competition between heterotrophs and nitrifiers will be a key determinant of their relative numbers in an environment, a negative correlation between HPC and AOB would be expected if the C/N model applied in the distribution systems included in this study. There is also support in the literature that the C/N model may not be applicable in chloraminated drinking water distribution systems. A number of authors have found species of AOB (Bollmann *et al.*, 2002; Regan *et al.*, 2002) and AOA (Martens-Habbena *et al.*, 2009) with high affinities for ammonia, such that they may not be vulnerable to competition from heterotrophic bacteria. There are also scenarios in which nitrifying microorganisms and heterotrophic bacteria could have a cooperative relationship, for example by removing toxic byproducts (Zhang *et al.*, 2009b).

The C/N model also implicitly assumes that organic carbon and ammonia-nitrogen are the only nutrients that may impose a limitation on the growth of microorganisms in drinking water distribution systems. However, other nutrients required for growth such as phosphorus (as phosphate) may also be present in limiting concentrations (Miettinen *et al.*, 1997).

From the work done here, the C/N model does not appear to make useful predictions about the ecological balance between ammonia oxidizing microorganisms and heterotrophic bacteria in distribution system environments. There are many possible explanations for this finding. First of all, distribution systems are heterogeneous environments, so there may be niches available for both nitrifiers and heterotrophs (e.g. at different depths within biofilms). Low nutrient distribution systems may select for species of ammonia-oxidizing bacteria that have a better ability to compete with heterotrophs than the laboratory strains of *Nitrosomonas europaea* used by Verhagen and Laanbroek (1991) in developing the C/N model (see Regan *et al.* 2002 and Bollmann *et al.* 2002). In chloraminated drinking water distribution systems, the effect of the disinfectant residual might overshadow any competitive effects that may exist. Finally, the possibility should be raised that the C/N model might prove to be a better fit to distribution systems if more precise data was available. Notably, the use of DOC to quantify the organic carbon substrate concentration could be improved by using assimilable organic carbon (AOC) or biodegradable dissolved organic carbon (BDOC) instead, since they provide more accurate data regarding the organic carbon that is available to microorganisms. Also, it would be better to measure ammonia oxidizers and heterotrophic bacteria by similar methods that can accurately assess both total cell counts and cell viability. However, the evaluation here is believed to be a good assessment of the operational usefulness of this model, since more precise data may not be feasible to collect.

Alternatives to Modelling

There are alternatives to modelling that can achieve the same goal. The models that have been discussed in this chapter offer predictions about the concentrations of constituents associated with nitrification, or conditions that could promote nitrification. Other options, ranging from trends in distribution system water quality data to batch testing, also exist for providing early warnings of nitrification episodes and for understanding the potential for nitrification at distribution system locations.

Based on a study conducted in one of the same distribution systems involved in the present study (Region of Waterloo) Pintar *et al.* (2005) concluded that a falling total chlorine residual can be an early warning of an incipient nitrification event. A number of other causes can underlie a decline in the disinfectant residual, as Zhang *et al.* (2009b) warn, but in distribution systems where nitrification is a concern, such a decline should at least trigger further investigation. This approach is much more simple than any of the models examined above, as it only depends on one variable. It is notable that all of the models examined in this chapter (with the exception of the carbon-to-nitrogen model which has a very limited scope) include the disinfectant residual—the only variable that is shared so widely. Therefore, watching for a falling trend in the disinfectant residual as Pintar *et al.* (2005) recommended accords well with the models presented in this chapter. Pintar *et al.* (2005) recommended that utilities monitor total chlorine rather than monochloramine for this purpose.

Another option is included as one of the recommendations of Wilczak *et al.* (1996), and that is to develop an accurate nitrogen balance for chloraminated drinking water distribution systems in which nitrification is a potential issue. At a fundamental level, nitrification is the oxidation of nitrogen from ammonia to nitrite and nitrate, so the nitrogen balance will always be affected. However, obtaining an accurate and precise nitrogen balance can be quite challenging in a full-scale distribution system. Nitrogen can be incorporated into growing biomass, background nitrate levels can fluctuate, and the target monochloramine residual concentration can change with time. Complications like these necessitate that care be taken when calculating a nitrogen balance in a full-scale distribution system. Wilczak *et al.* (1996) used a graphical framework of looking at the concentrations of ammonia, nitrite, and nitrate in parallel, compared to the concentrations entering the distribution system from the WTP to show changes occurring within the distribution system. Collecting this data is necessary prior to applying most of these models, in any case. Of the models discussed in this chapter, only the logistic regression risk model of Yang *et al.* (2007) does not include the concentrations of any nitrogen species as significant variables.

A significantly different approach was the focus of the previous chapter (Chapter 5) of this thesis. That is the batch test methodology for nitrification developed by Sathasivan

et al. (2005) and Sathasivan *et al.* (2008). In brief, this batch test methodology uses parallel batch tests that are inhibited or uninhibited against microbial activity in order to identify the relative contributions to the total chlorine decay rate by chemical and biologically-mediated processes. According to the authors, this method can identify nitrifying samples well in advance of any increase in nitrite, allowing mitigating actions to be taken before a severe nitrification episode develops. This method has been applied as part of a full-scale reservoir management strategy (Sathasivan *et al.*, 2010).

Together with the models presented above, these alternatives to modelling can serve as part of a diverse tool-kit for understanding nitrification in chloraminated drinking water distribution systems.

6.3 Conclusions and Recommendations

The above descriptions and evaluations of nitrification models should help drinking water distribution system operators select one that fits their individual situation and requirements. It is also hoped that the issues discussed will provide insight and guidance that will be useful in the development of future models for nitrification in chloraminated drinking water distribution systems. Table 6.3 lists strengths and weaknesses that have been identified for each of the models considered in this chapter.

The examination of these models has led to the following conclusions and recommendations:

- Due to its simplicity and the reasonable fit to an illustrative example using data from the present study, the Nitrification Potential Curve model (Fleming *et al.*, 2005) seems best suited for use in full-scale distribution systems.
- Simulations were conducted applying the kinetic nitrification model of Yang *et al.* (2008); it is recommended for research applications.
- The Nitrification Index model (Speital *et al.*, 2011), which incorporates THM cometabolism and toxicity effects, adds complexity to account for a phenomenon that was estimated to be insignificant in the distribution systems involved in the present study; this model is only expected to be worthwhile in cases where THM cometabolism is a prominent consideration.
- The carbon-to-nitrogen ratio model (Verhagen and Laanbroek, 1991; Zhang *et al.*, 2009b) did not fit the data from the full-scale distribution systems involved in the present study; however, the use of DOC measurements instead of a parameter that quantifies the assimilable organic carbon substrate concentration limited the evaluation of this model.
- The logistic regression risk factor model of Yang *et al.* (2007) could not be fit to the distribution systems involved in this study, probably due to insufficient data.
- Of the two kinetic models considered in this chapter, that of Yang *et al.* (2008) accounts for some reactions (e.g. chemical oxidation of nitrite) for which Liu *et al.* (2005) does not; however, the differences in the hydraulic regimes under which these models were developed may influence which one is preferred in a given scenario.
- The disinfectant concentration was a variable shared by almost all of the models examined in this work, highlighting the importance of maintaining a disinfectant residual for controlling distribution systems against nitrification.

Table 6.3: The strengths and weaknesses determined for the models evaluated.

Model	Strengths	Weaknesses
Pilot-scale Kinetic Model	Useful for conducting conceptual simulations Analyzing batch tests and heavily-monitored reservoirs Dynamic model Includes heterotrophic contribution to chloramine decay	Ignores biofilm; suspended growth only Most applicable to low surface-to-volume portions of distribution system Very complex
Plug-flow Kinetic Model	Contributes to understanding of nitrification	Requires HRT, which is often difficult to determine accurately in full-scale systems Steady-state only Treats chloramines as growth inhibitors rather than disinfecting agents Requires a biomass estimate Ignores chemical oxidation of nitrite
Nitrification Potential Curves	Conceptually straight-forward Mathematically simple Only requires easily obtained chemical measurements	Does not account for effect of factors such as pH and temperature Many possible curves can be fitted, so how significant are coefficients (R_{gi} , K_s)?
Nitrification Index	Allows inclusion of THM cometabolism effect in a nitrification model	Dedicates 4/6 variables to a marginal effect
Logistic Risk Model	Statistically strong Simple to apply	Complicated to fit, and requires a lot of data System specific
Carbon to Nitrogen Ratio	Interesting theory Reminder to be aware of limiting nutrients	Assumes substrate affinities that may not apply in distribution systems Not all organic carbon is readily available as a bacterial substrate

- Modelling is not the only means of predicting when there is a potential for nitrification in distribution system sites.

Overall, the Nitrification Potential Curve model of Fleming *et al.* (2005) seems to be the most feasible for application to full-scale distribution systems. The kinetic model of Yang *et al.* (2008) is expected to be useful in research applications and where frequent measurements of its parameters is possible. The continued development of models for nitrification in chloraminated drinking water distribution systems should consider the topics discussed in this chapter.

Chapter 7

Conclusions and Recommendations

The research presented in this thesis was undertaken with the goals of carrying out a study on nitrification in two full-scale chloraminated drinking water distribution systems, evaluating some models that have been proposed for nitrification using the data collected, and applying a batch test method for nitrification to samples from these distribution systems. By achieving these goals, an improved understanding of the water quality factors that are related to nitrification was obtained. A motivation for this was the need to better predict when the potential for nitrification episodes exists at sites in chloraminated drinking water distribution systems, ideally with enough advance warning to allow system operators to take action to avert them.

7.1 Major Findings

Two full-scale chloraminated drinking water distribution systems were involved in this study: Toronto Water and the Region of Waterloo (both in Ontario, Canada). The water source for Toronto is a Great Lake, while Waterloo uses a blend of highly-impacted surface water plus groundwater. The first experimental phase of this study was a nine month long sampling campaign from these distribution systems in which physical, chemical, and microbiological parameters relevant to nitrification were monitored at 7–8 sites in each system. The second experimental phase of this research involved applying a published batch test method—with an additional scheme for interpreting the results developed in the present research—to samples from the same two distribution systems. In addition to the experimental work included in this thesis, some models for nitrification were also assessed. Where possible, these models were applied to results from the full-scale sampling campaign.

Chapter 4 presented the results of the full-scale sampling campaign. The major results of this phase of the research were as follows:

- The sampling locations at both distribution systems generally remained well-controlled with respect to nitrification over the course of the study. There were small increases in the nitrite concentration on a few occasions, and mild reductions in the total chlorine residual at some sites, but there were no severe nitrification episodes with major losses of the disinfectant residual or prolonged elevations of nitrite levels.
- Ammonia oxidizing microorganisms (AOA and AOB) were found to be nearly ubiquitous in these distribution systems. This suggests that nitrification events could develop under favourable conditions.
- AOB were found to be more numerous than AOA at most of the sampling locations in this study, with the exception of some sites in the Waterloo distribution system.
- The levels of each type of microorganism (AOB, AOA, HPC) had negative Spearman correlations with the total chlorine residual, supporting the importance of maintaining a strong disinfectant residual in chloraminated distribution systems.
- A statistically significant Spearman correlation of interest was the positive correlation of nitrifiers with ammonia concentrations.
- A positive Spearman correlation was found between HPC and AOB, supporting the operational usefulness of HPC as an indicator of the general microbiological conditions in a distribution system.

The results of the second phase of experimental work, covered in Chapter 5, were as follows:

- The batch test method of Sathasivan *et al.* (2005) can be a useful tool for investigating distribution system nitrification.
- This method was supplemented with a proposed qualitative categorization scheme for four different types of results from these batch tests. These “total chlorine decay curve types” are based on the stage of the batch test when the total chlorine residual concentrations begin to diverge between inhibited and uninhibited samples.
- The phenomenon observed by Sathasivan *et al.* (2008) in which the decay rate of the chloramine residual increases past a point designated the Critical Threshold Residual (CTR) was confirmed.
- To interpret the results of these batch tests, it is not recommended to use the microbial decay factor (F_m) of Sathasivan *et al.* (2005) in isolation since it can have similar values under dissimilar conditions. Using the chemical (k_C) and microbial (k_m) decay coefficients in combination will avoid confusion.

- Almost all of the samples tested had greater decay of the chloramine residual in the uninhibited batch tests, confirming that microbial activity was contributing to the decay.
- The efficacy of silver nitrate as an inhibiting agent was supported by comparisons that were made between filtered and inhibited samples.
- Changes in the organic carbon fractions present were investigated with Liquid Chromatography with Organic Carbon Detection (LC-OCD). Liquid Chromatography with Organic Nitrogen Detection (LC-OND) showed some decreases in ammonium concentrations and increases in nitrite and nitrate concentrations, confirming the occurrence of nitrification processes in these samples.

In Chapter 6, some models for distribution system nitrification that have been proposed in the literature were assessed. The findings are as follows:

- The “Nitrification Potential Curves” model of Fleming *et al.* (2005) seems best suited for use in full-scale chloraminated distribution systems based on its feasibility of application in an illustrative scenario.
- The kinetic nitrification model of Yang *et al.* (2008) was too complex to apply to the data available from the full-scale sampling campaign; however some simulations were conducted to investigate the model. It appears promising for research applications.
- The logistic regression risk factor model of Yang *et al.* (2007) was straight-forward to apply, but seems to require more data to fit properly than was available in the current study.
- With the possible exception of some niche applications, the “Nitrification Index” model (Speital *et al.*, 2011) is not recommended. It includes the impact of THM cometabolism and toxicity on nitrification which was negligible in the distribution systems involved in this study, while accounting for it required a large increase in the model complexity.
- The Carbon-to-Nitrogen ratio model (Zhang *et al.*, 2009b; Verhagen and Laanbroek, 1991) is also not recommended. It claims to predict the ecological balance between heterotrophic bacteria and ammonia-oxidizers based on their competition for ammonia-nitrogen but it did not provide a good fit to the distribution systems studied here.
- All of the nitrification models considered in Chapter 6 (i.e. all of them except the carbon-to-nitrogen ratio model) include the disinfectant residual as a factor. Thus it may be regarded as a consensus choice as an important factor affecting distribution system nitrification.

- There are alternatives to modelling that can also provide an early warning of nitrification episodes. Such alternatives include monitoring for declining trends in the total chlorine residual (Pintar *et al.*, 2005), and developing an accurate nitrogen balance for the distribution system (Wilczak *et al.*, 1996).

The scope of this thesis was quite wide, looking at distribution system nitrification through a sampling campaign in two full-scale distribution systems, through models that have been proposed in the literature, and through a batch test method. There are some common themes that serve to unify these diverse approaches. The results of Chapters 4, 5, and 6 can all be applied to improving monitoring for distribution system nitrification. The correlations in Table 4.2 indicate some variables that are related to the abundance of AOA or AOB. Models can be applied to predict when nitrification may occur. The batch test method used in this study can identify the microbial component, which includes nitrification processes, of the chloramine decay rate in samples from distribution system sites. Another important theme is the importance of maintaining a disinfectant residual. The levels of nitrifying microorganisms were negatively correlated with the total chlorine concentration in Chapter 4. The batch test used in Chapter 5 is able to identify the Critical Threshold Residual (CTR) in samples, below which the total chlorine decay rate increases significantly. This may be useful in the operation of chloraminated drinking water reservoirs. Almost all of the nitrification models examined in Chapter 6 included the disinfectant concentration as a factor.

7.2 Recommendations

The findings of this study lead to the following recommendations for operations in chloraminated drinking water distribution systems where nitrification is a concern:

- Nitrifiers are likely to be present even at some sites that do not exhibit strong indications of nitrification therefore it is important to maintain good control over distribution system conditions.
- The batch test method of Sathasivan *et al.* (2005) applied in this research can provide useful information about the microbial contribution to the chloramine decay rate in distribution system samples.
- The Critical Threshold Residual (Sathasivan *et al.*, 2008) is a point at which the decay rate of the total chlorine residual increases; residual targets for reservoirs and other distribution system sites should be set above the CTR in practice.

- The importance of maintaining an appropriate residual concentration in chloraminated distribution systems was highlighted by the results of each portion of this study.
- Some statistically significant Spearman (non-parametric) correlations between AOB and HPC support the use of HPC bacteria as a general indicator of microbiological water quality in distribution systems.
- The Nitrification Potential Curve model of Fleming *et al.* (2005) achieved a reasonable fit to data in an illustrative example and has a low complexity, making it practical for use by system operators.

From the above points, some practical advice can be offered to utilities using a monochloramine disinfectant residual that wish to guard against nitrification: Utilities should continue normal monitoring practices and use some of the correlations discussed in this thesis (e.g. elevated HPCs) to identify any sites that may require further investigation. Applying the batch test method used Chapter 5 may be worthwhile at such sites, especially if they are reservoirs, which that method is well-suited to analyze. The Critical Threshold Residual (CTR) could then be used as a minimum residual at that site, with respect to preventing nitrification. The use of nitrification models is unlikely to be of much use in utilities where nitrification is not currently a significant problem since they require a sufficient number of nitrification episodes (which did not occur in the systems studied here) to provide data to fit and validate. It is also suggested that utilities watch for a gradual or accelerating trend in total chlorine residual over time at a given sampling location, particularly in association with an increasing trend in HPCs at that same location.

Further research is recommended on the following topics:

- The growth and inactivation kinetics of species of ammonia-oxidizing archaea (AOA) found in chloraminated drinking water distribution systems.
- The factors affecting the AOA:AOB ratio in the distribution system environment and their relative importance to nitrification.
- The net effect of pH changes on distribution system nitrification.
- The causes of the acceleration of the chloramine decay rate below the CTR should be identified.
- Follow up testing is recommended on the effects seen from LC-OCD analysis of the batch test samples, and on the effects seen with the addition of organic carbon and ammonia to samples.

- It is hoped that future models developed for distribution system nitrification can take advantage of the discussion points in Chapter 6 (“Evaluation of Models for Nitrification”) regarding such modelling efforts.

References

- Antoniou, P., J. Hamilton, B. Koopman, R. Jain, B. Holloway, G. Lyberatos, and S. Svoronos, 1990. Effect of Temperature and pH on the Effective Maximum Specific Growth Rate of Nitrifying Bacteria. *Water Research*, 24(1):97–101.
- APHA, AWWA, and WEF, 2005. *Standard Methods for the Examination of Water and Wastewater*. American Public Health Association, Washington, DC, 21st ed.
- AWWA, 2006. *Fundamentals and Control of Nitrification in Chloraminated Drinking Water Distribution Systems*. Manual of Water Supply Practices. American Water Works Association, Denver, 1st ed.
- Bollmann, A., M.-J. Bär-Gilissen, and H. J. Laanbroek, 2002. Growth at Low Ammonium Concentrations and Starvation Response as Potential Factors Involved in Niche Differentiation among Ammonia-Oxidizing Bacteria. *Applied and Environmental Microbiology*, 68(10):4751–4757.
- Cheyne, B. M., M. I. V. Dyke, W. B. Anderson, and P. M. Huck, 2010. The detection of *Yersinia enterocolitica* in surface water by quantitative PCR amplification of the *ail* and *yadA* genes. *Journal of Water and Health*, 8(3):487–499.
- City of Toronto, 2011. Drinking Water Systems Annual Report. Available online: http://www.toronto.ca/water/system_quality/pdf/2010_wts_annual_report.pdf; Accessed: 29-July-2011.
- Claros, J., E. Jiménez, L. Borrás, D. Aguado, A. Seco, J. Ferrer, and J. Serralta, 2010. Short-term effect of ammonia concentration and salinity on activity of ammonia oxidizing bacteria. *Water Science & Technology*, 61(12):3008–3016.
- Cunliffe, D. A., 1991. Bacterial Nitrification in Chloraminated Water Supplies. *Applied and Environmental Microbiology*, 57(11):3399–3402.
- de la Torre, J., C. B. Walker, A. E. Ingalls, M. Könneke, and D. A. Stahl, 2008. Cultivation of a thermophilic ammonia oxidizing archaeon synthesizing crenarchaeol. *Environmental Microbiology*, 10(1):810–818.

- de Vet, W. W. J. M., I. J. T. Dinkla, G. Muyzer, L. C. Rietveld, and M. C. M. van Loosdrecht, 2009. Molecular characterization of microbial populations in groundwater sources and sand filters for drinking water production. *Water Research*, 43:182–194.
- Di, H. J., K. C. Cameron, J.-P. Shen, C. S. Winefield, M. O’Callaghan, S. Bowatte, and J.-Z. He, 2010. Ammonia-oxidizing bacteria and archaea grow under contrasting soil nitrogen conditions. *FEMS Microbiology Ecology*, 72:386–394.
- Dodge, Y., 2010. *The Concise Encyclopedia of Statistics*. Springer Science+Business Media, LLC, New York, 1st ed.
- Dym, C. L., 2004. *Principles of Mathematical Modeling*. Elsevier Academic Press, Amsterdam, 2nd ed.
- Edwards, M. and S. Triantafyllidou, 2007. Chloride-to-sulfate mass ratio and lead leaching to water. *Journal AWWA*, 99(7):96–109.
- Fisher, I., A. Sathasivan, P. Chuo, and G. Kastl, 2009. Effects of stratification on chloramine decay in distribution system service reservoirs. *Water Research*, 43:1403–1413.
- Fleming, K. K., G. W. Harrington, and D. R. Noguera, 2005. Nitrification potential curves: a new strategy for nitrification prevention. *Journal AWWA*, 97(8):90–99.
- Fleming, K. K., G. W. Harrington, and D. R. Noguera, 2008. Using nitrification potential curves to evaluate full-scale drinking water distribution systems. *Journal AWWA*, 100(10):92–103.
- Francis, C. A., K. J. Roberts, J. M. Beman, A. E. Santoro, and B. B. Oakley, 2005. Ubiquity and diversity of ammonia-oxidizing archaea in water columns and sediments of the ocean. *PNAS*, 102(41):14683–14688.
- Hach, 2008. *Hach Water Analysis Handbook Procedures*. Hach Company, USA, 5th ed. Available online: <http://www.hach.com/download-resources>; Accessed: 5-May-2011.
- Hallam, S. J., K. T. Konstantinidis, N. Putnam, C. Schleper, Y. ichi Watanabe, J. Sugahara, C. Preston, J. de la Torre, P. M. Richardson, and E. F. DeLong, 2006. Genomic analysis of the uncultivated marine crenarchaeote *Cenarchaeum symbiosum*. *PNAS*, 103(48):18296–18301.
- Health Canada, 2002. From Source to Tap: the multi-barrier approach to safe drinking water. Available online: http://www.hc-sc.gc.ca/ewh-semt/alt_formats/hecs-sesc/pdf/water-eau/tap-source-robinet/tap-source-robinet-eng.pdf; Accessed: 5-May-2011.

- Health Canada, 2010. Guidelines for Canadian Drinking Water Quality—Summary Table. Available online: http://www.hc-sc.gc.ca/ewh-semt/alt_formats/hecs-sesc/pdf/pubs/water-eau/2010-sum_guide-res_recom/sum_guide-res_recom-eng.pdf; Accessed: 6-July-2011.
- Health Canada, 2011. Guidance on the Use of Heterotrophic Plate Counts in Canadian Drinking Water Supplies. Available online: http://www.hc-sc.gc.ca/ewh-semt/consult/_2011/Heterotrophic-heterotrophes/Heterotrophic-heterotrophes-eng.php; Accessed: 26-April-2011.
- Herrmann, M., A. Scheibe, S. Avrahami, and K. Küsel, 2011. Ammonium availability affects the ratio of ammonia-oxidizing bacteria to ammonia-oxidizing archaea in simulated creek ecosystems. *Applied and Environmental Microbiology*, 77(5):1896–1899.
- Hoefel, D., P. T. Monis, W. L. Grooby, S. Andrews, and C. P. Saint, 2005. Culture-Independent Techniques for Rapid Detection of Bacteria Associated with Loss of Chloramine Residual in a Drinking Water System. *Applied and Environmental Microbiology*, 71(11):6479–6488.
- Huber, S. A., A. Balz, M. Abert, and W. Pronk, 2011. Characterisation of aquatic humic and non-humic matter with size-exclusion chromatography – organic carbon detection – organic nitrogen detection (LC-OCD-OND). *Water Research*, 45:879–885.
- Huck, P. M. and G. A. Gagnon, 2004. Understanding the distribution system as a bioreactor: a framework for managing heterotrophic plate count levels. *International Journal of Food Microbiology*, 92:347–353.
- Karanfil, T., I. Erdogan, and M. A. Schlautman, 2003. Selecting filter membranes for measuring DOC and UV₂₅₄. *Journal AWWA*, 95(3):86–100.
- Kasuga, I., H. Nakagaki, F. Kurisu, and H. Furumai, 2010a. Abundance and diversity of ammonia-oxidizing archaea and bacteria on biological activated carbon in a pilot-scale drinking water treatment plant with different treatment processes. *Water Science & Technology*, 61(12):3070–3077.
- Kasuga, I., H. Nakagaki, F. Kurisu, and H. Furumai, 2010b. Predominance of ammonia-oxidizing archaea on granular activated carbon used in a full-scale advanced drinking water treatment plant. *Water Research*, 44:5039–5049.
- Kendall, M., 1942. Partial Rank Correlation. *Biometrika*, 32(3/4):277–283.

- Könneke, M., A. E. Bernhard, J. de la Torre, C. B. Walker, J. B. Waterbury, and D. A. Stahl, 2005. Isolation of an autotrophic ammonia-oxidizing marine archaeon. *Nature*, 437:543–546.
- Krishna, K. B. and A. Sathasivan, 2010. Does an unknown mechanism accelerate chemical chloramine decay in nitrifying waters? *Journal AWWA*, 102(10):82–90.
- LeChevallier, M. W., C. D. Lowry, and R. G. Lee, 1990. Disinfecting Biofilms in a Model Distribution System. *Journal AWWA*, 82(7):87–99.
- LeChevallier, M. W., N. J. Welch, and D. B. Smith, 1996. Full-Scale Studies of Factors Related to Coliform Regrowth in Drinking Water. *Applied and Environmental Microbiology*, 62(7):2201–2211.
- Leininger, S., T. Urich, M. Schloter, L. Schwark, J. Qi, G. W. Nicol, J. I. Prosser, S. C. Schuster, and C. Schleper, 2006. Archaea predominate among ammonia-oxidizing prokaryotes in soils. *Nature*, 442:806–809.
- Levin, R. B., P. R. Epstein, T. E. Ford, W. Harrington, E. Olson, and E. G. Reichard, 2002. U.S. Drinking Water Challenges in the Twenty-First Century. *Environmental Health Perspectives*, 110(Suppl. 1):43–52.
- Lipponen, M. T., P. J. Martikainen, R. E. Vasara, K. Servomaa, O. Zacheus, and M. H. Kontro, 2004. Occurrence of nitrifiers and diversity of ammonia-oxidizing bacteria in developing drinking water biofilms. *Water Research*, 38:4424–4434.
- Lipponen, M. T., M. H. Suutari, and P. J. Martikainen, 2002. Occurrence of nitrifying bacteria and nitrification in Finnish drinking water distribution systems. *Water Research*, 36:4319–4329.
- Liu, S., J. S. Taylor, A. Randall, and J. D. Dietz, 2005. Nitrification modeling in chloraminated distribution systems. *Journal AWWA*, 97(10):98–108.
- MacPhee, M. J., ed., 2005. *Distribution System Water Quality Challenges in the 21st Century: A Strategic Guide*. American Water Works Association, Denver, 1st ed.
- Martens-Habbena, W., P. M. Berube, H. Urakawa, J. de la Torre, and D. A. Stahl, 2009. Ammonia oxidation kinetics determine niche separation of nitrifying Archaea and Bacteria. *Nature*, 461:976–981.
- McGuire, M. J., X. Wu, N. K. Blute, D. Askenaizer, and G. Qin, 2009. Prevention of Nitrification Using Chlorite Ion: Results of a Demonstration Project in Glendale, Calif. *Journal AWWA*, 101(10):47–59.

- Miettinen, I. T., T. Vartiainen, and P. J. Martikainen, 1997. Phosphorus and Bacterial Growth in Drinking Water. *Applied and Environmental Microbiology*, 63(8):3242–3245.
- Murthy, D., N. Page, and E. Rodin, 1990. *Mathematical Modelling: A tool for problem solving in engineering, physical, biological and social sciences*. Pergamon Press, Oxford, 1st ed.
- National Research Council, 2006. *Drinking Water Distribution Systems: Assessing and Reducing Risks*. National Academies Press, Washington, DC. Committee on Public Water Supply Distribution Systems: Assessing and Reducing Risks.
- Nicolaisen, M. H. and N. B. Ramsing, 2002. Denaturing gradient gel electrophoresis (DGGE) approaches to study the diversity of ammonia-oxidizing bacteria. *Journal of Microbiological Methods*, 50:189–203.
- Odell, L. H., G. J. Kirmeyer, A. Wilczak, J. G. Jacangelo, J. P. Marcinko, and R. L. Wolfe, 1996. Controlling Nitrification in Chloraminated Systems. *Journal AWWA*, 88(7):86–98.
- Oldenburg, P. S., J. M. Regan, G. W. Harrington, and D. R. Noguera, 2002. Kinetics of *Nitrosomonas europaea* inactivation by chloramine. *Journal AWWA*, 94(10):100–110.
- Ontario Ministry of the Environment, 2006. Procedure for Disinfection of Drinking Water in Ontario. Available online: www.portal.gov.on.ca/drinkingwater/stel101_046942.pdf; Accessed: 21-Nov-2011.
- Peierls, S. R., 1980. Model-Making in Physics. *Contemporary Physics*, 21(1):3–17.
- Pintar, K. D. M., W. B. Anderson, R. M. Slawson, E. F. Smith, and P. M. Huck, 2005. Assessment of a distribution system nitrification critical threshold concept. *Journal AWWA*, 97(7):116–129.
- Pintar, K. D. M. and R. M. Slawson, 2003. Effect of temperature and disinfection strategies on ammonia-oxidizing bacteria in a bench-scale drinking water distribution system. *Water Research*, 37:1805–1817.
- Prosser, J. I. and G. W. Nicol, 2008. Relative contributions of archaea and bacteria to aerobic ammonia oxidation in the environment. *Environmental Microbiology*, 10(11):2931–2941.
- R Development Core Team, 2009. *R: A Language and Environment for Statistical Computing*. R Foundation for Statistical Computing, Vienna, Austria. <http://www.R-project.org>.

- Reed, D. W., J. M. Smith, C. A. Francis, and Y. Fujita, 2010. Responses of ammonia-oxidizing bacterial and archaeal populations to organic nitrogen amendments in low-nutrient groundwater. *Applied and Environmental Microbiology*, 76(8):2517–2523.
- Regan, J. M., G. W. Harrington, H. Baribeau, R. D. Leon, and D. R. Noguera, 2003. Diversity of nitrifying bacteria in full-scale chloraminated distribution systems. *Water Research*, 37:197–205.
- Regan, J. M., G. W. Harrington, and D. R. Noguera, 2002. Ammonia- and Nitrite-Oxidizing Bacterial Communities in a Pilot-Scale Chloraminated Drinking Water Distribution System. *Applied and Environmental Microbiology*, 68(1):73–81.
- Region of Waterloo, 2011. 2010 Water Quality Reports for Integrated Urban and Rural Water Supply Systems. Available online: <http://www.regionofwaterloo.ca/en/aboutTheEnvironment/resources/2010WQR.pdf>; Accessed: 29-July-2011.
- Rice, E. W., P. V. Scarpino, D. J. Reasoner, G. S. Logsdon, and D. K. Wild, 1991. Correlation of Coliform Growth Response with Other Water Quality Parameters. *Journal AWWA*, 83(7):98–102.
- Rittmann, B. E. and P. L. McCarty, 2001. *Environmental Biotechnology: Principles & Applications*, chap. 9. Nitrification, p. 470ff. McGraw Hill.
- Rittmann, B. E., J. M. Regan, and D. A. Stahl, 1994. Nitrification as a Source of Soluble Organic Substrate in Biological Treatment. *Water Science & Technology*, 30(6):1–8.
- Rittmann, B. E. and V. L. Snoeyink, 1984. Achieving Biologically Stable Drinking Water. *Journal AWWA*, 76(10):106–114.
- Rotthauwe, J.-H., K.-P. Witzel, and W. Liesack, 1997. The Ammonia Monooxygenase Structural Gene *amoA* as a Functional Marker: Molecular Fine-Scale Analysis of Natural Ammonia-Oxidizing Populations. *Applied and Environmental Microbiology*, 63(12):4704–4712.
- Sathasivan, A., I. Fisher, and G. Kastl, 2005. Simple Method for Quantifying Microbiologically Assisted Chloramine Decay in Drinking Water. *Environmental Science & Technology*, 39(14):5407–5413.
- Sathasivan, A., I. Fisher, and G. Kastl, 2010. Application of the microbial decay factor to maintain chloramine in large tanks. *Journal AWWA*, 102(4):94–103.
- Sathasivan, A., I. Fisher, and T. Tam, 2008. Onset of severe nitrification in mildly nitrifying chloraminated bulk waters and its relation to biostability. *Water Research*, 42:3623–3632.

- Sauder, L. A., K. Engel, J. C. Stearns, A. P. Massela, R. Pawliszyn, and J. D. Neufeld, 2011. Aquarium Nitrification Revisited: Thaumarchaeota are the Dominant Ammonia Oxidizers in Freshwater Aquarium Biofilters. *PLoS ONE*, 6(8):1–9.
- Schleper, C., 2010. Ammonia oxidation: different niches for bacteria and archaea? *The ISME Journal*, 4:1092–1094.
- Skadsen, J., 1993. Nitrification in a Distribution System. *Journal AWWA*, 85(7):95–103.
- Skadsen, J., 2002. Effectiveness of High pH in Controlling Nitrification. *Journal AWWA*, 94(7):73–83.
- Snoeyink, V. L. and D. Jenkins, 1980. *Water Chemistry*. John Wiley & Sons, Toronto.
- Speital, G. E., R. Kannappan, and B. M. Bayer, 2011. The nitrification index: a unified concept for quantifying the risk of distribution system nitrification. *Journal AWWA*, 103(1):69–80.
- Srinivasan, S. and G. W. Harrington, 2007. Biostability analysis for drinking water distribution systems. *Water Research*, 41:2127–2138.
- van der Wielen, P. W., S. Voost, and D. van der Kooij, 2009. Ammonia-Oxidizing Bacteria and Archaea in Groundwater Treatment and Drinking Water Distribution Systems. *Applied and Environmental Microbiology*, 75(14):4687–4695.
- Verhagen, F. J. and H. J. Laanbroek, 1991. Competition for Ammonium between Nitrifying and Heterotrophic Bacteria in Dual Energy-Limited Chemostats. *Applied and Environmental Microbiology*, 57(11):3255–3263.
- Vikesland, P. J., K. Ozekin, and R. L. Valentine, 2001. Monochloramine decay in model and distribution system waters. *Water Research*, 35(7):1766–1776.
- Villaverde, S., P. García-Encina, and F. Fdz-Polanco, 1997. Influence of pH over Nitrifying Biofilm Activity in Submerged Biofilters. *Water Research*, 31(5):1180–1186.
- Wahman, D. G., A. E. Henry, L. E. Katz, and G. E. Speital, 2006. Cometabolism of trihalomethanes by mixed culture nitrifiers. *Water Research*, 40:3349–3358.
- Wahman, D. G., M. J. Kirisits, L. E. Katz, and G. E. Speitel, 2011. Ammonia-oxidizing bacteria in biofilters removing Trihalomethanes are related to *Nitrosomonas oligotropha*. *Applied and Environmental Microbiology*, 77(7):2537–2540.

- Wahman, D. G., K. A. Wulfeck-Kleier, and J. G. Pressman, 2009. Monochloramine Disinfection Kinetics of *Nitrosomonas europaea* by Propidium Monoazide Quantitative PCR and Live/Dead BacLight Methods. *Applied and Environmental Microbiology*, 75(17):5555–5562.
- Westbrook, A. and F. A. Digiano, 2009. Rate of chloramine decay at pipe surfaces. *Journal AWWA*, 101(7):59–70.
- Wilczak, A., J. G. Jacangelo, J. P. Marcinko, L. H. Odell, and G. J. Kirmeyer, 1996. Occurrence of nitrification in chloraminated distribution systems. *Journal AWWA*, 88(7):74–85.
- Yang, J., G. W. Harrington, and D. R. Noguera, 2008. Nitrification Modeling in Pilot-Scale Chloraminated Drinking Water Distribution Systems. *Journal of Environmental Engineering*, 134(9):731–742.
- Yang, J., G. W. Harrington, D. R. Noguera, and K. K. Fleming, 2007. Risk Analysis of Nitrification Occurrence in Pilot-Scale Chloraminated Distribution Systems. *Journal of Water Supply: Research and Technology—AQUA*, 56(5):293–311.
- Zhang, M., M. J. Semmens, D. Schuler, and R. M. Hozalski, 2002. Biostability and microbiological quality in a chloraminated distribution system. *Journal AWWA*, 94(9):112–122.
- Zhang, Y. and M. Edwards, 2009. Accelerated chloramine decay and microbial growth by nitrification in premise plumbing. *Journal AWWA*, 101(11):51–62.
- Zhang, Y., A. Griffin, and M. Edwards, 2008. Nitrification in Premise Plumbing: Role of Phosphate, pH and Pipe Corrosion. *Environmental Science & Technology*, 42(12):4280–4284.
- Zhang, Y., A. Griffin, and M. Edwards, 2010a. Effect of Nitrification on Corrosion of Galvanized Iron, Copper, and Concrete. *Journal AWWA*, 102(4):83–93.
- Zhang, Y., A. Griffin, M. Rahman, A. Camper, H. Baribeau, and M. Edwards, 2009a. Lead Contamination of Potable Water Due to Nitrification. *Environmental Science & Technology*, 43(6):1890–1895.
- Zhang, Y., N. Love, and M. Edwards, 2009b. Nitrification in Drinking Water Systems. *Critical Reviews in Environmental Science and Technology*, 39:153–208.
- Zhang, Y., L. Zhou, G. Zeng, H. Deng, and G. Li, 2010b. Impact of total organic carbon and chlorine to ammonia ratio on nitrification in a bench-scale drinking water distribution system. *Frontiers of Environmental Science & Engineering in China*, 4(4):430–437.

Appendix A

Raw Sampling Data

The following tables (A.1, A.2, and A.3) contain the raw measurements from the sampling campaign described in Chapter 4. The parameters listed are temperature (Water Temp.), conductivity (Cond.), pH, total chlorine residual (Total Cl.), monochloramine (Monochlor.), nitrate (NO_3^-), nitrite (NO_2^-), ammonia (NH_3), dissolved organic carbon (DOC), dissolved oxygen (D.O.), chloride (Cl^-), sulfate (SO_4^{2-}), the chloride-to-sulfate mass ratio (CSMR), ammonia oxidizing bacteria (AOB), ammonia oxidizing archaea (AOA), and heterotrophic plate counts (HPC). AOB and AOA were determined by quantitative PCR and are reported in gene copies per 100 mL (gcp/100 mL) and HPC are reported in colony forming units per 100 mL (CFU/100 mL). Missing data is left blank.

Table A.1: Results for physical and chemical parameters from sampling in full-scale distribution systems in 2009–2010 (Part 1).

Site	Date	Water Temp. °C	Cond. $\mu\text{S}/\text{cm}$	pH	Total Cl. $\text{mg-Cl}_2/\text{L}$	Monochlor. $\text{mg-Cl}_2/\text{L}$	NO_3^- $\text{mg-N}/\text{L}$	
RCL	24-Nov	12.2	259	7.45	1.35	1.22		
	08-Dec	11	354	7.23	1.23	0.95		
	12-Jan	7.7	288	7.44	1.27	0.68	0.41	
	27-Jan	7.6	341	7.58	1.20	0.81	0.65	
	09-Feb	7.1	276	7.47	1.07	0.81	0.49	
	23-Feb	7.4	339	7.60	1.47	0.46	0.42	
	23-Mar	9.4	359	7.47	1.34	1.11	0.44	
	21-Apr	11.5	335	7.67	1.28	1.04	0.28	
	18-May	11.3	326	7.76	1.43	1.18	0.46	
	01-Jun	12.6	314	7.63	1.20	0.91	0.38	
	07-Jul	12.2	285	7.41	1.28	0.96	0.55	
	17-Aug			7.21	1.24	1.09	0.24	
	602	24-Nov	15	320	7.60	1.25	1.28	
		08-Dec	14.2	346	7.49	1.23	0.91	
12-Jan		10.7	340	7.37	1.16	0.86	0.58	
27-Jan		9.3	330	7.45	1.18	0.81	0.52	
09-Feb		9.7	325	7.27	1.09	0.76	0.48	
23-Feb		8.8	334	7.47	1.36	0.96	0.46	
23-Mar		9	360	7.45	1.26	0.99	0.39	
21-Apr		11.1	339	7.63	1.29	1.09	0.27	
18-May	13.5	325	7.38	1.31	1.12	0.53		

Table A.1: Results for physical and chemical parameters from sampling in full-scale distribution systems in 2009–2010 (Part 1).

Site	Date	Water Temp. °C	Cond. $\mu\text{S}/\text{cm}$	pH	Total Cl. $\text{mg-Cl}_2/\text{L}$	Monochlor. $\text{mg-Cl}_2/\text{L}$	NO_3^- $\text{mg-N}/\text{L}$
801	01-Jun	14.4	325	7.58	1.18	0.92	0.24
	07-Jul	15.9	285	7.49	1.23	0.29	0.31
	17-Aug	18		7.30	1.26	1.03	0.17
	24-Nov	19.4	325	7.53	1.07	1.03	
	08-Dec	15.6	347	7.56	1.12	0.81	
	12-Jan	14.8	334	7.57	1.01	0.65	0.37
	27-Jan	16.8	337	7.53	0.95	0.37	0.00
	09-Feb	13.8	327	7.67	1.05	0.76	0.50
	23-Feb	12	339	7.53	1.19	0.86	0.48
	23-Mar	12.2	364	7.61	1.06	0.92	0.48
	21-Apr	13.8	338	7.92	1.13	0.93	0.29
804	18-May	11.8	333	7.50	1.20	1.02	0.49
	01-Jun	18.1	318	7.41	1.01	0.87	0.37
	07-Jul	14.5	285	7.54	1.11	0.81	0.67
	17-Aug	19		7.50	0.90	0.66	0.16
	24-Nov	13.8	327	7.53	1.21	1.18	
	08-Dec	11.5	343	7.51	1.19	0.86	
	12-Jan	8	333	7.46	1.15	0.81	0.36
	27-Jan	7	341	7.74	1.22	0.81	0.29
	09-Feb	8.4	332	7.26	1.12	0.81	0.45
	23-Feb	6.9	343	7.59	1.30	0.96	0.50
	23-Mar	8.1	363	7.52	1.23	1.06	0.45
805	21-Apr	11.9	342		1.23	1.12	0.28
	18-May	13.5	330	7.46	1.27	1.08	0.47
	01-Jun	15.3	320	7.58	1.17	0.93	0.34
	07-Jul	15	287	7.53	1.23	0.89	0.42
	17-Aug	19		7.49	1.16	1.02	0.31
	24-Nov	12.6	322	7.52	1.10	1.06	
	08-Dec	11.3	336	7.43	1.08	0.71	
	12-Jan	8.4	354	7.44	1.15	0.76	0.37
	27-Jan	6.7	340	7.59	1.04	0.66	0.49
	09-Feb	6.3	331	7.35	1.20	0.86	0.46
	23-Feb	6.7	338	7.54	1.09	0.81	0.48
904	23-Mar	7.4	360	7.49	1.09	0.86	0.40
	21-Apr	9.4	326	7.69	1.10	0.95	0.15
	18-May	11	326	7.63	1.14	0.98	0.45
	01-Jun	13.4	315	7.74	1.08	0.93	0.29
	07-Jul	15.6	285	7.64	0.94	0.67	0.86
	17-Aug	18		7.51	0.92	0.66	0.15
	24-Nov	12.7	326	7.74	1.08	0.99	
	08-Dec	11.2	343	7.55	1.07	0.71	
	12-Jan	9	375	7.58	1.10	0.76	0.54
	27-Jan	8.3	341	7.77	1.01	0.66	0.67
	09-Feb	6.9	306	7.52	1.10	0.76	0.48
905	23-Feb	7.4	340	7.61	1.17	0.86	0.47
	23-Mar	8.6	367	7.55	1.08	0.82	0.51
	21-Apr	10.4	331	7.74	1.06	0.80	0.34
	18-May	11.7	331	7.52	1.06	0.84	0.52
	01-Jun	13.7	320	7.61	1.10	0.91	0.28
	07-Jul	14.8	290	7.66	1.00	0.67	0.36
	17-Aug	19		7.54	0.87	0.69	0.23
	24-Nov	14.2	319	7.62	1.05	0.51	
	08-Dec	14.5	335	7.52	1.16	0.81	
	12-Jan	10.7	334	7.44	1.19	0.65	0.68
	27-Jan	11.1	340	7.54	1.13	0.81	0.61
09-Feb	9.7	332	7.19	1.20	0.86	0.50	
23-Feb	13	331	7.50	1.14	0.86	0.39	

Table A.1: Results for physical and chemical parameters from sampling in full-scale distribution systems in 2009–2010 (Part 1).

Site	Date	Water Temp. °C	Cond. $\mu\text{S}/\text{cm}$	pH	Total Cl. $\text{mg-Cl}_2/\text{L}$	Monochlor. $\text{mg-Cl}_2/\text{L}$	NO_3^- $\text{mg-N}/\text{L}$	
K20S14	23-Mar	11.6	357	7.49	1.22	1.09	0.45	
	21-Apr	15.1	333	7.24	1.20	1.04	0.23	
	18-May	13.7	325	7.40	1.11	0.94	0.46	
	01-Jun	17.6	321	7.64	1.11	0.90	0.40	
	07-Jul	14.9	284	7.56	1.12	0.81	0.41	
	17-Aug			7.32	1.32	0.96	0.06	
	17-Feb	5.1	820	7.41	1.52	1.09	3.37	
	03-Mar	6	778	7.46	1.38	0.91	3.38	
	17-Mar	7.8	681	7.76	1.61	1.73	3.22	
	31-Mar	8.8	683	7.46	1.56	1.30	3.39	
	14-Apr	10.7	709	7.65	1.51	1.46	4.43	
	12-May	12.1	633	7.51	1.61	1.56	3.69	
	27-May	16.3	657	7.48	1.34	1.01	3.60	
	15-Jul	18.7	690	7.10	1.28	1.20	3.75	
W21	25-Aug	20.6		7.41	1.39	1.51	2.45	
	17-Feb	6.1	775	7.68	1.01		3.37	
	03-Mar	7.8	771	7.70	0.75	0.81	3.15	
	17-Mar	9.2	609	7.42	0.95	1.03	3.15	
	31-Mar	9.6	632	7.71	1.24	1.23	3.27	
	14-Apr	10.9	692	8.40	0.87	0.84	3.74	
	12-May	11.8	643	7.71	0.73	0.70	3.31	
	27-May	14.6	572	7.69	0.78	0.66	3.65	
	15-Jul	17.4	674	7.00	1.16	1.04	2.98	
	25-Aug	20.4		7.45	0.73	0.72	2.93	
	WOD08	17-Feb	8.6	769	7.42	1.07		3.38
		03-Mar	8	755	7.56	1.06	0.81	3.35
		17-Mar	9.4	760	7.52	1.07	1.06	3.23
		31-Mar	9.8	662	7.36	1.07	1.09	3.38
14-Apr		11.2	687	7.42	0.93	0.84	4.99	
12-May		13.6	661	7.41	0.94	0.85	2.98	
27-May		17	619	7.60	0.96	0.59	3.01	
15-Jul		20.2	681	7.08	0.83	0.79	3.04	
25-Aug		21.8		7.30	0.67	0.64	2.72	
WOD05		17-Feb	9.9	748	7.42			
		03-Mar	11.5	757	7.39	1.30	0.91	3.34
		17-Mar	10.5	733	7.54	1.27	1.20	3.28
		31-Mar	8.9	663	7.58	1.20	1.20	3.18
		14-Apr	11.9	691	7.66	0.98	0.92	4.51
	12-May	12.5	658	7.53	1.01	0.94	2.98	
	27-May	16.8	637	7.46	0.98	0.77	3.76	
	15-Jul	18.5	675	7.09	0.93	0.86	3.40	
	25-Aug	20.8		7.41	0.75	0.77	2.35	
	WOD06	17-Feb	8.4	745	7.46	0.84		3.25
		03-Mar	8.6	767	7.92	0.72	0.71	3.25
		17-Mar	8.4	745	7.57	1.04	1.08	2.96
		31-Mar	8.1	665	7.48	0.87	1.10	3.23
		14-Apr	12.1	689	7.54	0.69	0.61	4.05
12-May		13.3	661	7.40	0.91	0.81	3.42	
27-May		18.7	641	7.54	0.82	0.23	3.22	
15-Jul		21.2	691	7.10	0.46	0.43	3.77	
25-Aug		19.7		7.43	0.50	0.69	2.95	
WOD04		17-Feb	14.5	735	7.35	0.54		3.15
		03-Mar	13.7	740	7.52	0.16	0.18	3.35
		17-Mar	14.4	758	7.53	0.26	0.00	3.14
		31-Mar	13.6	715	7.57	0.63	0.00	3.32
		14-Apr	15.7	691	7.34	0.61	0.01	3.29
	12-May	14.8	665	7.57	0.61		3.49	

Table A.1: Results for physical and chemical parameters from sampling in full-scale distribution systems in 2009–2010 (Part 1).

Site	Date	Water Temp. °C	Cond. μS/cm	pH	Total Cl. mg-Cl ₂ /L	Monochlor. mg-Cl ₂ /L	NO ₃ ⁻ mg-N/L
E60T	27-May	17.9	645	7.60	0.51	0.00	3.83
	15-Jul	18.4	699	7.26	0.56	0.00	3.25
	25-Aug	19.8		7.52	0.45	0.00	2.76
	17-Feb	4.6	710	7.49	1.14		3.33
	03-Mar	8.1	781	7.44	1.26	0.96	3.30
	17-Mar	7.4	797	7.57	1.15	1.16	3.39
	31-Mar	8.7	672	7.53	1.16	1.18	3.13
	14-Apr	9.3	701	7.31	1.02	0.92	3.24
WOD61	12-May	12.3	675	7.48	1.07	0.96	3.37
	27-May	12.8	646	7.59	1.03	0.82	3.97
	15-Jul	16.4	697	7.14	0.91	0.84	3.39
	25-Aug	18.8		7.42	0.79	0.72	2.61
	17-Feb	6.6	740	7.41	0.81	0.50	3.12
	03-Mar	6.5	777	7.56	1.05	0.81	3.35
	17-Mar	12.6	749	7.48	0.73	0.64	3.14
	31-Mar	8.9	688	7.51	0.86	0.88	3.39
	14-Apr	9.4	707	7.61	0.84	0.76	3.53
	12-May	15.3	661	7.49	0.58	0.53	3.26
	27-May	16.4	642	7.56	0.74	0.49	4.08
	15-Jul	19.7	690	7.19	0.66	0.60	3.05
25-Aug	20.8		7.44	0.48	0.44	2.30	

Table A.2: Results for physical and chemical parameters from sampling in full-scale distribution systems in 2009–2010 (Part 2).

Site	Date	NO ₂ ⁻ mg-N/L	NH ₃ mg-N/L	DOC mg-C/L	D.O. mg/L	Cl ⁻ mg/L	SO ₄ ²⁻ mg/L	CSMR
RCL	24-Nov		0.22	2.59	7.9			
	08-Dec		0.18	2.27	9.9			
	12-Jan	0.000	0.04	1.80	6.8	30.8	38.3	0.80
	27-Jan	0.000	0.06	1.80	8.41	93.9	87.8	1.07
	09-Feb	0.000	0.00	1.90	11.2	21.9	29.0	0.76
	23-Feb	0.006	0.35	2.04	9.1	32.2	30.7	1.05
	23-Mar	0.000		1.93		36.5	33.3	1.10
	21-Apr	0.000	0.06	2.49		26.7	37.5	0.71
	18-May	0.000	0.04	3.34		33.0	30.8	1.07
	01-Jun	0.005	0.13	3.86		25.5	28.4	0.90
602	07-Jul	0.000	0.19	3.52		29.0	31.5	0.92
	17-Aug	0.000	0.13	4.19		32.5	29.4	1.11
	24-Nov		0.21	2.55	8.2			
	08-Dec		0.06	1.95	9.7			
	12-Jan	0.000		1.99	7.3	29.2	34.7	0.84
	27-Jan	0.000	0.05	1.84	9.2	99.3	94.9	1.05
	09-Feb	0.000	0.03	1.94	11.9	26.7	29.3	0.91
	23-Feb	0.000	0.01	2.00	8.4	34.5	36.2	0.95
	23-Mar	0.015	0.09	1.89		37.5	37.1	1.01
	21-Apr	0.000	0.08	1.74		28.9	30.4	0.95
801	18-May	0.000	0.10	2.02		32.2	36.6	0.88
	01-Jun	0.003	0.12	2.16		30.6	26.7	1.15
	07-Jul	0.009	0.27	2.70		28.5	32.6	0.87
	17-Aug	0.000	0.13	3.83		25.5	34.4	0.74
	24-Nov		0.28	2.37	9.2			
	08-Dec		0.07	2.21	9.7			
	12-Jan	0.000	0.04	1.87	8.2	28.9	34.7	0.83
	27-Jan	0.000	0.04	1.87				
	09-Feb	0.000	0.02	1.81	10.0	21.3	29.8	0.71

Table A.2: Results for physical and chemical parameters from sampling in full-scale distribution systems in 2009–2010 (Part 2).

Site	Date	NO ₂ ⁻ mg-N/L	NH ₃ mg-N/L	DOC mg-C/L	D.O. mg/L	Cl ⁻ mg/L	SO ₄ ²⁻ mg/L	CSMR
804	23-Feb	0.003	0.03	1.94	8.3	36.6	33.6	1.09
	23-Mar	0.000	0.13	1.75		34.1	36.9	0.92
	21-Apr	0.003	0.11	1.79		32.4	30.9	1.05
	18-May	0.000	0.11	1.71		27.6	33.4	0.83
	01-Jun	0.013	0.26	2.53		29.4	31.1	0.95
	07-Jul	0.000	0.20	2.85		24.5	36.8	0.66
	17-Aug	0.003	0.28	3.96		28.9	34.3	0.85
	24-Nov		0.09	2.35	9.9			
	08-Dec		0.06	1.93	9.1			
	12-Jan	0.000	0.05	1.91	9.5	27.9	34.5	0.81
	27-Jan	0.000	0.08	1.92	8.8	142.5	125.1	1.14
	09-Feb	0.000	0.04	1.98	11.4	26.7	29.0	0.92
	23-Feb	0.000	0.01	1.93	12.1	28.8	31.5	0.91
	23-Mar	0.000	0.14	1.74		32.8	31.3	1.05
805	21-Apr	0.000	0.11	2.30		27.6	35.7	0.77
	18-May	0.000	0.13	1.89		29.0	32.1	0.90
	01-Jun	0.006	0.17	3.02		24.0	26.7	0.90
	07-Jul	0.000	0.21	2.5		26.6	28.1	0.95
	17-Aug	0.000	0.09	3.62		28.2	29.7	0.95
	24-Nov		0.09	2.38	8.1			
	08-Dec		0.09	2.08	9.4			
	12-Jan	0.000	0.05	1.81	7.6	27.1	32.1	0.84
	27-Jan	0.000	0.08	1.84	8.3	88.9	101.6	0.87
	09-Feb	0.000	0.03	1.95	12.9	17.5	27.7	0.63
	23-Feb	0.000	0.12	1.96	11.7	28.3	30.7	0.92
	23-Mar	0.002	0.18	1.76		34.9	36.0	0.99
	21-Apr	0.000	0.11	1.68		23.1	29.6	0.78
	18-May	0.000	0.12	1.60		30.7	32.3	0.95
904	01-Jun	0.014	0.24	2.53		26.6	29.0	0.92
	07-Jul	0.000	0.32	3.60		30.8	34.4	0.89
	17-Aug	0.000	0.24	4.06		24.8	34.5	0.72
	24-Nov		0.24	2.49	9.5			
	08-Dec		0.08		11.2			
	12-Jan	0.000	0.03	1.97	9.9	29.9	48.7	0.62
	27-Jan	0.000	0.06	2.01	7.2	93.5	94.8	0.99
	09-Feb	0.000	0.04	1.93	9.6	24.9	28.6	0.87
	23-Feb	0.002	0.05	2.02	12.0	29.5	32.3	0.92
	23-Mar	0.000	0.18	1.80		35.1	33.4	1.05
	21-Apr	0.016	0.12	1.62		29.0	26.7	1.09
	18-May	0.017	0.14	1.77		28.1	36.8	0.76
	01-Jun	0.002	0.18	2.82		28.4	32.5	0.88
	07-Jul	0.000	0.28	3.35		27.6	32.0	0.86
905	17-Aug	0.000	0.30	3.81		28.1	31.1	0.90
	24-Nov		0.50	2.24	8.5			
	08-Dec		0.07	2.05	9.7			
	12-Jan	0.000		1.87	8.7	30.5	38.1	0.80
	27-Jan	0.000	0.07	1.97	10.2	108.2	109.6	0.99
	09-Feb	0.000	0.01	1.93	11.3	27.0	28.1	0.96
	23-Feb	0.000	0.05	2.12	9.3	26.8	30.6	0.87
	23-Mar	0.005	0.11	1.70		36.8	35.4	1.06
	21-Apr	0.000	0.09	1.70		29.8	32.6	0.91
	18-May	0.000	0.14	2.12		28.0	30.2	0.93
	01-Jun	0.027	0.19	3.01		25.9	32.5	0.80
	07-Jul	0.000	0.22	3.60		24.2	32.3	0.76
	17-Aug	0.004	0.20	3.57		25.3	31.8	0.80

Table A.2: Results for physical and chemical parameters from sampling in full-scale distribution systems in 2009–2010 (Part 2).

Site	Date	NO ₂ ⁻ mg-N/L	NH ₃ mg-N/L	DOC mg-C/L	D.O. mg/L	Cl ⁻ mg/L	SO ₄ ²⁻ mg/L	CSMR
K20S14	17-Feb	0.004	0.12	3.29	14.9	76.9	57.5	1.34
	03-Mar	0.009	0.08	2.56	10.1	83.1	52.3	1.59
	17-Mar	0.003	0.21	2.45		66.0	87.2	0.76
	31-Mar	0.009	0.13	2.42		67.0	42.1	1.59
	14-Apr	0.000	0.20	3.91		55.2	47.6	1.16
	12-May	0.000	0.16	2.9		55.6	42.3	1.31
	27-May	0.006	0.16	5.69		70.9	39.8	1.78
	15-Jul	0.004	0.20	5.80	8.0	62.0	43.9	1.41
W21	25-Aug	0.000	0.09	3.12	6.4	81.0	40.5	2.00
	17-Feb	0.005	0.08	2.41	9.8	63.8	53.8	1.19
	03-Mar	0.003	0.17	2.08		71.0	56.8	1.25
	17-Mar	0.009	0.22	2.02		70.7	51.5	1.37
	31-Mar	0.000	0.24	1.66		56.8	52.8	1.08
	14-Apr	0.000	0.15	1.81		50.0	46.8	1.07
	12-May	0.000	0.36	1.66		53.6	57.4	0.93
	27-May	0.045	0.36	4.08		74.6	42.4	1.76
WOD08	15-Jul	0.005	0.17	3.85	6.7	57.8	46.6	1.25
	25-Aug	0.006	0.30	4.18	5.1	59.1	40.4	1.46
	17-Feb	0.005	0.10	2.28	8.3	62.7	54.0	1.16
	03-Mar	0.003	0.14	2.09	10.2	71.9	60.6	1.19
	17-Mar	0.005	0.32	1.87		72.5	52.2	1.39
	31-Mar	0.000	0.17	1.33		53.0	57.0	0.93
	14-Apr	0.003	0.12	1.69		50.9	43.5	1.17
	12-May	0.000	0.37	2.16		53.2	56.2	0.95
WOD05	27-May	0.014	0.37	3.46		72.9	45.9	1.59
	15-Jul	0.008	0.26	2.60	7.3	73.2	41.9	1.75
	25-Aug	0.004	0.38	2.92	6.7	54.9	49.4	1.11
	17-Feb		0.08		9.7			
	03-Mar	0.007		2.00	8.2	71.1	50.6	1.40
	17-Mar	0.006	0.25	1.69		65.9	52.9	1.25
	31-Mar	0.007	0.12	1.31		52.7	53.0	1.01
	14-Apr	0.000	0.23	2.56		56.1	54.8	1.02
WOD06	12-May	0.000	0.00	2.20		55.6	51.4	1.09
	27-May	0.030	0.00	2.78		68.1	46.1	1.48
	15-Jul	0.000	0.22	5.20	6.8	54.2	52.5	1.03
	25-Aug	0.000	0.25	3.85	7.2	69.3	46.4	1.50
	17-Feb	0.009	0.09	2.18	9.1	61.6	63.8	0.97
	03-Mar	0.000	0.17	1.94	10.5	74.7	54.0	1.38
	17-Mar	0.005	0.18	1.82		74.5	59.7	1.25
	31-Mar	0.007	0.23	1.29		52.5	47.4	1.11
WOD04	14-Apr	0.000	0.14	1.80		50.4	51.8	0.97
	12-May	0.000	0.51	2.13		55.7	55.3	1.01
	27-May	0.043	0.51	4.07		65.9	42.9	1.54
	15-Jul	0.003	0.33	3.10	6.8	61.1	49.1	1.25
	25-Aug	0.003	0.32	3.56	4.3	59.7	40.0	1.49
	17-Feb	0.000	0.00	2.43	7.4	68.9	51.1	1.35
	03-Mar	0.000	0.02	1.79	6.4	66.2	61.3	1.08
	17-Mar	0.001	0.01	2.06		73.8	58.9	1.25
E60T	31-Mar	0.000	0.02	1.49		58.8	48.1	1.22
	14-Apr	0.000		1.64		55.4	51.6	1.07
	12-May	0.000	0.04	1.74		53.8	52.7	1.02
	27-May	0.000	0.04	4.06		67.8	49.8	1.36
	15-Jul	0.002	0.06	6.22	6.9	74.1	49.7	1.49
	25-Aug	0.004	0.03	2.91	4.5	62.2	41.3	1.51
	17-Feb	0.005	0.09	2.40	9.7	62.9	54.0	1.16
	03-Mar	0.003	0.12	1.85		73.5	54.3	1.36
	17-Mar	0.004	0.17	1.75		65.4	56.9	1.15

Table A.2: Results for physical and chemical parameters from sampling in full-scale distribution systems in 2009–2010 (Part 2).

Site	Date	NO ₂ ⁻ mg-N/L	NH ₃ mg-N/L	DOC mg-C/L	D.O. mg/L	Cl ⁻ mg/L	SO ₄ ²⁻ mg/L	CSMR
WOD61	31-Mar	0.010	0.15	1.30		55.1	49.7	1.11
	14-Apr	0.000	0.17	1.77		52.5	48.5	1.09
	12-May	0.000	0.33	2.67		57.1	52.2	1.09
	27-May	0.051	0.33	2.31		69.9	45.5	1.54
	15-Jul	0.000	0.27	6.26	6.9	55.8	52.3	1.07
	25-Aug	0.000	0.36	4.75	4.0	69.7	40.8	1.71
	17-Feb	0.004	0.10	2.22	9.3	67.5	58.5	1.16
	03-Mar	0.006	0.24	2.12	8.3	68.9	52.3	1.32
	17-Mar	0.000	0.20	1.96		77.9	54.2	1.44
	31-Mar	0.003	0.17	2.54		52.0	47.5	1.09
	14-Apr	0.003	0.33	1.82		56.5	51.2	1.10
	12-May	0.000	0.38	1.80		57.4	50.4	1.14
	27-May	0.045	0.38	2.90		64.9	49.7	1.31
	15-Jul	0.006	0.32	4.72	6.7	64.9	48.9	1.32
	25-Aug	0.013	0.31	3.13	3.9	68.6	44.9	1.54

Table A.3: Results for microbiological parameters from sampling in full-scale distribution systems in 2009–2010.

Site	Date	AOB gcp/100 mL	AOA gcp/100 mL	HPC CFU/100 mL	
RCL	24-Nov	0	0	3.0×10 ¹	
	08-Dec	0	0	2.0×10 ¹	
	12-Jan	0	0	0	
	27-Jan	5	6	5.5×10 ¹	
	09-Feb	1.2×10 ¹	0	1.70×10 ²	
	23-Feb	0	0	5.0×10 ¹	
	23-Mar	0	2	2.0×10 ¹	
	21-Apr	0	4	3.0×10 ¹	
	18-May	2	1	3.5×10 ¹	
	01-Jun	1.7×10 ¹	0	2.0×10 ¹	
	07-Jul	0	0	4.0×10 ¹	
	17-Aug	0	7	6.0×10 ¹	
	602	24-Nov	1.18×10 ³	0	5.30×10 ³
		08-Dec	4.86×10 ³	0	2.00×10 ³
		12-Jan	4.34×10 ²	0	4.97×10 ³
		27-Jan	5.95×10 ²	0	8.03×10 ³
		09-Feb	1.64×10 ²	0	2.74×10 ⁴
23-Feb		1.21×10 ³	0	1.83×10 ⁴	
23-Mar		1.31×10 ³	0	1.21×10 ⁴	
21-Apr		1.68×10 ³	0	4.28×10 ⁴	
18-May		4.86×10 ²	0	3.06×10 ⁴	
01-Jun		1.13×10 ³	0	2.54×10 ⁴	
801	07-Jul	1.51×10 ³	0	1.43×10 ⁴	
	17-Aug	5.46×10 ³	0	1.37×10 ⁴	
	24-Nov	3.18×10 ²	1.2×10 ¹	2.90×10 ³	
	08-Dec	1.88×10 ²	1.4×10 ¹	1.12×10 ³	
	12-Jan	3.00×10 ²	2.2×10 ¹	2.10×10 ³	
	27-Jan	5.95×10 ²	4.1×10 ¹	3.29×10 ⁴	
	09-Feb	8.3×10 ¹	4	3.90×10 ³	
	23-Feb	3.53×10 ²	1.43×10 ²	8.95×10 ³	
	23-Mar	3.01×10 ²	0	2.53×10 ⁴	
	21-Apr	1.21×10 ²	0	9.90×10 ²	
18-May	3.18×10 ²	0	2.75×10 ³		

Table A.3: Results for microbiological parameters from sampling in full-scale distribution systems in 2009–2010.

Site	Date	AOB	AOA	HPC
		gcp/100 mL	gcp/100 mL	CFU/100 mL
804	01-Jun	3.37×10^2	2.0×10^1	3.65×10^3
	07-Jul	7.14×10^2	0	7.95×10^3
	17-Aug	1.28×10^3	1.3×10^1	8.85×10^3
	24-Nov	5.3×10^1	5.0×10^1	6.50×10^3
	08-Dec	1.50×10^2	1.4×10^1	1.80×10^2
	12-Jan	7.2×10^1	2.3×10^1	8.30×10^2
	27-Jan	7.9×10^1	0	5.30×10^3
	09-Feb	6.7×10^1	0	5.50×10^3
	23-Feb	5.20×10^2	0	9.90×10^3
	23-Mar	4.18×10^2	1.33×10^2	1.38×10^4
	21-Apr	6.45×10^2	0	1.65×10^3
	18-May	4.5×10^1	0	2.21×10^4
	01-Jun	6.6×10^1	0	2.45×10^3
	07-Jul	8.7×10^1	1.0×10^1	5.20×10^3
805	17-Aug	1.08×10^2	0	1.27×10^3
	24-Nov	2.21×10^3	2.9×10^1	3.20×10^3
	08-Dec	6.75×10^2	3.0×10^1	5.10×10^2
	12-Jan	2.33×10^2	4.8×10^1	3.60×10^3
	27-Jan	2.49×10^3	0	4.45×10^3
	09-Feb	9.6×10^1	7	1.90×10^3
	23-Feb	1.33×10^2	1.4×10^1	4.35×10^3
	23-Mar	3.00×10^2	2.1×10^1	4.50×10^3
	21-Apr	2.34×10^2	4.6×10^1	5.65×10^3
	18-May	1.23×10^3	0	4.90×10^3
	01-Jun	2.22×10^2	1.9×10^1	6.85×10^3
	07-Jul	4.92×10^3	9	5.95×10^3
	17-Aug	5.09×10^3	3.2×10^1	4.45×10^3
	24-Nov	1.13×10^4	0	5.50×10^3
904	08-Dec	1.11×10^4	0	9.55×10^2
	12-Jan	9.40×10^2	0	1.17×10^4
	27-Jan	9.20×10^2	0	8.40×10^3
	09-Feb	6.60×10^2	0	7.75×10^3
	23-Feb	4.89×10^3	0	3.84×10^4
	23-Mar	2.31×10^3	0	2.21×10^4
	21-Apr	4.23×10^3	0	1.14×10^4
	18-May	7.25×10^3	0	2.33×10^4
	01-Jun	1.35×10^4	3.31×10^2	2.72×10^4
	07-Jul	7.56×10^3	0	4.10×10^3
	17-Aug	1.17×10^4	4.7×10^1	7.15×10^3
	24-Nov	8.99×10^2	4.9×10^1	1.10×10^4
	08-Dec	2.94×10^2	4.3×10^1	1.25×10^2
	12-Jan	3.68×10^2	1.1×10^1	3.43×10^2
905	27-Jan	8.9×10^1	0	1.28×10^3
	09-Feb	1.18×10^2	0	1.35×10^3
	23-Feb	4.2×10^1	0	3.06×10^4
	23-Mar	4.0×10^1	0	1.06×10^4
	21-Apr	5.1×10^1	0	1.23×10^4
	18-May	9.0×10^1	4.33×10^2	6.05×10^3
	01-Jun	1.51×10^2	9.80×10^2	7.37×10^4
	07-Jul	2.05×10^2	0	6.55×10^3
	17-Aug	1.58×10^2	9	2.80×10^3

Table A.3: Results for microbiological parameters from sampling in full-scale distribution systems in 2009–2010.

Site	Date	AOB gcp/100 mL	AOA gcp/100 mL	HPC CFU/100 mL
K20S14	17-Feb	0	2.1×10^1	1.45×10^2
	03-Mar	0	2.9×10^1	1.0×10^1
	17-Mar	9	4.9×10^1	5.0×10^1
	31-Mar	1	8.2×10^1	2.0×10^1
	14-Apr	1	5.1×10^1	2.0×10^1
	12-May	5	9.2×10^1	3.0×10^1
	27-May	1	3.6×10^1	3.0×10^1
	15-Jul	7	2.37×10^2	6.45×10^2
W21	25-Aug	0	1.1×10^1	2.46×10^4
	17-Feb	1.27×10^3	2.40×10^3	2.35×10^3
	03-Mar	1.68×10^3	2.56×10^3	2.10×10^3
	17-Mar	2.20×10^2	7.30×10^2	1.20×10^4
	31-Mar	4.73×10^2	8.95×10^2	4.45×10^3
	14-Apr	3.51×10^2	8.65×10^2	2.90×10^3
	12-May	2.19×10^2	8.10×10^2	3.00×10^3
	27-May	7.45×10^2	1.89×10^3	5.30×10^3
WOD08	15-Jul	5.41×10^2	9.7×10^1	6.30×10^3
	25-Aug	4.25×10^2	3.3×10^1	5.52×10^4
	17-Feb	1.0×10^1	5.1×10^1	5.40×10^2
	03-Mar	1.5×10^1	6.0×10^1	1.55×10^2
	17-Mar	1.1×10^1	1.7×10^1	1.04×10^3
	31-Mar	2.7×10^1	3.7×10^1	2.75×10^2
	14-Apr	7.2×10^1	1.14×10^2	5.60×10^2
	12-May	5.5×10^1	6.6×10^1	3.80×10^2
WOD05	27-May	9	3.8×10^1	2.00×10^2
	15-Jul	2.09×10^2	1.52×10^2	4.84×10^4
	25-Aug	1.85×10^2	5.0×10^1	3.55×10^4
	17-Feb	6.30×10^2	8.9×10^1	1.82×10^4
	03-Mar	1.19×10^3	9.8×10^1	2.07×10^4
	17-Mar	5.8×10^1	1.7×10^1	1.58×10^4
	31-Mar	1.62×10^3	5.20×10^2	5.07×10^4
	14-Apr	3.96×10^2	1.36×10^2	1.30×10^3
WOD06	12-May	4.56×10^2	1.50×10^2	2.01×10^4
	27-May	1.25×10^3	1.77×10^2	1.08×10^4
	15-Jul	4.07×10^3	1.33×10^2	6.41×10^4
	25-Aug	7.86×10^2	9.9×10^1	1.39×10^4
	17-Feb	1.93×10^4	1.04×10^2	5.15×10^4
	03-Mar	9.75×10^4	4.77×10^2	4.25×10^4
	17-Mar	3.66×10^4	5.2×10^1	6.52×10^4
	31-Mar	4.65×10^4	1.26×10^2	3.40×10^4
WOD04	14-Apr	1.73×10^4	2.46×10^2	3.35×10^4
	12-May	6.90×10^2	2.49×10^2	3.94×10^4
	27-May	2.42×10^3	3.62×10^2	7.65×10^3
	15-Jul	9.13×10^3	6.85×10^2	5.35×10^4
	25-Aug	1.08×10^4	7.73×10^2	1.25×10^4
	17-Feb	1	0	5.35×10^3
	03-Mar	1	0	1.04×10^4
	17-Mar	2.4×10^1	0	3.90×10^3
WOD04	31-Mar	4	0	2.69×10^4
	14-Apr	0	0	1.88×10^4
	12-May	5.8×10^1	2.1×10^1	2.55×10^3
	27-May	2	0	1.30×10^4
	15-Jul	0	0	2.10×10^3

Table A.3: Results for microbiological parameters from sampling in full-scale distribution systems in 2009–2010.

Site	Date	AOB gcp/100 mL	AOA gcp/100 mL	HPC CFU/100 mL
E60T	25-Aug	7.5×10^1	1.8×10^1	2.32×10^4
	17-Feb	1.22×10^2	3	2.70×10^3
	03-Mar	8.7×10^1	8.45×10^2	2.10×10^3
	17-Mar	5	2	1.60×10^3
	31-Mar	7.0×10^1	1.4×10^1	5.90×10^3
	14-Apr	1.72×10^2	3.3×10^1	2.70×10^3
	12-May	3.5×10^1	1.8×10^1	2.70×10^3
	27-May	2.1×10^1	1.2×10^1	3.45×10^2
	15-Jul	5.9×10^1	3.7×10^1	1.10×10^5
	25-Aug	4.9×10^1	1.3×10^1	3.52×10^4
WOD61	17-Feb	3.08×10^2	4.4×10^1	8.60×10^3
	03-Mar	4.22×10^2	4.0×10^1	1.60×10^4
	17-Mar	1.88×10^2	4.0×10^1	1.45×10^4
	31-Mar	9.15×10^2	7.9×10^1	1.39×10^4
	14-Apr	2.34×10^2	7.5×10^1	8.20×10^3
	12-May	2.73×10^2	5.6×10^1	1.85×10^4
	27-May	3.55×10^2	1.15×10^2	TNTC
	15-Jul	5.55×10^3	5.96×10^2	6.92×10^4
	25-Aug	2.34×10^2	1.84×10^2	4.75×10^4

Nitrification Batch Tests

The following figures present the results of nitrification batch tests that were not shown in Chapter 5.

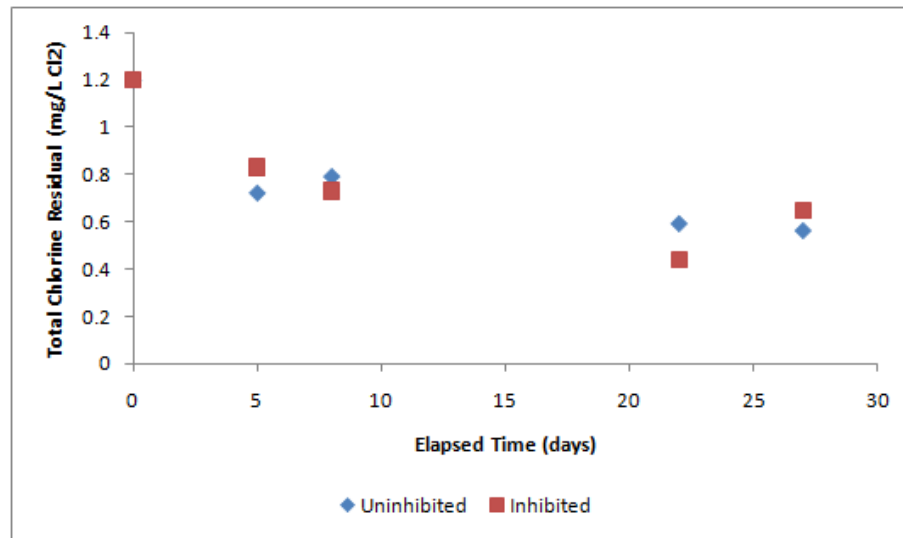


Figure A.1: Nitrification batch test on sample from site RCL in the Toronto distribution system. Sample date was 17 Aug 2010.

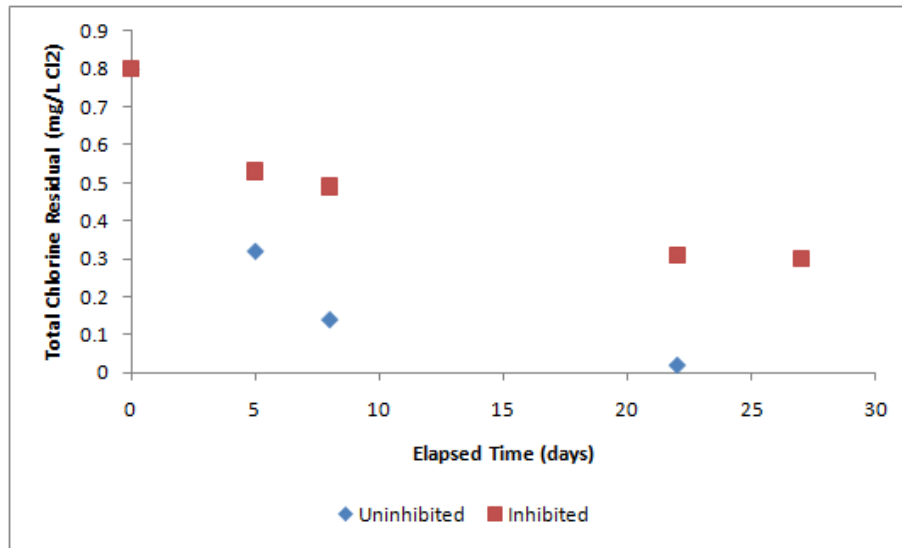


Figure A.2: Nitrification batch test on sample from site RCL in the Toronto distribution system. Sample date was 17 Aug 2010.

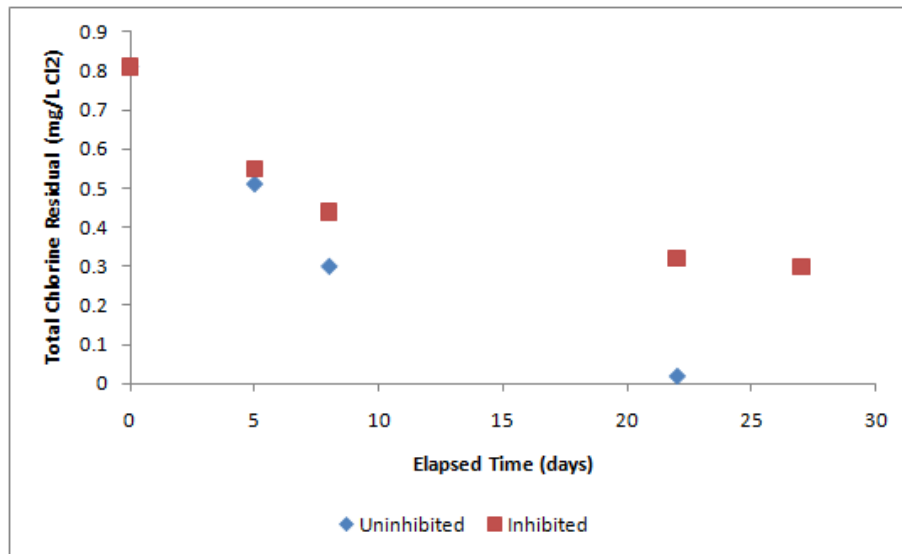


Figure A.3: Nitrification batch test on sample from site RCL in the Toronto distribution system. Sample date was 17 Aug 2010.

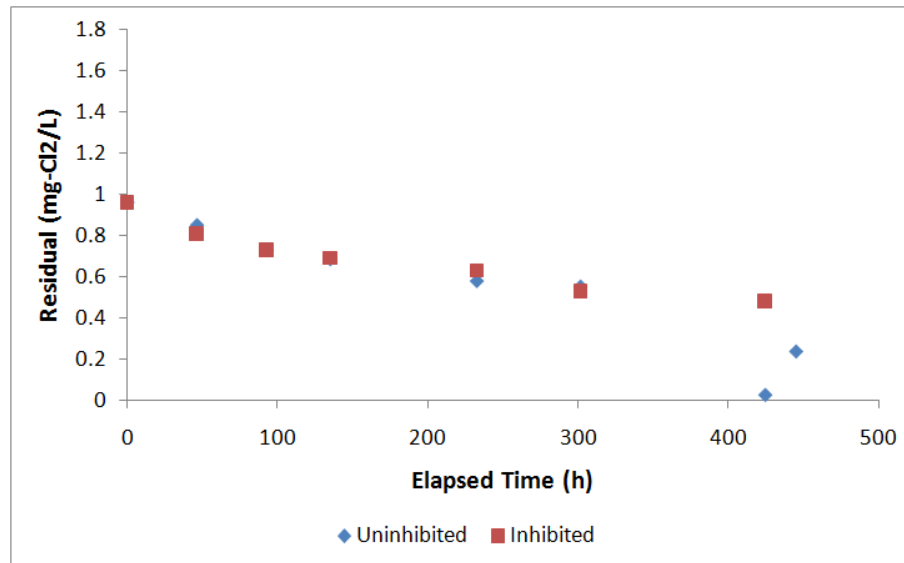


Figure A.4: Nitrification batch test on sample from site RCL in the Toronto distribution system. Sample date was 17 Oct 2010.

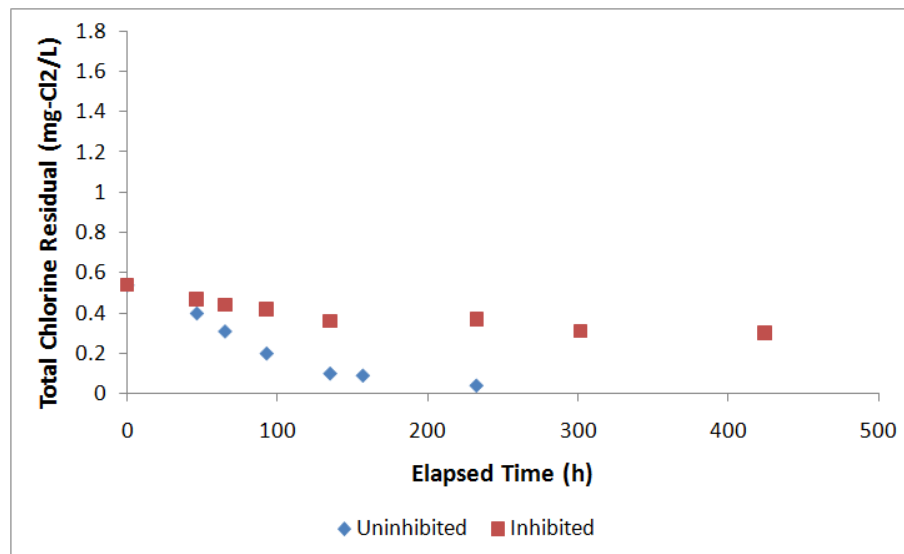


Figure A.5: Nitrification batch test on sample from site 801 in the Toronto distribution system. Sample date was 17 Oct 2010.

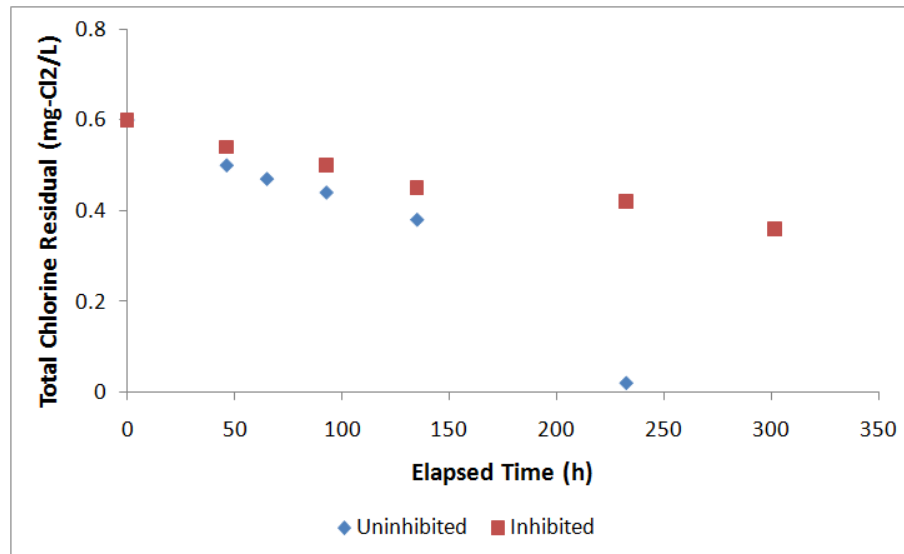


Figure A.6: Nitrification batch test on sample from site 904 in the Toronto distribution system. Sample date was 17 Oct 2010.

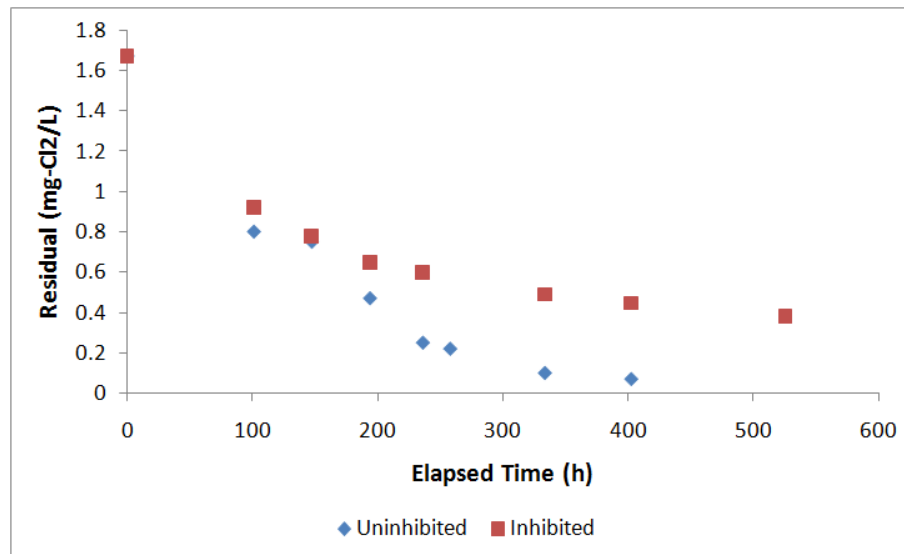


Figure A.7: Nitrification batch test on sample from site K20S14 in the Waterloo distribution system. Sample date was 12 Oct 2010.

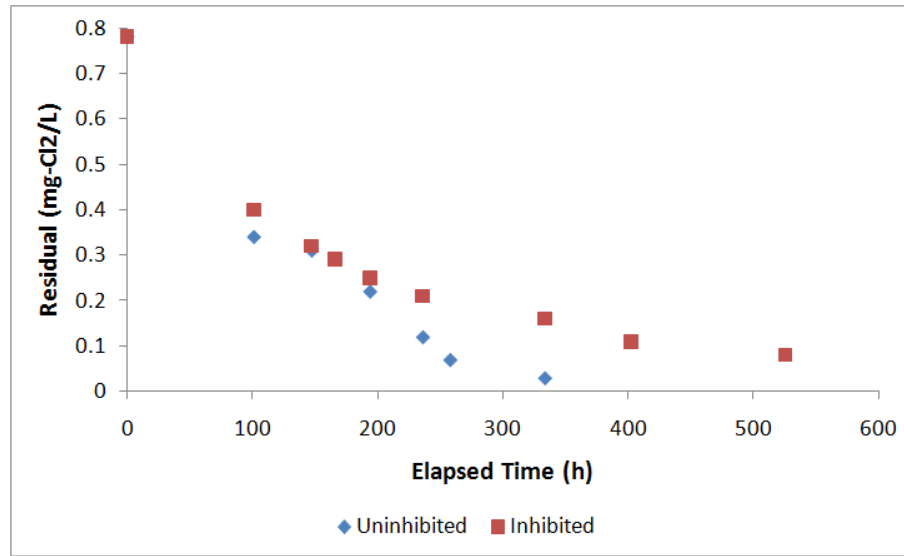


Figure A.8: Nitrification batch test on sample from site WOD61 in the Waterloo distribution system. Sample date was 12 Oct 2010.

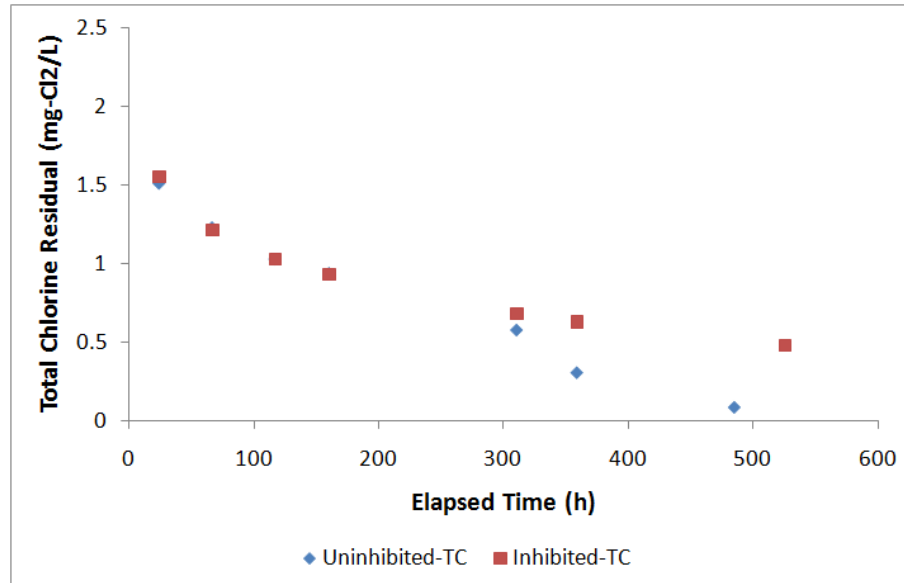


Figure A.9: Nitrification batch test on sample from site K20S14 in the Waterloo distribution system with 1.5 mg-C/L of acetate added. Sample date was 24 Nov 2010.

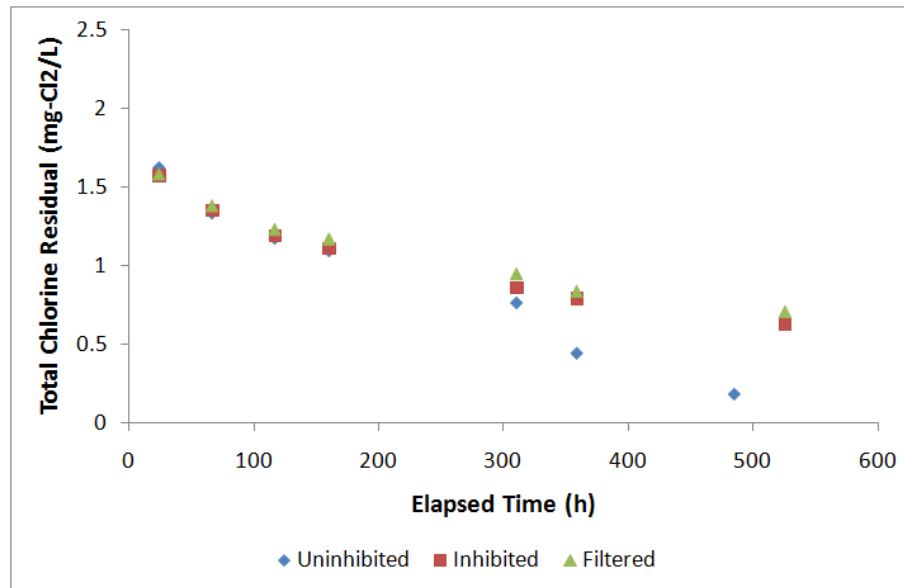


Figure A.10: Nitrification batch test on sample from site K20S14 in the Waterloo distribution system with 0.2 mg-N/L of ammonia added. Sample date was 24 Nov 2010.

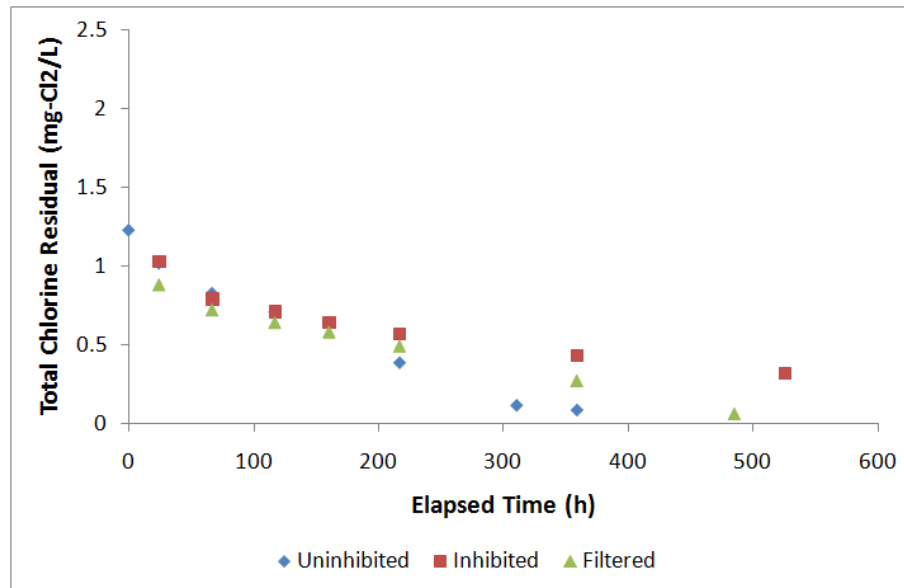


Figure A.11: Nitrification batch test on sample from site WOD06 in the Waterloo distribution system. Sample date was 24 Nov 2010.

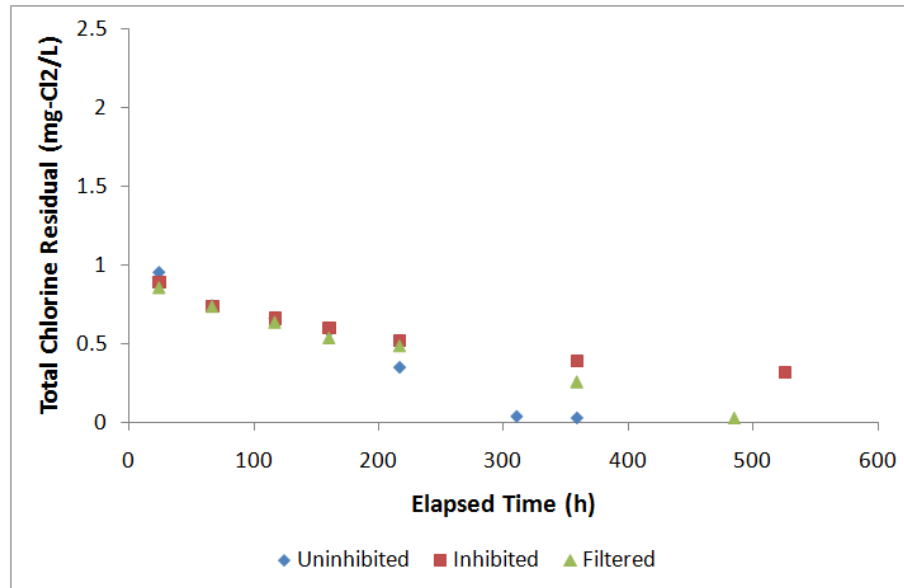


Figure A.12: Nitrification batch test on sample from site WOD06 in the Waterloo distribution system with 1.5 mg-C/L of acetate added. Sample date was 24 Nov 2010.

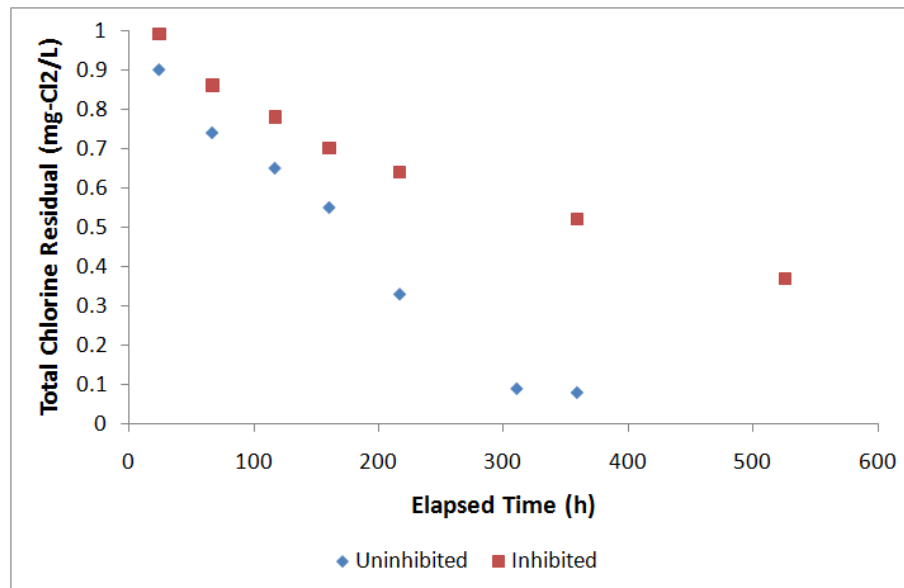


Figure A.13: Nitrification batch test on sample from site WOD06 in the Waterloo distribution system with 0.2 mg-N/L of ammonia added. Sample date was 24 Nov 2010.

Appendix B

Nitrifier Enumeration Methods

B.1 Quantitative PCR of AOB and AOA

Samples that were frozen at -80°C were subjected to three freeze-thaw cycles (-80°C followed by 50°C for 15 minutes), and the vials were then placed on a Dynal rotary mixer for at least 1 hour. The GITC buffer was next transferred to a sterile 2 mL centrifuge tube, then centrifuged at 13 000 rpm for 5 minutes. The supernatant was collected and the DNA was purified using the Qiagen DNeasy tissue kit. The supernatant was passed through a Qiagen column, and the column was washed following the manufacturer's instructions. The column was eluted in a final 100 μL elution buffer. This method resulted in a sample concentration 10 000 times the original sample. This procedure for DNA extraction and purification has been described in Cheyne *et al.* (2010).

Real-time PCR was performed using the following parameters. AOB primers used were described by Rotthauwe *et al.* (1997) while primers for AOA were described by de la Torre *et al.* (2008). Each 50 μL PCR reaction contained 20 μL of DNA sample (corresponding to 200 mL of distribution system sample), 300 nM of each primer, 25 μL of 2x SsoFast EvaGreen supermix (BioRad), and 20 μg BSA (Sigma). The cycling conditions for the AOA assay were 1 cycle at 95°C for 2 minutes; 40 cycles at 95°C for 15 s, 54°C for 30 s and 72°C for 60 s. The same conditions were used for the AOB assay, but with an annealing temperature of 59°C . PCR templates were *amoA* genes cloned into the pCR 4-TOPO vector (Invitrogen). The bacterial *amoA* gene was obtained from a pure culture of *Nitrosomonas europaea*. The archaeal *amoA* gene was amplified from a river water sample. The vector was linearized using the PstI enzyme, and template concentrations were determined using the Quant-iT PicoGreen kit (Invitrogen). For the real-time PCR assays, the standard curves were calculated as *amoA* gene copies. The specificity of all PCR reactions were confirmed by melt curve analysis and by agarose gel electrophoresis.

Cell quantities were estimated from *amoA* gene copy numbers based on conversion factors described by van der Wielen *et al.* (2009) and Hallam *et al.* (2006). The factors used were 2 copies of *amoA* gene per cell for AOB and 1 copy of *amoA* gene per cell for archaea. However, these should be regarded as estimates as Kasuga *et al.* (2010b) found possible evidence for 2 copies of the *amoA* gene per cell for archaea, and Nicolaisen and Ramsing (2002) found that some strains of AOB may have only one copy of the *amoA* gene.

B.2 Culture-based Detection of Nitrifiers

In addition to the PCR-based detection of nitrifying microorganisms that was done for all samples, a culture-based detection method for ammonia-oxidizing bacteria was applied to one set of samples to verify that viable cells were present. Samples were collected from sites in the Toronto distribution system on 17 August 2010 and from sites in the Region of Waterloo distribution system on 25 August 2010. Each sample was filtered through a 0.2 μm Supor 200 membrane as described above, and the membranes were placed in a growth media solution (APHA *et al.*, 2005) and incubated at 28°C for 28 days. The growth media contained a pH indicator in addition to an ammonia substrate and other necessary nutrients. A pH decrease indicated by a colour change at the end of the incubation period was taken as a sign of nitrification. As further confirmation, the solution was tested after the 28 d incubation for the presence of nitrite and nitrate using NitriVer and NitraVer reagents from Hach. Samples that exhibited a colour change for pH, nitrite, and nitrate were marked positive for the presence of ammonia-oxidizing microorganisms. Samples that did not exhibit a colour change for pH, but did have detectable nitrite and nitrate were also marked positive for ammonia oxidizers. This test provided an indication of the presence of ammonia oxidizing microorganisms but was not quantitative. It is based on Standard Method 9245 (APHA *et al.*, 2005).

Appendix C

Supplemental Information

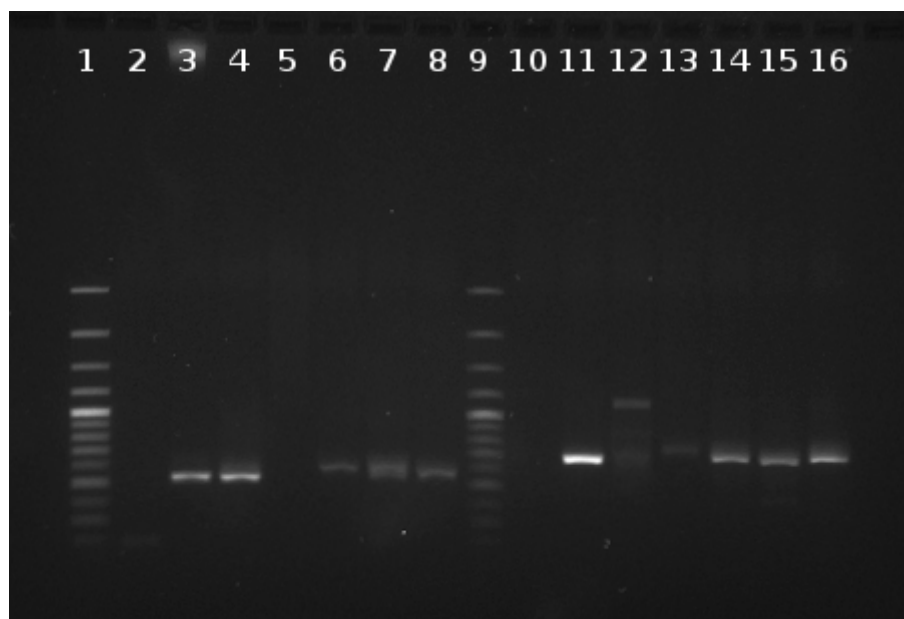


Figure C.1: Agarose gel showing the presence of ammonia-oxidizing archaea (AOA) and ammonia-oxidizing bacteria (AOB) in the surface water sources for each distribution system involved in this study (Lake Ontario for Toronto, and the Grand River for the Region of Waterloo; the groundwater source for the Region of Waterloo was not sampled). Lane descriptions: 1—100 bp ladder, 2—negative control, 3—AOB standard, 4—AOB from Lake Ontario (Oct. 2010), 5–8—AOB from Grand River (2007/2008), 9—100 bp ladder, 10—negative control, 11—AOA standard, 12—AOA from Lake Ontario (Oct. 2010), 13–16—AOA from Grand River (2007/2008).

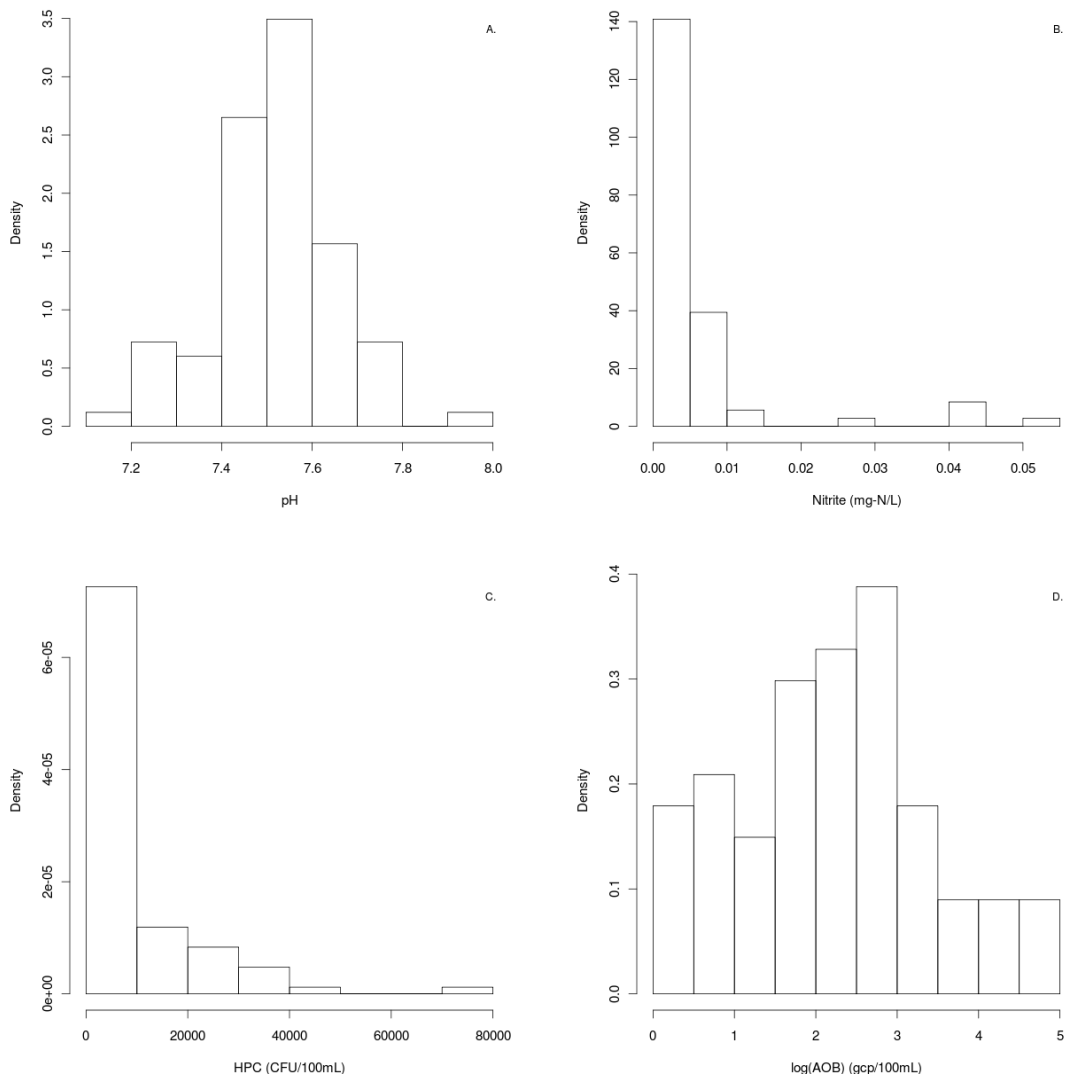


Figure C.2: Histograms showing the frequency distributions of selected parameters monitored in this study. A: pH (Toronto), B: Nitrite (Waterloo), C: HPC (Toronto), D: the base-10 logarithm of AOB amoA gene copy numbers (Waterloo).

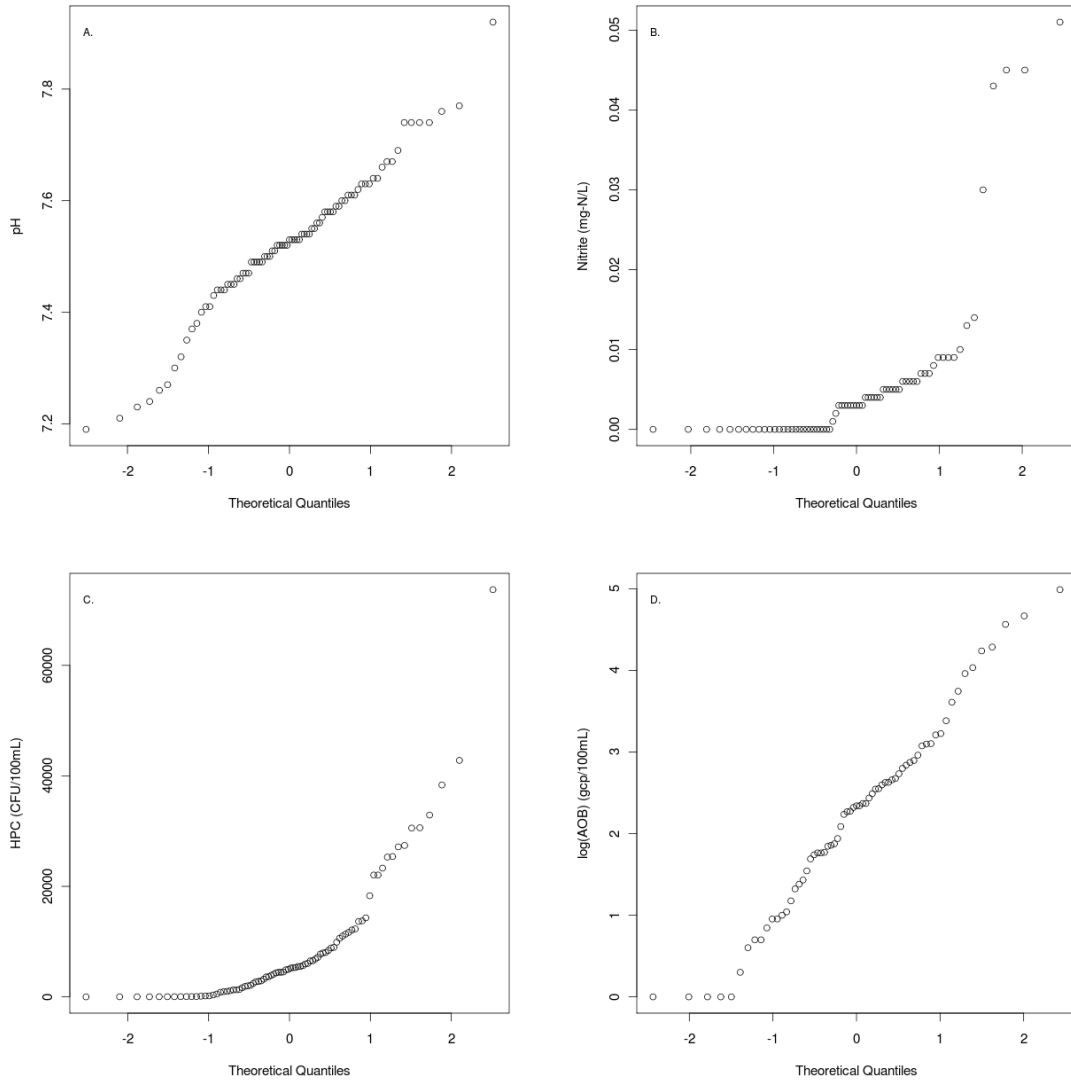


Figure C.3: Quantile-quantile (“Q-Q”) plots examining the statistical distributions of selected parameters monitored in this study. A straight line on these plots indicates a good fit to the normal distribution. A: pH (Toronto), B: Nitrite (Waterloo), C: HPC (Toronto), D: the base-10 logarithm of AOB amoA gene copy numbers (Waterloo).

Appendix D

Calibration of Instruments and Methods

Accuracy and precision information for instruments and methods used in this research:

- Hach method # 10200 has a range of 0.04–4.50 mg-Cl₂/L for monochloramine and a range of 0.01–0.50 mg NH₃-N/L for ammonia; 95% confidence limits on the precision are ± 0.06 and ± 0.014, respectively (Hach, 2008)
- Hach method # 8167 (total chlorine) has a range of 0.02–2.00 mg-Cl₂/L and 95% confidence limits on precision of ± 0.02 (Hach, 2008)
- The Hach CO150 Conductivity Meter has a maximum accuracy of ± 9 μS in the range 200–1999 μS for conductivity and an accuracy of ± 1.0°C for temperature
- Average relative standard deviation (RSD) for dissolved organic carbon standards run on 21 June 2010 was 4.8%
- Average RSD (values for peak heights and areas for all anions were included) for the ion chromatograph at low ranges (0.1–0.4 mg/L Cl⁻; 0.05–0.2 mg/L for NO₂⁻ and NO₃⁻; 0.15–0.6 mg/L for SO₄²⁻) was determined to be 32% on 14 July 2010

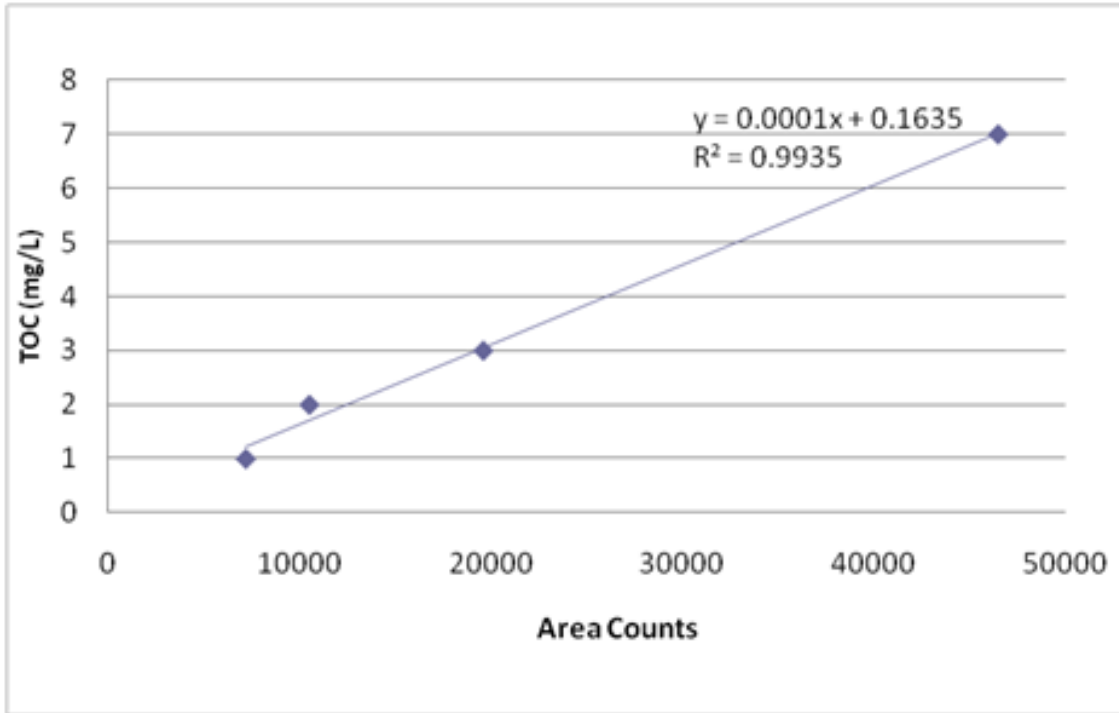


Figure D.1: Example calibration curve for DOC samples (22 Sept. 2010).

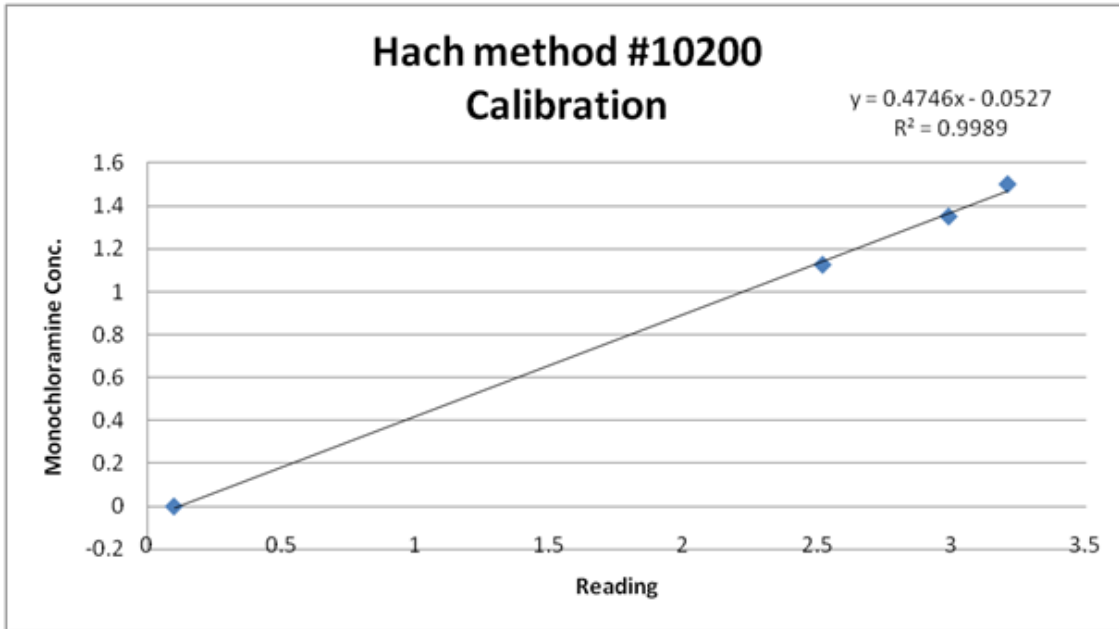


Figure D.2: This curve was developed to provide a calibration factor for monochloramine readings from the spectrophotometer being used.

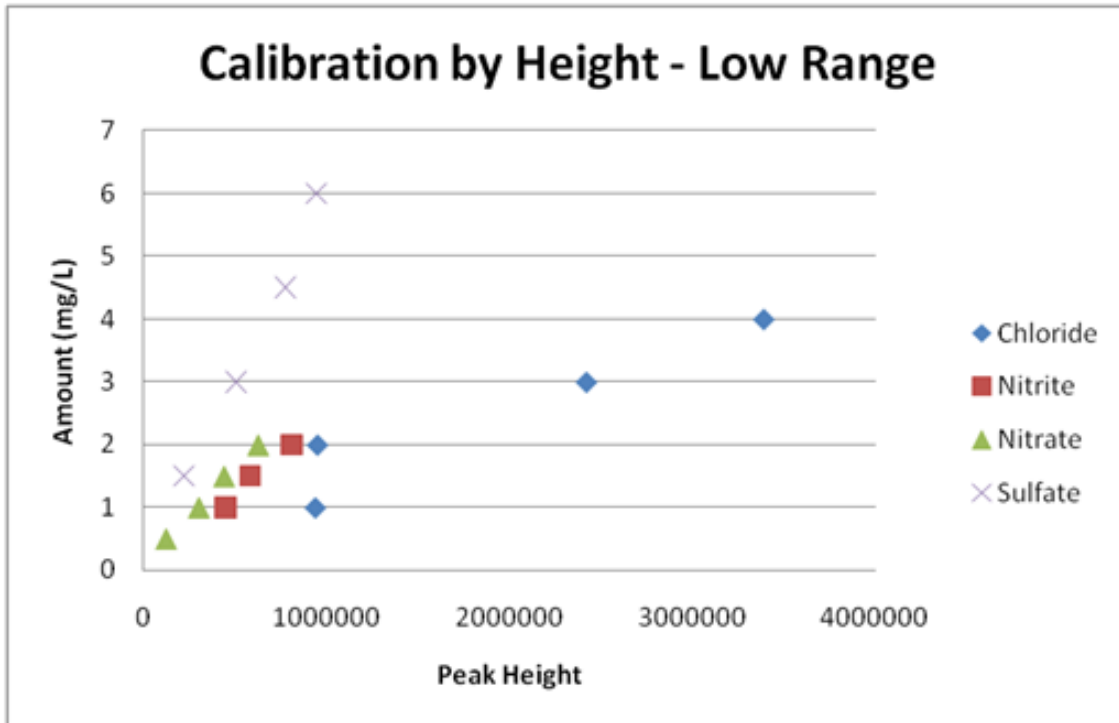


Figure D.3: Example calibration curve for anion (ion chromatography measurements) samples from 7 April 2010. This calibration curve was used to derive low range concentrations from chromatograph peak heights.

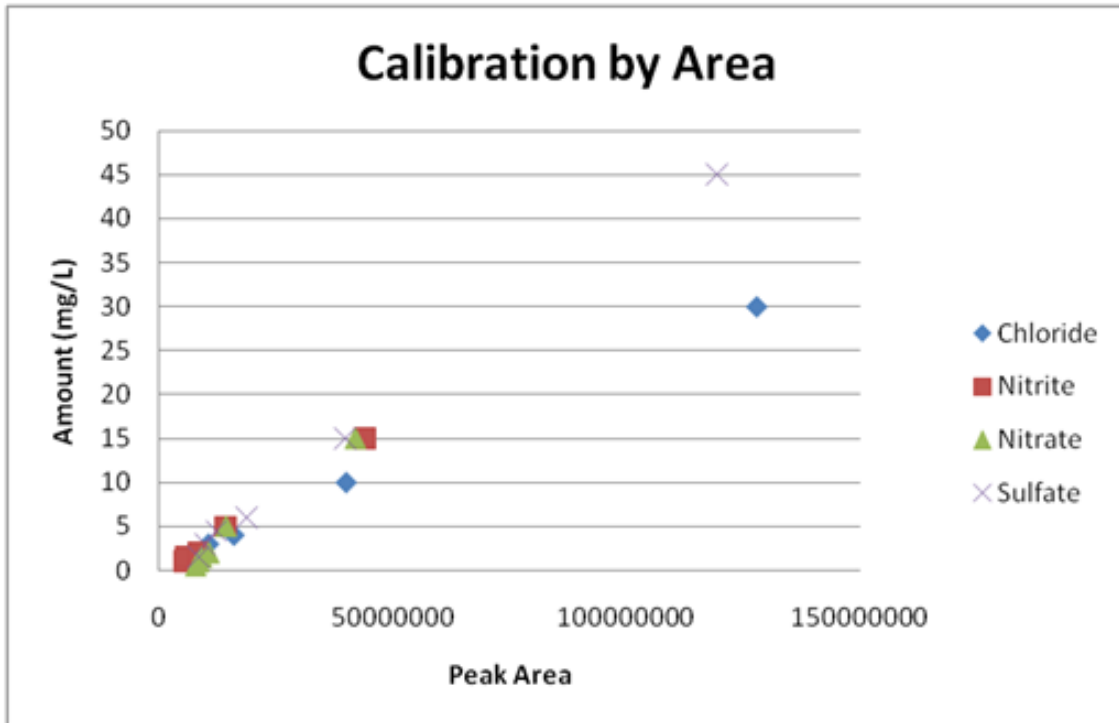


Figure D.4: Example calibration curve for anion (ion chromatography measurements) samples from 7 April 2010. This calibration curve was used to derive high range concentrations from chromatograph peak areas.

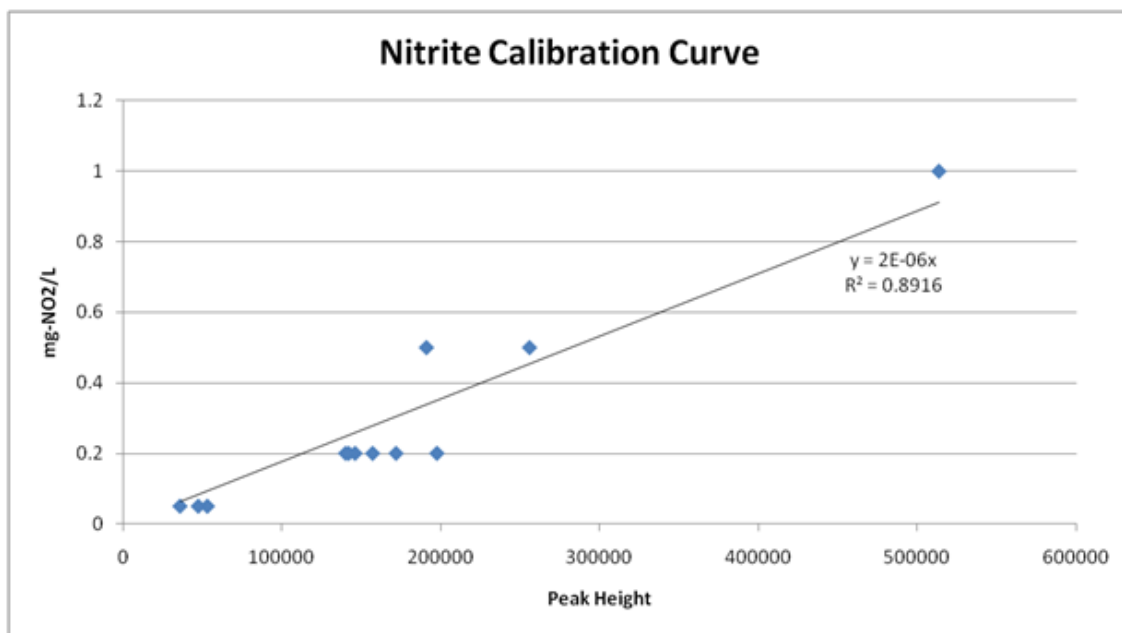


Figure D.5: The calibration curve used for all nitrite samples analyzed in the ion chromatograph, determined using low concentration standards.

Appendix E

Sample Model Calculations

Here are sample calculations for the nitrification batch tests described in Chapter 5. These calculations were done in Microsoft Excel spreadsheets. The label “y-values” signifies a column of natural logarithms of total chlorine concentrations, while “x-values” denotes a column of the corresponding times (in hours).

- $k_{T1} = -1 * \text{SLOPE}(\text{y-values}, \text{x-values})$, for data points before a visible break-point in the decay rate
- $b_1 = \text{INTERCEPT}(\text{y-values}, \text{x-values})$, for data points before a visible break-point in the decay rate
- $k_{T2} = -1 * \text{SLOPE}(\text{y-values}, \text{x-values})$, for data points after a visible break-point in the decay rate
- $b_2 = \text{INTERCEPT}(\text{y-values}, \text{x-values})$, for data points after a visible break-point in the decay rate
- $k_C = -1 * \text{SLOPE}(\text{y-values}, \text{x-values})$, for inhibited batch samples
- $\text{Time to CTR} = (b_2 - b_1) / (k_{T2} - k_{T1})$
- $\text{CTR} = \text{EXP}(-1 * k_{T1} * (\text{Time to CTR}) + b_1)$

Two methods were used to fit the coefficients for the Nitrification Potential Curve model of Fleming *et al.* (2005) presented in Chapter 6. In the notation used to describe these methods, C_d is the disinfectant concentration and C_s is the substrate (ammonia) concentration. The first method was adapted from Srinivasan and Harrington (2007):

1. Pick point 1 such that it has the highest C_d from the set of nitrifying points

2. Pick point 2 such that $C_{d2} < C_{d1}$ and $C_{s2} < C_{s1}$
3. Calculate $R_{gi} = [C_{d1}C_{d2}(C_{s1} - C_{s2})]/[C_{s1}C_{d2} - C_{s2}C_{d1}]$
4. Calculate $K_s = [C_{s1}C_{s2}(C_{d1} - C_{d2})]/[C_{s2}C_{d1} - C_{s1}C_{d2}]$
5. Check the following inequality for all nitrifying points in the data set and adjust point 2 to minimize violations, if necessary: $C_{di}K_s + C_{di}C_{si} - R_{gi}C_{si} \leq 0$; non-nitrifying points should mostly be >0

The second method for fitting coefficients was modified from Fleming *et al.* (2005, 2008):

1. Pick point 1 such that it has the highest C_d from the set of nitrifying points
2. Pick point 2 such that it appears to lie near the nitrifying/non-nitrifying boundary (e.g. lowest C_d or highest C_s from non-nitrifying set of data points or lowest C_s from set of nitrifying points)
3. Assuming $C_{d2} < C_{d1}$, calculate $K_s = (C_{s2}C_{d1} - C_{d2}C_{s2})/C_{d2}$
4. Calculate the following statement for both points 1 and 2 and take the maximum value for R_{gi} : $C_{di} \frac{K_s + C_{si}}{C_{si}}$

The following R (R Development Core Team, 2009) code is provided as an example of the calculations done for Spearman correlations (Table 4.2) and logistic regression (evaluating model of Yang *et al.* (2007):

Calc_ex.R

```

1  ## Calc_ex.R - shows examples of calculations notable to my thesis done using R
  # Commands are on lines beginning with a right angle bracket (>)
  # Output is also shown

6  ## Spearman Correlation Example

  > cor.test(Toronto$Temp, Toronto$Total.Cl, method="spearman")

  Spearman's rank correlation rho

11 data:  Toronto$Temp and Toronto$Total.Cl
   S = 112632.1, p-value = 0.04133
  alternative hypothesis: true rho is not equal to 0
  sample estimates:
16      rho
   -0.2258476

21 ## Logistic Regression Example

```

```

> W.Risk.Model <- glm(W.event[complete.cases(W.Risk.Factors,W.event) & Waterloo$Site != "
  K2OS14" & Waterloo$Site != "WOD61"] ~ W.Risk.Factors$Waterloo.Ammonia[complete.cases(W.
  Risk.Factors,W.event) & Waterloo$Site != "K2OS14" & Waterloo$Site != "WOD61"] + W.Risk.
  Factors$W.pH_diff[complete.cases(W.Risk.Factors,W.event) & Waterloo$Site != "K2OS14" &
  Waterloo$Site != "WOD61"] + W.Risk.Factors$Waterloo.Total.Cl[complete.cases(W.Risk.
  Factors,W.event) & Waterloo$Site != "K2OS14" & Waterloo$Site != "WOD61"] + W.Risk.
  Factors$Waterloo.Temp[complete.cases(W.Risk.Factors,W.event) & Waterloo$Site != "K2OS14"
  & Waterloo$Site != "WOD61"], binomial ("logit"))

26 > summary(W.Risk.Model)

Call:
glm(formula = W.event[complete.cases(W.Risk.Factors, W.event) &
  Waterloo$Site != "K2OS14" & Waterloo$Site != "WOD61"] ~ W.Risk.Factors$Waterloo.Ammonia[
  complete.cases(W.Risk.Factors,
31   W.event) & Waterloo$Site != "K2OS14" & Waterloo$Site != "WOD61"] +
  W.Risk.Factors$W.pH_diff[complete.cases(W.Risk.Factors, W.event) &
  Waterloo$Site != "K2OS14" & Waterloo$Site != "WOD61"] +
  W.Risk.Factors$Waterloo.Total.Cl[complete.cases(W.Risk.Factors,
36   W.event) & Waterloo$Site != "K2OS14" & Waterloo$Site !=
  "WOD61"] + W.Risk.Factors$Waterloo.Temp[complete.cases(W.Risk.Factors,
  W.event) & Waterloo$Site != "K2OS14" & Waterloo$Site != "WOD61"],
  family = binomial("logit"))

Deviance Residuals:
41   Min       1Q   Median       3Q      Max
   -1.4536  -0.2954  -0.1279  -0.0609   1.8715

Coefficients:
                                Estimate
46 (Intercept)                   -14.1935
   W.Risk.Factors$Waterloo.Ammonia[...]  2.0375 ###Subset defined above
   W.Risk.Factors$W.pH_diff[...]       -6.8197
   W.Risk.Factors$Waterloo.Total.Cl[...]  7.6418
51   W.Risk.Factors$Waterloo.Temp[...]    0.5926

                                Std. Error
   (Intercept)                   7.7465
   W.Risk.Factors$Waterloo.Ammonia[...]  4.9364
   W.Risk.Factors$W.pH_diff[...]       3.8599
56   W.Risk.Factors$Waterloo.Total.Cl[...]  5.2411
   W.Risk.Factors$Waterloo.Temp[...]    0.3243

                                z value
   (Intercept)                   -1.832
61   W.Risk.Factors$Waterloo.Ammonia[...]  0.413
   W.Risk.Factors$W.pH_diff[...]       -1.767
   W.Risk.Factors$Waterloo.Total.Cl[...]  1.458
   W.Risk.Factors$Waterloo.Temp[...]    1.827

                                Pr(>|z|)
66   (Intercept)                   0.0669
   W.Risk.Factors$Waterloo.Ammonia[...]  0.6798
   W.Risk.Factors$W.pH_diff[...]       0.0773
   W.Risk.Factors$Waterloo.Total.Cl[...]  0.1448
71   W.Risk.Factors$Waterloo.Temp[...]    0.0676

```

```

(Intercept) .
W.Risk.Factors$Waterloo.Ammonia[...] .
W.Risk.Factors$W.pH_diff[...] .
76 W.Risk.Factors$Waterloo.Total.Cl[...] .
W.Risk.Factors$Waterloo.Temp[...] .
---
Signif. codes:  0   ***    0.001   **   0.01   *    0.05   .    0.1    1

81 (Dispersion parameter for binomial family taken to be 1)

      Null deviance: 28.042  on 50  degrees of freedom
Residual deviance: 18.365  on 46  degrees of freedom
AIC: 28.365

86 Number of Fisher Scoring iterations: 7

```

The following R code was written to conduct simulations using the model of Yang *et al.* (2008):

Nitrification_Model.R

```

### Nitrification_Model.R
2 #
# This R script implements the semi-mechanistic nitrification model of
# Yang et al. (2008). It's been adapted/simplified to batch conditions
# (no inflow or outflow). A pH of 7.5 and temperature of 20 C are assumed.
#
7 # Set the initial conditions prior to running this script:
# Initial <- data.frame(D = 1.3, HPC = 0.0001, S = 0.20, Xa = 0.0001, Xn = 0.00002, N =
#   0.01, Na = 1.0)
#
# Dataframes: Initial--initial conditions; Previous--used to calculate deltas
# (changes); Current--Tracking present concentrations; Record--sparse
12 # snapshots of Current
#
# Constituents/Variables: D--disinfectant (assumed to be all monochloramine)
# concentration, mg-Cl2/L; HPC--Heterotrophs, mg/L; S--substrate (ammonia)
# conc., mg-N/L; Xa--AOB, mg/L; Xn--NOB, mg/L; N--nitrite, mg-N/L; Na--
17 # nitrate, mg-N/L; day--time, days
#
# Other: i,j--index variables; delta.t--time step, days; i.max--endpoint of loop;
# NRec--number of records
#
22
##Initialize variables
Previous <- data.frame(day = 0, D = 0, HPC = 0, S = 0, Xa = 0, Xn = 0, N = 0, Na = 0)
Current <- data.frame(day = 0, D = 0, HPC = 0, S = 0, Xa = 0, Xn = 0, N = 0, Na = 0)
27 delta.t <- 0.005
i.max <- ((30/delta.t) + 1) #end after 30 days; plus 1 to index to include zero
NRec <- 30*8 #keep simulation results from every 3 hours (8x daily) for 30 days
Record <- data.frame(day = numeric(NRec), D = numeric(NRec), S = numeric(NRec), Xa = numeric
  (NRec), Xn = numeric(NRec), N = numeric(NRec), Na = numeric(NRec))
j <- 1
32
Current$D <- Initial$D
Current$HPC <- Initial$HPC
Current$S <- Initial$S
Current$Xa <- Initial$Xa
37 Current$Xn <- Initial$Xn
Current$N <- Initial$N
Current$Na <- Initial$Na

##Step through simulation
42 for (i in 1:i.max){
  #Write Current to Previous
  Previous$day <- Current$day
  Previous$D <- Current$D
  Previous$HPC <- Current$HPC #HPCs are assumed to be constant
47 Previous$S <- Current$S
  Previous$Xa <- Current$Xa
  Previous$Xn <- Current$Xn
  Previous$N <- Current$N
  Previous$Na <- Current$Na
52 if ((Current$day%0.125)<0.005){#Record Current every 3 hours (0.125 days)

```

```

Record$day[j] <- Current$day
Record$D[j] <- Current$D
Record$S[j] <- Current$S
57 Record$Xa[j] <- Current$Xa
Record$Xn[j] <- Current$Xn
Record$N[j] <- Current$N
Record$Na[j] <- Current$Na
j <- j + 1
}
62 #Calculate deltas for each variable based on Previous and delta.t and
# use to determine Current
Current$day <- Previous$day + delta.t
rmn <- (84000*10^(-7.5)*Previous$D*Previous$N*(1 + 0.016*Previous$N))/(39*((10^(-9.32)*
Previous$S)/((10^(-9.32) + 10^(-7.5)))) + (1 + 0.016*Previous$N)) #reaction between
monochloramine and nitrite
Current$D <- Previous$D - delta.t*(0.032*Previous$D^2 + 0.34*Previous$D + rmn + 70*
Previous$HPC*Previous$D)
67 Current$S <- Previous$S + delta.t*((14/71)*((1/3)*0.032*Previous$D^2 + 0.34*Previous$D +
rmn + 70*Previous$HPC*Previous$D) - (1/0.33)*((0.47*Previous$S*Previous$Xa)/(0.023 +
Previous$S)))
Current$N <- Previous$N + delta.t*((0.97/0.33)*((0.47*Previous$S*Previous$Xa)/(0.023 +
Previous$S)) - (14/71)*rmn - (1/0.083)*0.21*Previous$Xn)
Current$Na <- Previous$Na + delta.t*((14/71)*rmn + (0.97/0.083)*0.21*Previous$Xn)
Current$Xa <- Previous$Xa + delta.t*(Previous$Xa*((0.47*Previous$S)/(0.023 + Previous$S) -
0.096 - 0.97*Previous$D))
Current$Xn <- Previous$Xn + delta.t*(Previous$Xn*(0.21-0.096))
72 }

##Make graphs of simulation results
png("Sim_Nitrogen.png",width=640,height=640)
par(cex=1.25,mar=c(4.1,4,2,4))
77 plot(Record$day,Record$D,ylim=range(Record$D,Record$S,Record$N,Record$Na),type="l", lty=1,
xlab="Day",ylab="Concentration (mg/L)",main="") #graph of nitrogen species
lines(Record$day,Record$S,lty=2)
lines(Record$day,Record$N,lty=3)
lines(Record$day,Record$Na,lty=4)
dev.off()
82
png("Sim_Nitrifiers.png",width=640,height=640)
par(cex=1.25,mar=c(4.1,4,2,4))
plot(Record$day,Record$Xa,ylim=range(Record$Xa,Record$Xn),type="l", lty=1, xlab="Day",ylab="
Concentration",main="") #graph of nitrifying bacteria
lines(Record$day,Record$Xn,lty=2)
87 dev.off()

```